

12-17-2010

## Geology & Geochemistry of the Kingman Feldspar, Rare Metals and Wagon Bow Pegmatites

TJ Brown  
*University of New Orleans*

Follow this and additional works at: <https://scholarworks.uno.edu/td>

---

### Recommended Citation

Brown, TJ, "Geology & Geochemistry of the Kingman Feldspar, Rare Metals and Wagon Bow Pegmatites" (2010). *University of New Orleans Theses and Dissertations*. 1280.  
<https://scholarworks.uno.edu/td/1280>

This Thesis is protected by copyright and/or related rights. It has been brought to you by ScholarWorks@UNO with permission from the rights-holder(s). You are free to use this Thesis in any way that is permitted by the copyright and related rights legislation that applies to your use. For other uses you need to obtain permission from the rights-holder(s) directly, unless additional rights are indicated by a Creative Commons license in the record and/or on the work itself.

This Thesis has been accepted for inclusion in University of New Orleans Theses and Dissertations by an authorized administrator of ScholarWorks@UNO. For more information, please contact [scholarworks@uno.edu](mailto:scholarworks@uno.edu).

Geology & Geochemistry of the Kingman Feldspar, Rare Metals and Wagon Bow Pegmatites

A Thesis

Submitted to the Graduate Faculty of the  
University of New Orleans  
in Partial Fulfillment of the  
requirements for the Degree of

Master of Science  
in  
Earth & Environmental Science

By

T.J. Allen Brown

August 2010

B.A., Adrian College, 2008

## **Acknowledgements**

Throughout this endeavor a small group of people assisted in the completion of this project and I would now like to take this opportunity to thank them for all they did help make this thesis a reality.

Firstly I would like to thank the Earth & Environmental Department at the University of New Orleans for both for supplying partial funding for my field work as well as my laboratory research.

I would like to thank my committee member Karen Webber and my fiancée Heather Piehl for supplying their invaluable editing skills to this manuscript to correct the countless misspellings that existed in the beginning.

I owe a special debt of gratitude to Dr. Sarah Hanson for all she has helped me accomplish. From guiding my way as an undergrad and giving me a job where I could smash and break things, both good and bad, to helping me survive in the desert collecting radioactive minerals in banjo country. I would also like to thank Dr. Hanson for introducing me to Jerry Baird who was able to supply me with samples that he was able to retrieve thanks to his time spent exploring the area.

Next I would like to thank Dr. Wm. "Skip" Simmons for his assistance in the field, his countless suggestions for improving the manuscript and for teaching me how to start a moving company.

I would like also thank Al Falster for all of his troubleshooting assistance, time spent in data collection, sharing confusion over new computer programs and for showing me that truly disgusting foods do exist.

Finally, I would like to thank my close friend Jeremy James Milton McKinney, without whom I would have ended up being a biologist and nobody wants that.

## Table of Contents

	<u>Page</u>
List of Tables .....	v
List of Figures .....	vii
Abstract .....	ix
Introduction.....	1
General Geology .....	2
Cerbat Mountain Range .....	6
Kingman Feldspar Quarry Pegmatite.....	10
Aquarius Mountain Range .....	13
Rare Metals Pegmatite .....	15
Wagon Bow Pegmatites .....	19
Petrography .....	22
Host Rock.....	22
Quartz Diorite .....	22
Granite.....	23
Pegmatite.....	25
Mineralogy .....	26
Microcline Feldspar .....	26
Muscovite.....	37
Biotite.....	37
Fe/Ti Oxides.....	41
Allanite.....	50
Monazite .....	59

Beryl.....	65
Apatite.....	65
Bastnaesite & Ca-rich Bastnaesite .....	70
Titanite .....	75
Zircon.....	77
Quartz.....	80
Epidote .....	80
Thorogummite.....	82
Uraninite .....	87
Goethite.....	89
Major and Trace Element Chemistry.....	91
Discussion & Conclusions .....	120
References.....	126
Analytical Methods.....	130
Petrographic Analysis .....	130
Heavy Mineral Separation .....	130
Scanning Electron Microscopy .....	130
Direct Coupled Plasma Spectroscopy .....	130
Electron Microprobe Analyses .....	131
X-Ray Diffraction .....	132
Whole Rock Analyses.....	132
Appendix.....	134
Vita.....	170

## List of Tables

Table	Page
1. Representative Chemical Composition of Microcline from the Kingman, Rare Metals and Wagon Bow Pegmatites.....	31
2. Representative Chemical Composition of Plagioclase exsolution lamellae from the Kingman, Rare Metals and Wagon Bow Pegmatites .....	33
3. Average Microcline Content from all Sampling Location .....	34
4. Average Plagioclase Content from all Sampling Locations .....	35
5. Microcline & Plagioclase Reintegration Compositions.....	36
6. Chemical Composition of Muscovite from the Rare Metals Mine .....	39
7. Representative Chemical Composition of Biotite from the Kingman, Rare Metals and Wagon Bow Pegmatite.....	40
8. Representative Chemical Composition of Ilmenite from the Kingman Pegmatite.....	42
9. Chemical Composition of Magnetite from the Kingman Pegmatite .....	43
10. Representative Chemical Composition of Hematite from the Kingman, Rare Metals and Wagon Bow Pegmatites.....	44
11. Chemical Composition of Rutile from the Kingman, Rare Metals and Wagon Bow Pegmatites .....	45
12. Representative Chemical Composition of Allanite from the Kingman Pegmatite ....	53
13. Representative Chemical Composition of Monazite from the Rare Metals and Wagon Bow Pegmatites .....	60
14. Chemical Composition of Beryl from the Rare Metals Mine .....	66
15. Chemical Composition of Apatite from the Kingman and Wagon Bow Pegmatites .....	67
16. Chemical Composition of Bastnaesite from the Kingman Pegmatite .....	71
17. Chemical Composition of Ca-rich bastnaesite from the Kingman Pegmatite .....	72
18. Chemical Composition of Titanite from the Kingman and Wagon Bow Pegmatites .....	76
19. Chemical Composition of Zircon from the Kingman Pegmatite .....	78
20. Chemical Composition of Epidote from the Kingman and Wagon Bow Pegmatite.....	81
21. Chemical Composition of Thorogummite from the Kingman Pegmatite.....	83
22. Chemical Composition of Uraninite from the Kingman Pegmatite.....	88
23. Chemical Composition of Goethite from the Kingman Pegmatite .....	90
24. XRF Whole Rock Data for Major Elements .....	97
25. XRF Whole Rock Data for Trace Elements .....	98
26. Chemical Composition of Biotite from the Kingman, Rare Metals and Wagon Bow Pegmatites continued .....	134
27. Chemical Composition of Microcline from the Kingman, Rare Metals and Wagon Bow Pegmatites continued .....	138

28. Chemical Composition of Plagioclase from the Kingman, Rare Metals and Wagon Bow Pegmatites continued .....	141
29. Chemical Composition of Ilmenite from the Kingman Pegmatite continued.....	143
30. Chemical Composition of Hematite from the Kingman, Rare Metals and Wagon Bow Pegmatites continued .....	145
31. Chemical Composition of Nd-dominant Allanite from the Kingman Pegmatite.....	147
32. Chemical Composition of Allanite from the Kingman Pegmatite continued .....	149
33. Chemical Composition of Monazite from the Rare Metals and Wagon Bow Pegmatites continued .....	161
34. Rubidium DCP analysis.....	166
35. Lithium DCP analysis .....	167
36. Thallium DCP analysis .....	168
37. Boron DCP analysis .....	169

## List of Figures

<u>Figure</u>	<u>Page</u>
1. A. State and Field Map of Study Area.....	4
B. Model of Terranes Docking With North America .....	5
C. Rifting Model .....	5
2. Geologic Map of the Cerbat Mountain Range .....	8
3. Geologic Map of the Kingman Feldspar Pegmatite.....	9
4. Satellite image of the Kingman Feldspar Pegmatite, Cut A .....	11
5. Satellite image of the Kingman Feldspar Pegmatite, Cuts B & C .....	11
6. Geologic Map of the Rare Metals Pegmatite .....	14
7. Field Shot at Rare Metals Mine of Line Rock .....	17
8. Geologic Map of the Wagon Bow #3 Pegmatite .....	18
9. Satellite Image of the three Wagon Bow Pegmatites.....	20
10. Field Shot at Wagon Bow #3 of Line Rock .....	21
11. Graph Plotting the Proper Naming of Host Rock .....	23
12. Field Shot at Wagon Bow #1 of Spotted Granite Boulder.....	25
13. Field Shot of Allanite in Microcline showing Radiating Fracturing .....	27
14. Petrographic Thin Section of Microcline from the Kingman Feldspar Pegmatite, Cut B. Maximum Dimension 2.5 mm.....	28
15. A. Field Shot of Massive Microcline, Finger for Scale .....	29
B. Binary Phase Diagram.....	30
16. Ternary Diagram of Microcline and Plagioclase Comparing Orthoclase, Albite, and Anorthite Compositions .....	32
17. Field Shot at Rare Metals Mine of Muscovite Pods near Core Zone .....	38
18. Ternary Diagram of Fe/Ti oxides and the Respective Zones they fall into .....	47
19. Ternary Diagram of Rutile Illustrating Slight Ti Replacement by Fe .....	48
20. Ternary Diagram of Rutile showing a separation by Ca from HREE and LREE.....	48
21. Field Shot at Kingman Feldspar Cut B of Allanite in Microcline .....	51
22. Petrography Thin Section of Allanite under Plane Polarized Light .....	52
23. Petrography Thin Section of Allanite under Crossed Nichols.....	52
24. Ternary diagram of allanite showing near equal amounts of dominance for Ca and REE.....	55
25. Ternary Diagram of Allanite Showing an Absence of HREE and the Equal Dominance of Ca and LREE .....	56
26. Ternary Diagram Showing Allanite and Epidote Falling into their Respective Zones .....	57
27. Ternary Diagram of Allanite Showing the Existence of a New Mineral; Allanite-Nd .....	58
28. Ternary Diagram of Monazite Showing Elemental Dominance.....	63
29. Ternary Diagram of Monazite Showing High Amounts of LREE	

over Th and HREE.....	62
30. Radiation damage seen in Quartz .....	64
31. Ternary Diagram of Apatite with Ca Dominant over Both Mn and Fe .....	68
32. Ternary Diagram of Apatite Plotted to Determine Which Type of Apatite is in the Sample .....	69
33. Ternary Diagram of Bastnaesite and Ca-rich bastnaesite Showing a Lack of HREE and LREE Dominance over Ca .....	73
34. Ternary Diagram of Bastnaesite & Ca-rich bastnaesite Showing Ce Dominance....	74
35. Ternary Diagram of Thorogummite Showing Small Amounts of Ca and REE in Comparison to the Th Content .....	85
36. Ternary Diagram of Thorogummite Showing no HREE and Th Dominant Over LREE.....	86
37. Major Element Harker Diagrams.....	99
38. Trace Element Harker Diagrams .....	102
39. Rb versus Sr Variation Diagram .....	110
40. K <sub>2</sub> O and CaO versus Rb and Sr Variation Diagrams.....	111
41. Eby Ternary Diagram Showing Likely Origin for Host Rock.....	112
42. Pearce Tectonic Discrimination Diagram .....	113
43. Pearce Tectonic Discrimination Diagram .....	114
44. Pearce Tectonic Discrimination Diagram .....	115
45. Harris Ternary Diagram for Tectonic Discrimination .....	116
46. Spider Diagrams of Host Rock Normalized to Ocean Ridge Granites .....	117
47. Chondrite Diagram for Host Rock LREE .....	119

## Abstract

In the Mojave Pegmatite district, located in northwestern AZ, numerous pegmatites intrude syn- to post-collisional Paleoproterozoic granitic rocks. The slightly older Cerbat plutons are associated with the suturing of the Mojave and Yavapai terranes whereas Aquarius granites were emplaced during the Yavapai Orogeny as the sutured terranes docked with North America. A detailed study of 5 pegmatites shows that they are zoned with composite cores and contain REE minerals characteristic of NYF pegmatites. However, they exhibit characteristics atypical for NYF pegmatites including F depletion, white microcline, an absence of columbite and, in the Rare Metals pegmatite, have muscovite and beryl. With the exception of the Kingman pegmatite, they exhibit normal LREE-HREE distributions. The Kingman pegmatite is extremely LREE enriched, HREE depleted and exhibits an unusual Nd enrichment which, in some cases, is sufficiently high that allanite is Nd dominant, thus a new mineral species, allanite-Nd.

Key words: Mojave County, pegmatite, rare-earth-element, allanite

## **Introduction**

The Mojave County Pegmatite district is located 168 km southeast of Las Vegas, Nevada.

Pegmatites in this district are most well known for an abundance of radioactive, rare earth element (REE)-bearing minerals. The first published study was done in the early 1960's by Heinrich (1960), who described in detail the mineralogy and zonation of two pegmatites, the Kingman Feldspar Mine and the Rare Metals Mine. It was later discovered that the location of the Rare Metals Mine was incorrectly located in the literature which led to a several year search for the mine (Hanson et. al., 2007). After several failed attempts, the mine was eventually located with the help of a local collector, Jerry Baird.

This study represents the first detailed petrographic and geochemical study that encompasses all of the large REE-bearing pegmatites in the Mojave County Pegmatite District. This includes the Kingman Feldspar and Rare Metals Mine as well as three others, the Wagon Bow 1, 2 and 3 quarries. The objectives of the study include (a) collecting representative samples from each zone at each locality, (b) complete mapping of all pegmatite zones, (c) verifying the existence of a potentially new mineral, allanite-Nd, (d) analyzing all REE-minerals to determine composition and fractionation trends with respect to select REE's, and (e) examining whole rock and mineral species to determine the relationship between host rock and pegmatite.

## **General Geology**

The period between 1780 and 1650 Ma was one of major crustal growth in North America (Karlstrom and Bowring, 1988; Hoffman, 1988). In the southwestern United States, isotopic and geochronological data define three Paleoproterozoic crustal provinces, the Mazatzal, Yavapai, and Mojave (Fig. 1a) (Karlstrom and Bowring, 1993; based on Silver, 1965; Silver et al., 1977; Nelson and DePaolo, 1985; Bennett and DePaolo, 1987; Wooden et al., 1988). Of these three provinces, the only two relevant to this study are the Mojave and Yavapai provinces as the Kingman pegmatite lies in the Mojave province and the Rare Metals and all of the Wagon Bow pegmatite lie in the Boundary zone, a transitional zone that exhibits characteristics of both the Mojave and Yavapai provinces. Differences in Pb isotopic signatures, deformational styles and grades of metamorphism suggest that the Mojave and Yavapai provinces represent two separate terranes that were sutured together between 1740 and 1720 Ma (Figure 1b, Part A). Subsequently, between 1710 and 1685 Ma, these provinces were docked to terranes that are currently located in Colorado, thus becoming part of the North American continent (Figure 1b, Part B). (Duebendorfer et. al., 2001). While the eastern boundary of the Mojave Province is ill defined, Duebendorfer et al. (2001) suggest that the eastern edge of this province corresponds to the eastern edge of the Boundary zone (Figure 1a). Differences in Pb isotopic signatures between the Mojave and Boundary zones are attributed to isotopic mixing during modification of the eastern margin of the Mojave province either prior to, or during juxtaposition of the two provinces.

The Mojave Province, is composed predominantly of recycled crustal material.

Conversely, the Yavapai province is composed of a series of tectonic blocks composed largely of island arc and associated marginal basin material. The Boundary zone shows mixed affinities with areas preexisting continental crustal material that are separated by juvenile material that was added during extension prior to the juxtaposition of the two terrane (Figure 1c).

Pegmatites are classified into two groups on the basis of trace element abundances (Černý, 2005; Wise, 1999). Enriched in Li, Cs and Ta, LCT type pegmatites are generally associated with orogenic granites. NYF pegmatites, enriched in Nb, Y and F, are generally associated with rift zones. Typically pegmatites that are enriched in REE elements fall into the NYF category. However, the mineralogy of the Mojave pegmatites does not correspond to typical NYF pegmatites as all are F poor and the Kingman Feldspar pegmatite is extremely LREE enriched and HREE are nearly absent.

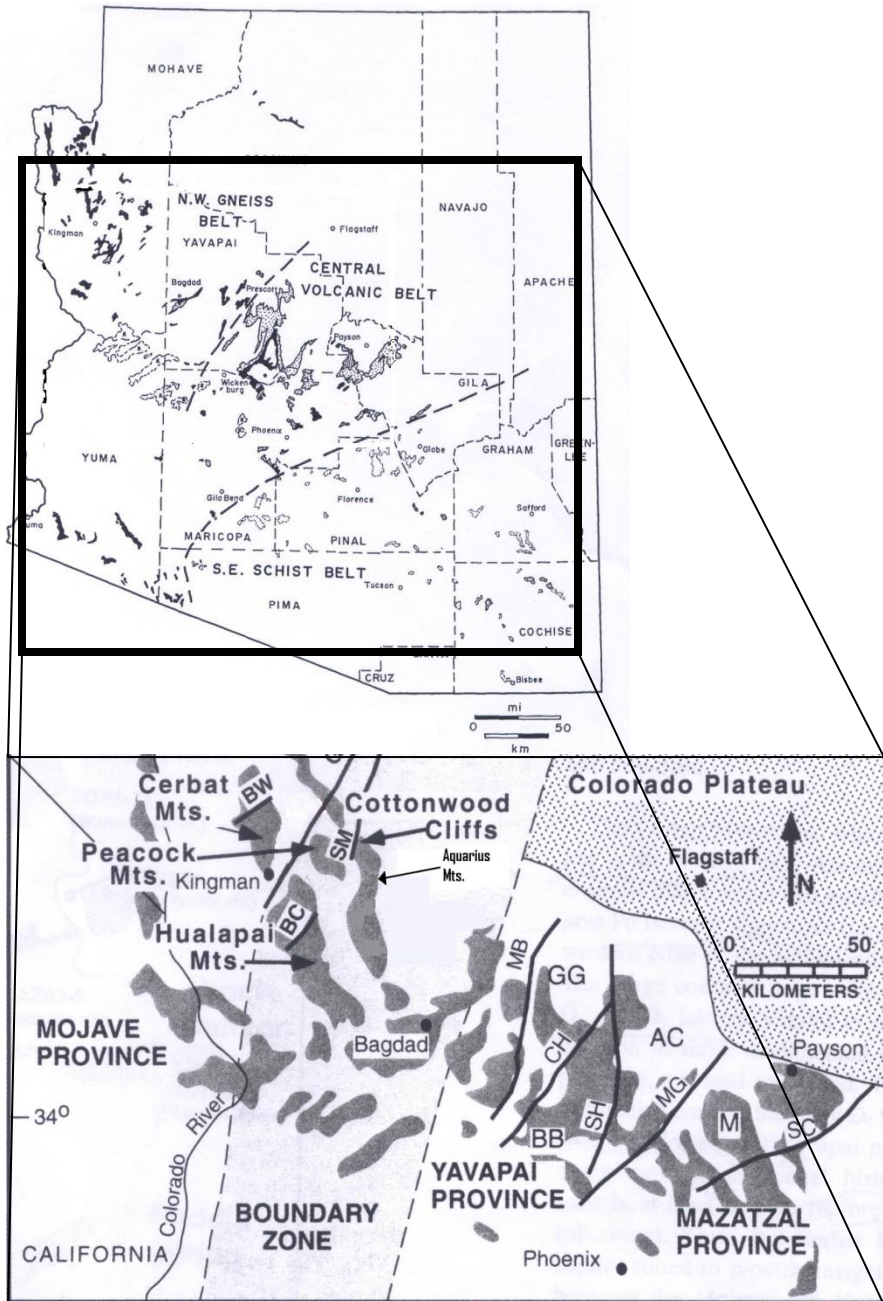
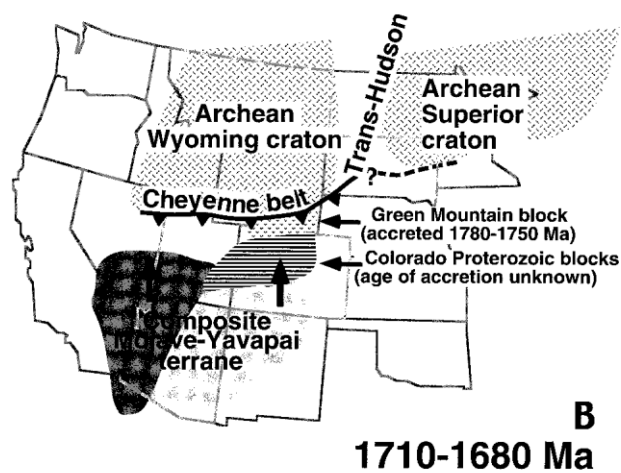


Figure 1a. Arizona state map, modified from Anderson (1989), with study area pulled out, modified from Duebendorfer (2001)

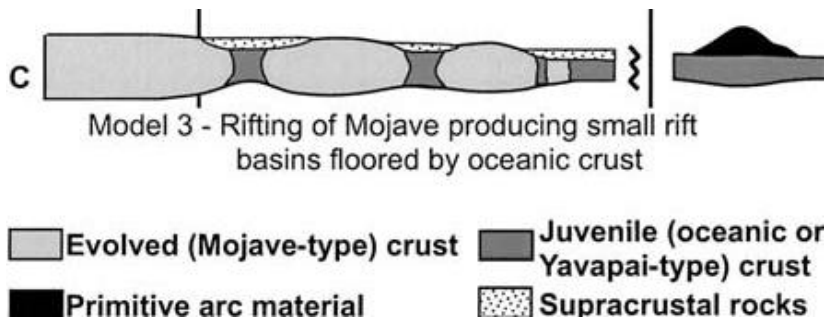


**A**  
1740-1720 Ma



**B**  
1710-1680 Ma

Figure 1b. Part A (top) shows the Mojave and Yavapai terranes suturing together. Part B (bottom) shows the amalgamated terranes docking with North America (Duebendorfer et al., 2006)



**C**  
Model 3 - Rifting of Mojave producing small rift basins floored by oceanic crust

Evolved (Mojave-type) crust	Juvenile (oceanic or Yavapai-type) crust
Primitive arc material	Supracrustal rocks

Figure 1c. Proposed rifting model to explain the origin of the pre-collisional crust of the Boundary Zone. Modified from Duebendorfer (2006)

## Cerbat Mountain Range

The southernmost portion of the Cerbat range, just north of Kingman, Arizona, extends northward for roughly 55 km (Fig. 2). It lies in the easternmost portion of the Mojave province as determined by Pb isotopic signatures (Duebendorfer et. al., 2001). Two periods of granulite facies metamorphism associated with the two docking episodes described above produced a series of discontinuous metasedimentary and metavolcanic rocks. Intruding into these Precambrian metamorphic rocks are a series of Paleoproterozoic Laramide stocks and dikes. These igneous rocks account for upwards of 80% of all the exposures in the range. Some of these rocks are covered by more recently eroded debris. The Paleoproterozoic rocks are further intruded by a late Cretaceous granite stock (Duebendorfer et. al., 2001). It is noteworthy to point out that no Paleozoic strata have been identified in the range. The entire complex of intruding granites and dikes is batholithic in size and resides in an up thrown fault block that is tilted 15° eastward (Wolfhard, 1984; Duebendorfer et. al., 2001). In the western portion of the range, the granite is gneissic in texture and contains three distinct granitic intrusions, the Diana, Chloride and Big Wash granites (Duebendorfer et. al., 2001). Based on Pb/U age dates the Chloride is  $1721 \pm 2$  Ma, the Diana is  $1719 \pm 1$  Ma. and the Big Wash granite is  $1737 \pm 4.3$  Ma (Duebendorfer et. al., 2001). In the northern portion of the Cerbat range, older successions of steeply dipping layers of hornblende-diopsidic schist, amphibolites, biotite schist and quartzite are exposed. Based on relict bedding in the quartzite and the disposition of the layered rocks in large folds, they represent a series of stratified deposits. Also in the northern portion is the Water Tank granite ( $1768 \pm 5.5$  Ma), which contains inclusions of foliated amphibolite (Duebendorfer et. al., 2001). In the eastern central portion of the range a series of  $1682.5 \pm 2.3$  Ma granite dikes are exposed in Vock Canyon (Duebendorfer et. al., 2001). The very southern and eastern

portions of the range is covered by Miocene volcanic, including the  $18.5 \pm 0.2$  Ma Peach Springs tuff (Nielson et. al., 1990) that range between felsic and intermediate in composition (Duebendorfer et. al., 2001). The Kingman Feldspar pegmatite is exposed in the southeastern Cerbat Mountain Range (Figure 3), just north of the Miocene volcanics.

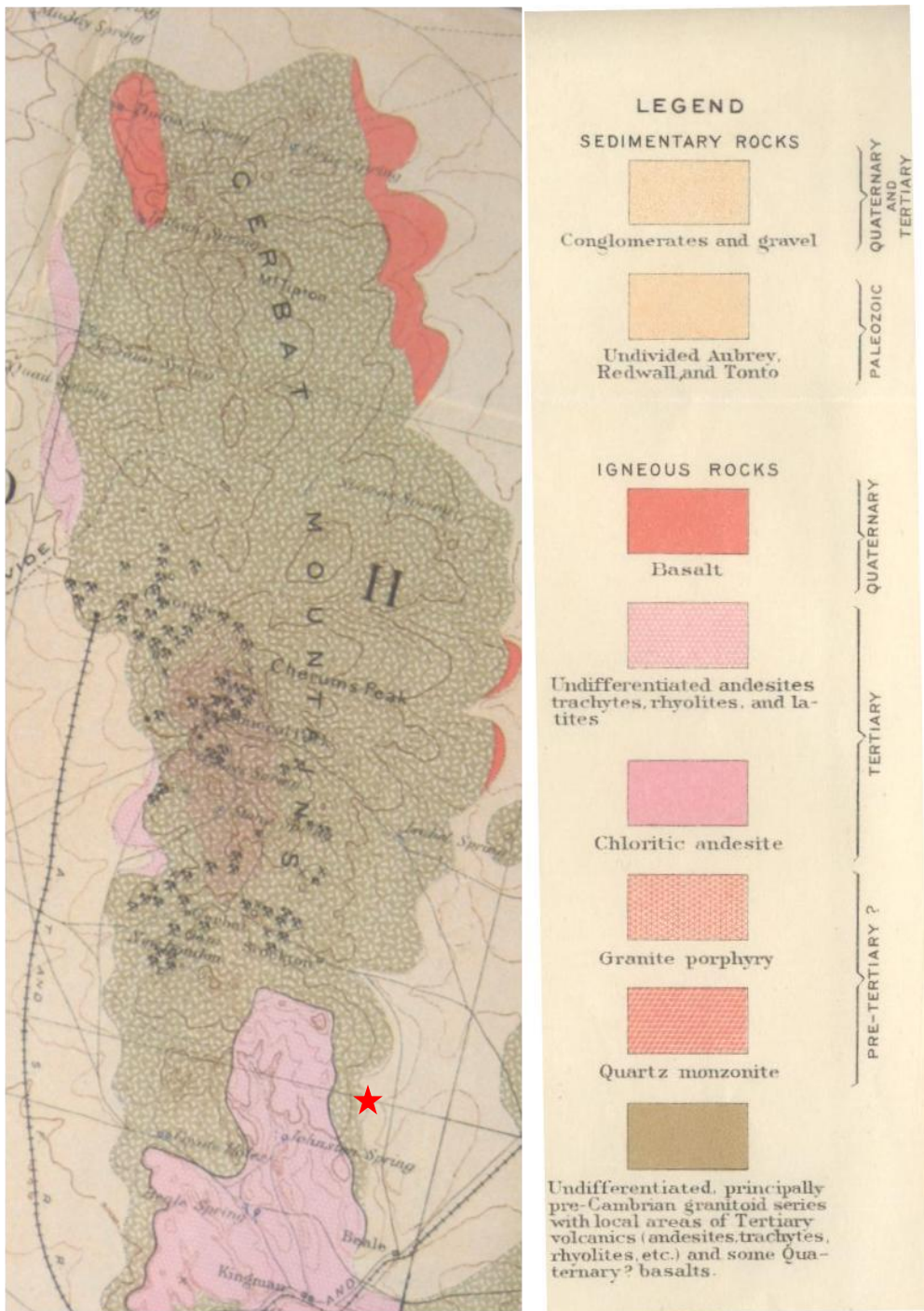


Figure 2. Geologic map of the Cerbat Mountain range. Scale: 1 in. = 4 miles. Modified from Schrader (1909). The star shows the location of the Kingman Feldspar mine.

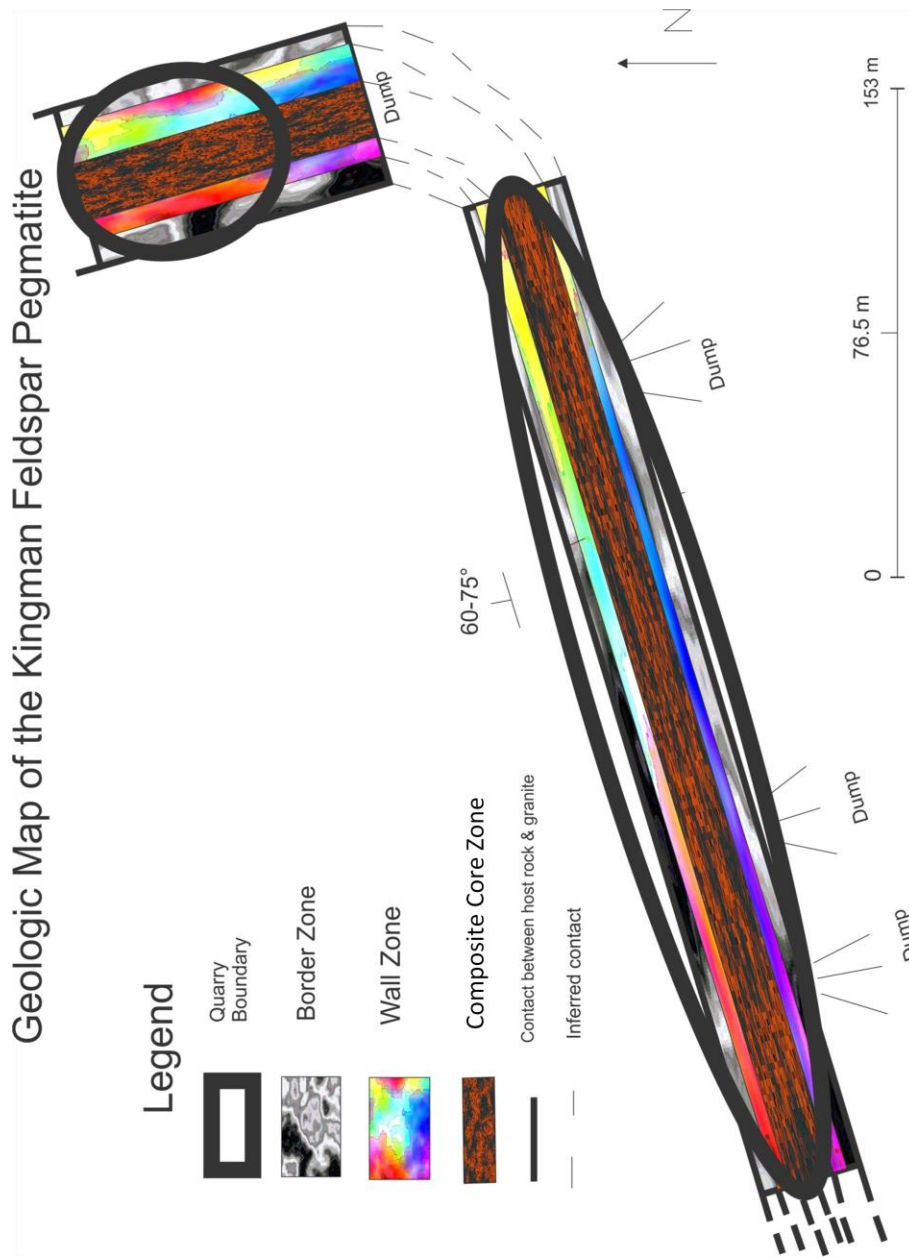


Figure 3. Idealized geologic map of the Kingman Feldspar

## **Kingman Feldspar Quarry Pegmatite**

The Kingman Feldspar Pegmatite is located at 35° 16'6.71"N, 114° 3'34.68"W. It crops out 8 km north of Kingman at the south eastern tip of the Cerbat Range and is only accessible through washed out jeep trails (Figure 2. Red star).

This large pegmatite is hosted by a coarse to medium grained granite that locally exhibits a well developed gneissic texture and, in other locations a porphyritic texture with 1.2 cm megaphenocrysts of potassium feldspar (Heinrich, 1960). Contacts between the pegmatite and the wall rock are well defined and, in some locations, exhibit significant reaction boundaries (~1/3 m wide) in the granite. Near the northern end of the pegmatite there are several roof pendants of gneissic metamorphic rocks exposed within the granite and pegmatite. Additionally, there is an almost horizontal diabase dike, 0.1-0.6m thick exposed in this northernmost portion of the quarry. The only unweathered granite in the area was exposed by mining at the southernmost end of the quarry.

The Kingman pegmatite is the largest pegmatite included in this study, is 460 m in length and ranges in thickness from 20 to 60 m. This sill-like body trends N50-65°E and dips 60-75°NW (Heinrich, 1960). Much of the pegmatite material was mined circa 1950's for feldspar, in some places down to the country rock leaving behind only minimal exposures of the wall zone and little of the core zone. The mining process has left the pegmatite exposed in three separate cuts, herein referred to as cuts A, B and C with A being the northernmost cut and C the southernmost.



Figure 4. Satellite image of Cut A in the Kingman pegmatite.

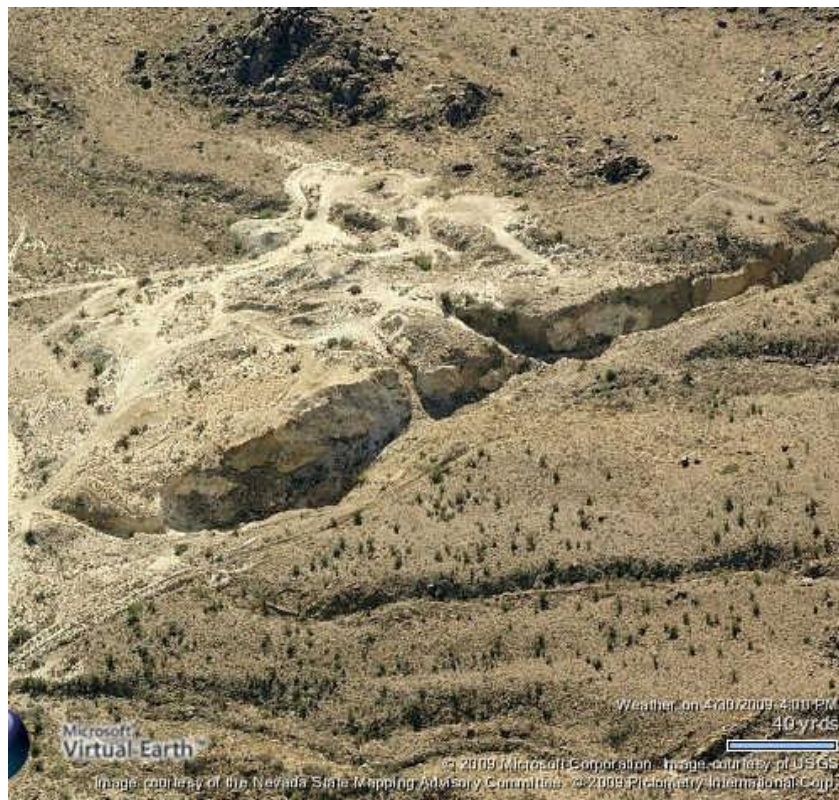


Figure 5. Satellite image of Cuts B and C in the Kingman pegmatite.

This pegmatite exhibits several characteristics that are not typical of NYF pegmatites. It is HREE, F and Nb depleted and microcline in the core and wall zone is very light in color, nearly white in some places. This is unusual for NYF pegmatites as microcline in others such as the in the Wausau Complex, Wisconsin, and the South Platte district, Colorado, are shades of pink and red (Falster et. al. 2000, Simmons & Heinrich, 1980).

#### *Border Zone*

The border zone is a thin discontinuous layer 0.1-0.5 m thick, and is composed entirely of microcline and fine grained quartz. The overall appearance of the zone was white with an aplitic texture throughout.

#### *Wall Zone*

The wall zone ranges in thickness from 3 to 6 m with an average of approximately 4 m. It is comprised mainly of quartz, white microcline and biotite. The most abundant accessory mineral, allanite occurs as large pods up to 0.4 m in diameter. Heinrich (1944) stated that during one excavation 20 tons of allanite were sent off to an unknown buyer in 1944. Thorogummite inclusions are occasional in the allanite. Other accessory minerals include magnetite, zircon, titanite, bastnaesite, synchisite, uraninite, apatite, hematite, ilmenite and rutile. In cut A only, small amounts of muscovite and several mm sized garnet are present as well as hematite and titanite. In some areas of the wall zone there are 2-5 mm quartz veinlets cutting across the zone. Most of the wall zone has a somewhat layered appearance that is parallel to the border zone and host rock contacts.

#### *Composite Core*

The quartz-microcline composite core ranges in thickness from 10-60 m with microcline masses averaging 3-4 m across (Heinrich, 1960). Heinrich also reported pods of grey quartz,

while less abundant than the microcline, reached 1.5 m X 2 m X 4.5 m. Stringers of quartz from these pods cut through the large microcline masses.

### **Aquarius Mountain Range**

The Aquarius Range lies in the Boundary zone between the Mohave and Yavapai provinces as described by Duebendorfer et. al., (2001). It extends from the Mohon mountains in the east to the Big Sandy Valley in the west. Its northern boundary is Trout Creek and terminates to the south at Burro Creek (Fig 1.). The Aquarius cliffs, which mark the western front of the Aquarius Range, represent the location of a normal fault that uplifted the range during Basin and Range extension. Thus the Aquarius Range is a large up-thrown fault block. This ridge is composed of Precambrian and younger granitic rocks that exhibit a northward trending fracture pattern. Also, exposed along the cliffs are numerous aplite and pegmatite dikes. Many of these dikes, the Rare Metals and three Wagon Bow pegmatites were evaluated in this study, have quartz veins associated with them. To the south and east, this granite is overlain by a thick series of Tertiary volcanic basalt flows that covers more than 1000 sq miles (Wilson, 1941).

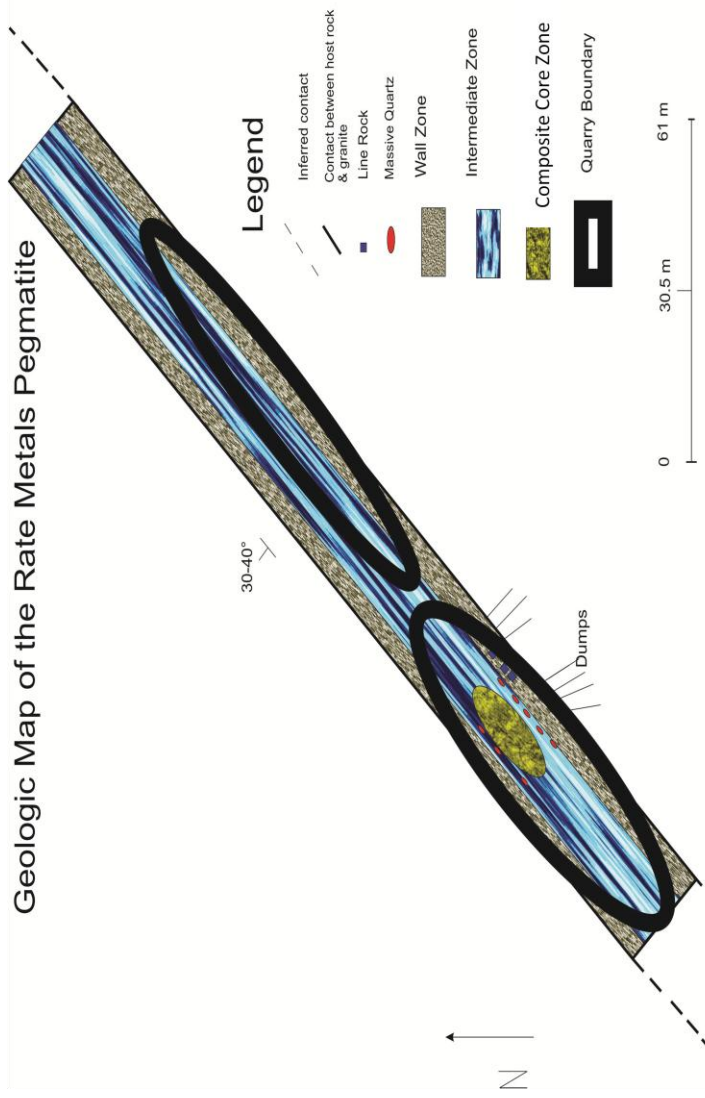


Figure 6. Idealized Geologic map of the Rare Metals Pegmatite

## Rare Metals Pegmatite

The Rare Metals pegmatite (Figure 6) is located at 34° 50'27.00"N, 113° 33'16.00"W. It outcrops on a ridge top just above an arroyo that, when wet, is tributary to the Big Sandy River. This pegmatite is only accessible through rough trails and a quarter mile hike through scrub brush.

This pegmatite intruded into a coarse grained peraluminous granite that contains small segregations of intergrown quartz and grey muscovite along with minor amounts of biotite and plagioclase. The contact, where exposed is sharp and shows no significant reaction boundaries. Locally present within the pegmatite are blocky xenoliths of altered granite that range in size from 10-20 cm in length and 8 cm thick. These xenoliths contain primarily muscovite, quartz and feldspar. Several pits have been cut laterally through the pegmatite at different locations along the length of the dike.

The Rare Metals pegmatite is a medium sized pegmatite, 183 m in length and ranges in thickness from 0.5 – 12 m. This dike strikes between N82-85°E and dips 30-40°NW. There are reports of large amounts of minerals removed during the mining process; 7-8 tons of yttriotantalite ore, 6 tons of beryl, some bismuth minerals, small amounts of monazite and gadolinite (Heinrich, 1960). However, a reevaluation of the original Heinrich samples by Hanson et al. (2007) has shown that the samples originally thought to be yttriotantalite are euxenite-(Y) and polycrase-(Y), some with intergrowths of betafite. Additionally, one of the samples appears to be a mixture of betafite and possibly fergusonite. The identity of monazite was confirmed and was shown to be Ce-dominant thus is monazite-(Ce) (Hanson, 2007). No gadolinite or bismuth minerals were located either in this study or the Hanson (2005; 2007) studies so the presence of these mineral remains unconfirmed.

This pegmatite also does not lie distinctly in the NYF field as F is notably absent. Additionally, microcline from this quarry, like microcline from the Kingman mine, exhibits the unusual, nearly white color.

#### *Wall zone*

The wall zone ranges in thickness from 3-5 m with an average thickness of approximately 4 m. It is comprised entirely of coarse and medium grained quartz, white feldspar, grey to green muscovite and garnet. The contacts where the wall zone and the host granite meet are poorly exposed and those that are exposed are generally weathered.

#### *Intermediate zone*

The intermediate zone ranges in thickness from 1-3 m and is comprised primarily of quartz and feldspar. Accessory minerals include; monazite, hematite, biotite, muscovite, and beryl. Albited replacement units are present within the intermediate zone at the core-intermediate zone boundary on the footwall side of the core. In addition to albite, they contain several REE bearing minerals including euxenite-(Y), polycrase-(Y), betafite and possibly fergusonite (Hanson et. al., 2007).

#### *Composite Core*

The composite core averages 6 m in thickness and 18 m in length and is comprised of quartz and microcline. Marginal to both sides of the core are scattered muscovite pods and beryl crystals (Heinrich, 1960). Heinrich also stated that on either side of the main core smaller pods of massive quartz and 1-2 m long microcline were present.

#### *Line Rock*

The line rock, a discontinuous unit, measured 1.8 m thick and had a fine-grained, aplitic texture. The unit is comprised of sugary textured quartz, blue-green muscovite and white albite. This line rock is formed by alternating bands of muscovite and albite that formed during the crystallization process. This has resulted in a wavy, banded look throughout this unit. While a local mine operator reported 12 pound masses of gadolinite were removed from this line rock in the 1950's (Heinrich, 1960), no gadolinite was recovered at the time of this expedition or by Heinrich in 1955 thus, the presence of gadolinite cannot be confirmed.



Figure 7. Line rock from Rare Metals Mine showing the scallopy, wavy, pattern.



Figure 8. Idealized Geologic map of the Wagon Bow #3 Pegmatite.

## **Wagon Bow Pegmatites**

The Wagon Bow Pegmatites, three included this study, are located in the general area of  $34^{\circ} 91'4.92''\text{N}$ ,  $113^{\circ} 52'3.85''\text{W}$ . The 3 pegmatites, herein referred to as Wagon Bow #1, #2 and #3 (Figure 8), are all located within a few kilometers of each other (Figure 9). Each pegmatite was sampled and analyzed but only #3 was mapped and extensively sampled. This is because Wagon Bows #1 and #2 are poorly exposed. Wagon Bow #1 has only a small quarry and #2 has only a prospect pits cut into the pegmatite.

The Wagon Bow #3 pegmatite, the smallest pegmatite in the study, intrudes into fine grained granite which is composed of quartz, biotite and feldspar up to 1.5 cm. Contacts with the wall zone are only exposed on the southwestern edge of the pegmatite and are sharply defined. No reaction boundaries with the host rock are evident.

This tabular pegmatite has an average thickness of 9 m and measured approximately 100 m in length. The pegmatite strikes  $295^{\circ}$  and dips  $40\text{-}65^{\circ}$  NE. This pegmatite has undergone extensive mining and removal of most of the core and wall zone leaving only approximately 10 m of pegmatite unexposed. At least four small, 15 m, unexplored and pegmatites are found in the nearby vicinity, all with roughly the same attitude. Accessory minerals collected from the mine dumps include xenotime, monazite with xenotime inclusions and ilmenorutile with cassiterite inclusions (Hanson et. al, 2005).

Like the Kingman Feldspar and Rare Metals pegmatites, the Wagon Bow pegmatites are F poor with white microcline, features that are atypical for NYF pegmatites.



Figure 9. Satellite image of the three Wagon Bow pegmatites. Provided by Google.

#### *Wall zone*

The wall zone varies in thickness from 1-2 m and is composed of massive feldspars and minor amounts of REE-bearing minerals. Small pockets contained monazite crystals, some measuring up to 5-5.5 cm. These pockets on average contained 4-6 monazite crystals ranging in size from 3-5.5 cm. Accessory minerals include; epidote, hematite and goethite. Replacement units bearing HREE oxides are notably absent. While it is possible that they were completely removed during mining, this is unlikely as no HREE oxides were found in the dump material.

#### *Core zone*

The composite core of the pegmatite was 7-8 m thick and 60 m long, comprised of massive quartz and flesh-toned microcline with lesser amounts of muscovite near the margins.

#### *Line Rock*

Mining has exposed the line rock unit only along the southeastern end of the pegmatite where it is 1.4 m thick. This unit is comprised of grey muscovite, fine grained quartz and white albite. The fabric of this unit is distinct from the Rare Metals line rock as it exhibits a more linear layering which dips downward into the pegmatite (Figure 10).



Figure 10. Line rock from Wagon Bow #3, student for scale.

## **Petrography**

### **Host Rock**

All of the pegmatites are intruded into granitic rocks with the composition and texture of these host rocks different for each of the pegmatites in the Cerbat and Aquarius ranges. The Kingman pegmatite is hosted by coarse grained, biotite-rich quartz diorite, the Rare Metals pegmatite intrudes into coarse-grained granite and the Wagon Bow series intrudes into locally weathered medium-grained granite. Also recovered from the Wagon Bow series, pegmatite #1, were pieces from a boulder of spotted granite.

#### *Quartz Diorite*

In the Cerbat range, the porphyritic quartz diorite (Figure 11) was recovered from several locations around the Kingman pegmatite. This mesocratic quartz diorite is metaluminous, although nearly peraluminous, exhibits a coarse grained, porphyritic texture with approximately 30% subhedral feldspar megaphenocrysts up to 7 cm. The ground mass is holocrystalline, hypidiomorphic and is composed entirely of medium grained (<2 mm) material which consists entirely of subhedral biotite, subhedral microcline, anhedral quartz and plagioclase. This quartz diorite shows severe discoloration where it meets the wall zone of the pegmatite, ranging from a bluish in color closest to the pegmatite contact and becoming deep orange further away. The gradation in color from the contact to unaltered granite averages 33 cm across. The unaltered gneiss-like granite exhibits a mesocratic, coarse grained, phaneritic texture and is hypidiomorphic with several millimeter grains of subhedral biotite, microcline, plagioclase and quartz.

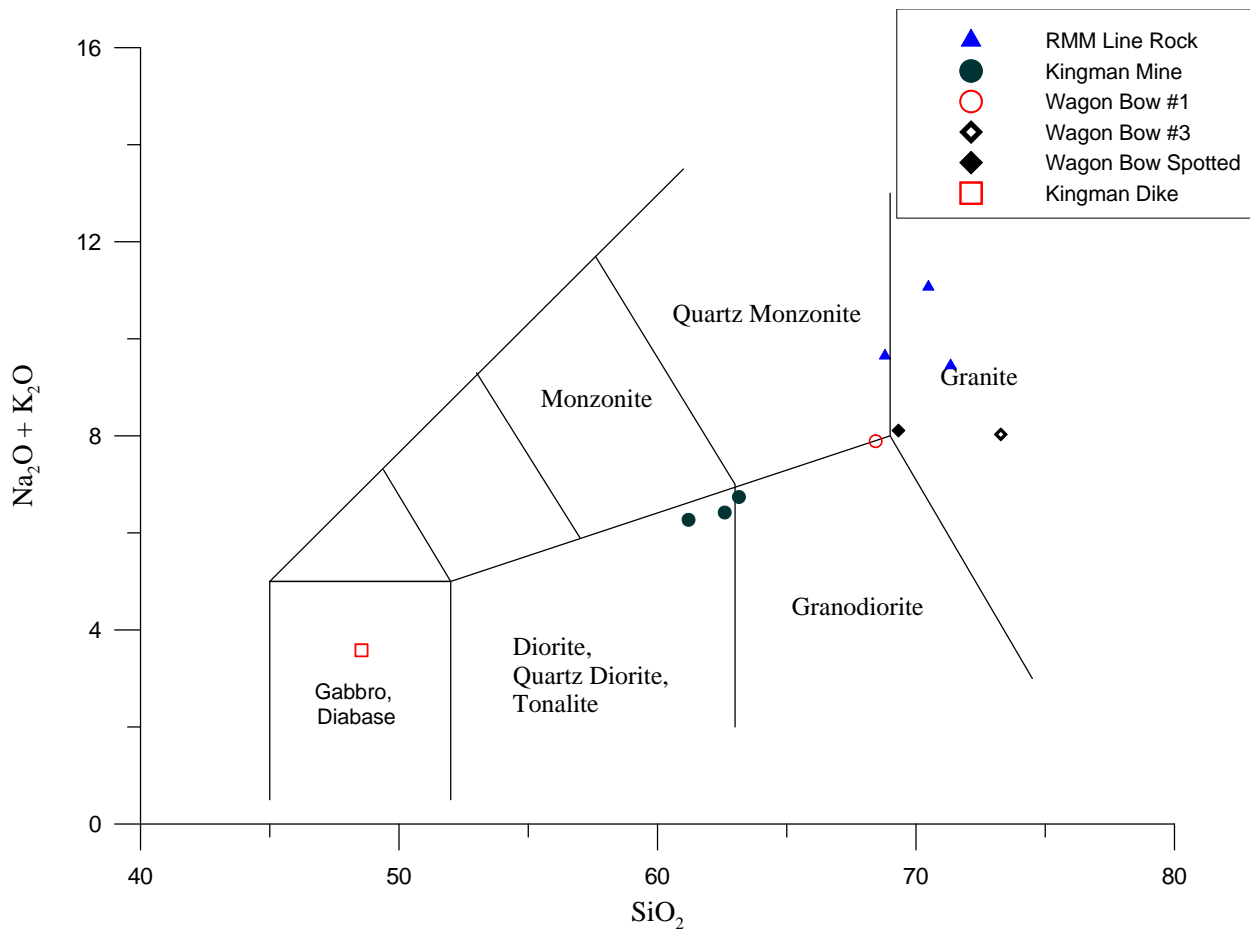


Figure 11. Total alkali versus silica diagram showing the proper names for the host rocks and pegmatite samples. Modified from Le Maitre, (1989).

### *Granite*

The granite into which the Rare Metals pegmatite is intruded is mildly peraluminous, leucocratic, holocrystalline and exhibits a coarse grained, phaneritic texture. It is hypidiomorphic and is composed of subhedral microcline, euhedral muscovite, subhedral plagioclase and anhedral quartz with all grains averaging ~1 mm. This granite contains small pods of muscovite which is intergrown, in some places, with quartz and minor amounts of biotite and plagioclase. The presence of muscovite suggests that this granite is peraluminous. Unlike granite at the Kingman Feldspar mine, contacts with the wall zone show no significant reaction boundaries.

The Wagon Bow pegmatites all intrude compositionally and texturally similar mildly peraluminous granite. This leucocratic granite is holocrystalline and exhibits a medium grained texture. It is hypidiomorphic with subhedral quartz, euhedral biotite, subhedral plagioclase and subhedral. The contacts with the wall zone are only seen on the southwestern end and, where exposed, show sharp definition and no significant reaction boundaries.

A much darker spotted granite was found only in one boulder at the Wagon Bow #1 pegmatite (Figure 12). The overall appearance of the granite is somewhat reddish in color with white spots that average 5 cm in diameter and encompass approximately 25% of the rock. The granite straddles the boundary between granodiorite and quartz monzanite (Figure 11). The spots are mineralogically identical to the remainder of the rock and are likely the result of a lack of oxidation in these areas. This mesocratic granite as a whole is also medium-grained in texture. It is holocrystalline and is comprised of euhedral biotite, anhedral quartz, subhedral plagioclase and subhedral feldspar. It differs from the other granites in the area as a large amount of euhedral muscovite is present, which contains 154 ppm of Tl (Table 53). This boulder was probably moved during the mining process, thus the possible relationship to the pegmatite is impossible to ascertain.



Figure 12. Photo of spotted granite boulder at Wagon Bow #1, crazed short person for scale.

### Pegmatite

Altered granite xenoliths were present only in the wall zone of the Rare Metals pegmatite and averaged 40 cm in diameter. These xenoliths are holocrystalline, mesocratic, and exhibit a coarse grained phaneritic texture. The granite is composed of medium grained subhedral biotite, subhedral muscovite, medium to coarse-grained subhedral microcline and anhedral quartz resulting in a hypidiomorphic texture.

## Mineralogy

### **Microcline Feldspar**

Microcline,  $KAlSi_3O_8$ , is a major mineral in all of the pegmatites in this study.

The color of the microcline is variable and depends on the pegmatite zone in which it occurs.

Microcline in the core of the pegmatites are white in color, blocky in nature and, on average, about 1.8-2.4 m wide and 0.3 m thick. Border zone microcline is light grey in color and crumbly to the touch. The crumbly nature of this microcline is attributed to radiation damage caused by allanite and monazite that are included in microcline (Figure 13). This radiation damage has caused the microcline to become structurally unstable and damage patterns, or halos, can be seen clearly in the microcline. In thin section microcline exhibits grid-iron twinning and minimal inclusions (Figure 14).

The perthitic microcline (Figure 15a) was further examined using EMP and SEM analysis. Microcline host compositions are given in Table 1 and plagioclase exsolution lamellae compositions in Table 2, these compositions are representative analyses with the entire data set residing in Appendix I. Ions were calculated based on eight oxygen a.p.f.u. Both the host microcline and the plagioclase exsolution lamellae have a nearly ideal formula (Figure 16). The percentages of lamellae (Table 3) and blebs (Table 4) were determined in an effort to find the original composition of the host microcline (Table 5) as well as the temperature of exsolution. Both host and lamellae are near ideal, thus exsolution occurred at very low temperatures, perhaps as low as 200 ° C (Bowen & Tuttle, 1950). However, the slope of the solvus curve is very steep at these high Ab and Or values, thus even a small analytical or plotting error could yield a several hundred degrees variation in temperature (Figure 15b). For this reason this temperature is, at best, an estimate. In other samples, the plagioclase component in the microcline perthite is unusually high, possibly hinting at a late stage albitization.



Figure 13. Allanite in Microcline showing radial fracturing.

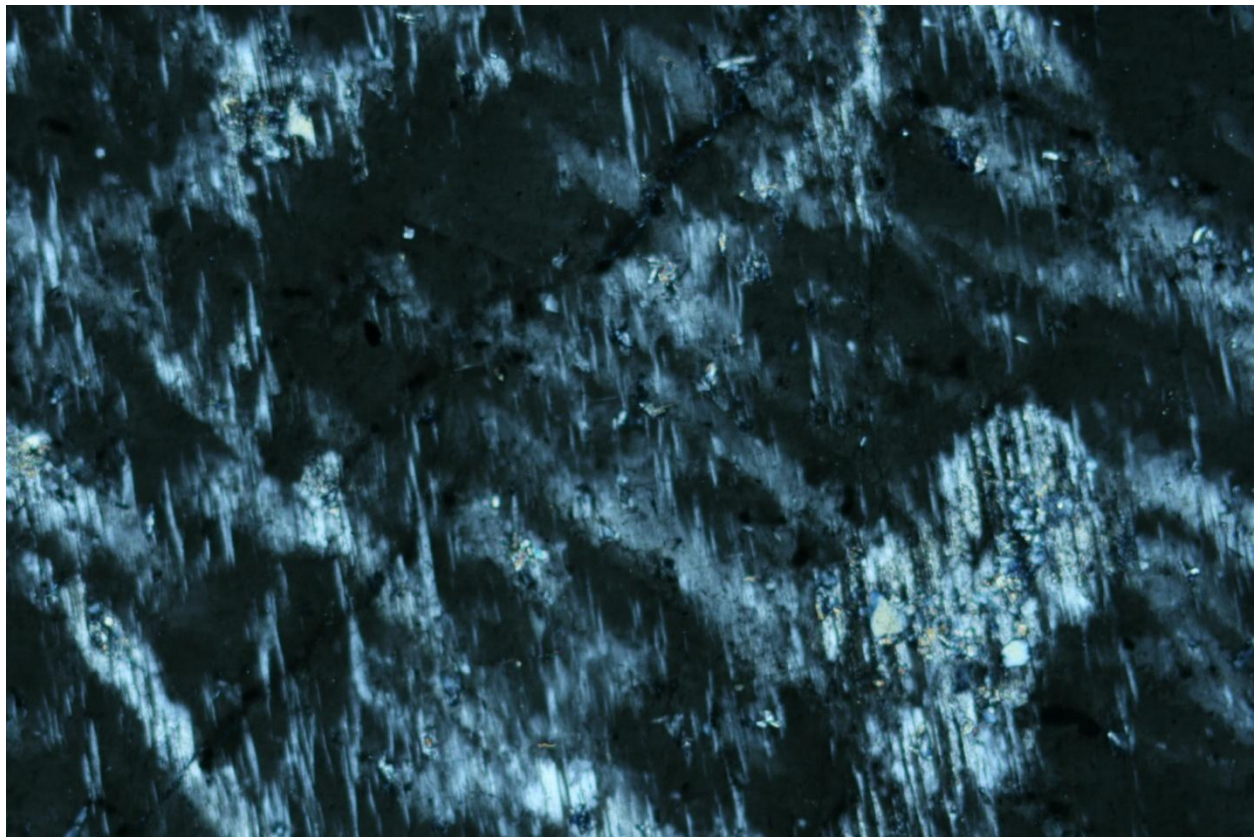


Figure 14. Thin section of feldspar from the Kingman Feldspar Mine, Cut B. Maximum dimension 2.5 mm.



Figure 15a. Photograph of massive feldspars found in the Kingman Feldspar Pegmatite, Cut B. Finger for scale.

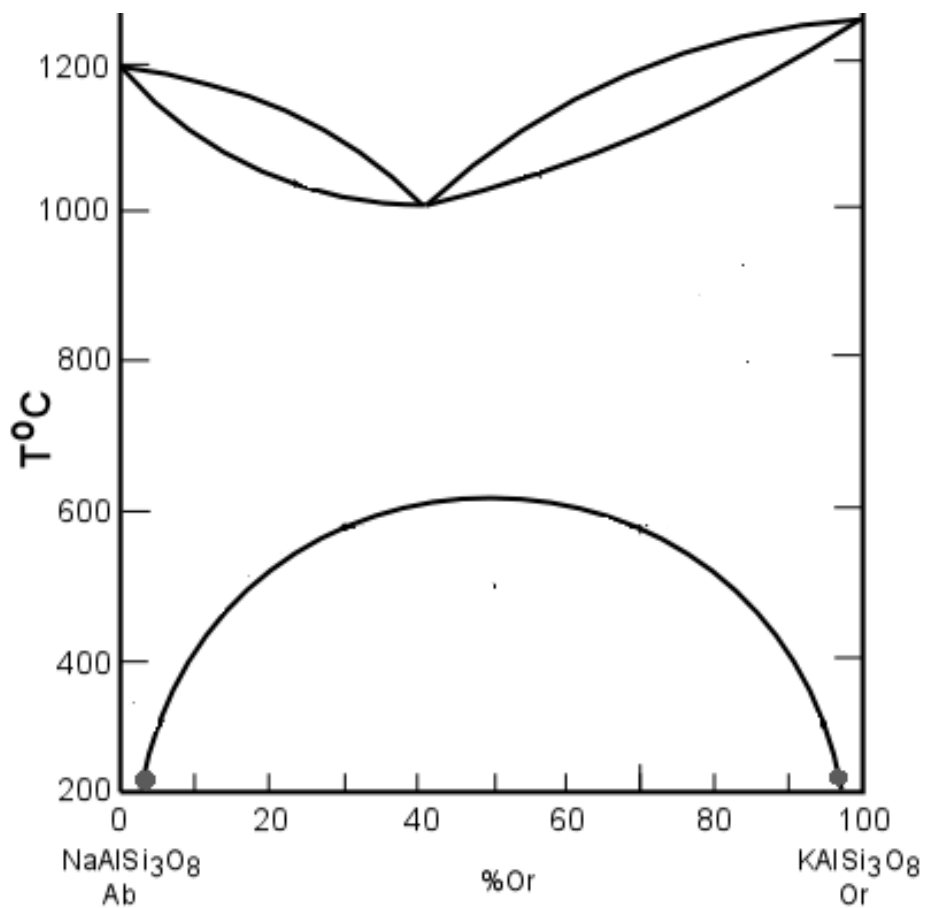
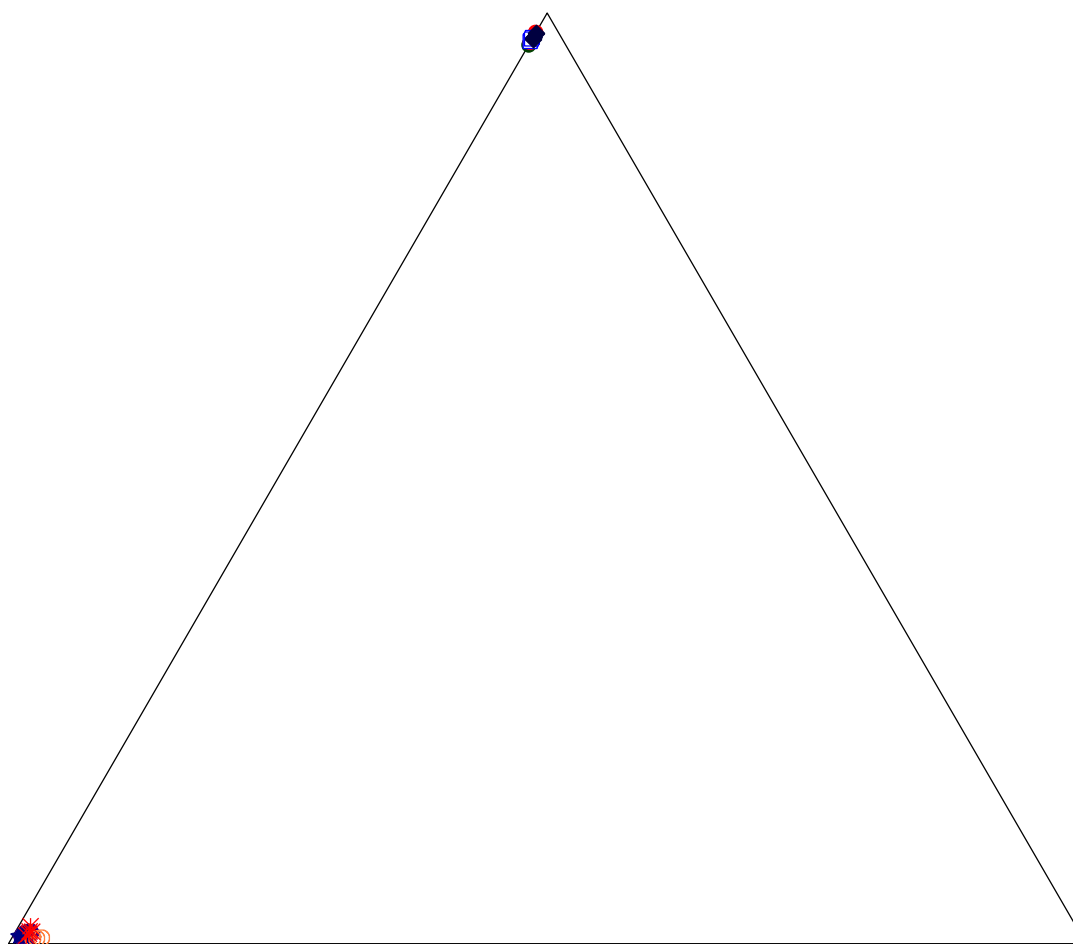


Figure 15b. Binary albite/k-feldspar phase diagram showing approximate host and lamellae compositions for Mojave County Pegmatite District perthite versus temperature

Table 1. Representative Chemical Composition of Microcline from the Kingman, Rare Metals and Wagon Bow Pegmatites

Oxides	Kingman Mine		Rare Metals Mine			Wagon Bow #2		Wagon Bow #3	
	KFM-entrance	KFM-site-X-8	RMMF-1	RMM-24-3	RMMF-4	WH2RAD-2	WH2RAD-4	WH-1-7	WH-1-9
SiO <sub>2</sub>	64.91	64.88	64.83	64.71	64.85	64.59	64.61	64.69	64.6
TiO <sub>2</sub>	0.01	0.01	0.01	0.01	0.01	0.01	0.01	0.02	0.01
Al <sub>2</sub> O <sub>3</sub>	18.34	18.3	18.39	18.35	18.36	18.41	18.66	18.3	18.32
MgO	0	0	0	0	0	0	0	0.01	0
CaO	0.04	0.02	0.02	0.02	0.03	0.02	0.02	0.03	0.03
MnO	0	0	0	0	0	0.01	0.01	0	0
FeO	0.01	0	0.02	0.01	0.02	0.03	0.04	0.02	0.01
Na <sub>2</sub> O	0.33	0.29	0.29	0.27	0.23	0.31	0.29	0.3	0.23
K <sub>2</sub> O	16.41	16.22	16.33	16.31	16.29	16.23	16.41	16.34	16.32
Rb <sub>2</sub> O	0.07	0.05	0.07	0.06	0.06			0.05	0.06
Total	100.12	99.76	99.94	99.74	99.83	99.61	100.05	99.76	99.57
Ions									
Ti	0	0	0	0	0	0	0	0.001	0
Mg	0	0	0	0	0	0	0	0.001	0
Ca	0.002	0.001	0.001	0.001	0	0.001	0	0.002	0.001
Mn	0	0	0	0	0	0	0	0	0
Fe 2+	0	0	0.001	0.001	0	0.001	0	0.001	0
Na	0.03	0.026	0.026	0.024	0.02	0.028	0.03	0.027	0.021
K	0.967	0.956	0.963	0.961	0.96	0.957	0.97	0.963	0.962
Rb	0.002	0.002	0.002	0.002	0	0	0	0.002	0.002
Σ X-Site	1.001	0.984	0.991	0.988	0.98	0.986	0.99	0.994	0.986
Σ Al	0.999	0.997	1.001	1	1	1.003	1.02	0.997	0.998
Σ Si	3	2.998	2.996	2.99	3	2.985	2.99	2.99	2.985
Anorthite	0.2	0.1	0.1	0.1	0.1	0.1	0.1	0.2	0.1
Albite	3	2.6	2.6	2.4	2.1	2.8	2.6	2.7	2.1
Orthoclase	96.8	97.3	97.3	97.5	97.8	97.1	97.3	97.1	97.7

## Potassium Feldspar & Plagioclase Orthoclase



Albite

Anorthite

### Legend

- Kingman K-Spar
- Rare Metals K-Spar
- Wagon Bow #2 K-Spar
- ◆ Wagon Bow #3 K-Spar
- Kingman Plagioclase
- ★ Rare Metals Plagioclase
- Wagon Bow #2 Plagioclase
- ✖ Wagon Bow #3 Plagioclase

Figure 16. Ternary diagram comparing orthoclase, albite, and Anorthite content for host microcline and plagioclase exsolution lamellae

Table 2. Representative Chemical Composition of Plagioclase Exsolution Lamellae from the Kingman, Rare Metals and Wagon Bow Pegmatites

Oxides	Wagon Bow #2			Kingman Mine			Wagon Bow # 3		Rare Metals Mine		
	WH2RAD-1	WH2RAD-5	WH2REC-2	KFM-entrance area-2	KFM-entrance area-5	KFM-site-X-2	WH-1-5	WH-1-3	RMM-24-7	RMMF-7	RMMF-10
SiO <sub>2</sub>	68.79	68.67	68.61	68.61	68.7	68.7	68.68	68.68	68.69	68.68	68.6
TiO <sub>2</sub>	0	0	0	0	0	0	0	0	0	0	0
Al <sub>2</sub> O <sub>3</sub>	19.34	19.44	19.51	19.44	19.58	19.47	19.31	19.33	19.44	19.47	19.55
MgO	0	0	0	0	0	0	0	0	0	0	0
CaO	0.48	0.54	0.4	0.16	0.28	0.26	0.26	0.23	0.23	0.22	0.12
MnO	0	0	0	0	0	0	0	0	0	0	0
FeO	0.01	0.02	0.01	0	0.01	0	0	0	0	0	0
Na <sub>2</sub> O	10.87	10.56	10.89	11.61	11.52	11.46	11.22	11.31	11.29	11.39	11.33
K <sub>2</sub> O	0.09	0.1	0.09	0.15	0.17	0.11	0.15	0.33	0.23	0.11	0.13
Total	99.58	99.34	99.52	99.96	100.25	99.99	99.62	99.89	99.88	99.87	99.73
Ions											
Ti	0	0	0	0	0	0	0	0	0	0	0
Mg	0	0	0	0	0	0	0	0	0	0	0
Ca	0.022	0.026	0.019	0.007	0.013	0.012	0.012	0.011	0.011	0.01	0.005
Mn	0	0	0	0	0	0	0	0	0	0	0
Fe 2+	0	0.001	0	0	0	0	0	0	0	0	0
Na	0.922	0.897	0.924	0.983	0.973	0.969	0.952	0.959	0.956	0.965	0.961
K	0.005	0.006	0.005	0.008	0.009	0.006	0.008	0.019	0.013	0.006	0.007
Σ X-Site	0.95	0.929	0.948	0.999	0.996	0.987	0.973	0.988	0.98	0.981	0.974
Σ Al	0.997	1.004	1.007	1.001	1.005	1.002	0.996	0.996	1.001	1.002	1.007
Σ Si	3.009	3.008	3.003	2.998	2.994	2.999	3.007	3.003	3.001	3	3
Anorhtite	2.3	2.7	2	0.7	1.3	1.2	1.2	1.1	1.1	1.1	0.6
Albite	97.1	96.6	97.5	98.5	97.8	98.2	97.9	97	97.6	98.3	98.7
Orthoclase	0.6	0.6	0.5	0.8	0.9	0.6	0.9	1.9	1.3	0.6	0.8

Table 3. Average Microcline Content from all Sampling Locations

	WB						
	Rare Metals		Wagon Bow 2		3	Kingman	
	RMMF	RMM24	WH2 REC	WH2 RAD	KFM WH1	ENT	KFMX
SiO <sub>2</sub>	64.87	64.77	64.55	64.60	64.65	64.90	64.81
TiO <sub>2</sub>	0.01	0.01	0.02	0.01	0.01	0.01	0.00
Al <sub>2</sub> O <sub>3</sub>	18.37	18.35	18.30	18.47	18.33	18.39	18.34
MgO	0.00	0.00	0.00	0.00	0.00	0.00	0.00
CaO	0.03	0.02	0.02	0.02	0.02	0.04	0.02
MnO	0.00	0.00	0.00	0.01	0.00	0.00	0.00
FeO	0.01	0.01	0.03	0.03	0.02	0.01	0.00
Na <sub>2</sub> O	0.31	0.29	0.34	0.31	0.26	0.31	0.31
K <sub>2</sub> O	16.32	16.27	16.23	16.30	16.30	16.33	16.30
Rb <sub>2</sub> O	0.06	0.06		0.05	0.06	0.05	
Total	99.98	99.78	99.50	99.75	99.65	100.04	99.84
Ions							
Ti	0.00	0.00	0.000	0.00	0.00	0.00	0.00
Mg	0.00	0.00	0.000	0.00	0.00	0.00	0.00
Ca	0.00	0.00	0.000	0.00	0.00	0.00	0.00
Mn	0.00	0.00	0.000	0.00	0.00	0.00	0.00
Fe 2+	0.00	0.00	0.000	0.00	0.00	0.00	0.00
Na	0.03	0.03	0.030	0.03	0.02	0.03	0.03
K	0.96	0.96	0.960	0.96	0.96	0.96	0.96
Rb	0.00	0.00	0.000	0.00	0.00	0.00	0.00
Σ X-Site	0.99	0.99	0.990	0.99	0.99	0.99	0.99
Σ Al	1.00	1.00	1.000	1.01	1.00	1.00	1.00
Σ Si	3.00	2.99	2.980	2.99	2.99	3.00	3.00
Anorthite	0.15	0.08	0.1	0.08	0.11	0.20	0.12
Albite	2.75	2.66	3.1	2.83	2.41	2.78	2.81
Orthoclase	97.10	97.27	96.8	97.09	97.48	97.03	97.07
% Feldspar	83.22	77.19	58.65	58.65	58.65	80.90	76.57

Table 4. Average Plagioclase Content from all Sampling Locations

	WB						
	Rare Metals		Wagon Bow 2		3	Kingman	
	RMMF	RMM24	WH2RAD	WH2RED	WH1	KFM ENT	KFM X
SiO <sub>2</sub>	68.62	68.71	68.73	68.61	68.69	68.64	68.69
TiO <sub>2</sub>	0.00	0.00	0.00	0.00	0.00	0.00	0.00
Al <sub>2</sub> O <sub>3</sub>	19.46	19.41	19.39	19.51	19.33	19.50	19.45
MgO	0.00	0.00	0.00	0.00	0.00	0.00	0.00
CaO	0.17	0.23	0.51	0.40	0.27	0.20	0.29
MnO	0.00	0.00	0.00	0.00	0.00	0.00	0.00
FeO	0.00	0.00	0.02	0.01	0.00	0.00	0.00
Na <sub>2</sub> O	11.36	11.33	10.72	10.89	11.25	11.57	11.36
K <sub>2</sub> O	0.15	0.22	0.10	0.09	0.20	0.18	0.14
Total	99.76	99.90	99.46	99.52	99.73	100.11	99.95
Ions							
Ti	0.00	0.00	0.00	0.000	0.00	0.00	0.00
Mg	0.00	0.00	0.00	0.000	0.00	0.00	0.00
Ca	0.01	0.01	0.02	0.019	0.01	0.01	0.01
Mn	0.00	0.00	0.00	0.000	0.00	0.00	0.00
Fe 2+	0.00	0.00	0.00	0.000	0.00	0.00	0.00
Na	0.96	0.96	0.91	0.924	0.95	0.98	0.96
K	0.01	0.01	0.01	0.005	0.01	0.01	0.01
Σ X-Site	0.98	0.98	0.94	0.948	0.98	1.00	0.98
Σ Al	1.00	1.00	1.00	1.007	1.00	1.00	1.00
Σ Si	3.00	3.00	3.01	3.003	3.01	3.00	3.00
Anorthite	0.82	1.07	2.55	2.0	1.28	0.95	1.39
Albite	98.34	97.70	96.86	97.5	97.59	98.04	97.81
Orthoclase	0.84	1.23	0.59	0.5	1.13	1.01	0.80
%							
Plagioclase	16.78	22.81	41.35	41.35	41.35	19.11	23.43

Table 5. Microcline and Plagioclase Reintegration Compositions

	RMMF	RMM24	WH2REC	WH2RAD	WH1	KFMENT	KFM x
SiO <sub>2</sub>	65.51	65.68	66.26	66.24	66.31	65.61	65.70
TiO <sub>2</sub>	0.01	0.01	0.01	0.01	0.01	0.01	0.00
Al <sub>2</sub> O <sub>3</sub>	18.56	18.60	18.75	18.89	18.74	18.60	18.60
MgO	0.00	0.00	0.00	0.00	0.00	0.00	0.00
CaO	0.05	0.06	0.22	0.17	0.12	0.07	0.09
MnO	0.00	0.00	0.00	0.00	0.00	0.00	0.00
FeO	0.01	0.00	0.02	0.02	0.01	0.01	0.00
Na <sub>2</sub> O	2.19	2.83	4.59	4.65	4.77	2.45	2.85
K <sub>2</sub> O	13.57	12.58	9.62	9.65	9.70	13.26	12.58
Rb <sub>2</sub> O	0.05	0.05	0.00	0.00	0.05	0.05	0.04
Total	99.94	99.80	99.49	99.71	99.66	100.05	99.86
Ions							
Ti	0.00	0.00	0.00	0.00	0.00	0.00	0.00
Mg	0.00	0.00	0.00	0.00	0.00	0.00	0.00
Ca	0.00	0.00	0.01	0.00	0.00	0.00	0.00
Mn	0.00	0.00	0.00	0.00	0.00	0.00	0.00
Fe 2+	0.00	0.00	0.00	0.00	0.00	0.00	0.00
Na	0.19	0.24	0.23	0.23	0.24	0.25	0.24
K	0.80	0.74	0.74	0.74	0.74	0.74	0.74
Rb	0.17	0.00	0.00	0.00	0.01	0.00	0.00
Σ X-Site	0.82	0.99	0.97	0.97	0.98	0.99	0.99
Σ Al	1.00	1.00	1.00	1.01	1.00	1.00	1.00
	0.00						
Σ Si	3.00	3.00	2.99	2.99	2.99	3.00	3.00
	0.00						
Anorthite	0.26	0.31	1.10	0.86	0.59	0.34	0.41
Albite	19.00	24.52	41.54	41.63	41.43	20.88	24.66
Orthoclase	80.74	75.18	57.36	57.51	57.97	78.78	74.92

## **Muscovite**

Muscovite,  $KAl_2AlSi_3O_{10}(OH)_2$  was only present in sufficient quantities to analyze at the Rare Metals Mine. It occurs in pods, up to 15 cm in length, and often was 5-10 cm thick (Figure 17). These pods most commonly occur in clusters of four or five. The individual flakes are metallic blue and, on average, about 10 cm in diameter. The muscovite pods occur marginally to the core on the south side, none are present on the north side as the core/wall zone boundary is still unexposed. Muscovite within the pods is associated with microcline, quartz, and small crystals of beryl and monazite. These pods appeared to be radioactive and exhibit radiation damage due to nearby monazite crystals.

The microprobe analyses were recalculated based on twenty oxygen a.p.f.u. and are found in Table 6. DCP analysis (Table 36) shows that the muscovite has a small amount of Rb (>500 ppm) along with a smaller amount (~250 ppm) of Li.

## **Biotite**

Biotite,  $K(Mg,Fe)_3AlSi_3O_{10}(OH)_2$ , was recovered in small quantities from each sampling locality at contact points with the host rock. These biotite flakes are black in color and averaged 2.5 cm in diameter. Though found in all locations, it was only recovered in large quantities in the Kingman Feldspar Quarry. In the other two pegmatites, biotite was only found during heavy mineral separations of material from the wall and border zones.

The microprobe analyses were recalculated based on twenty oxygen a.p.f.u. and representative data are presented in Table 7 with the entire data set in Appendix I. The low analytical totals, as well as low K values, for this biotite suggest that they are anhydrous. DCP analyses of Kingman biotite show that, as with the muscovite, it is enriched in Rb (>400 ppm). However, in contrast to the muscovite, Li values are much lower (~235 ppm) and also contains

small amounts of B (~6 ppm, Table 39) as well as the highest total of Ti with 21.2 ppm (Table 38).



Figure 17. Muscovite pods shown in the wall zone near the core zone, camera case for scale.

Table 6. Chemical Composition of Muscovite from the Rare Metal Pegmatite.

	RM1	RM2	RM3	RM4	RM5
<b>Oxides</b>					
SiO <sub>2</sub>	45.443	45.377	45.522	45.393	45.423
TiO <sub>2</sub>	0.234	0.254	0.244	0.264	0.269
Al <sub>2</sub> O <sub>3</sub>	36.366	36.465	36.384	36.411	36.432
FeO	3.677	3.77	3.83	3.823	3.734
MnO	0.045	0.038	0.033	0.042	0.043
MgO	0.544	0.563	0.609	0.562	0.555
CaO	0.023	0.042	0.032	0.019	0.022
Na <sub>2</sub> O	0.344	0.356	0.42	0.383	0.344
K <sub>2</sub> O	9.889	9.978	10.112	9.789	9.884
F	1.677	1.91	1.891	1.771	1.565
Subtotal	98.242	98.753	99.077	98.457	98.271
Less O=F	0.706101	0.804206	0.796206	0.74568	0.6589433
Total	97.5359	97.94879	98.28079	97.71132	97.612057
<b>Ions</b>					
Si	5.260309	5.228118	5.233901	5.245127	5.2600805
Al to A	2.739691	2.771882	2.766099	2.754873	2.7399195
Σ A-Site	8	8	8	8	8
Ti	0.020369	0.022007	0.021097	0.02294	0.0234255
Al to B	2.221951	2.180013	2.164506	2.204027	2.2326996
Fe 2+	0.711802	0.363197	0.368209	0.369371	0.3615615
Mn	0.10666	0.054935	0.059299	0.054996	0.0544299
Mg	0.007937	0.007213	0.005484	0.003272	0.0037974
Σ B-Site	3.06872	2.627364	2.618595	2.654607	2.6759139
Ca	0.085322	0.043943	0.051735	0.047413	0.0426778
Na	2.219232	2.228739	2.253966	2.192864	2.2189905
K	0.247605	0.280689	0.277318	0.261017	0.2311606
Σ C-Site	2.55216	2.553371	2.583019	2.501293	2.4928289
OH	2.772399	2.608373	2.625086	2.705907	2.8539313
F	1.227601	1.391627	1.374914	1.294093	1.1460687
Σ Hydroxyl	4	4	4	4	4

Table 7. Representative Chemical Composition of Biotite from the Wagon Bow #2, Rare Metals, and Kingman Pegmatite

Sample	Wagon Bow #2			Rare Metals Mine			Kingman Mine		
	WHM-2-4	WHM-2-5	B-1-D-1	RMM-3-1	RMM-3-2	RMM-3-3	D-4-D-1	D-4-D-2	D-4-D-3
SiO <sub>2</sub>	38.56	38.66	38.23	38.57	38.62	38.57	38.11	38.24	38.13
TiO <sub>2</sub>	2.78	2.94	3.13	3.02	2.98	3.01	2.92	2.79	2.92
Al <sub>2</sub> O <sub>3</sub>	14.34	14.53	14.25	14.32	14.29	14.41	13.83	13.78	13.87
SFeO	25.66	25.73	24.68	25.54	25.34	25.34	25.21	25.12	25.17
MnO	1.10	1.12	1.27	1.21	1.13	1.26	1.12	1.09	1.13
MgO	3.77	3.87	4.11	4.12	4.09	3.89	3.66	4.01	3.79
CaO	0.21	0.14	0.18	0.19	0.22	0.18	0.20	0.19	0.21
Na <sub>2</sub> O	0.31	0.29	0.21	0.30	0.28	0.31	0.18	0.18	0.19
K <sub>2</sub> O	7.89	7.80	6.77	7.05	7.23	7.66	7.00	6.34	6.22
F	0.98	1.02	0.63	0.89	1.09	1.01	0.56	0.51	0.52
Cl	0.02	0.03	0.01	0.01	0.03	0.02	0.01	0.02	0.01
Sub-Total	95.61	96.12	93.48	95.22	95.31	95.64	92.81	92.27	92.18
Ions									
Si	2.979	2.969	2.983	3.010	3.018	3.009	3.041	3.053	3.047
Al(iv)	0.984	1.031	1.017	0.990	0.982	0.991	0.959	0.947	0.953
Ti(iv)	0.000	0.000	0.000	0.000	0.000	0.000	0.000	0.000	0.000
Al(vi)	0.338	0.285	0.294	0.328	0.334	0.335	0.343	0.349	0.354
Ti(vi)	0.163	0.170	0.183	0.177	0.175	0.176	0.175	0.167	0.175
Fe <sub>3</sub>	0.332	0.331	0.322	0.067	0.066	0.066	0.067	0.067	0.067
Fe <sub>2</sub>	1.326	1.322	1.288	1.601	1.590	1.587	1.615	1.610	1.615
Mn	0.072	0.073	0.084	0.080	0.075	0.083	0.076	0.074	0.076
Mg	0.434	0.443	0.478	0.479	0.476	0.452	0.435	0.477	0.451
Vacancy(vi)	0.336	0.377	0.351	0.268	0.284	0.300	0.289	0.255	0.260
Sum Oct Cat	2.664	2.623	2.649	2.732	2.716	2.700	2.711	2.745	2.740
Ca	0.017	0.012	0.015	0.016	0.019	0.015	0.017	0.016	0.018
Na	0.047	0.043	0.032	0.045	0.042	0.046	0.028	0.028	0.030
K	0.778	0.764	0.673	0.701	0.721	0.762	0.713	0.646	0.634
Sum(A site)	0.842	0.818	0.721	0.762	0.781	0.823	0.758	0.690	0.682
F	0.240	0.247	0.156	0.220	0.270	0.250	0.140	0.130	0.132
Cl	0.003	0.004	0.001	0.002	0.004	0.002	0.002	0.002	0.002
OH	1.757	1.749	1.842	1.778	1.726	1.748	1.858	1.868	1.866
SUM Hydroxyl	2.000	2.000	2.000	2.000	2.000	2.000	2.000	2.000	2.000

## **Fe/Ti Oxides**

Magnetite ( $\text{Fe}^{2+}\text{Fe}_2^{3+}\text{O}_4$ ) and ilmenite ( $\text{Fe}^{2+}\text{TiO}_3$ ) were found only in the Kingman Feldspar Quarry whereas hematite ( $\text{Fe}_2\text{O}_3$ ) was found in all three pegmatites. Rutile ( $\text{TiO}_2$ ) was found at the Kingman Quarry and Wagon Bow 2 & 3. All four of these oxides were only found once the heavy mineral separation test was done on select specimens. All are anhedral and range in size from .5 to 1 cm.

The microprobe analyses were calculated using three oxygen apfu for ilmenite (Table 8), four for magnetite (Table 9), three for hematite (Table 10) and two for rutile (Table 11), the ilmenite and hematite tables are representative data sets with the entire data set in Appendix I. Magnetite, ilmenite and hematite are nearly ideal whereas rutile exhibits variable amounts of Fe substitution (Figure 18). This Fe substitution is particularly prominent for the Wagon Bow # 3 pegmatite where it is coupled with the REE substitution (Figure 19). The HREE was then compared to LREE content to determine which rutile would have a greater affinity for, which in this case was the HREE (Figure 20).

The Fe/Ti oxides all occur in the wall zones of their respective pegmatites and are associated with similar mineral assemblages and occasionally with each other. Hematite and ilmenite are most commonly associated with quartz, microcline and allanite. Magnetite is associated with quartz, microcline and biotite. Rutile is associated with quartz, microcline, biotite and muscovite.

Table 8. Representative Chemical Composition of Ilmenite from the Kingman Pegmatite

Oxides	KFMAX-3	B-3-A-2	B-3-A-5	B-4-B-1	B-4-B-1	B-4-B-2	B-4-B-3
WO <sub>3</sub>	0.02	0	0	0	0	0	0
Nb <sub>2</sub> O <sub>5</sub>	0.08	0.09	0.09	0.02	0.02	0.02	0.03
Ta <sub>2</sub> O <sub>5</sub>	0.01	0.01	0	0	0	0.01	0.02
TiO <sub>2</sub>	51.43	52.12	52.01	55.23	55.23	53.34	55.65
ZrO <sub>2</sub>	0.01	0	0	0	0	0	0
SnO <sub>2</sub>	0.21	0.07	0.09	0	0	0	0.01
ThO <sub>2</sub>	0.01	0	0	0	0	0	0
Al <sub>2</sub> O <sub>3</sub>	0.13	0.25	0.29	0.15	0.15	0.23	0.21
MgO	0.14	0.33	0.26	0.17	0.17	0.21	0.19
CaO	0	0.03	0.05	0	0	0.02	0.02
MnO	0.45	1.45	1.34	0.09	0.09	0.08	0.1
FeO	46.77	45.98	45.9	41.67	41.67	44.88	42.34
Total	99.99	100.34	100.03	99.99	99.99	99.99	100
Ions							
Mg	0.005	0.012	0.01	0.006	0.006	0.008	0.007
Mn	0.01	0.031	0.029	0.002	0.002	0.002	0.002
Fe 2+	0.978	0.968	0.969	0.82	0.82	0.919	0.852
Σ A-Site	0.993	1.011	1.007	0.828	0.828	0.928	0.861
W	0	0	0	0	0	0	0
Nb	0.001	0.001	0.001	0	0	0	0
Ta	0	0	0	0	0	0	0
Ti	0.967	0.986	0.987	0.978	0.978	0.982	1.007
Zr	0	0	0	0	0	0	0
Sn	0.002	0.001	0.001	0	0	0	0
Th	0	0	0	0	0	0	0
Al	0.004	0.007	0.009	0.004	0.004	0.007	0.006
Ca	0	0.001	0.001	0	0	0.001	0
Σ B-Site	0.991	0.994	0.996	0.982	0.982	0.988	1.013

Table 9. Chemical Composition of Magnetite  
from the Kingman Pegmatite

Oxides	KMB-X-M-1	KMB-X-M-2	KMB-X-M-3	KFMAX-5
TiO <sub>2</sub>	0.07	0.06	0.06	0.54
Al <sub>2</sub> O <sub>3</sub>	0.06	0.07	0.06	0.12
Sc <sub>2</sub> O <sub>3</sub>	0.07	0.08	0.07	0.08
Fe <sub>2</sub> O <sub>3</sub>	68.37	68.92	69.51	67.76
FeO	29.80	30.02	30.34	29.87
MgO	0.05	0.06	0.04	0.01
CaO	0.05	0.04	0.04	0.07
MnO	0.88	0.87	0.93	0.79
Total	99.28	100.12	101.05	99.24
Ions				
Mn	0.028	0.028	0.030	0.026
Ca	0.002	0.002	0.002	0.003
Fe <sup>2+</sup>	0.966	0.967	0.966	0.967
Mg	0.003	0.003	0.002	0.001
Σ A-Site	0.999	0.967	1.000	0.997
Ti	0.002	0.002	0.002	0.016
Sc	0.002	0.003	0.002	0.003
Fe <sup>3+</sup>	1.995	1.993	1.992	1.973
Al	0.003	0.003	0.003	0.005
Σ B-Site	2.002	2.001	1.999	1.99

Table 10. Representative Chemical Composition of Hematite from the Kingman Feldspar, Rare Metals, and Wagon Bow #2 & #3 Pegmatites

Oxides	Kingman Feldspar Mine			Wagon Bow #2			Wagon Bow # 3			Rare Metals Mine		
	KFMAA-3	KFMAA-4	KFMCM-1-5	S-2-A-3	S-2-A-5	WHM-1-1	WHM-1-1	WHM-1-2	RMM-4-3	RMM-4-4	RMM-4-5	
TiO <sub>2</sub>	0.00	0.00	0.12	0.03	0.04	0.00	0.00	0.00	0.21	0.23	0.11	
Al <sub>2</sub> O <sub>3</sub>	0.98	0.97	0.03	0.15	0.16	0.57	0.57	0.23	0.09	0.09	0.05	
Sc <sub>2</sub> O <sub>3</sub>	0.03	0.03	0.00	0.01	0.02	0.02	0.02	0.03	0.00	0.00	0.00	
Fe <sub>2</sub> O <sub>3</sub>	96.58	96.73	98.30	99.03	98.86	96.81	96.81	96.79	99.54	98.86	99.04	
MgO	0.00	0.02	0.01	0.02	0.04	0.00	0.00	0.02	0.00	0.00	0.00	
CaO	0.11	0.12	0.06	0.02	0.03	0.01	0.01	0.01	0.02	0.01	0.04	
MnO	0.11	0.14	0.06	0.52	0.63	0.22	0.22	0.20	0.09	0.15	0.15	
Total	97.80	98.01	98.59	99.83	99.78	97.62	97.62	97.27	99.94	99.34	99.39	
Ions												
Ti	0.000	0.000	0.002	0.001	0.002	0.000	0.000	0.000	0.008	0.009	0.005	
Al	0.031	0.031	0.001	0.005	0.005	0.018	0.018	0.007	0.003	0.003	0.001	
Sc	0.001	0.001	0.000	0.000	0.000	0.000	0.000	0.001	0.000	0.000	0.000	
Fe <sup>3+</sup>	1.964	1.964	1.993	1.944	1.934	1.952	1.952	1.968	1.973	1.968	1.975	
Mg	0.000	0.001	0.000	0.002	0.003	0.000	0.000	0.001	0.000	0.000	0.000	
Ca	0.003	0.004	0.002	0.001	0.002	0.001	0.001	0.001	0.001	0.001	0.002	
Mn	0.003	0.003	0.001	0.023	0.028	0.010	0.010	0.009	0.004	0.006	0.007	
Σ A-Site	2.002	2.002	2.000	1.978	1.974	1.981	1.981	1.987	1.989	1.987	1.990	

Table 11. Chemical Composition of Rutile from the Kingman and Wagon Bow Pegmatites

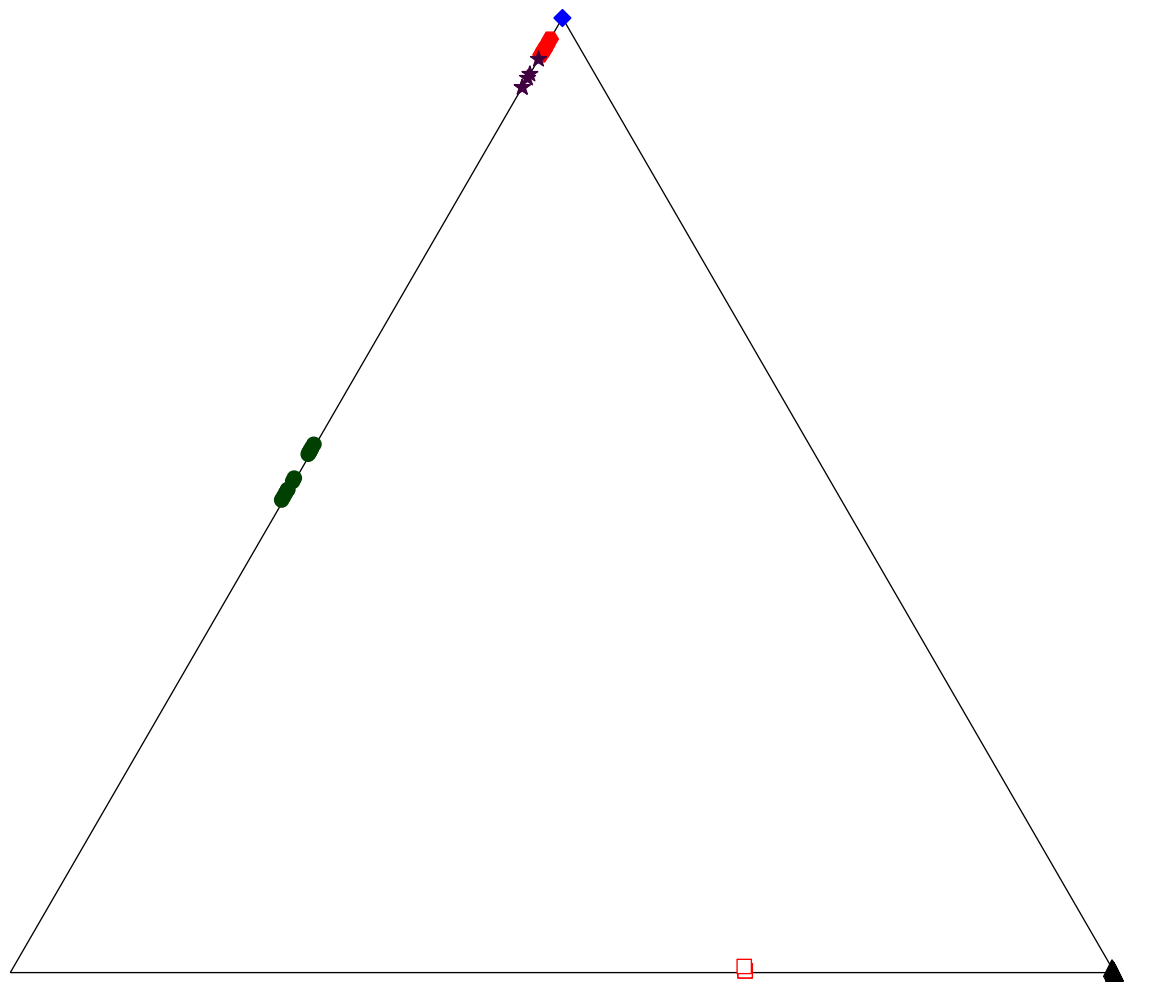
Oxides	Kingman Mine		Wagon Bow #3					Wagon Bow #2				
	KFMAX-1	KFMAX-2	WHRADS-1	WHRADS-2	WHRADS-3	WHRADS-4	WHRADS-5	S-6-B-1	S-6-B-2	S-6-B-3	S-6-B-4	S-6-B-5
Nb <sub>2</sub> O <sub>5</sub>	0.12	0.14	3.23	2.95	3.11	3.23	2.45	0.00	0.00	0.02	0.02	0.01
Ta <sub>2</sub> O <sub>5</sub>	0.02	0.03	1.11	0.93	1.46	1.21	1.85	0.00	0.00	0.00	0.00	0.00
SiO <sub>2</sub>	0.00	0.00	0.00	0.00	0.00	0.00	0.00	0.00	0.00	0.00	0.03	0.00
TiO <sub>2</sub>	98.69	98.54	79.02	79.56	77.66	80.57	81.12	93.03	95.57	93.00	92.63	93.00
ZrO <sub>2</sub>	0.01	0.02	0.01	0.00	0.00	0.00	0.01	0.00	0.00	0.00	0.00	0.00
SnO <sub>2</sub>	0.07	0.09	0.00	0.00	0.01	0.00	0.01	0.00	0.00	0.01	0.00	0.00
ThO <sub>2</sub>	0.01	0.01	0.00	0.01	0.00	0.02	0.00	0.00	0.00	0.00	0.00	0.00
Al <sub>2</sub> O <sub>3</sub>	0.15	0.09	0.11	0.10	0.09	0.10	0.09	0.01	0.09	0.06	0.03	0.04
Sc <sub>2</sub> O <sub>3</sub>	0.00	0.00	0.03	0.04	0.03	0.03	0.03	0.00	0.00	0.00	0.00	0.00
Y <sub>2</sub> O <sub>3</sub>	0.04	0.04	5.77	4.09	2.96	2.99	4.65	0.00	0.00	0.00	0.00	0.00
La <sub>2</sub> O <sub>3</sub>	0.01	0.01	0.93	1.21	1.00	1.22	1.43	0.00	0.00	0.00	0.00	0.00
Ce <sub>2</sub> O <sub>3</sub>	0.01	0.01	1.57	1.76	1.34	1.50	1.21	0.00	0.00	0.00	0.00	0.00
Pr <sub>2</sub> O <sub>3</sub>	0.00	0.00	0.05	0.03	0.04	0.04	0.04	0.00	0.00	0.00	0.00	0.00
Nd <sub>2</sub> O <sub>3</sub>	0.01	0.01	2.11	1.93	2.46	2.88	2.51	0.00	0.00	0.00	0.00	0.00
Sm <sub>2</sub> O <sub>3</sub>	0.00	0.00	0.02	0.03	0.02	0.02	0.02	0.00	0.00	0.00	0.00	0.00
Eu <sub>2</sub> O <sub>3</sub>	0.00	0.00	0.00	0.00	0.01	0.02	0.00	0.00	0.00	0.00	0.00	0.00
Gd <sub>2</sub> O <sub>3</sub>	0.00	0.00	0.05	0.04	0.04	0.03	0.04	0.00	0.00	0.00	0.00	0.00
Tb <sub>2</sub> O <sub>3</sub>	0.00	0.00	0.03	0.04	0.04	0.03	0.03	0.00	0.00	0.00	0.00	0.00
Dy <sub>2</sub> O <sub>3</sub>	0.00	0.00	0.05	0.06	0.06	0.05	0.07	0.00	0.00	0.00	0.00	0.00
Ho <sub>2</sub> O <sub>3</sub>	0.00	0.00	0.04	0.05	0.07	0.03	0.03	0.00	0.00	0.00	0.00	0.00
Er <sub>2</sub> O <sub>3</sub>	0.00	0.00	0.02	0.02	0.02	0.02	0.02	0.00	0.00	0.00	0.00	0.00
Tm <sub>2</sub> O <sub>3</sub>	0.00	0.00	0.02	0.02	0.01	0.01	0.09	0.00	0.00	0.00	0.00	0.00
Yb <sub>2</sub> O <sub>3</sub>	0.01	0.01	0.34	0.29	0.30	0.27	0.32	0.00	0.00	0.00	0.00	0.00
Lu <sub>2</sub> O <sub>3</sub>	0.00	0.00	0.01	0.00	0.00	0.00	0.01					
MgO	0.09	0.12	0.01	0.01	0.01	0.01	0.01	0.02	0.02	0.02	0.02	0.01
CaO	0.00	0.00	0.67	0.83	0.57	0.73	0.66	0.00	0.00	0.00	0.00	0.00
MnO	0.09	0.09	1.21	0.85	0.89	1.54	1.15	0.21	0.19	0.14	0.12	0.16
FeO	0.01	0.02	2.88	2.50	2.09	2.54	1.66	5.66	3.89	6.57	6.54	5.23
Σ REE	0.08	0.08	#	11.00	9.57	8.36	9.11	10.47	0.00	0.00	0.00	0.00
PbO	0.00	0.00	0.01	0.00	0.00	0.02	0.02	0.00	0.00	0.00	0.00	0.00
Total	99.34	99.24	99.30	97.34	94.26	99.11	99.51	98.94	99.77	99.82	99.41	98.46

Table 11 cont. Chemical Formula of Rutile from the Kingman and Wagon Bow Pegmatites

Ions	Kingman Mine		Wagon Bow #3					Wagon Bow #2				
	KFMAX-1	KFMAX-2	WHRADS-1	WHRADS-2	WHRADS-3	WHRADS-4	WHRADS-5	S-6-B-1	S-6-B-2	S-6-B-3	S-6-B-4	S-6-B-5
Nb	0.001	0.001	0.022	0.020	0.022	0.022	0.016	0.000	0.000	0.000	0.000	0.000
Ta	0.000	0.000	0.004	0.004	0.006	0.005	0.007	0.000	0.000	0.000	0.000	0.000
Si	0.000	0.000	0.000	0.000	0.000	0.000	0.000	0.000	0.000	0.000	0.000	0.000
Ti	0.995	0.995	0.880	0.894	0.899	0.892	0.896	0.966	0.975	0.960	0.960	0.968
Zr	0.000	0.000	0.000	0.000	0.000	0.000	0.000	0.000	0.000	0.000	0.000	0.000
Sn	0.000	0.000	0.000	0.000	0.000	0.000	0.000	0.000	0.000	0.000	0.000	0.000
Th	0.000	0.000	0.000	0.000	0.000	0.000	0.000	0.000	0.000	0.000	0.000	0.000
Al	0.002	0.001	0.002	0.002	0.002	0.002	0.002	0.000	0.001	0.001	0.001	0.001
Sc	0.000	0.000	0.000	0.001	0.000	0.000	0.000	0.000	0.000	0.000	0.000	0.000
Y	0.000	0.000	0.045	0.033	0.024	0.023	0.036	0.000	0.000	0.000	0.000	0.000
La	0.000	0.000	0.005	0.007	0.006	0.007	0.008	0.000	0.000	0.000	0.000	0.000
Ce	0.000	0.000	0.008	0.010	0.008	0.008	0.007	0.000	0.000	0.000	0.000	0.000
Pr	0.000	0.000	0.000	0.000	0.000	0.000	0.000	0.000	0.000	0.000	0.000	0.000
Nd	0.000	0.000	0.011	0.010	0.014	0.015	0.013	0.000	0.000	0.000	0.000	0.000
Sm	0.000	0.000	0.000	0.000	0.000	0.000	0.000	0.000	0.000	0.000	0.000	0.000
Eu	0.000	0.000	0.000	0.000	0.000	0.000	0.000	0.000	0.000	0.000	0.000	0.000
Gd	0.000	0.000	0.000	0.000	0.000	0.000	0.000	0.000	0.000	0.000	0.000	0.000
Tb	0.000	0.000	0.000	0.000	0.000	0.000	0.000	0.000	0.000	0.000	0.000	0.000
Dy	0.000	0.000	0.000	0.000	0.000	0.000	0.000	0.000	0.000	0.000	0.000	0.000
Ho	0.000	0.000	0.000	0.000	0.000	0.000	0.000	0.000	0.000	0.000	0.000	0.000
Er	0.000	0.000	0.000	0.000	0.000	0.000	0.000	0.000	0.000	0.000	0.000	0.000
Tm	0.000	0.000	0.000	0.000	0.000	0.000	0.000	0.000	0.000	0.000	0.000	0.000
Yb	0.000	0.000	0.002	0.001	0.001	0.001	0.001	0.000	0.000	0.000	0.000	0.000
Lu	0.000	0.000	0.000	0.000	0.000	0.000	0.000	0.000	0.000	0.000	0.000	0.000
Mg	0.002	0.002	0.000	0.000	0.000	0.000	0.000	0.000	0.000	0.000	0.000	0.000
Ca	0.000	0.000	0.011	0.013	0.009	0.012	0.010	0.000	0.000	0.000	0.000	0.000
Mn	0.001	0.001	0.015	0.011	0.012	0.019	0.014	0.002	0.002	0.002	0.001	0.002
Fe 2+	0.000	0.000	0.036	0.031	0.027	0.031	0.020	0.065	0.044	0.075	0.075	0.061
Pb	0.000	0.000	0.000	0.000	0.000	0.000	0.000	0.000	0.000	0.000	0.000	0.000
Σ A-Site	1.002	1.002	1.043	1.038	1.031	1.039	1.034	1.034	1.024	1.039	1.039	1.031

## Fe/Ti Oxides

TiO<sub>2</sub>



FeO

Fe<sub>2</sub>O<sub>3</sub>

### Legend

- Ilmenite
- Magnetite
- ▲ Hematite
- ◆ Kingman Rutile
- Wagon Bow #3 Rutile
- ★ Wagon Bow #2 Rutile

Figure 18. Ternary diagram showing the chemical composition of Fe-Ti oxides.

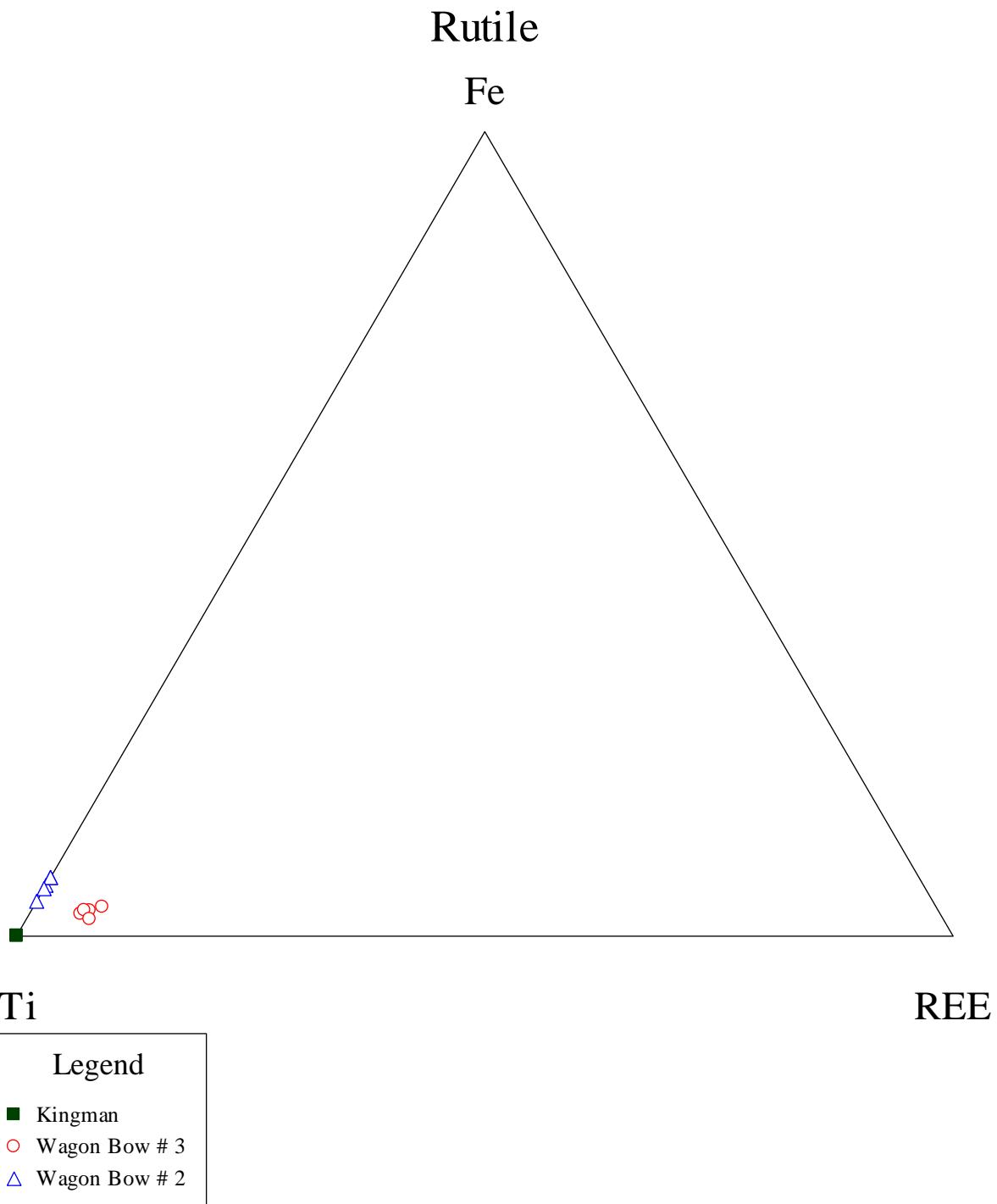


Figure 19. Ternary composition of rutile from the Kingman and Wagon Bow pegmatites showing Fe and REE substitutions for Ti.

# Rutile

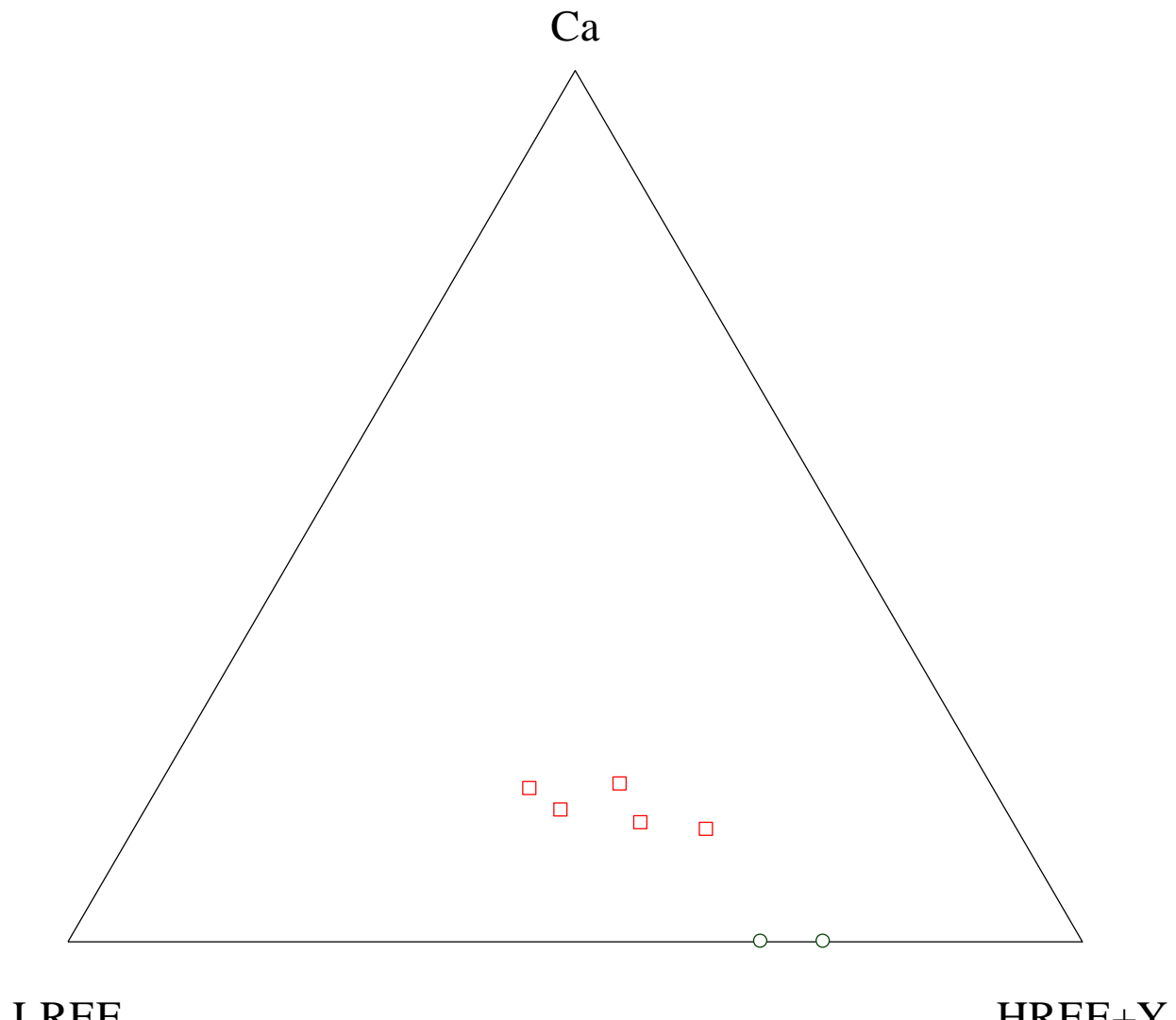


Figure 20. Ternary diagram showing the relative abundance of Ca and REE substitutions for rutile from the Kingman and Wagon Bow #3 pegmatites.

## Allanite

Allanite,  $\{\text{CaCe}\}\{\text{Al}_2\text{Fe}^{2+}\}[\text{O}|\text{OH}|\text{SiO}_4|\text{Si}_2\text{O}_7]$ , is only present in the wall zone at Kingman Feldspar Mine where large pods, Figure 21, crop out in Cuts B and C. Additionally, small, 3 cm, allanites were present in Cut A. More specifically, allanite was present only on the south face of the pegmatite in cuts B and C whereas it was exposed only on the north face of the A cut. These locations are the result of incomplete mining leaving exposures of wall zone material at these locations. The allanite is dark brown to black in color and is mildly radioactive. Most of the allanite was exposed in large pods of euhedral to subhedral crystals. The pods reach over 0.4 m length, with the largest one showing an intergrowth with another pod. These pods are extensively fractured due, in large part, to their metamict nature. On all of the exposed surfaces the allanite was coated with a red crust of oxidized iron. Within the allanite were small (0.3 cm) inclusions of thorogummite.

An examination of thin sections of allanite under both plane polarized light (Figure 22) and crossed nichols (Figure 23) show that there is little to no internal zonation. Microprobe data were recalculated using thirteen oxygen a.p.f.u, as suggested by Ercit (2002), a representative recalculated analyses are given in Table 12 and the rest can be found in Appendix I. A plot of the dominant A-site cations shows that Ca is only slightly dominant over REE and there is little to no Th present (Figure 24). Allanites are also enriched in LREE over HREE (Figure 25). Allanite analyses were plotted using a system for differentiating allanite versus epidote that was developed by Ercit (2002). These Kingman specimens all clearly lie in the allanite field (Figure 26).

Levinson (1966) outlined the method of adding suffixes to rare earth mineral names depending on rare earth element dominance. Using this nomenclature, three allanite species are

currently recognized; allanite-(Ce), allanite-(La) and allanite-(Yb). A plot of the three most abundant REE's shows that allanite from the Kingman pegmatite is Ce dominant in most cases. However, some of the samples are Nd dominant, thus indicating a new species in the allanite group; allanite-(Nd) ( $\{\text{CaNd}\}\{\text{Al}_2\text{Fe}^{2+}\}[\text{O}|\text{OH}|\text{SiO}_4|\text{Si}_2\text{O}_7]$ ) , (Figure 27).



Figure 21. Photo of allanite pod in wall zone microcline, large pod measured at 45 cm tall.

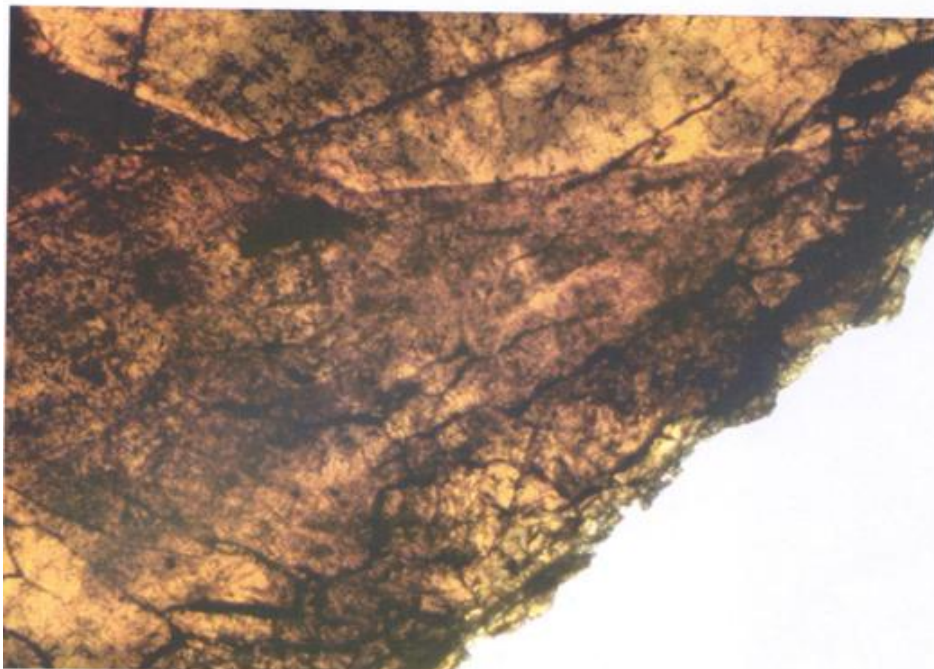


Figure 22. Petrographic thin section of allanite under plane polarized light. 2.5 mm

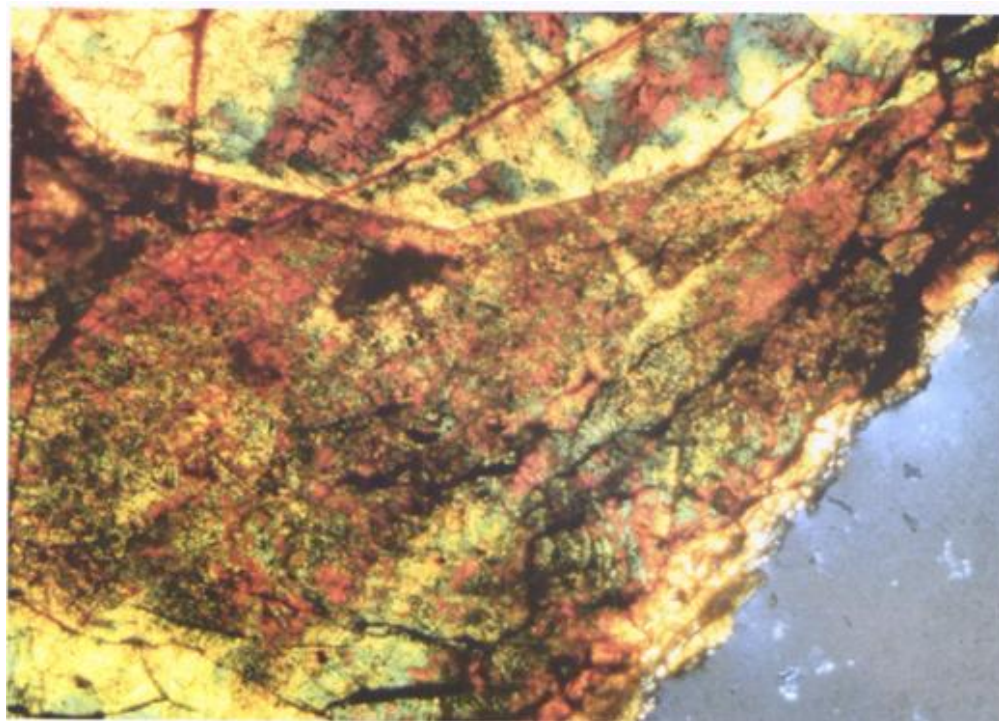


Figure 23. Petrographic thin section of allanite under crossed nichols. 2.5 mm

Table 12. Representative Chemical Analyses of the Compositions of Allanite from the Kingman Pegmatite

	KFMBA-1-1	KFMBA-1-2	KFMBA-1-3	KFMBA-1-3b	KFMBA-3-1	KFMBX-3-4	KFMCA-3-4	KFMCF-2-1	KFMCSW-5	KFMCM-1-6
WO <sub>3</sub>	0.02	0.01	0.01	0.01	0.00	0.01	0.01	0.00	0.00	0.00
P <sub>2</sub> O <sub>5</sub>	0.00	0.00	0.00	0.00	0.01	0.00	0.05	0.02	0.04	
Nb <sub>2</sub> O <sub>5</sub>	0.01	0.01	0.01	0.01	0.00	0.00	0.00	0.00	0.00	0.00
Ta <sub>2</sub> O <sub>5</sub>	0.00	0.00	0.00	0.00	0.02	0.00	0.00	0.00	0.00	0.00
SiO <sub>2</sub>	29.59	29.66	29.58	29.57	30.02	29.64	29.63	29.78	29.83	30.03
TiO <sub>2</sub>	0.45	0.62	0.34	0.31	0.77	0.59	0.51	0.87	0.87	0.90
ZrO <sub>2</sub>	0.02	0.01	0.01	0.01	0.02	0.00	0.00	0.00	0.00	0.00
SnO <sub>2</sub>	0.00	0.00	0.00	0.00	0.00	0.00	0.00	0.00	0.00	0.00
HfO <sub>2</sub>	0.00	0.00	0.00	0.00	0.00	0.00	0.00	0.00	0.00	0.00
ThO <sub>2</sub>	0.90	0.90	0.87	0.90	0.57	0.44	0.69	0.95	0.98	1.06
UO <sub>2</sub>	0.11	0.14	0.13	0.14	0.05	0.03	0.09	0.11	0.10	0.09
Al <sub>2</sub> O <sub>3</sub>	12.20	12.32	12.72	12.45	12.68	12.55	13.22	12.88	13.78	14.45
Sc <sub>2</sub> O <sub>3</sub>	0.06	0.05	0.06	0.06	0.06	0.06	0.07	0.08	0.07	0.07
Y <sub>2</sub> O <sub>3</sub>	0.20	0.20	0.19	0.25	0.09	0.08	0.09	0.23	0.14	0.09
La <sub>2</sub> O <sub>3</sub>	3.09	3.01	2.98	3.01	4.55	5.65	3.45	4.10	3.95	4.22
Ce <sub>2</sub> O <sub>3</sub>	7.88	8.10	7.89	9.33	8.88	8.43	9.99	9.88	9.70	9.00
Pr <sub>2</sub> O <sub>3</sub>	1.83	1.89	1.78	1.81	1.46	1.23	2.08	1.00	1.23	1.12
Nd <sub>2</sub> O <sub>3</sub>	9.03	8.78	8.60	8.90	6.79	7.23	6.21	6.12	7.13	7.67
Sm <sub>2</sub> O <sub>3</sub>	1.15	1.15	1.32	1.30	0.94	1.28	1.44	0.88	0.53	0.54
Eu <sub>2</sub> O <sub>3</sub>	0.01	0.01	0.01	0.01	0.00	0.02	0.02	0.02	0.02	0.02
Gd <sub>2</sub> O <sub>3</sub>	0.00	0.01	0.01	0.00	0.02	0.02	0.03	0.02	0.00	0.00
Tb <sub>2</sub> O <sub>3</sub>	0.00	0.01	0.00	0.00	0.00	0.00	0.00	0.00	0.00	0.00
Dy <sub>2</sub> O <sub>3</sub>	0.02	0.03	0.03	0.03	0.03	0.00	0.00	0.03	0.04	0.04
Ho <sub>2</sub> O <sub>3</sub>	0.00	0.01	0.00	0.00	0.00	0.03	0.00	0.00	0.00	0.00
Er <sub>2</sub> O <sub>3</sub>	0.01	0.00	0.00	0.00	0.00	0.00	0.00	0.00	0.00	0.00
Tm <sub>2</sub> O <sub>3</sub>	0.00	0.00	0.00	0.00	0.00	0.00	0.00	0.00	0.00	0.00
Yb <sub>2</sub> O <sub>3</sub>	0.19	0.18	0.19	0.21	0.06	0.14	0.10	0.15	0.08	0.09
Lu <sub>2</sub> O <sub>3</sub>	0.00	0.00	0.00	0.00	0.00	0.00	0.00	0.00	0.00	0.00
MgO	0.30	0.30	0.24	0.27	0.16	0.17	0.15	0.55	0.30	0.27
CaO	9.00	9.45	9.93	9.43	9.65	9.90	9.90	9.86	10.04	10.77
MnO	1.23	1.33	1.13	1.20	1.23	1.10	0.72	1.33	1.01	0.98
FeO	16.43	16.39	16.84	15.46	17.79	16.89	16.05	17.00	16.45	15.99
PbO	0.02	0.02	0.04	0.04	0.03	0.03	0.04	0.16	0.09	0.11
Na <sub>2</sub> O	0.00	0.00	0.00	0.00	0.00	0.00	0.00	0.00	0.00	0.00
K <sub>2</sub> O	0.00	0.03	0.00	0.02	0.01	0.00	0.02	0.02	0.00	0.00
H <sub>2</sub> O	6.155	5.315	4.999	5.197	4.115	4.43	5.442	3.841	3.552	2.383
F	0.021	0	0.013	0	0.011	0	0.009	0.033	0.034	0.044
Cl	0.055	0.062	0.068	0.055	0.022	0.033	0.028	0.065	0.034	0.044
Re-calculated										
Subtotal	100	100	100	100	100	100	100	100	100	100
Less O=F	0.01	0.00	0.01	0.00	0.00	0.00	0.01	0.02	0.01	0.01
Less O=Cl	0.01	0.01	0.02	0.01	0.00	0.01	0.01	0.01	0.01	0.01
Total	99.98	99.99	99.98	99.99	99.99	99.99	99.99	99.97	99.98	99.98

Table 12 cont. Representative Chemical Analyses of the Formula of Allanite from the Kingman Pegmatite

Ions	KFMBA-1-1	KFMBA-1-2	KFMBA-1-3	KFMBA-1-3b	KFMBA-3-1	KFMBX-3-4	KFMCA-3-4	KFMCF-2-1	KFMCSW-5	KFMCM-1-6
W	0.000	0.000	0.000	0.000	0.000	0.000	0.000	0.000	0.000	0.000
P	0.000	0.000	0.000	0.000	0.000	0.001	0.000	0.004	0.002	0.004
Nb	0.001	0.001	0.000	0.001	0.000	0.000	0.000	0.000	0.000	0.000
Ta	0.000	0.000	0.000	0.000	0.001	0.000	0.000	0.000	0.000	0.000
Zr	0.001	0.001	0.001	0.001	0.001	0.000	0.000	0.000	0.000	0.000
Sn	0.000	0.000	0.000	0.000	0.000	0.000	0.000	0.000	0.000	0.000
Hf	0.000	0.000	0.000	0.000	0.000	0.000	0.000	0.000	0.000	0.000
Th	0.021	0.021	0.020	0.021	0.013	0.010	0.016	0.022	0.023	0.024
U	0.003	0.003	0.003	0.003	0.001	0.001	0.002	0.002	0.002	0.002
Sc	0.006	0.005	0.005	0.005	0.005	0.005	0.006	0.007	0.006	0.006
Y	0.011	0.011	0.010	0.013	0.005	0.004	0.005	0.012	0.007	0.005
La	0.116	0.112	0.112	0.113	0.167	0.211	0.129	0.152	0.146	0.155
Ce	0.292	0.300	0.293	0.347	0.325	0.312	0.370	0.364	0.357	0.329
Pr	0.068	0.070	0.066	0.067	0.053	0.045	0.077	0.037	0.045	0.041
Nd	<b>0.327</b>	<b>0.317</b>	<b>0.311</b>	0.323	0.242	0.261	0.225	0.220	0.256	0.273
Sm	0.040	0.040	0.046	0.045	0.032	0.045	0.050	0.031	0.018	0.019
Eu	0.000	0.000	0.000	0.000	0.000	0.001	0.001	0.001	0.001	0.001
Gd	0.000	0.000	0.000	0.000	0.001	0.001	0.001	0.001	0.000	0.000
Tb	0.000	0.000	0.000	0.000	0.000	0.000	0.000	0.000	0.000	0.000
Dy	0.001	0.001	0.001	0.001	0.001	0.000	0.000	0.001	0.001	0.001
Ho	0.000	0.000	0.000	0.000	0.000	0.001	0.000	0.000	0.000	0.000
Er	0.000	0.000	0.000	0.000	0.000	0.000	0.000	0.000	0.000	0.000
Tm	0.000	0.000	0.000	0.000	0.000	0.000	0.000	0.000	0.000	0.000
Yb	0.006	0.005	0.006	0.007	0.002	0.004	0.003	0.005	0.002	0.003
Lu	0.000	0.000	0.000	0.000	0.000	0.000	0.000	0.000	0.000	0.000
Ca	0.977	1.024	1.079	1.025	1.033	1.073	1.074	1.064	1.081	1.152
Mn	0.105	0.114	0.097	0.103	0.104	0.094	0.062	0.114	0.086	0.083
Pb	0.001	0.001	0.001	0.001	0.001	0.001	0.001	0.004	0.002	0.003
Na	0.000	0.000	0.000	0.000	0.000	0.000	0.000	0.000	0.000	0.000
K	0.000	0.004	0.000	0.003	0.002	0.000	0.004	0.003	0.000	0.000
$\Sigma$ A-Site	1.976	2.030	2.051	2.079	1.989	2.070	2.026	2.044	2.035	2.101
Al	1.458	1.469	1.521	1.489	1.493	1.496	1.578	1.529	1.634	1.702
Ti	0.035	0.047	0.026	0.024	0.058	0.045	0.039	0.066	0.066	0.068
Mg	0.046	0.045	0.037	0.040	0.023	0.026	0.023	0.083	0.045	0.039
Fe 2+	1.393	1.386	1.428	1.311	1.486	1.430	1.358	1.432	1.383	1.335
$\Sigma$ M-Site	2.932	2.947	3.012	2.864	3.060	2.997	2.998	3.110	3.128	3.144
$\Sigma$ Si	3.000	3.000	3.000	3.000	3.000	3.000	3.000	3.000	3.000	3.000
OH	4.058	3.982	3.992	3.994	4.000	4.017	4.011	3.972	3.978	3.985
F	0.007	0.000	0.004	0.000	0.003	0.000	0.003	0.011	0.011	0.014
Cl	0.009	0.011	0.012	0.009	0.004	0.006	0.005	0.011	0.006	0.007
$\Sigma$ Hydroxyl	4.179	3.597	3.398	3.527	2.750	2.996	3.683	2.603	2.399	1.609

-Bold portions indicate Nd-dominance

Allanite

Th x 10

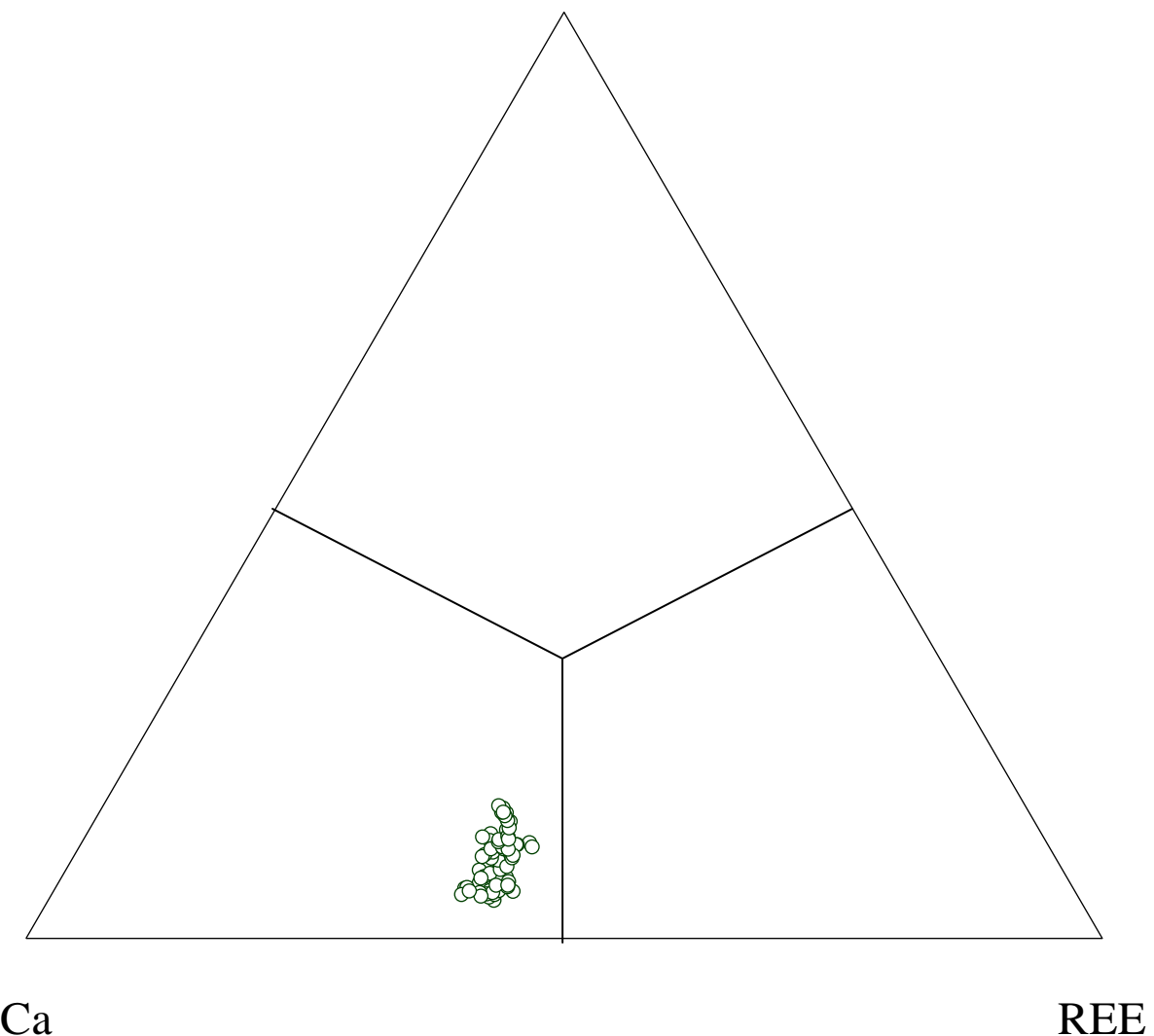


Figure 24. Ternary diagram for A-site cations in allanite from the Kingman pegmatite showing an almost equal proportion of Ca to the REE's and only minor substitution of Th.

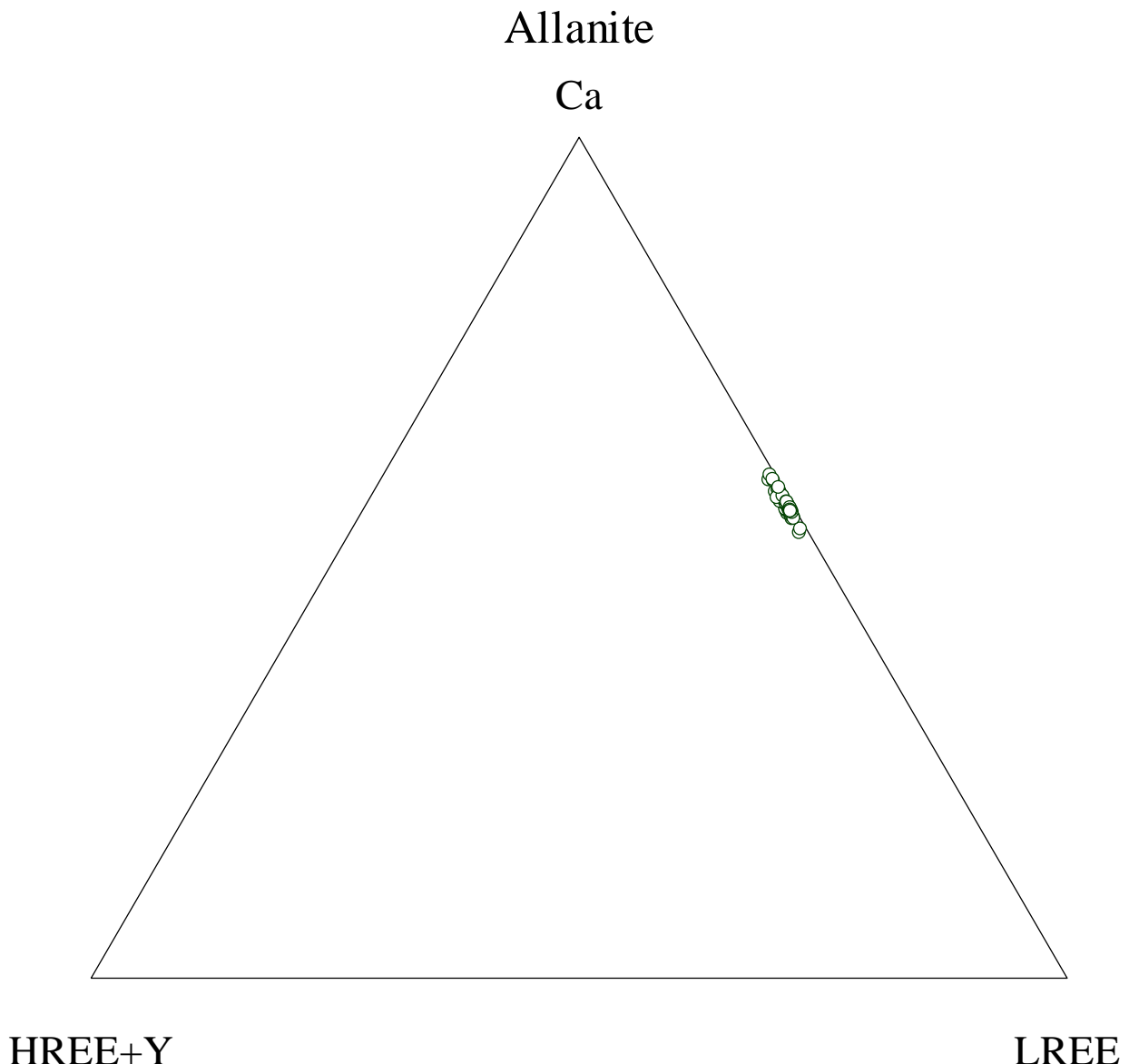


Figure 25. Ternary diagram for allanite from the Kingman pegmatite showing an extreme LREE enrichment relative to HREE.

## Allanite & Epidote

A2 Ca+M3<sup>3+</sup> -2 A1

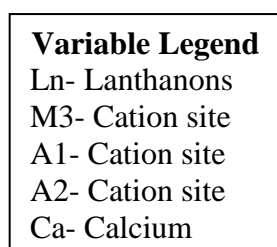
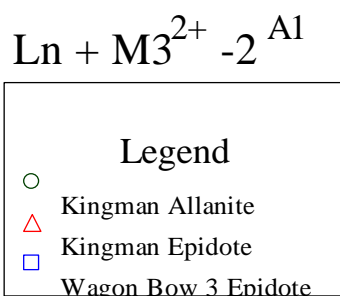
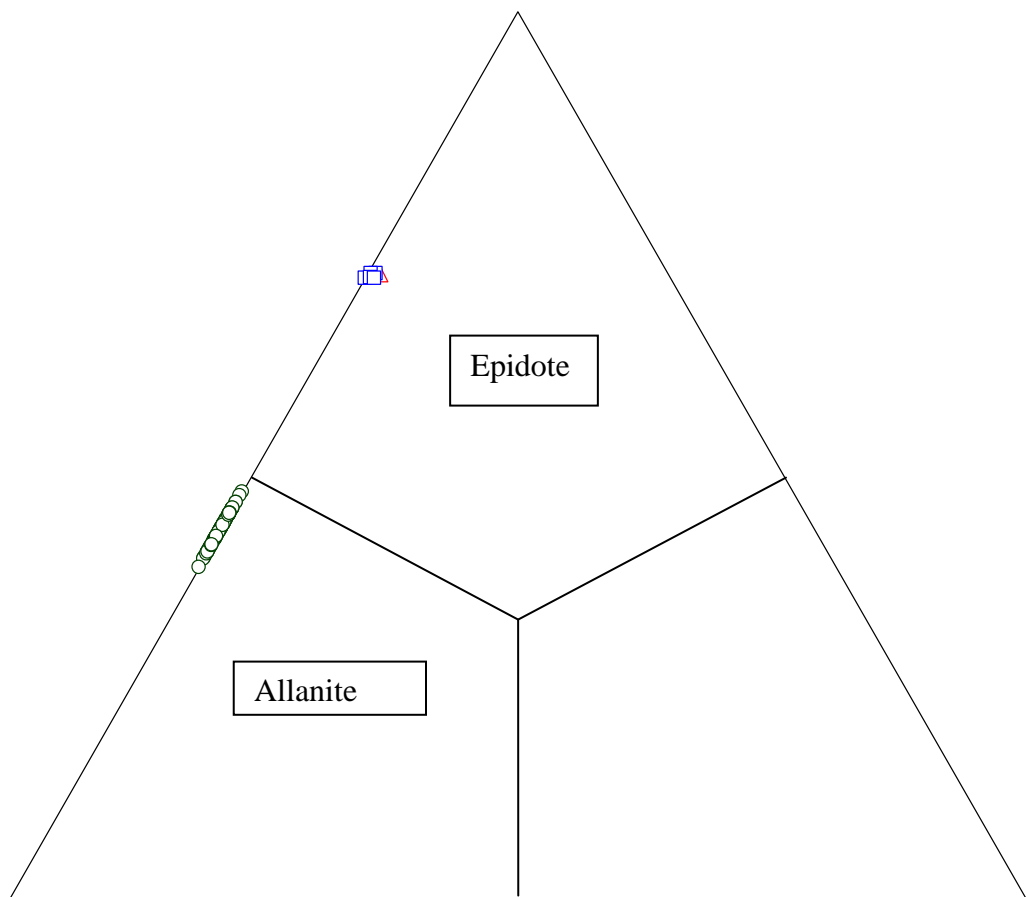
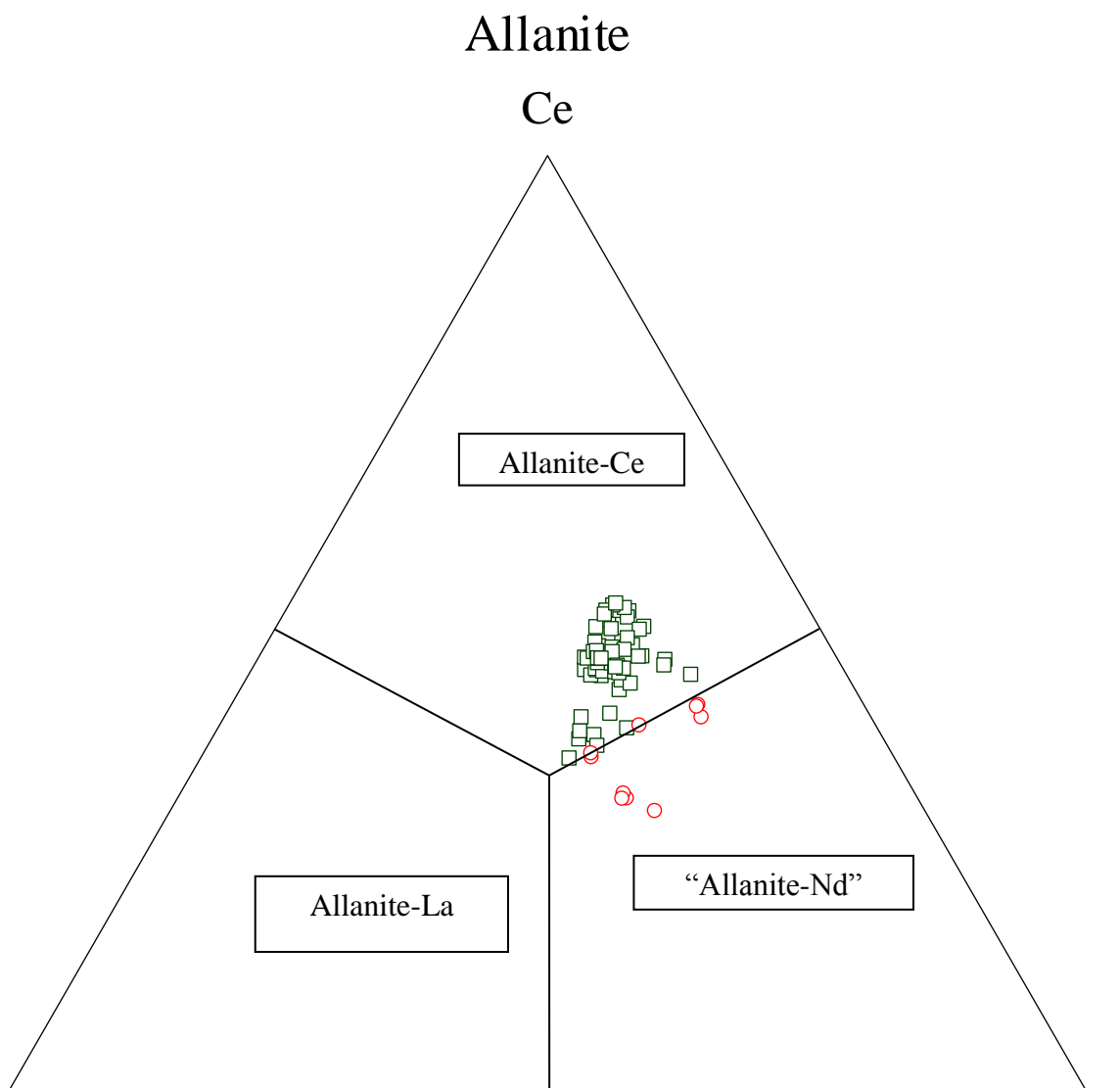


Figure 26. Ternary diagram plotting the Ercit (2002) variables and fields that confirm the identification of allanite from the Kingman pegmatite and epidote from the Kingman pegmatite and Wagon Bow # 3 mines.



La

Nd

**Legend**

- Ce-dominant Allanite
- Nd-dominant Allanite

Figure 27. Ternary diagram for allanite from the Kingman pegmatite showing the three most abundant REE's which indicate the proper suffix to be used. Since the Nd-dominant species is not a currently recognized mineral species, samples lying in that field are a new mineral.

## **Monazite**

Monazite,  $(\text{Ce}, \text{La}, \text{Nd}, \text{Th})\text{PO}_4$ , was recovered from both the Rare Metals and Wagon Bow #3 mine. It is brownish-red in color and averaged 2.5-3 cm in length. The intact crystals are subhedral to almost completely euhedral. They were found in the wall zones of the pegmatites associated with quartz, microcline biotite and, at the Rare Metals mine, muscovite.

The monazite microprobe analyses were recalculated to four oxygen a.p.f.u.. Representative analyses can be found in Table 13 with the entire data set found in Appendix I. A plot of the dominant A-site cations shows that the monazite has a greater affinity for the LREE (Figure 28). A plot of the dominant REE's show that the monazite is Ce-dominant, although they do lie very close to the Nd dominant field (Figure 29). Monazite has a strong radioactive signature due to the presence of U and Th which has produced a red/brown halo of radiation damage in the enclosing quartz (Figure 30).

Table 13. Representative Chemical Analyses of Monazite from the Wagon Bow #3 and Rare Metals Pegmatites

Oxides	Wagon Bow # 3					Rare Metals Mine				
	WHRADM-3	WHRADM-4	WHRADM-5	WHRADM-1	WHRADM-2	MONWH-4	RMM-1-1	RMM-1-2	WHRADM-3	WHRADM-4
P <sub>2</sub> O <sub>5</sub>	29.92	30.01	29.82	30.12	29.88	29.56	29.5	29.54	29.92	30.01
SiO <sub>2</sub>	1.43	1.33	1.56	1.43	1.57	1.27	0.88	0.92	1.43	1.33
TiO <sub>2</sub>	0.01	0.01	0.01	0.01	0.01	0	0	0	0.01	0.01
ThO <sub>2</sub>	3.23	2.88	3.03	2.9	3	2.7	3.11	2.93	3.23	2.88
ThO <sub>2</sub>	0.22	0.28	0.26	0.23	0.31	0.31	0.33	0.38	0.22	0.28
UO <sub>2</sub>	0.08	0.23	0.19	0.09	0.11	0.12	0.21	0.18	0.08	0.23
Sc <sub>2</sub> O <sub>3</sub>	0.04	0.04	0.03	0.03	0.04	0.03	0.04	0.04	0.04	0.04
Y <sub>2</sub> O <sub>3</sub>	0.28	0.23	0.25	0.27	0.31	0.14	0.12	0.15	0.28	0.23
La <sub>2</sub> O <sub>3</sub>	7.99	8.22	8.3	8.21	8.44	8.44	7.9	8.23	7.99	8.22
Ce <sub>2</sub> O <sub>3</sub>	22.01	20.94	22.33	22.12	21.57	22.92	23.55	22.13	22.01	20.94
Pr <sub>2</sub> O <sub>3</sub>	3.63	3.3	3.42	3.54	3.41	3.32	3.23	3.18	3.63	3.3
Nd <sub>2</sub> O <sub>3</sub>	19.22	21.43	19.83	20.99	19.91	20.04	18.77	19.34	19.22	21.43
Sm <sub>2</sub> O <sub>3</sub>	4.77	4.3	4.23	4.54	4.32	2.78	3.11	3.21	4.77	4.3
Eu <sub>2</sub> O <sub>3</sub>	0.2	0.21	0.21	0.26	0.22	0.16	0.15	0.13	0.2	0.21
Gd <sub>2</sub> O <sub>3</sub>	2.09	2.33	2.3	2.57	2.22	1.77	1.54	1.57	2.09	2.33
Tb <sub>2</sub> O <sub>3</sub>	0.51	0.5	0.52	0.55	0.46	0.06	0.05	0.05	0.51	0.5
Dy <sub>2</sub> O <sub>3</sub>	0.23	0.23	0.24	0.25	0.21	0.1	0.07	0.09	0.23	0.23
Ho <sub>2</sub> O <sub>3</sub>	0	0	0.01	0.01	0.01	0	0	0	0	0
Er <sub>2</sub> O <sub>3</sub>	0.01	0.01	0.01	0.01	0.02	0.02	0	0	0.01	0.01
Tm <sub>2</sub> O <sub>3</sub>	0	0.01	0.02	0.01	0.01	0.01	0	0	0	0.01
Yb <sub>2</sub> O <sub>3</sub>	0.14	0.12	0.12	0.13	0.12	0.1	0.06	0.05	0.14	0.12
Lu <sub>2</sub> O <sub>3</sub>	0	0	0.01	0	0	0	0	0	0	0
MgO	0.24	0.21	0.18	0.21	0.16	0.09	0.1	0.11	0.24	0.21
CaO	0.89	0.83	0.73	0.79	0.94	0.54	0.43	0.42	0.89	0.83
MnO	0.08	0.05	0.05	0.06	0.06	0.03	0.08	0.21	0.08	0.05
FeO	0.78	0.78	0.46	0.57	0.91	0.78	1.21	1	0.78	0.78
PbO	0.23	0.2	0.22	0.21	0.2	0.16	0.18	0.17	0.23	0.2
Total	98.23	98.69	98.37	100.11	98.42	95.46	94.62	94.04	98.23	98.69

Table 13cont. Representative Chemical Formula of Monazite from then Wagon Bow and Rare Metals Pegmatites

Ions	Wagon Bow # 3					Rare Metals Mine				
	WHRADM-3	WHRADM-4	WHRADM-5	WHRADM-1	WHRADM-2	MONWH-4	RMM-1-1	RMM-1-2	WHRADM-3	WHRADM-4
Ti	0	0	0	0	0	0	0	0	0	0
Th	0.029	0.025	0.027	0.025	0.026	0.024	0.028	0.027	0.029	0.025
U	0.004	0.005	0.005	0.004	0.005	0.003	0.003	0.003	0.004	0.005
Al	0.003	0.011	0.009	0.004	0.005	0.006	0.01	0.008	0.003	0.011
Sc	0.001	0.001	0.001	0.001	0.001	0.001	0.001	0.001	0.001	0.001
Y	0.006	0.005	0.005	0.005	0.006	0.003	0.003	0.003	0.006	0.005
La	0.114	0.117	0.119	0.116	0.12	0.124	0.117	0.122	0.114	0.117
Ce	0.313	0.296	0.317	0.311	0.305	0.334	0.346	0.326	0.313	0.296
Pr	0.051	0.046	0.048	0.05	0.048	0.048	0.047	0.047	0.051	0.046
Nd	0.266	0.296	0.275	0.287	0.275	0.285	0.269	0.278	0.266	0.296
Sm	0.064	0.057	0.057	0.06	0.058	0.038	0.043	0.045	0.064	0.057
Eu	0.003	0.003	0.003	0.003	0.003	0.002	0.002	0.002	0.003	0.003
Gd	0.027	0.03	0.03	0.033	0.029	0.023	0.021	0.021	0.027	0.03
Tb	0.007	0.006	0.007	0.007	0.006	0.001	0.001	0.001	0.007	0.006
Dy	0.003	0.003	0.003	0.003	0.003	0.001	0.001	0.001	0.003	0.003
Ho	0	0	0	0	0	0	0	0	0	0
Er	0	0	0	0	0	0	0	0	0	0
Tm	0	0	0	0	0	0	0	0	0	0
Yb	0.002	0.001	0.001	0.002	0.001	0.001	0.001	0.001	0.002	0.001
Lu	0	0	0	0	0	0	0	0	0	0
Mg	0.028	0.024	0.021	0.012	0.018	0.005	0.006	0.007	0.028	0.024
Ca	0.074	0.069	0.061	0.032	0.078	0.023	0.019	0.018	0.074	0.069
Mn	0.005	0.003	0.003	0.002	0.004	0.001	0.003	0.007	0.005	0.003
Fe 2+	0.05	0.051	0.03	0.018	0.059	0.026	0.041	0.034	0.05	0.051
Pb	0.005	0.004	0.004	0.002	0.004	0.002	0.002	0.002	0.005	0.004
$\Sigma$ A-Site	1.053	1.054	1.025	0.978	1.056	0.951	0.962	0.953	1.053	1.054
P	0.983	0.982	0.98	0.978	0.979	0.995	1.002	1.006	0.983	0.982
Si	0.056	0.052	0.061	0.055	0.061	0.051	0.035	0.037	0.056	0.052
$\Sigma$ B-Site	1.039	1.034	1.04	1.033	1.039	1.045	1.038	1.043	1.039	1.034

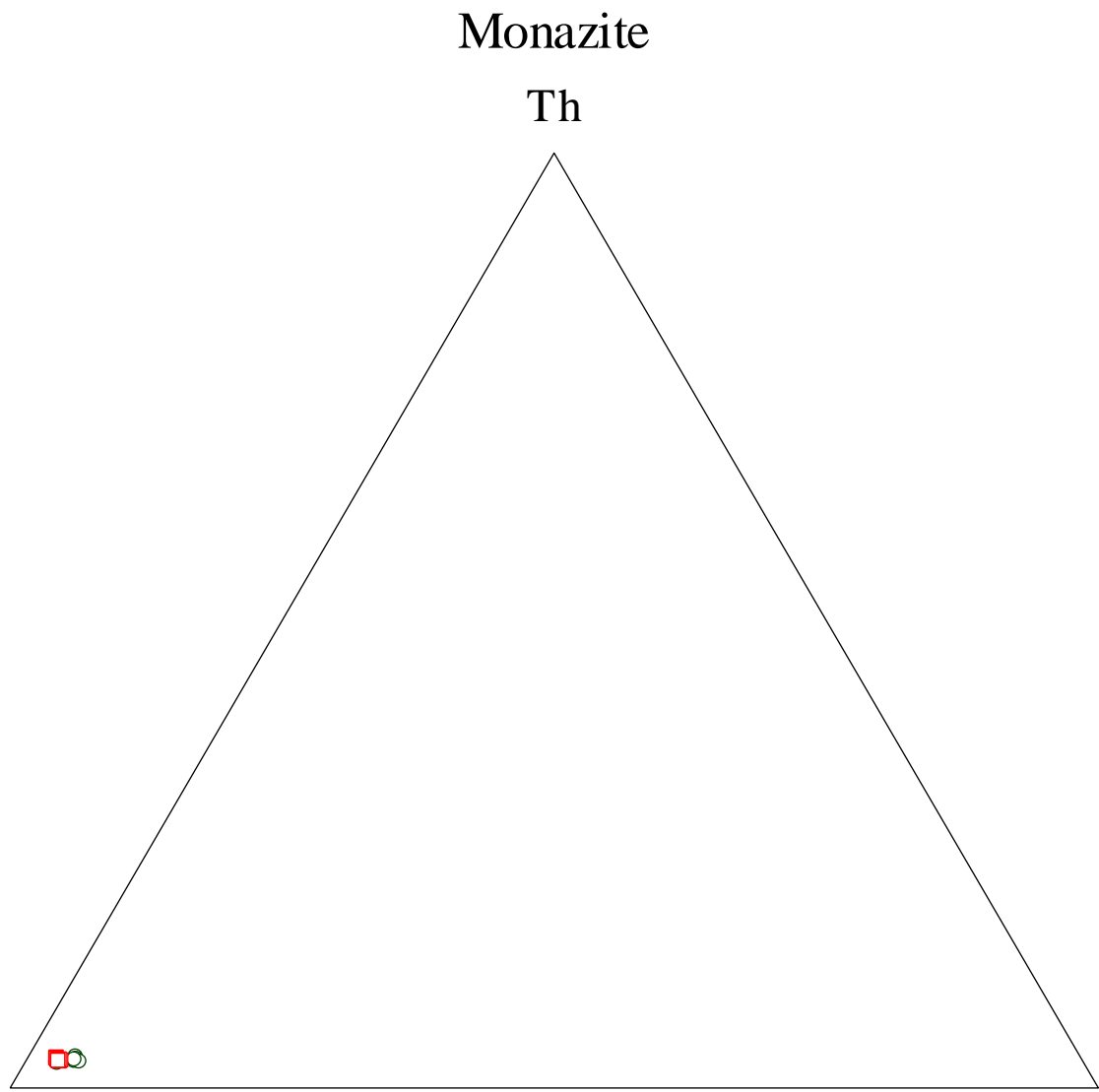
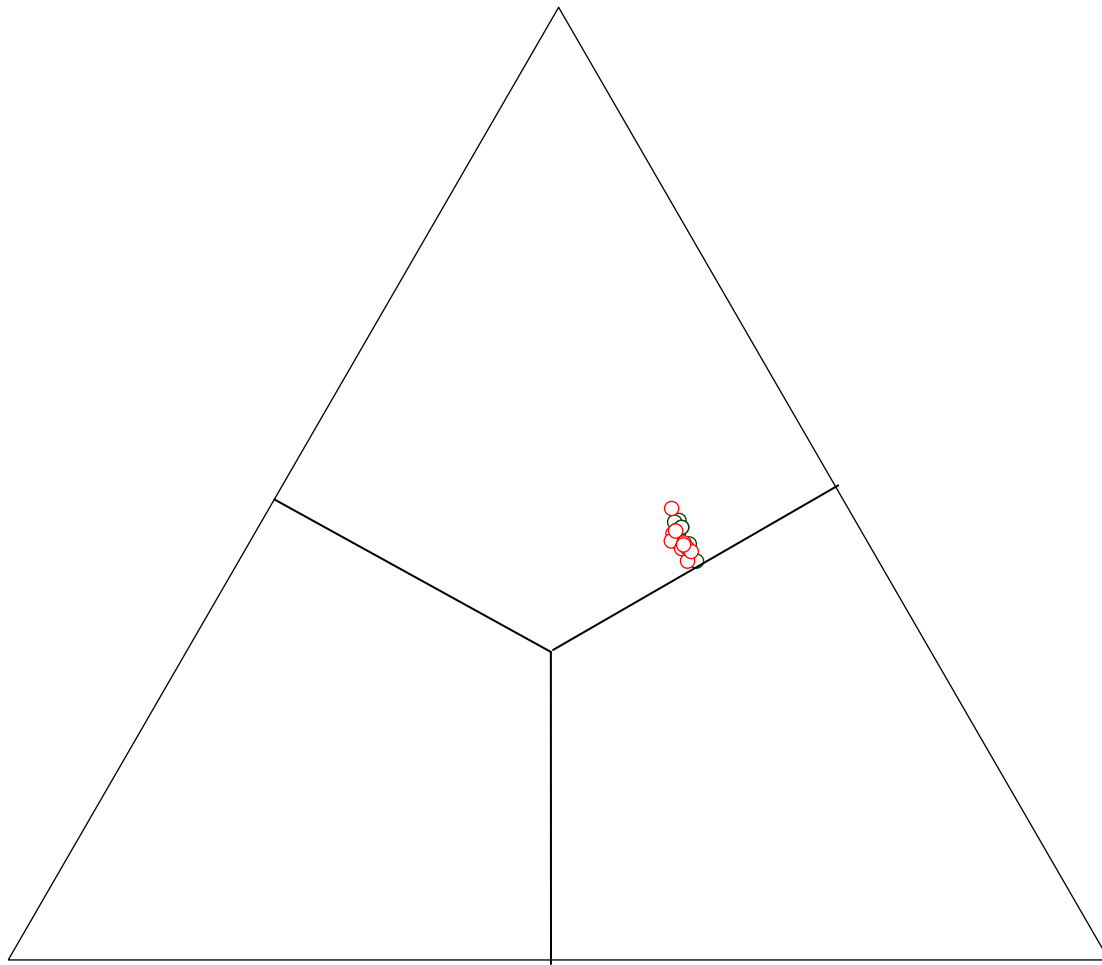


Figure 28. Ternary diagram for monazite showing an extreme LREE enrichment relative to HREE and minor Th substitutions.

Monazite

Ce



La

Nd

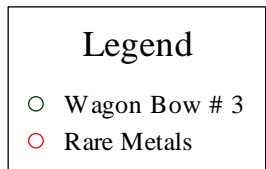


Figure 29. Ternary diagram for Wagon Bow #3 and Rare Metals monazite showing Ce-dominance.



Figure 30. Radiation damage halo from monazite seen in quartz. 3 mm.

## **Beryl**

Only one specimen of beryl,  $\text{BeAl}_2\text{Si}_6\text{O}_{18}$ , was found in loose rubble at the Rare Metals Mine. It is light blue in color, measured 1 cm high by 1 cm wide and is associated with muscovite, biotite, microcline and quartz.

The microprobe data were recalculated using 18 a.p.f.u. and can be found in Table 14. DCP analysis (Table 37) shows that this specimen has trace amounts of Li (>350 ppm). Schaller et al. says that the presence of Li may have been brought in through digestion of the country rock (1962)

## **Apatite**

Apatite,  $\text{Ca}_5(\text{PO}_4)_3\text{F}$  was recovered in small amounts from the Kingman Feldspar and Wagon Bow #2 mines. The Wagon Bow #3 apatites were found through SEM identification whereas the Kingman specimens were found after the heavy mineral separation test was run. They were all recovered from wall zone material and are associated with quartz and microcline. They are yellow in color and approximately 1 cm in height.

Microprobe data were recalculated on the basis of thirteen O, F and Cl apfu and are given in Table 15. Minor substitutions of Mn and Fe for Ca can be seen in Figure 31. Samples from the Kingman mine have slightly higher Mn content.

A plot of the hydroxyl site shows that the samples from the Wagon Bow #3 and the Kingman mine are Cl poor and have F as the dominant hydroxyl, thus the apatites are fluorapatite (Figure 32).

Table 14. Chemical Composition of Beryl from the Rare Metal Pegmatite.

	RB1	RB2	RB3	RB4	RB5
Oxides					
SiO <sub>2</sub>	65.349	65.411	65.332	65.512	65.465
TiO <sub>2</sub>	0	0	0	0	0
Al <sub>2</sub> O <sub>3</sub>	18.215	18.334	18.347	18.4	18.341
FeO	0.361	0.317	0.345	0.341	0.327
MnO	0	0	0	0	0
BeO	13.6	13.625	13.615	13.65	13.63
MgO	0	0	0	0	0
CaO	0	0	0	0	0
Na <sub>2</sub> O	0.073	0.077	0.083	0.074	0.067
K <sub>2</sub> O	0.045	0.056	0.056	0.039	0.033
Total	97.643	97.82	97.778	98.016	97.863
Ions					
Σ Si	6.002377	5.996794	5.993514	5.994298	5.99818949
Ti	0	0	0	0	0
Al	1.971965	1.981122	1.983838	1.984362	1.98070421
Fe	0.027726	0.024301	0.026465	0.026089	0.02505244
Mn	0	0	0	0	0
Mg	0	0	0	0	0
Σ B-Site	1.99969	2.005423	2.010303	2.010451	2.00575665
Σ Be	3.000437	3.00031	3.000092	2.999932	2.99963333
Ca	0	0	0	0	0
Na	0.012999	0.013686	0.014762	0.013127	0.01190123
K	0.005272	0.006548	0.006553	0.004552	0.00385663

Normalized to 3 Be, Be calculated stoichiometrically

Table 15. Chemical Compositions of Apatite from the Wagon Bow #3 and Kingman Pegmatites

	Wagon Bow #3		Kingman Feldspar Mine				
	WH2REC-4	WH2REC-5	B-6-C-1	B-6-C-2	B-6-C-3	B-6-C-4	B-6-C-5
P <sub>2</sub> O <sub>5</sub>	41.89	41.96	41.78	41.73	41.81	41.78	41.73
SiO <sub>2</sub>	0.23	0.20	0.17	0.21	0.18	0.13	0.15
Al <sub>2</sub> O <sub>3</sub>	0.02	0.03	0.03	0.02	0.02	0.02	0.01
Y <sub>2</sub> O <sub>3</sub>	0.02	0.01	0.03	0.03	0.03	0.03	0.02
Ce <sub>2</sub> O <sub>3</sub>	0.01	0.01	0.00	0.00	0.00	0.01	0.00
Nd <sub>2</sub> O <sub>3</sub>	0.00	0.01	0.00	0.00	0.00	0.00	0.00
Yb <sub>2</sub> O <sub>3</sub>	0.00	0.00	0.01	0.01	0.00	0.01	0.00
MgO	0.02	0.02	0.11	0.11	0.12	0.11	0.10
CaO	55.32	54.98	55.45	55.34	55.39	55.52	55.35
MnO	0.02	0.02	0.03	0.03	0.02	0.03	0.03
FeO	0.01	0.01	0.01	0.02	0.02	0.02	0.01
F	2.45	2.61	2.57	2.66	2.85	2.73	2.82
Cl	0.03	0.04	0.05	0.06	0.05	0.04	0.04
H <sub>2</sub> O	0.00	0.11	0.00	0.00	0.00	0.00	0.00
Subtotal	100.66	100.00	100.24	100.20	100.49	100.45	100.26
Less O=F	1.04	1.10	1.08	1.12	1.20	1.15	1.19
Less O=Cl	0.01	0.01	0.01	0.01	0.01	0.01	0.01
Sum	99.62	98.90	99.63	99.07	99.73	99.29	99.61
<b>Ions</b>							
Al	0.002	0.003	0.003	0.003	0.002	0.002	0.001
Y	0.001	0.000	0.001	0.001	0.001	0.002	0.001
Ce	0.001	0.000	0.000	0.000	0.000	0.000	0.000
Nd	0.000	0.000	0.000	0.000	0.000	0.000	0.000
Yb	0.000	0.000	0.000	0.000	0.000	0.000	0.000
Mg	0.002	0.002	0.014	0.014	0.015	0.028	0.012
Ca	4.930	4.893	4.930	4.915	4.896	4.992	4.901
Mn	0.001	0.001	0.002	0.002	0.001	0.004	0.002
Fe	0.001	0.001	0.001	0.001	0.001	0.001	0.001
$\Sigma$ A-Site	4.938	4.899	4.948	5.018	5.015	5.030	5.018
P	2.950	2.951	2.935	2.925	2.920	2.969	2.928
Si	0.019	0.017	0.014	0.017	0.015	0.011	0.012
$\Sigma$ B-Site	2.969	2.971	2.952	2.945	2.935	2.980	2.937
F	0.644	0.686	0.674	0.697	0.764	0.713	0.737
Cl	0.004	0.006	0.007	0.008	0.007	0.005	0.006
OH	0.352	0.308	0.319	0.223	0.249	0.282	0.257
$\Sigma$ Hydroxyl	1.000	1.000	1.000	1.000	1.000	1.000	1.000

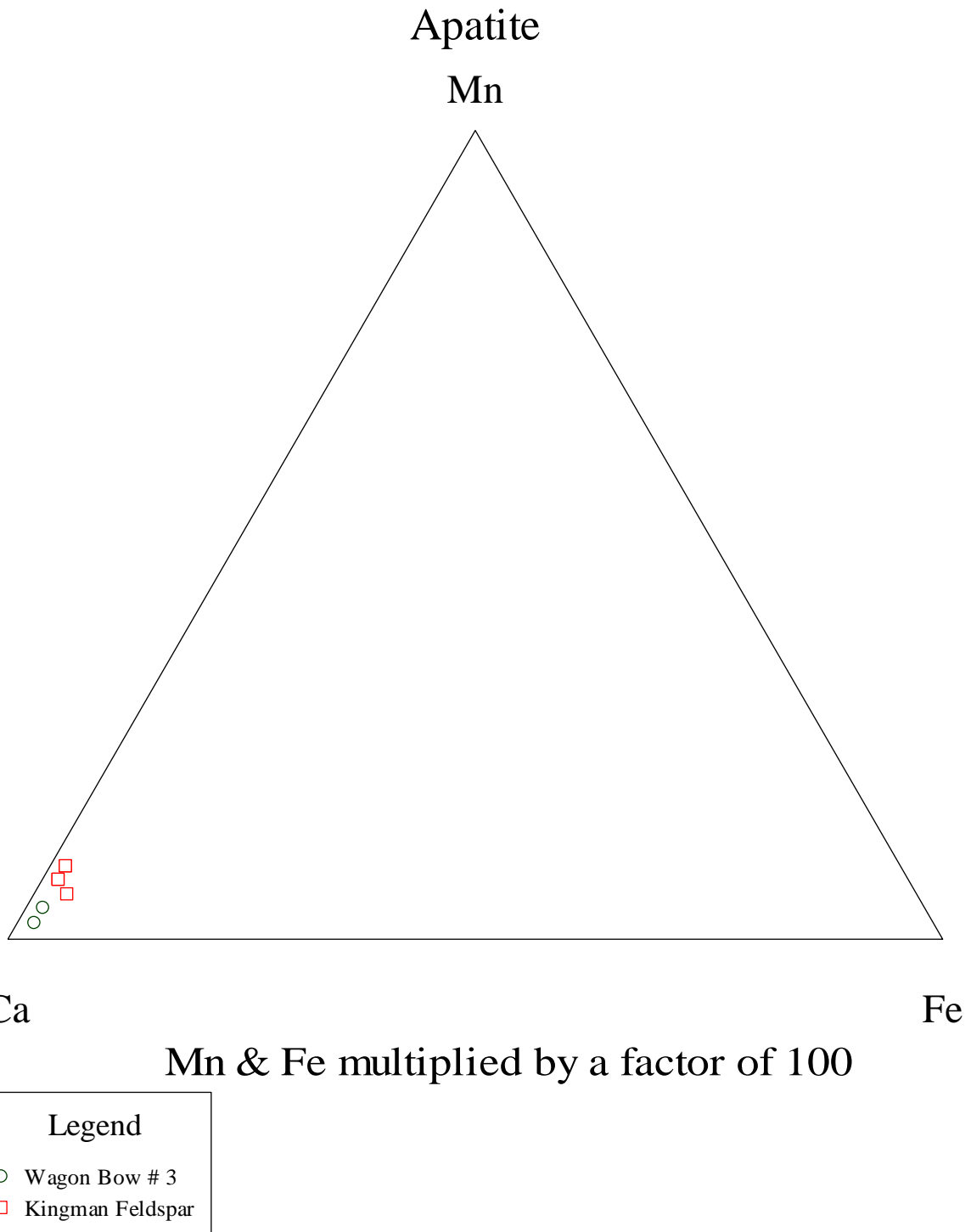


Figure 31. Ternary diagram for apatite showing extreme Ca dominance over Fe and Mn.

# Apatite

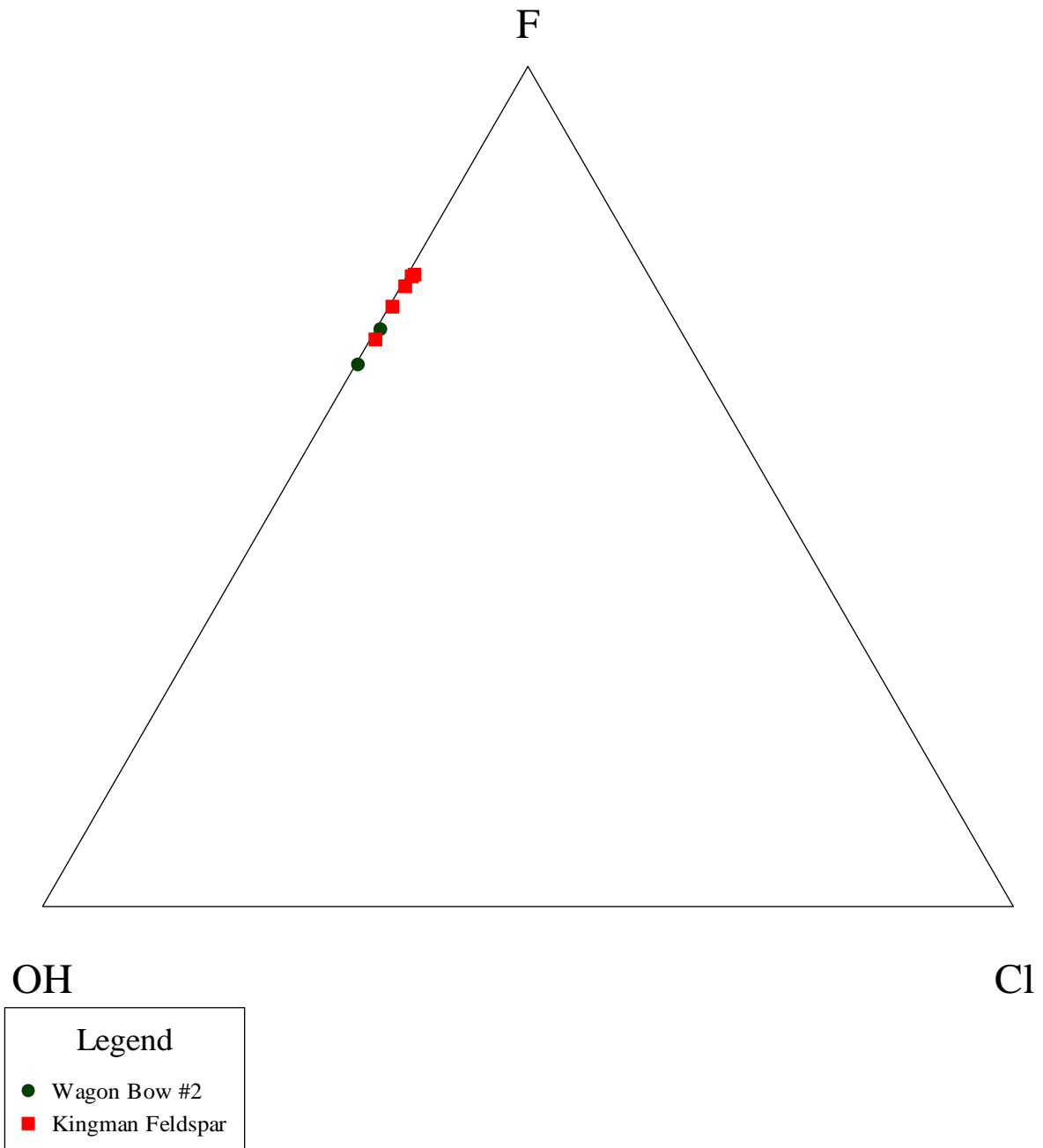


Figure 32. Ternary diagram for apatite hydroxyl site occupancy. The Wagon Bow and Kingman apatites are well within the fluorapatite domain.

## Bastnaesite and Ca-rich bastnaesite

Bastnaesite((Ce,La)[F|CO<sub>3</sub>]) and Ca-rich bastnaesite were present only in the C cut in the Kingman Feldspar Quarry. The bastnaesite is yellowish brown to dark brown and measured up to 1 cm in size. The Ca-rich bastnaesites are whitish brown in color and measured up to 1 cm in size. The bastnaesite was identified by SEM analysis whereas the Ca-rich bastnaesite was found after heavy mineral separation. Both are from wall zone material and are associated with quartz, microcline, and biotite.

Chemical data were acquired using the EMP and are given in Tables 16 (bastnaesite) and 17 (Ca-rich bastnaesite). Ions were calculated using four O and F a.p.f.u for bastnaesite and Ca-rich bastnaesite. Both bastnaesite and Ca-rich bastnaesite are LREE enriched (Figure 33) with Nd, Ce, and La ranging from 0.17-0.2 a.p.f.u's in bastnaesite and 0.21-0.29 a.p.f.u's in Ca-rich bastnaesite. A plot of these elements shows that both bastnaesite and Ca-rich bastnaesite are Ce-dominant (Figure 34). It is noteworthy that the Ca-rich bastnaesite yields low analytical totals possibly related to hydrate water or absorbed water.

Table 16. Chemical Composition of  
Bastnaesite from the Kingman  
Pegmatite

Oxides	KFMCM- 1-3	KFMCM- 1-4
SiO <sub>2</sub>	0.07	0.05
TiO <sub>2</sub>	0.00	0.00
ThO <sub>2</sub>	3.56	3.34
UO <sub>2</sub>	0.07	0.07
Al <sub>2</sub> O <sub>3</sub>	0.23	0.32
Sc <sub>2</sub> O <sub>3</sub>	0.07	0.08
Y <sub>2</sub> O <sub>3</sub>	0.04	0.05
La <sub>2</sub> O <sub>3</sub>	14.63	14.26
Ce <sub>2</sub> O <sub>3</sub>	17.77	17.33
Pr <sub>2</sub> O <sub>3</sub>	1.76	1.65
Nd <sub>2</sub> O <sub>3</sub>	17.65	17.43
Sm <sub>2</sub> O <sub>3</sub>	1.00	1.01
Eu <sub>2</sub> O <sub>3</sub>	0.04	0.05
Gd <sub>2</sub> O <sub>3</sub>	0.05	0.04
Dy <sub>2</sub> O <sub>3</sub>	0.01	0.00
Yb <sub>2</sub> O <sub>3</sub>	0.02	0.02
MgO	0.09	0.07
CaO	8.88	8.33
MnO	0.11	0.09
FeO	4.65	5.03
PbO	0.68	0.70
H <sub>2</sub> O	0.85	1.36
CO <sub>2</sub>	23.18	24.00
F	7.85	8.10
Cl	0.05	0.03
Sub-Total	103.31	103.42
Less O=F	3.30	3.41
Less O=Cl	0.01	0.01
Total	100.00	100.00
Ions		
Ti	0.000	0.000
Th	0.026	0.024
U	0.000	0.000
Al	0.009	0.012
Sc	0.002	0.002
Y	0.001	0.001
La	0.175	0.166
Ce	0.211	0.200
Pr	0.021	0.019
Nd	0.204	0.196
Sm	0.011	0.011
Eu	0.000	0.001
Gd	0.001	0.000
Dy	0.000	0.000
Yb	0.000	0.000
Mg	0.004	0.003
Ca	0.308	0.281
Mn	0.003	0.002
Fe 2+	0.126	0.132
Pb	0.006	0.006
Σ A-Site	1.107	1.056
Si	0.002	0.002
OH	0.183	0.286
CO <sub>2</sub>	1.024	1.032
F	0.803	0.806
Cl	0.003	0.002
Σ B-Site	2.017	2.128

Table 17. Chemical Composition of Ca-rich bastnaesite from the Kingman Pegmatite

Oxides	B-4-D-1	B-4-D-2	B-4-D-3	B-4-D-4	B-4-D-5
SiO <sub>2</sub>	0.99	0.89	0.79	0.95	0.57
TiO <sub>2</sub>	0.01	0.00	0.00	0.00	0.00
ThO <sub>2</sub>	1.46	1.46	1.56	1.89	1.77
UO <sub>2</sub>	0.00	0.01	0.00	0.00	0.00
Al <sub>2</sub> O <sub>3</sub>	0.11	0.00	0.00	0.09	0.13
Sc <sub>2</sub> O <sub>3</sub>	0.02	0.03	0.02	0.02	0.03
Y <sub>2</sub> O <sub>3</sub>	0.03	0.05	0.04	0.04	0.04
La <sub>2</sub> O <sub>3</sub>	13.14	12.93	13.55	13.43	12.78
Ce <sub>2</sub> O <sub>3</sub>	18.57	18.00	18.67	17.78	17.67
Pr <sub>2</sub> O <sub>3</sub>	2.32	2.12	2.46	2.66	2.41
Nd <sub>2</sub> O <sub>3</sub>	17.90	16.97	17.90	17.98	18.01
Sm <sub>2</sub> O <sub>3</sub>	1.57	1.65	1.57	1.70	1.46
Eu <sub>2</sub> O <sub>3</sub>	0.09	0.07	0.09	0.08	0.09
Gd <sub>2</sub> O <sub>3</sub>	0.00	0.00	0.00	0.00	0.00
Dy <sub>2</sub> O <sub>3</sub>	0.00	0.00	0.00	0.00	0.00
Yb <sub>2</sub> O <sub>3</sub>	0.02	0.02	0.02	0.02	0.02
MgO	0.03	0.06	0.11	0.09	0.09
CaO	4.54	5.10	4.89	4.26	3.89
MnO	0.46	0.56	0.49	0.73	0.72
FeO	4.55	2.23	6.78	4.12	2.54
PbO	0.12	0.09	0.08	0.09	0.06
H <sub>2</sub> O	1.80	1.60	2.19	1.48	1.13
CO <sub>2</sub>	29.65	33.58	26.38	29.62	33.48
F	4.54	4.45	4.12	5.10	5.34
Cl	0.00	0.00	0.00	0.00	0.00
Subtotal	101.91	101.86	101.73	102.14	102.24
Less O=F	1.91	1.87	1.73	2.14	2.25
Total	99.99	99.99	100.00	99.99	99.99
Ions					
Ti	0.000	0.000	0.000	0.000	0.000
Th	0.015	0.014	0.016	0.019	0.017
U	0.000	0.000	0.000	0.000	0.000
Al	0.006	0.000	0.000	0.005	0.007
Sc	0.001	0.001	0.001	0.001	0.001
Y	0.001	0.001	0.001	0.001	0.001
La	0.215	0.201	0.232	0.220	0.200
Ce	0.301	0.277	0.317	0.290	0.274
Pr	0.038	0.032	0.042	0.043	0.037
Nd	0.283	0.255	0.297	0.286	0.273
Sm	0.024	0.024	0.025	0.026	0.021
Eu	0.001	0.001	0.001	0.001	0.001
Gd	0.000	0.000	0.000	0.000	0.000
Dy	0.000	0.000	0.000	0.000	0.000
Yb	0.000	0.000	0.000	0.000	0.000
Mg	0.002	0.004	0.008	0.006	0.006
Ca	0.216	0.230	0.243	0.203	0.177
Mn	0.017	0.020	0.019	0.028	0.026
Fe 2+	0.168	0.079	0.263	0.153	0.090
Pb	0.001	0.001	0.001	0.001	0.001
Σ A-Site	1.290	1.139	1.466	1.284	1.132
Si	0.044	0.037	0.036	0.042	0.024
OH	0.532	0.449	0.678	0.439	0.320
CO <sub>2</sub>	1.794	1.928	1.671	1.799	1.938
F	0.637	0.592	0.605	0.717	0.717
Cl	0.000	0.000	0.000	0.000	0.000
Σ B-Site	3.007	3.005	2.991	2.997	2.999

## Bastnaesite & Ca-rich bastnaesite

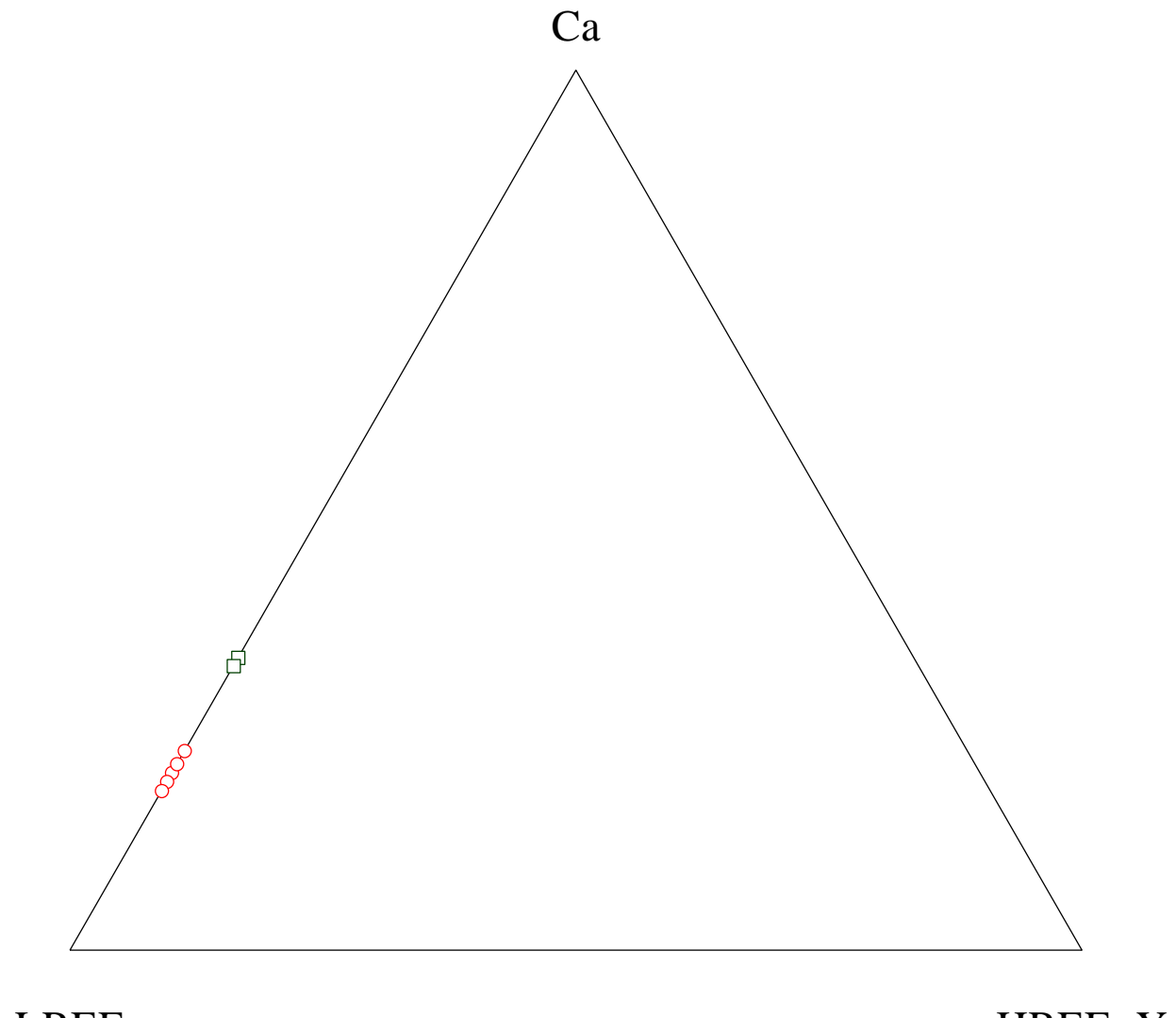


Figure 33. Ternary diagram for bastnaesite and Ca-rich bastnaesite showing both are LREE-enriched.

## Bastnaesite & Ca-rich bastnaesite

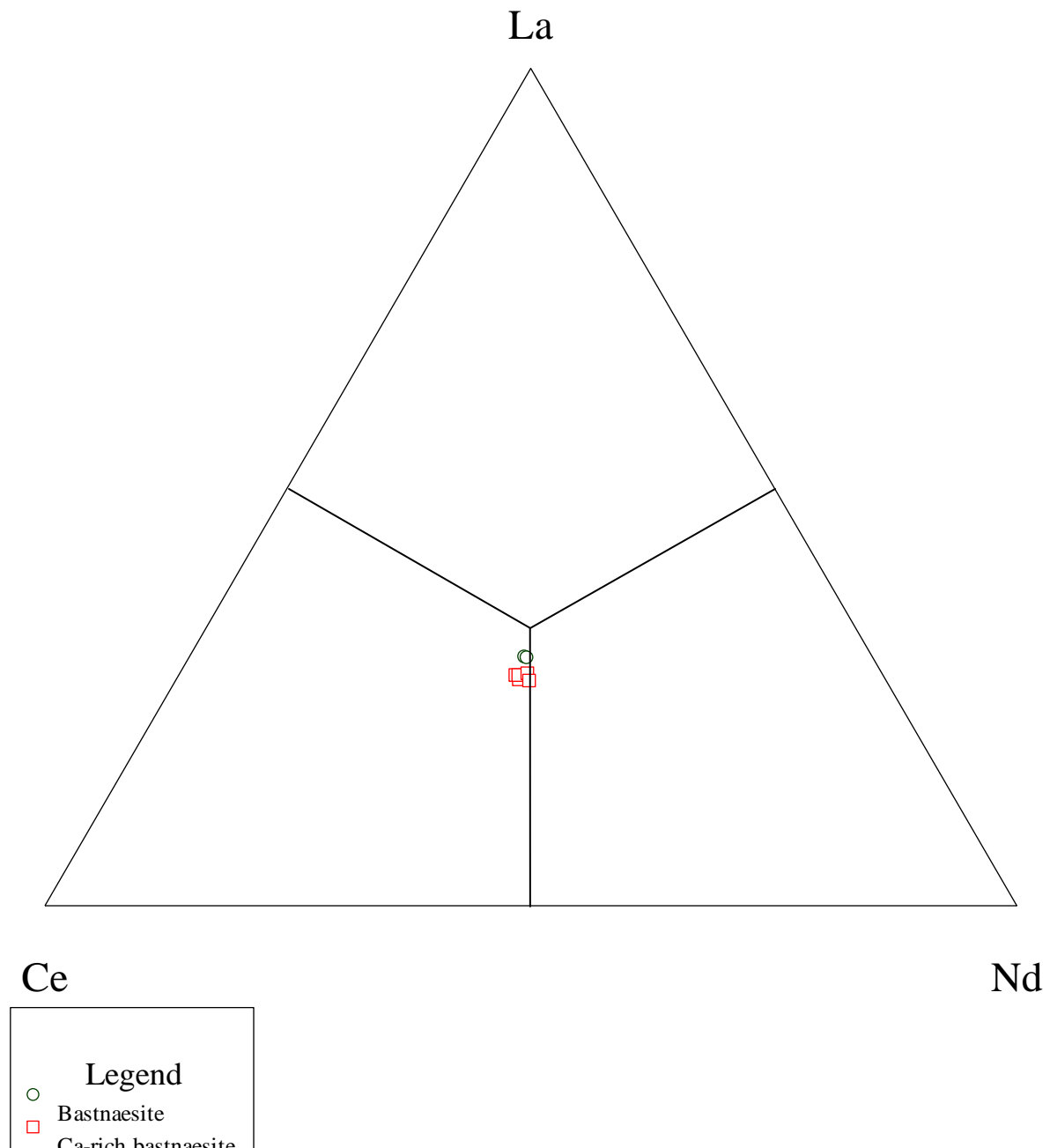


Figure 34. Ternary diagram showing the three most abundant REE's for bastnaesite and Ca-rich bastnaesite showing Ce-dominance.

## **Titanite**

Titanite,  $\text{CaTiSiO}_5$ , specimens were found in the Kingman Feldspar and Wagon Bow #2 mines. Only a few grains were recovered from the heavy mineral separate of wall zone material. It is associated with quartz and microcline, approximately 0.6 mm in size and are dark grey to black.

Microprobe analyses (Table 18) show that titanite is close to stoichiometrically ideal with only minor HREE substituting for Ca.

Table 18. Chemical Composition of Titanite from the Kingman and Wagon Bow Pegmatites

Oxides	Wagon Bow # 2					Kingman Mine				
	B-5-E-1	B-5-E-2	B-5-E-3	B-5-E-4	B-5-E-5	B-6-B-1	B-6-B-2	B-6-B-3	B-6-B-4	B-6-B-5
Nb <sub>2</sub> O <sub>5</sub>	0.02	0.03	0.03	0.03	0.02	0.03	0.03	0.04	0.03	0.03
SiO <sub>2</sub>	30.46	30.66	30.72	30.40	30.38	30.63	30.55	30.52	30.23	30.28
TiO <sub>2</sub>	39.12	39.21	39.23	39.09	39.10	39.22	39.30	39.41	38.93	39.41
Al <sub>2</sub> O <sub>3</sub>	0.32	0.27	0.25	0.33	0.24	0.22	0.09	0.06	0.11	0.08
Sc <sub>2</sub> O <sub>3</sub>	0.01	0.00	0.01	0.02	0.00	0.01	0.01	0.01	0.01	0.02
La <sub>2</sub> O <sub>3</sub>	0.02	0.02	0.03	0.03	0.02	0.02	0.02	0.02	0.02	0.02
Ce <sub>2</sub> O <sub>3</sub>	0.03	0.04	0.04	0.04	0.04	0.03	0.03	0.04	0.03	0.03
Pr <sub>2</sub> O <sub>3</sub>	0.01	0.00	0.00	0.01	0.00	0.00	0.00	0.01	0.01	0.01
Nd <sub>2</sub> O <sub>3</sub>	0.03	0.03	0.04	0.04	0.04	0.03	0.03	0.03	0.03	0.04
MgO	0.16	0.21	0.24	0.20	0.10	0.21	0.19	0.23	0.22	0.16
CaO	28.32	28.23	28.44	28.37	28.37	28.41	28.38	28.40	28.38	28.44
MnO	0.23	0.20	0.18	0.18	0.19	0.26	0.27	0.22	0.21	0.27
FeO	0.21	0.17	0.19	0.20	0.23	0.19	0.18	0.19	0.18	0.17
Total	98.95	99.05	99.40	98.94	98.74	99.27	99.10	99.18	98.41	98.97
Ions										
Nb	0.000	0.000	0.000	0.000	0.000	0.001	0.000	0.001	0.000	0.000
Si	1.004	1.019	1.016	1.005	1.005	1.013	1.011	1.009	1.000	1.002
Ti	0.970	0.980	0.976	0.972	0.972	0.976	0.977	0.980	0.968	0.980
Al	0.013	0.010	0.010	0.013	0.010	0.009	0.004	0.002	0.004	0.003
Sc	0.000	0.000	0.000	0.001	0.000	0.000	0.000	0.000	0.000	0.001
La	0.000	0.000	0.000	0.000	0.000	0.000	0.000	0.000	0.000	0.000
Ce	0.000	0.000	0.001	0.000	0.000	0.000	0.000	0.000	0.000	0.000
Pr	0.000	0.000	0.000	0.000	0.000	0.000	0.000	0.000	0.000	0.000
Nd	0.000	0.000	0.000	0.000	0.000	0.000	0.000	0.000	0.000	0.000
Mg	0.008	0.010	0.012	0.010	0.005	0.011	0.009	0.011	0.011	0.008
Ca	1.000	1.005	1.008	1.005	1.005	1.007	1.006	1.006	1.006	1.008
Mn	0.007	0.006	0.005	0.005	0.005	0.007	0.008	0.006	0.006	0.008
Fe 2+	0.006	0.005	0.005	0.005	0.006	0.005	0.005	0.005	0.005	0.005
Σ A-Site	1.995	2.007	2.004	2.001	1.999	2.003	1.999	2.001	1.989	2.003

## **Zircon**

Zircon,  $\text{ZrSiO}_4$ , is very rare in these pegmatites, only one sample was recovered from the Kingman Feldspar Quarry. Found intergrown in the wall zone with feldspar and quartz, it is black in color, measured 1 cm in diameter and is subhedral in shape.

Electron microprobe analysis (Table 19) reveals a near end-member formula with only trace amounts of U, P, REE's, Fe and Ca. Of these impurities, Fe and Ca were the most abundant; averaging 0.019 and 0.029 a.p.f.u. respectively.

Table 19. Chemical Composition of Zircon  
from the Kingman Pegmatite

Oxides	KFMCF- 1-1	KFMCF- 1-2	KFMCF- 1-3
P <sub>2</sub> O <sub>5</sub>	0.23	0.18	0.21
Nb <sub>2</sub> O <sub>5</sub>	0.01	0.00	0.00
Ta <sub>2</sub> O <sub>5</sub>	0.01	0.00	0.00
SiO <sub>2</sub>	32.12	32.21	32.19
TiO <sub>2</sub>	0.11	0.09	0.14
ZrO <sub>2</sub>	64.83	64.57	64.80
HfO <sub>2</sub>	1.45	1.60	1.55
ThO <sub>2</sub>	0.09	0.12	0.09
UO <sub>2</sub>	0.13	0.15	0.09
Al <sub>2</sub> O <sub>3</sub>	0.23	0.11	0.34
Sc <sub>2</sub> O <sub>3</sub>	0.06	0.03	0.04
Y <sub>2</sub> O <sub>3</sub>	0.21	0.19	0.21
Ce <sub>2</sub> O <sub>3</sub>	0.01	0.01	0.00
Nd <sub>2</sub> O <sub>3</sub>	0.00	0.00	0.01
Gd <sub>2</sub> O <sub>3</sub>	0.01	0.01	0.01
Tb <sub>2</sub> O <sub>3</sub>	0.01	0.01	0.01
Dy <sub>2</sub> O <sub>3</sub>	0.02	0.01	0.01
Ho <sub>2</sub> O <sub>3</sub>	0.01	0.00	0.00
Er <sub>2</sub> O <sub>3</sub>	0.02	0.02	0.02
Tm <sub>2</sub> O <sub>3</sub>	0.01	0.00	0.01
Yb <sub>2</sub> O <sub>3</sub>	0.02	0.02	0.02
MgO	0.10	0.09	0.08
CaO	0.66	0.44	0.24
MnO	0.02	0.02	0.02
FeO	0.43	0.54	0.37
PbO	0.02	0.02	0.02
Cl	0.00	0.01	0.01
Subtotal	100.81	100.44	100.49
Less			
O=Cl	0.00	0.00	0.00
Total	100.81	100.44	100.48

Table 19 cont. Chemical Formula of Zircon  
from the Kingman Pegmatite

Ions	KFMCF- 1-1	KFMCF- 1-2	KFMCF- 1-3
Nb	0.000	0.000	0.000
Ta	0.000	0.000	0.000
Ti	0.003	0.002	0.003
Zr	0.965	0.965	0.966
Hf	0.013	0.014	0.013
Th	0.001	0.001	0.001
U	0.002	0.002	0.001
Al	0.008	0.004	0.012
Sc	0.001	0.001	0.001
Y	0.003	0.003	0.003
Ce	0.000	0.000	0.000
Nd	0.000	0.000	0.000
Gd	0.000	0.000	0.000
Tb	0.000	0.000	0.000
Dy	0.000	0.000	0.000
Ho	0.000	0.000	0.000
Er	0.000	0.000	0.000
Tm	0.000	0.000	0.000
Yb	0.000	0.000	0.000
Mg	0.009	0.008	0.007
Ca	0.043	0.029	0.016
Mn	0.001	0.001	0.001
Fe 2+	0.011	0.028	0.019
Pb	0.000	0.000	0.000
$\sum$ A-Site	1.062	1.059	1.046
P	0.006	0.005	0.005
Si	0.981	0.988	0.985
Cl	0.000	0.001	0.001
$\sum$ B-Site	0.987	0.993	0.991

## **Quartz**

Quartz,  $\text{SiO}_2$ , is an abundant mineral in all of the pegmatites. It is present in large amounts both in the wall zone and core zone, where it is one of the two main components. Quartz from all the locations is cloudy to white and generally subhedral. In the intermediate and core zones it can occur in masses up to 12 m in length and is intergrown with microcline.

## **Epidote**

Epidote,  $\{\text{Ca}_2\}\{\text{Al}_2\text{Fe}^{3+}\}[\text{O}|\text{OH}|\text{SiO}_4|\text{Si}_2\text{O}_7]$ , was recovered in one sample from the Kingman Feldspar Quarry and at multiple sites at the Wagon Bow #3 Quarry. In both instances the epidote is approximately 0.6 cm in size and is dark green to black. The samples that were recovered are the result of secondary alteration of the wall zone and associated with quartz and microcline.

Mineral chemistry of epidote was collected using the EMP and the data is given in Table 20. Ions were calculated using thirteen oxygen plus F a.p.f.u. The epidote shows only minor substitution of LREE and using variables determined by Ercit (2002) plots clearly within the epidote field (Figure 26).

Table 20. Chemical Composition of Epidote from the Kingman &amp; Wagon Bow Pegmatites

Oxides	Kingman Mine			Wagon Bow # 3		
	KFMCF-1-4	WHM-1-5	WHM-2-1	WHM-2-2	WHM-2-3	WHM-1-3
P <sub>2</sub> O <sub>5</sub>	0.00	0.03	0.01	0.03	0.02	0.03
Nb <sub>2</sub> O <sub>5</sub>	0.00	0.00	0.01	0.01	0.01	0.00
SiO <sub>2</sub>	36.44	36.21	36.00	36.09	36.10	36.32
TiO <sub>2</sub>	0.05	0.29	0.68	0.65	0.68	0.32
ZrO <sub>2</sub>	0.01	0.00	0.00	0.00	0.00	0.01
ThO <sub>2</sub>	0.01	0.00	0.01	0.00	0.00	0.01
UO <sub>2</sub>	0.00	0.00	0.01	0.00	0.00	0.00
Al <sub>2</sub> O <sub>3</sub>	20.13	20.03	19.91	19.87	19.83	19.92
Sc <sub>2</sub> O <sub>3</sub>	0.03	0.04	0.04	0.05	0.05	0.03
Y <sub>2</sub> O <sub>3</sub>	0.00	0.03	0.02	0.02	0.02	0.03
La <sub>2</sub> O <sub>3</sub>	0.04	0.08	0.08	0.07	0.08	0.09
Ce <sub>2</sub> O <sub>3</sub>	0.06	0.09	0.10	0.93	0.10	0.11
Pr <sub>2</sub> O <sub>3</sub>	0.00	0.03	0.03	0.04	0.04	0.02
Nd <sub>2</sub> O <sub>3</sub>	0.05	0.08	0.09	0.07	0.08	0.08
Sm <sub>2</sub> O <sub>3</sub>	0.01	0.03	0.04	0.03	0.03	0.03
Eu <sub>2</sub> O <sub>3</sub>	0.00	0.00	0.01	0.00	0.00	0.00
Gd <sub>2</sub> O <sub>3</sub>	0.00	0.00	0.01	0.00	0.01	0.00
Dy <sub>2</sub> O <sub>3</sub>	0.00	0.00	0.01	0.01	0.00	0.01
Yb <sub>2</sub> O <sub>3</sub>	0.00	0.00	0.00	0.00	0.01	0.00
MgO	0.05	0.11	0.21	0.19	0.23	0.09
CaO	23.12	23.11	22.96	22.89	22.94	22.99
MnO	0.56	0.69	1.12	1.33	1.28	0.73
FeO	16.75	16.57	16.12	16.09	16.20	16.84
H <sub>2</sub> O	2.57	2.59	2.52	1.62	2.27	2.16
F	0.23	0.00	0.02	0.00	0.02	0.27
Cl	0.00	0.00	0.00	0.00	0.02	0.00
Subtotal	100.09	100.00	100.01	100.00	100.01	100.11
Less O=F	0.10	0.00	0.01	0.00	0.01	0.12
Less O=Cl	0.00	0.00	0.00	0.00	0.01	0.00
Total	100.00	100.00	100.00	100.00	100.00	99.99
Ions						
P	0.000	0.000	0.000	0.000	0.000	0.000
Nb	0.000	0.000	0.000	0.000	0.000	0.000
Ti	0.003	0.018	0.042	0.040	0.043	0.020
Zr	0.000	0.000	0.000	0.000	0.000	0.000
Th	0.000	0.000	0.000	0.000	0.000	0.000
U	0.000	0.000	0.000	0.000	0.000	0.000
Sc	0.002	0.003	0.003	0.003	0.003	0.002
Y	0.000	0.001	0.001	0.001	0.001	0.001
La	0.001	0.002	0.002	0.002	0.003	0.003
Ce	0.002	0.003	0.003	0.028	0.003	0.003
Pr	0.000	0.001	0.001	0.001	0.001	0.001
Nd	0.001	0.002	0.003	0.002	0.002	0.002
Sm	0.000	0.001	0.001	0.001	0.001	0.001
Eu	0.000	0.000	0.000	0.000	0.000	0.000
Gd	0.000	0.000	0.000	0.000	0.000	0.000
Dy	0.000	0.000	0.000	0.000	0.000	0.000
Yb	0.000	0.000	0.000	0.000	0.000	0.000
Ca	2.039	2.052	2.050	2.038	2.043	2.034
Σ A-Site	2.046	2.067	2.066	2.080	2.059	2.051
Al	1.954	1.956	1.956	1.947	1.943	1.940
Mg	0.006	0.014	0.026	0.023	0.028	0.011
Mn	0.039	0.048	0.079	0.094	0.090	0.051
Fe <sup>3+</sup>	1.281	1.275	1.249	1.243	1.251	1.292
Σ M-Site	3.279	3.293	3.310	3.307	3.312	3.294
Σ Si	3.000	3.000	3.000	3.000	3.000	3.000
OH	1.411	1.431	1.401	0.898	1.258	1.190
F	0.060	0.000	0.006	0.000	0.004	0.071
Cl	0.000	0.000	0.000	0.000	0.003	0.000
Σ Hydroxyl	1.471	1.431	1.407	0.898	1.266	1.261

Normalized to 3 Si a.p.f.u.

## **Thorogummite**

Thorogummite,  $(\text{Th}, \text{U})[(\text{OH})_{4x} | (\text{SiO}_4)_{1-x}]$ , occurs only as inclusions in wall zone allanite from the C cut in the Kingman Feldspar Quarry. The specimens recovered measured 0.3 cm long and were a mottled brown color.

Thorogummite was analyzed using the EMP and is given in Table 21. Ions were recalculated from the microprobe data using four oxygen a.p.f.u. Th is the dominant cation (Figure 35) in the A site with 0.56 a.p.f.u. Lesser amounts of U, Ce and Ca are present with 0.205, 0.115 and 0.063 a.p.f.u respectively. These inclusions are also enriched in LREE with very low HREE (Figure 36). There is also a small amount of Pr, 0.001 a.p.f.u., possibly left from the radioactive decay of the uranium.

Table 21. Recalculated  
Chemical Composition of  
Thorogummite from the  
Kingman Pegmatite

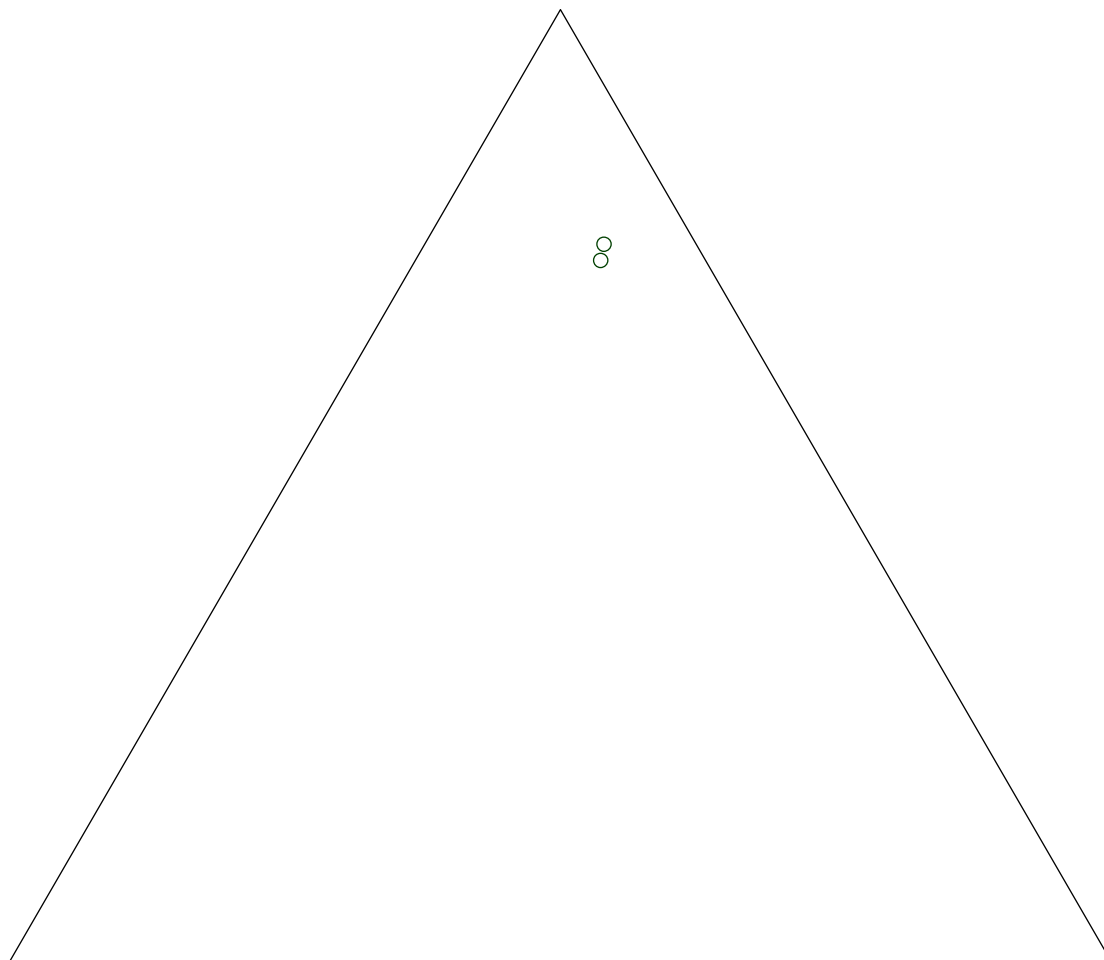
Oxides	KFMCM- 1-1	KFMCM- 1-2
P <sub>2</sub> O <sub>5</sub>	1.22	1.00
SiO <sub>2</sub>	14.33	13.99
TiO <sub>2</sub>	0.10	0.12
ZrO <sub>2</sub>	0.08	0.05
SnO <sub>2</sub>	0.08	0.06
ThO <sub>2</sub>	55.76	54.35
UO <sub>2</sub>	9.99	10.43
Al <sub>2</sub> O <sub>3</sub>	0.32	0.42
Sc <sub>2</sub> O <sub>3</sub>	0.22	0.25
Y <sub>2</sub> O <sub>3</sub>	0.11	0.11
La <sub>2</sub> O <sub>3</sub>	0.21	0.17
Ce <sub>2</sub> O <sub>3</sub>	6.98	7.34
Pr <sub>2</sub> O <sub>3</sub>	0.04	0.02
Nd <sub>2</sub> O <sub>3</sub>	0.21	0.20
Sm <sub>2</sub> O <sub>3</sub>	0.08	0.03
Dy <sub>2</sub> O <sub>3</sub>	0.02	0.00
Yb <sub>2</sub> O <sub>3</sub>	0.06	0.06
MgO	0.02	0.01
CaO	0.66	0.74
MnO	0.02	0.01
FeO	0.99	1.45
PbO	2.46	2.66
H <sub>2</sub> O	6.05	6.52
Total	100.00	100.00

Table 21 cont. Chemical  
Composition of Thorogummite  
from the Kingman Pegmatite

Ions	KFMCM- 1-1	KFMCM- 1-2
Ti	0.003	0.004
Zr	0.002	0.001
Sn	0.001	0.001
Th	0.571	0.552
U	0.200	0.207
Al	0.017	0.022
Sc	0.009	0.010
Y	0.003	0.002
La	0.004	0.003
Ce	0.115	0.120
Pr	0.001	0.000
Nd	0.003	0.003
Sm	0.001	0.000
Dy	0.000	0.000
Yb	0.001	0.001
Mg	0.003	0.001
Ca	0.063	0.071
Mn	0.002	0.001
Fe 2+	0.074	0.108
Pb	0.057	0.061
$\sum$ A-Site	1.130	1.169
P	0.047	0.038
Si	0.645	0.624
$\sum$ B-Site	0.692	0.662
$\sum$ Hydroxyl	1.816	1.940

## Thorogummite

Th



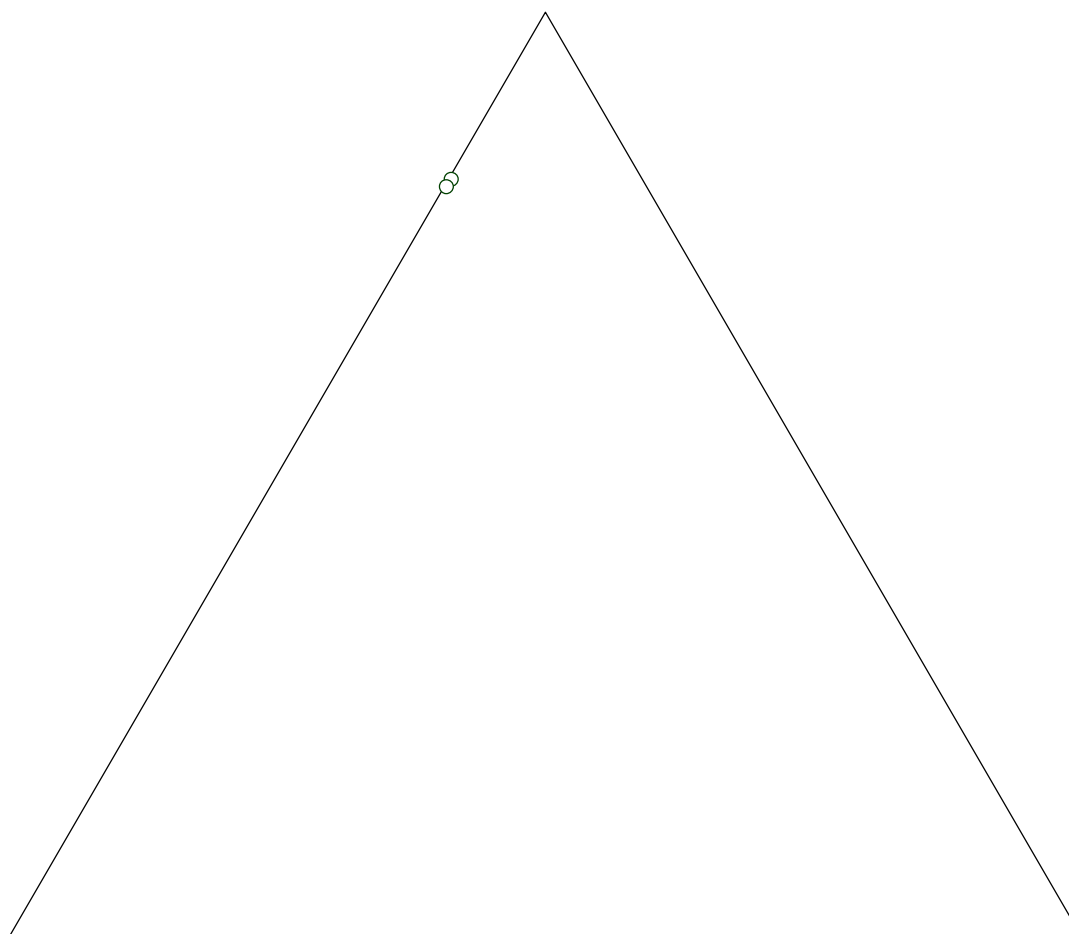
Ca

REE

Figure 35. Ternary diagram showing A-site occupancy for thorogummite from the Kingman Feldspar mine. Only a small amount of Ca and REE are substituting for Th in the samples

Thorogummite

Th



LREE

HREE+Y

Figure 36. Ternary diagram for thorogummite from the Kingman Feldspar mine showing very low HREE and Th > LREE.

## **Uraninite**

Uraninite,  $\text{UO}_2$ , specimens were only recovered from the C cut in the Kingman Feldspar Quarry. The uraninite samples measured 2 cm in length and had a yellowish brown color. The uraninite was found in the wall zone material associated with quartz and microcline.

Uraninite chemistry was analyzed using the EMP analytical results are given in Table 22. Ions were calculated from the microprobe data using two oxygen a.p.f.u (Table 22). U is the dominant cation at the A-site with an average of 0.75 apfu. Substituting for U are minor amounts of Th (0.046-0.052 a.p.f.u),  $\text{Fe}^{2+}$  (0.019 a.p.f.u.), Pb (0.023 apfu) and minor REE's.

Table 22. Chemical Composition of Uraninite from the Kingman Pegmatite

Oxides	KFMCF- 2-4	KFMCF- 2-5	KFMCM- 2-6	B-3- D-1	B-3- D-2	B-3- D-3	B-3- D-4	B-3- D-5
P <sub>2</sub> O <sub>5</sub>	0.02	0.03	0.06	0.02	0.00	0.00	0.04	0.04
SiO <sub>2</sub>	0.00	0.00	0.00	0.00	0.00	1.54	0.98	2.83
TiO <sub>2</sub>	0.21	0.34	0.29	0.45	0.22	0.39	0.41	0.17
ZrO <sub>2</sub>	0.03	0.05	0.05	0.02	0.00	0.00	0.02	0.01
ThO <sub>2</sub>	4.98	5.23	5.66	4.57	4.87	5.23	4.98	5.42
UO <sub>2</sub>	89.87	88.79	88.98	87.79	88.46	89.22	88.34	87.93
Al <sub>2</sub> O <sub>3</sub>	0.02	0.12	0.07	0.02	0.03	0.03	0.08	0.10
Y <sub>2</sub> O <sub>3</sub>	0.11	0.09	0.05	0.00	0.00	0.03	0.01	0.03
Ce <sub>2</sub> O <sub>3</sub>	0.00	0.00	0.00	0.05	0.12	0.16	0.09	0.22
CaO	0.12	0.22	0.09	0.54	0.03	0.05	0.12	0.09
MnO	0.01	0.01	0.01	0.00	0.00	0.01	0.00	0.00
FeO	0.79	1.09	0.66	0.85	0.34	0.46	0.52	0.15
PbO	2.23	2.34	2.45	2.11	2.57	2.61	2.16	2.32
Total	98.41	98.32	98.36	96.42	96.64	99.74	97.76	99.30

Ions	P	Si	Ti	Zr	Th	U	Al	Y	Ce	Ca	Mn	Fe <sup>2+</sup>	Pb	$\sum$ A-Site
P	0.001	0.001	0.002	0.001	0.000	0.000	0.001	0.000	0.000	0.001	0.000	0.005	0.000	0.001
Si	0.000	0.000	0.000	0.000	0.000	0.000	0.057	0.037	0.037	0.012	0.000	0.000	0.000	0.112
Ti	0.006	0.010	0.009	0.012	0.006	0.011	0.012	0.005	0.000	0.000	0.000	0.000	0.000	0.000
Zr	0.001	0.001	0.001	0.000	0.000	0.000	0.000	0.000	0.000	0.000	0.000	0.000	0.000	0.000
Th	0.046	0.047	0.052	0.037	0.041	0.044	0.043	0.049	0.000	0.000	0.000	0.000	0.000	0.000
U	0.809	0.788	0.797	0.701	0.726	0.733	0.741	0.771	0.000	0.000	0.000	0.000	0.000	0.000
Al	0.001	0.006	0.003	0.001	0.001	0.001	0.004	0.005	0.001	0.001	0.000	0.000	0.000	0.005
Y	0.002	0.002	0.001	0.000	0.000	0.001	0.000	0.001	0.001	0.000	0.000	0.000	0.000	0.001
Ce	0.000	0.000	0.000	0.001	0.002	0.002	0.001	0.003	0.001	0.002	0.000	0.000	0.000	0.003
Ca	0.005	0.010	0.004	0.021	0.001	0.002	0.005	0.004	0.001	0.002	0.000	0.000	0.000	0.004
Mn	0.000	0.000	0.000	0.000	0.000	0.000	0.000	0.000	0.000	0.000	0.000	0.000	0.000	0.000
Fe <sup>2+</sup>	0.027	0.036	0.022	0.026	0.011	0.014	0.016	0.005	0.000	0.000	0.000	0.000	0.005	0.000
Pb	0.023	0.024	0.025	0.020	0.024	0.025	0.021	0.024	0.000	0.000	0.000	0.000	0.000	0.024
$\sum$ A-Site	1.032	1.041	1.030	1.042	1.024	1.121	1.026	1.019	0.000	0.000	0.000	0.000	0.000	0.000

## **Goethite**

Goethite,  $\alpha\text{-Fe}^{3+}\text{O(OH)}$ , specimens were recovered only from the Wagon Bow #3 Quarry and were found clustered together. The goethite was found when a radiation detector picked up a large monazite crystal and, once found, others crystals were found in the vicinity. The goethite measured 1 cm in size and was a reddish brown color. They were found in place in the wall zone associated with monazite, microcline, and quartz.

Goethite was analyzed using the EMP and analytical results are given in Table 23. Ions were calculated from the microprobe analysis on the basis of two oxygen and hydroxyl a.p.f.u. In order to balance the equation, 1 a.p.f.u of  $\text{OH}^-$  was added by hand to the 0.98  $\text{Fe}^{3+}$  a.p.f.u.

Table 23. Chemical Composition of Goethite from the Wagon Bow #3 Pegmatite

Oxides	WH1MY-1	WH1MY-2	WH1MY-3	WH1MY-4	WH1MY-5
Al <sub>2</sub> O <sub>3</sub>	0.33	0.18	0.42	0.26	0.23
Fe <sub>2</sub> O <sub>3</sub>	88.74	89.03	88.95	89.14	88.52
CaO	0.02	0.10	0.09	0.07	0.13
Mn <sub>2</sub> O <sub>3</sub>	0.13	0.11	0.16	0.13	0.03
H <sub>2</sub> O	10.09	10.09	10.14	10.13	10.05
Total	99.31	99.51	99.76	99.73	98.96
Ions					
Al	0.006	0.003	0.007	0.004	0.004
Fe 3+	0.993	0.996	0.990	0.993	0.994
Ca	0.000	0.002	0.001	0.001	0.002
Mn3+	0.001	0.001	0.002	0.002	0.000
Σ A-Site	1.000	1.000	1.000	1.000	1.000
Σ Hydroxyl	1.000	1.000	1.000	1.000	1.000

## **Major & Trace Element Chemistry**

Whole rock samples from the Wagon Bow and Kingman Feldspar Mine host rocks, and the dike that intrudes the Kingman Feldspar host rock, were analyzed using X-Ray Fluorescence (XRF) for both major and trace elements. Analytical results for the major elements are presented in Table 24 and trace elements in Table 25. Trace elements were also analyzed by Direct-Coupled Plasma Spectrometry (DCP) and Inductively-Coupled Plasma Spectrometry-Mass Spectrometry (ICP-MS), Tables 34-37. Abbreviations for the samples are as follows: Kingman (Site-F, HGO-A, KFMB-1, and KFM-C), Kingman Dike (DM-1), Wagon Bow #1 (WH-1), Wagon Bow #3 (WH-3) and Wagon Bow Spotted Granite (SGWH-1). Water was determined by loss on ignition (LOI).

### *Major Elements*

Oxides versus silica diagrams for the major elements are shown in Figure 37. In general, the more compatible elements including Fe<sub>2</sub>O<sub>3</sub>, MgO and CaO decrease with increasing silica content. However, the more incompatible elements do not produce clear trends. Though TiO<sub>2</sub> and MnO show a clear decreasing trend Al<sub>2</sub>O<sub>3</sub>, Na<sub>2</sub>O and K<sub>2</sub>O exhibit considerable variation over a small range of SiO<sub>2</sub>. The P<sub>2</sub>O<sub>5</sub> plot also shows considerable variation with a distinct enrichment in P<sub>2</sub>O<sub>5</sub> for the Kingman samples.

### *Trace Elements*

Silica vs. trace element (ppm) diagrams for trace elements are shown in Figure 38. The generally compatible elements including Cr, Ni, Cu, and Zn show the expected decrease with increasing silica. As with the major elements, the relationship between the more strongly incompatible trace elements and silica are more complex. Sr, V, Pr, and Zr decrease with increasing SiO<sub>2</sub>. Rb and Ga also generally increase with the exception of samples from the Rare

Metals line rock, which exhibit considerable variation. Ba, Y, Nb, La, Ga, Ce, Sm, Yb, Pb, Th, and U exhibit considerable scatter. In general, the REE's are higher in the Kingman quartz monzonite as compared to the granites from the Aquarius Range. Several of these elements, Ba, Zr and Hf are unusually high in quartz diorite from the Kingman Feldspar mine. The high Ba is attributed to the presence of K-feldspar megacrysts. The Zr and Hf enrichment is attributed to the presence of inherited zircon which is present in the Cerbat Range intrusions (DUEBENDORFER et al., 2001).

Variation diagrams showing Rb versus Sr, Rb versus K<sub>2</sub>O and CaO, and Sr versus K<sub>2</sub>O and CaO are shown in Figures 39 and 40. Rb versus Sr crudely exhibits the typical antithetic behavior as Rb decreases with increasing Sr. The remainder of the diagrams show mixed results. In general, Rb decreases and Sr increases with increasing CaO, however, no real trend emerges when Sr and Rb are plotted against K<sub>2</sub>O.

Trace element data were evaluated in an effort to determine the tectonic origin of the host rocks. On an Y-Nb-GaX3 variation diagram based on work done by EBY (1992), all of the granitic host rocks lie, within analytical error, in the A2 field, suggesting a collisional, post-collisional or anorogenic origin (Figure 41). In an effort to further constrain the tectonic affiliation, host rock chemistry was plotted on discrimination diagrams from Pearce et al. (1984) (Figures 42-44) and the Hf-Rb/30-TaX3 discrimination diagram of Harris et al. (1986) (Figure 45). Additionally, spider diagrams normalized to the Ocean Ridge Granite of Pearce (1984) are given in Figure 46 and a chondrite normalized REE diagram in Figure 47. Note that line rock from the Rare Metals mine was not included in this evaluation as it represents a pegmaticic segregation rather than a granitic host rock. A cursory examination of these diagrams reveals that the nature of these host rocks is complex and they cannot easily be classified based on the

tectonic origin. For this reason, the following discussion will evaluate host rocks from each pegmatite individually.

The Kingman Feldspar quartz diorite falls within the within plate granite in all three Pearce discrimination diagrams (Figures 42-44). While it lies in the volcanic arc field of the Harris diagram (Figure 45), this may be an artifact of Hf enrichment due to the presence of inherited Zr and not indicative of the melt source. The spider diagrams also yield conflicting evidence. Consistent with a within plate origin, both Rb and Th are high and enriched relative to Ta and Nb and Ce and Sm are enriched relative to adjacent elements (Figure 46b). However, the distinguishing negative Ba anomaly is absent, giving the overall enrichment and depletion trends more of an attenuated within plate crust appearance (Figure 46d). The REE plot exhibits a negative slope with a small Eu anomaly, indicative of fractionation of plagioclase (Figure 47).

The Wagon Bow # 3 granite lies in the within plate field on all 3 of the Pearce diagrams (Figures 42-44) yet lies just above the post-collisional / within plate boundary in the post-collisional field on the Harris diagram (Figure 46). The spider diagrams show further conflicting evidence. The large Ba anomaly is consistent with a within plate origin (Figure 46b) yet the Rb and Th spikes, as well as low Hf and Zr (which generally remain in the melt residues) are more consistent with attenuate within plate and syn-collisional granites (Figure 46a and 46c). Further evidence suggesting an orogenic or post-orogenic origin lies in the generally lower REE concentrations as compared to the Kingman host rock (Figure 47). Additionally, the granite exhibits a strong negative Eu anomaly consistent with the fractionation of plagioclase.

The Wagon Bow #1 plots as a within plate granite on the Yb versus Ta diagram, just beyond that field into the volcanic arc / syn-collisional granite on the Nb versus Y diagram and at the intersection of all three zones on the Y+Nb versus Rb diagram (Figures 42-44). On the

Harris diagram, this granite lies clearly within the post-collisional zone (Figure 45). Again the spider diagrams provide conflicting evidence. It exhibits spikes for Rb and Th and has generally lower less incompatible elements (Hf – Yb), thus are comparable to the syn-collisional granites of Pearce (1984) (Figure 46a).

The Wagon Bow spotted granite lies in the volcanic arc field of the Pearce diagrams (Figures 41-43) and the Harris diagram (Figure 45). The spider diagrams for this granite are even more difficult to evaluate it does not clearly fall into any of the fields. The most incompatible elements generally lie above the fields for within plate, orogenic and volcanic arc granites whereas the less incompatible elements lie above the orogenic and volcanic arc fields and below the within plate granite field. Additionally, the REE composition lies sandwiched between the Kingman quartz monzonites and the Wagon Bow granites.

The conflicting signatures of these granites are a direct result of the complex plate boundary that existed in the area during the Paleoproterozoic. In the early Proterozoic, pre-collision rifting of the eastern Mojave margin generated isolated domains of Mojave and isotopically distinct juvenile crust. Immediately following rifting, between 1.74 and 1.72 Ga, the Yavapai and Mojave provinces sutured together. This event was closely followed by the Yavapai Orogeny (1.71 – 1.68 Ga) during which time the diminishing subduction boundary became collisional as the sutured terranes docked with North American continent (Duebendorfer et al., 2001.). Thus, it is unlikely that these granites are of within plate origin. However, the geochemistry does not clearly suggest an attenuated within plate, volcanic arc or syn-collisional origin. Thus, it is likely that these granites are all post-collisional. Pearce et al., (1984) report that major problems exist when classifying post-orogenic granites as they often cannot be attributed to a single mantle or crustal source. Thus, they can be of within plate, volcanic arc or

syn-collisional composition. Furthermore, if they originate during a time when both thermal relaxation in the lower crust and adiabatic decompression in the upper mantle are occurring, the resulting chemical signature will contain components from crustal and upper mantle sources (Harris et al., 1986). This upper mantle contribution can be varied, from either “within plate” or “arc” composition (Pearce, 1984; England and Thomas, 1984 and Harris, 1981). In these cases, the discrimination diagrams can be used to evaluate the potential contributions from each source (Pearce et al., 1984). The Kingman quartz diorite, which lies in the within plate field on the Pearce diagrams, generally exhibits both an attenuated within plate as well as a within plate signature on the spider diagrams. Alternatively, the Wagon Bow granites, which show mixed affiliations on the Pearce diagrams, show affinities to both lower crustal within plate and attenuated within plate granites on the Spider diagrams. Additionally, they lie in the post-collisional field on the Hf vs. Rb/30 vs. TaX3 diagram. This suggests that both the Kingman quartz diorite and the Wagon Bow granites are hybrid granites that are the result of partial melting of predominantly rift related granitic protoliths. The Wagon Bow spotted granite exhibits similar within plate and attenuated within plate characteristics yet also exhibits minor volcanic arc affinities suggesting there may also be a volcanic arc contribution to the melt. In summary, while these granites were formed during the collisional events associated with the suturing of the Yavapai and Mojave terranes as well as the subsequent Yavapai Orogeny, they exhibit a strong attenuated within plate (rift) signature that is representative of the rift related protolith.

Finally, it is important to note that there are no timing implications with regard to the above argument. While the mixed signatures suggests these granitic rocks are “post collisional,” the complexity of collisional zones allow for a non-sequential formation of syn- and post-

collisional granites. Instead, the timing of these events is dependent on the rates of crustal thickening and subsidiary subduction (Harris et al., 1986). It has been demonstrated that in the Alps, the syn-collisional Novate intrusion postdates the post-collisional Bergell suite (Gulson and Krogh, 1973).

Table 24. Whole rock data for the major elements.(XRF)

Sample	HGO-A	KFMB-1	KFM-C	DM-1	RMM-B	RMM-M	RMM-T	WH-3	WH-1	SGWH-1
SiO <sub>2</sub>	62.6	61.2	63.15	48.55	68.8	71.34	70.48	73.28	69.32	68.44
TiO <sub>2</sub>	0.86	1.01	1	2.02	0.03	0.02	0.02	0.04	0.15	0.38
Al <sub>2</sub> O <sub>3</sub>	13.73	13.55	13.63	14.47	17.64	17.03	19.67	15.24	13.78	14.11
Fe <sub>2</sub> O <sub>3</sub>	6.13	6.51	6.43	15.47	0.48	0.39	0.19	0.64	1.6	3.55
MnO	0.09	0.11	0.1	0.18	0.01	0.01	0	0.01	0.03	0.05
MgO	1.38	1.48	1.48	5.07	0.07	0.06	0.02	0.13	0.32	0.57
CaO	3.03	3.64	3.44	7.79	0.4	0.3	0.38	0.15	0.99	1.64
Na <sub>2</sub> O	3.37	3.22	2.89	2.76	8.81	8.84	10.89	6.99	3.16	2.24
K <sub>2</sub> O	3.05	3.05	3.85	0.82	0.84	0.61	0.18	1.04	4.95	5.65
P <sub>2</sub> O <sub>5</sub>	0.32	0.39	0.37	0.31	0.01	0.02	0.01	0.01	0.04	0.12
Subtotal	94.56	94.16	96.34	97.44	97.09	98.62	101.84	97.53	94.34	96.75
LOI	5.16	5.53	3.39	2.43	2.83	1.33	0	2.41	5.54	3.03
Total	99.72	99.69	99.73	99.87	99.92	99.95	101.84	99.94	99.88	99.78

Table 25. Whole rock data for the trace elements.

Sample	HGO-A	KFMB-1	KFM-C	DM-1	RMM-B	RMM-M	RMM-T	WH-3	WH-1	SGWH-1
Ni (PPM)	5	7	6	92	0	0	0	bf	bf	2
Cu (PPM)	51	22	7	71	0	0	0	11	bf	8
Zn (PPM)	95	94	98	111	35	37	9	13	40	43
Rb (PPM)	190	171	130	22	438	270	42	212	270	218
Sr (PPM)	259	271	304	307	44	54	72	40	122	188
Zr (PPM)	586	652	600	145	50	57	64	21	129	379
Ga (PPM)*	52.94	55.9	49.42	47.66	84.53	103.73	61.25	67.39	51.36	58.39
Ba (PPM) <sup>1</sup>	1340.46	1397.97	1308.45	299.81	13.52	20.77	15	50.74	647.68	1234.16
La (PPM) <sup>1</sup>	80.64	89.41	78.95	15.96	10.61	8.78	6.64	12.39	24.72	100.8
Ce (PPM) <sup>1</sup>	176.4	208	169.3	33.65	24.93	23.53	14.82	46.75	72.47	223.2
Pr (PPM) <sup>1</sup>	21.93	28.52	23.32	4.93	4.07	4.18	2.57	5.63	5.1	21.43
Nd (PPM) <sup>1</sup>	85.39	119.4	92.31	22.57	14.92	15.84	9.45	21.94	16.43	66.98
Sm (PPM) <sup>1</sup>	16.4	25	19.5	5.81	6.43	6.95	4.81	6.9	3.04	9.9
Eu (PPM) <sup>1</sup>	2.4	3.63	3.19	1.87	0.14	0.17	0.18	0.17	0.55	1.15
Gd (PPM) <sup>1</sup>	14.6	21.9	17.8	6.08	6.89	8.19	6.46	6.48	3.44	8.32
Y (PPM) <sup>1</sup>	67.3	109	90.7	30.9	61.8	106	91.9	55.9	26.9	28
Dy (PPM) <sup>1</sup>	11.4	18.6	15.2	5.44	6.93	9.87	10.1	6.78	3.95	5.22
Ho (PPM) <sup>1</sup>	2.33	3.85	3.22	1.15	0.72	1.19	1.16	0.99	0.76	0.85
Er (PPM) <sup>1</sup>	6.08	10.43	8.67	3.11	1.32	2.38	2.46	2.63	2.23	2.24
Lu (PPM) <sup>1</sup>	0.68	1.17	0.99	0.38	0.2	0.31	0.38	0.52	0.41	0.4
Yb (PPM) <sup>1</sup>	4.93	8.88	7.48	2.83	1.07	2.1	2.54	3.41	2.54	2.35
Tb (PPM) <sup>1</sup>	2.16	3.41	2.81	0.99	1.25	1.65	1.45	1.06	0.58	1.01
V (PPM) <sup>1</sup>	51.42	57.91	59.84	319.68	10.85	11.8	12.35	17.67	17.5	52.21
Cr (PPM) <sup>1</sup>	10.03	11.9	10.94	37.06	2.21	2.37	2.15	3.02	3.26	14.92
Nb (PPM) <sup>1</sup>	25.6	36.9	33.3	6.33	26.1	32.9	31.3	23	24.6	16.6
Hf (PPM) <sup>1</sup>	13.07	15.1	13.99	4.02	6.86	9.46	10.69	3.11	3.91	8.44
Ta (PPM) <sup>1</sup>	1.01	1.53	1.65	0.39	27.2	34.4	35.8	9.02	3.5	1.3
Pb (PPM) <sup>1</sup>	15.5	14.7	15.9	3.63	16	18.3	21.3	9.25	64.7	36.5
Th (PPM) <sup>1</sup>	8.38	7.69	9.97	2.13	3.59	5.5	10.3	12.4	34.2	40.3
U (PPM) <sup>1</sup>	2.71	2.61	2.54	0.4	4.1	6.76	5.91	2.37	9.14	3.23

\* Analyzed by DCP

<sup>1</sup> Analyzed by ICP-MS

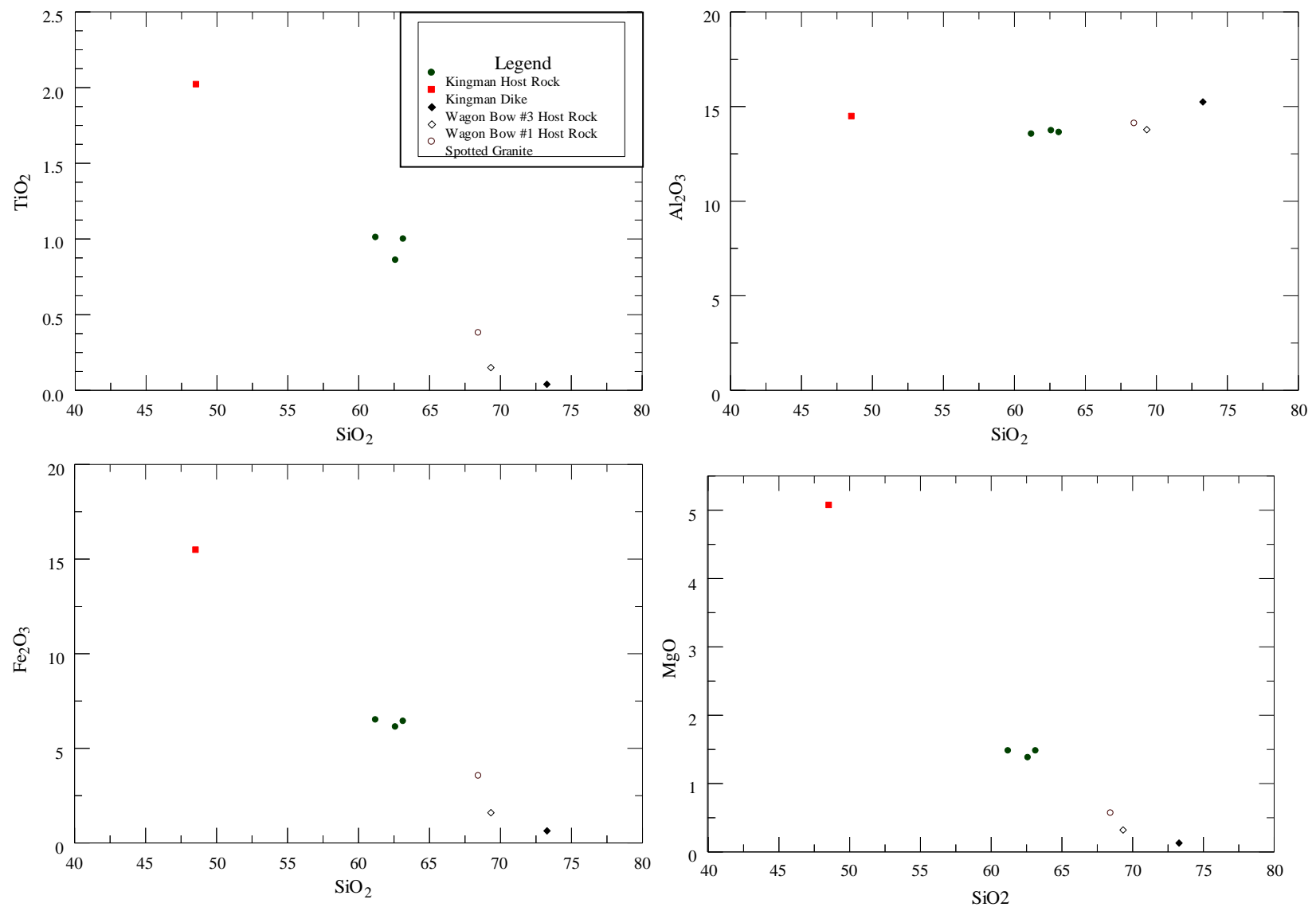


Figure 37. Variation diagrams showing major elements versus silica for pegmatite and host rocks.

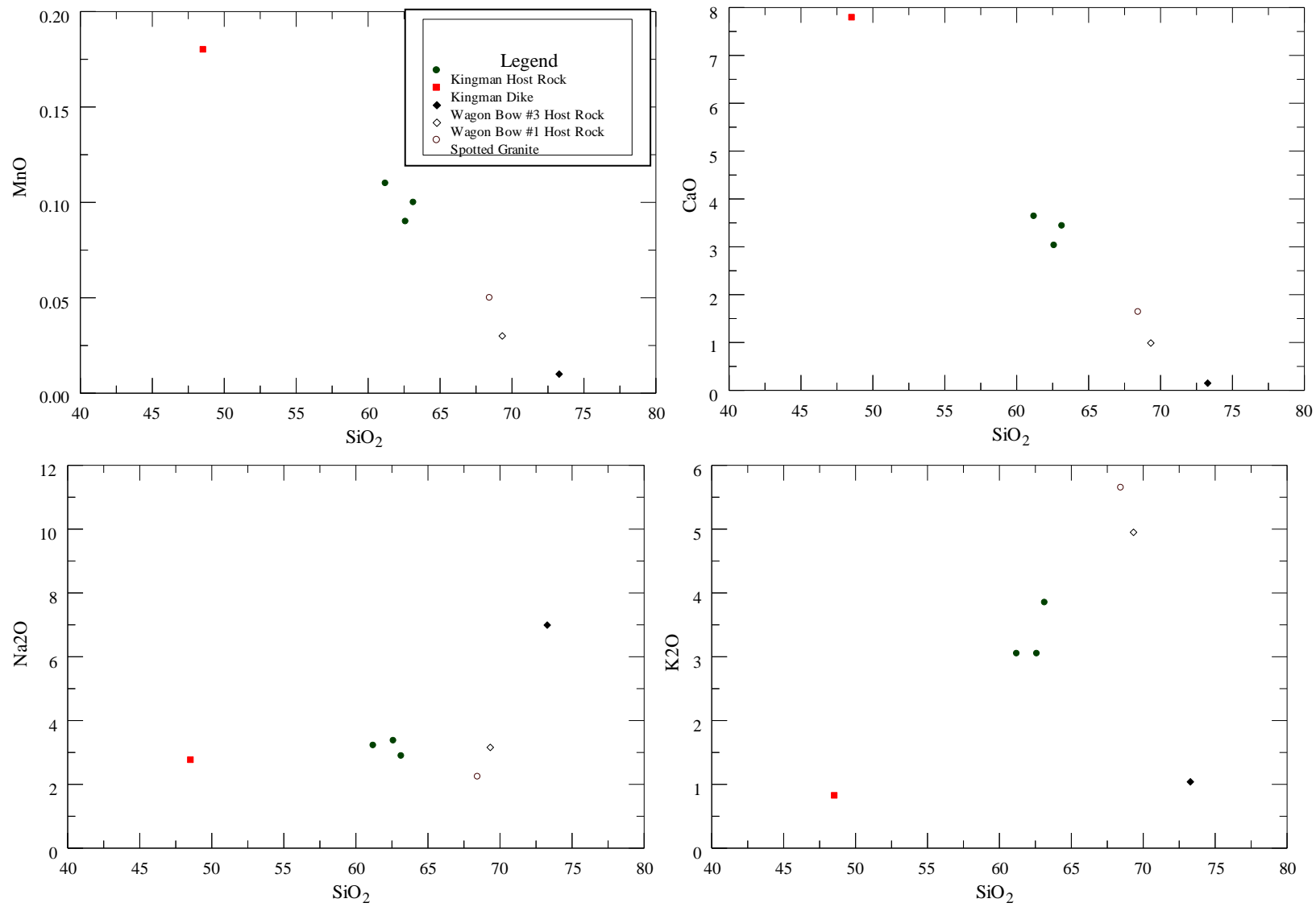


Figure 37. Continued.

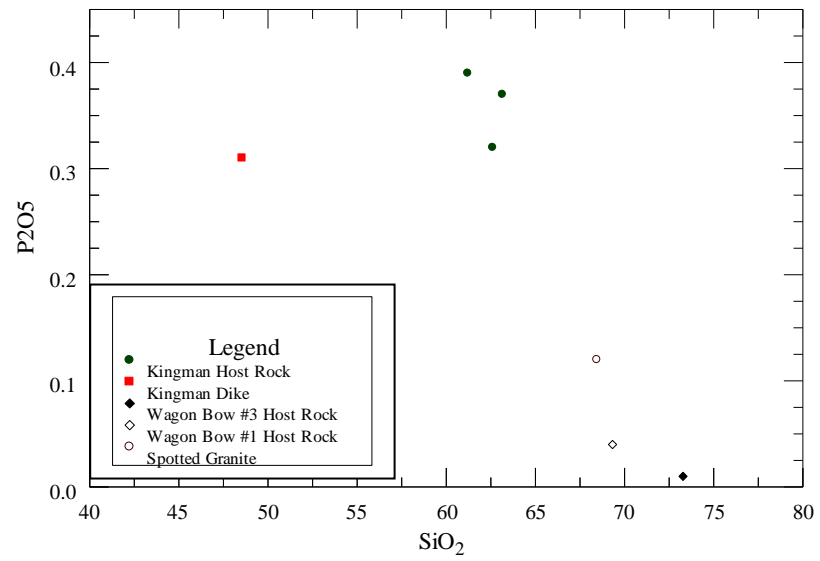


Figure 37. Continued.

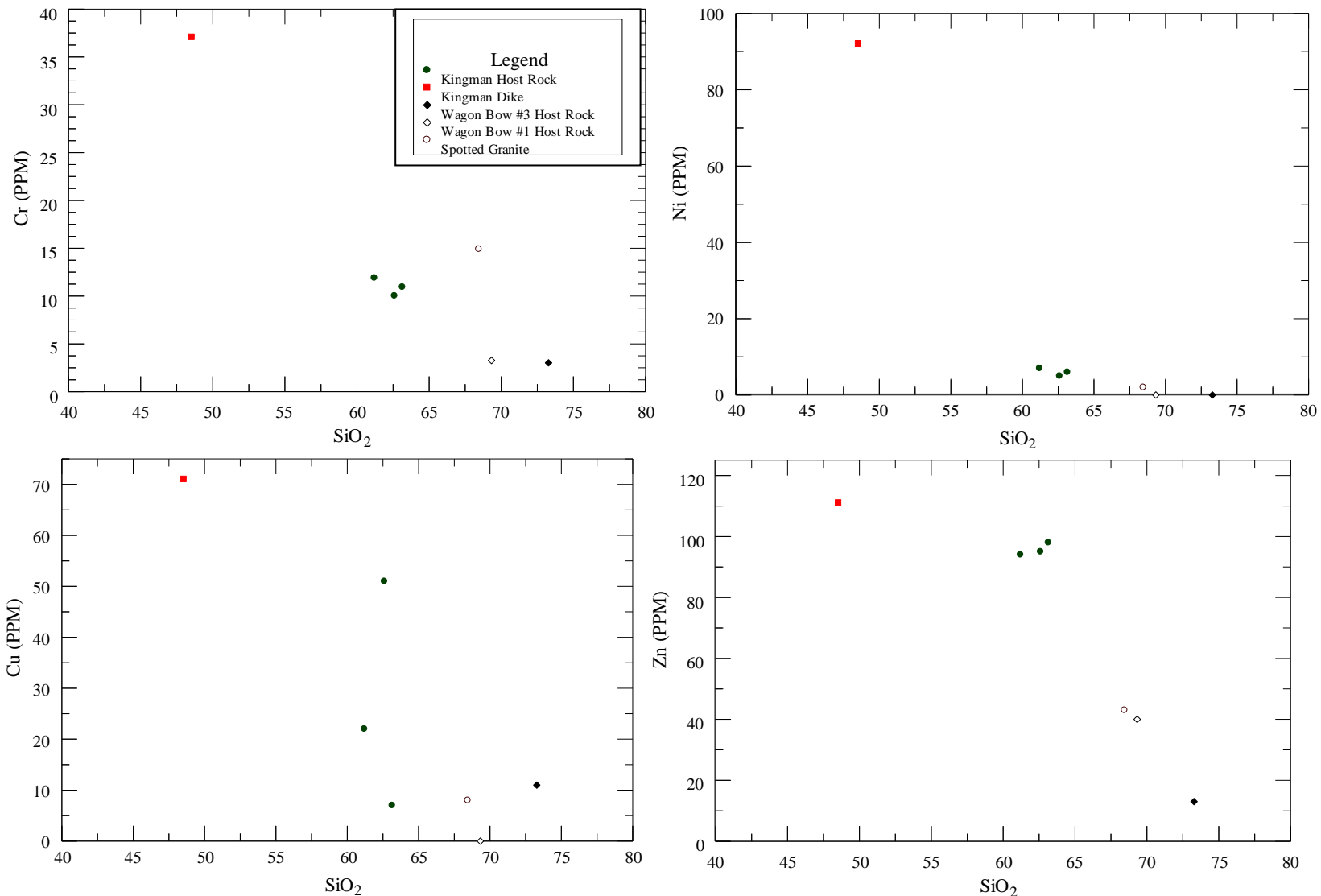


Figure 38. Variation diagrams showing trace elements versus silica for pegmatite and host rocks.

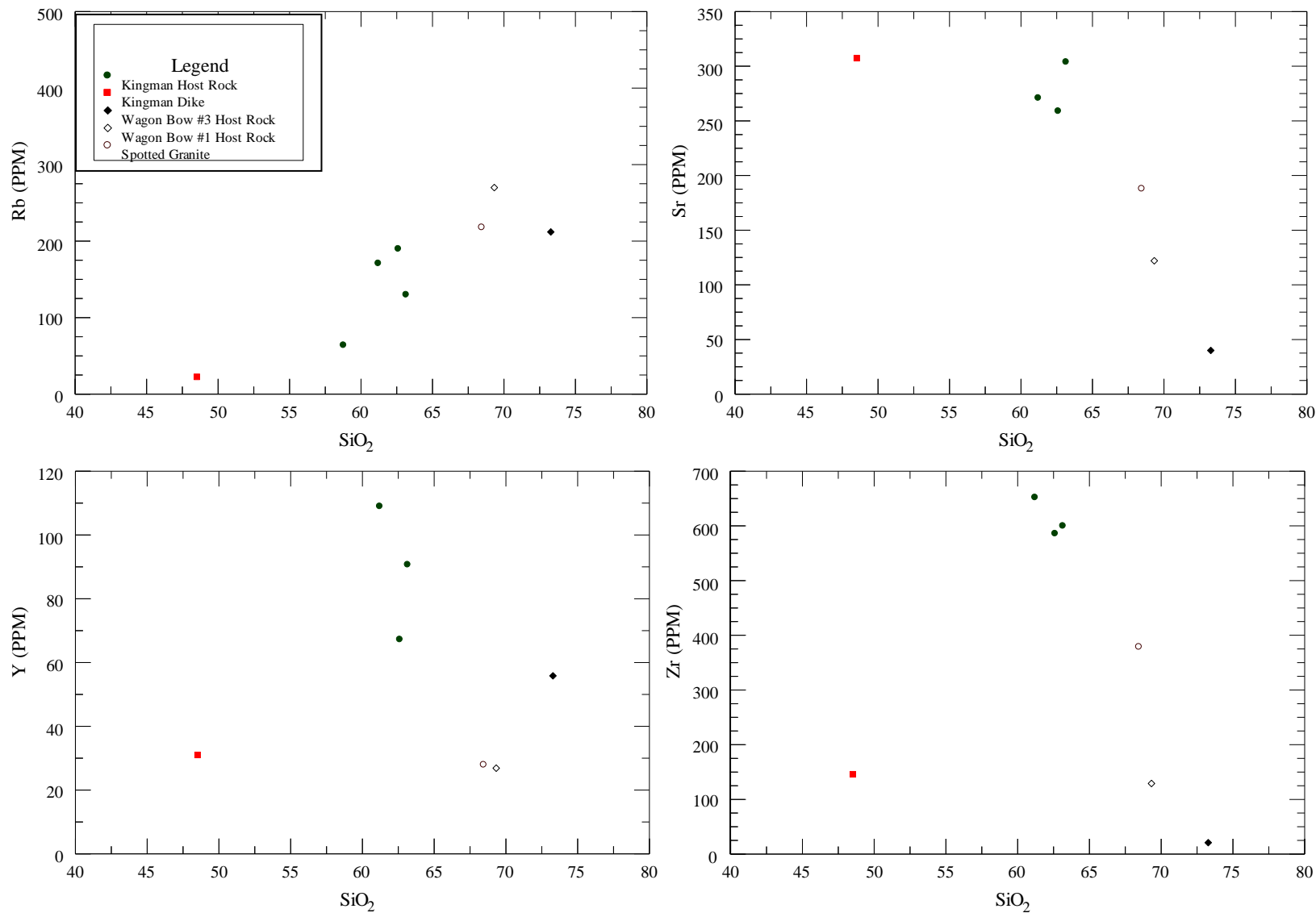


Figure 38. Continued

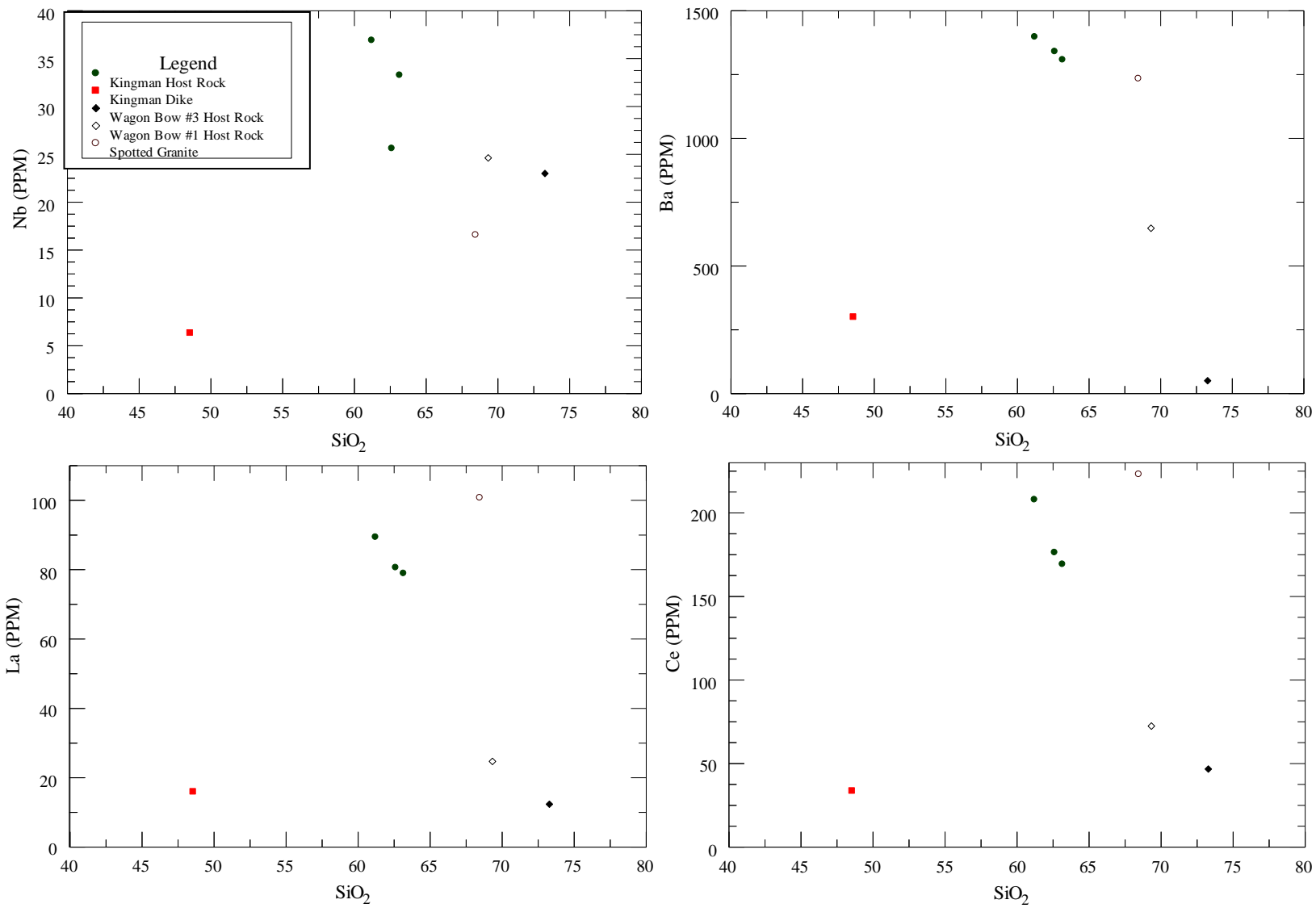


Figure 38. Continued

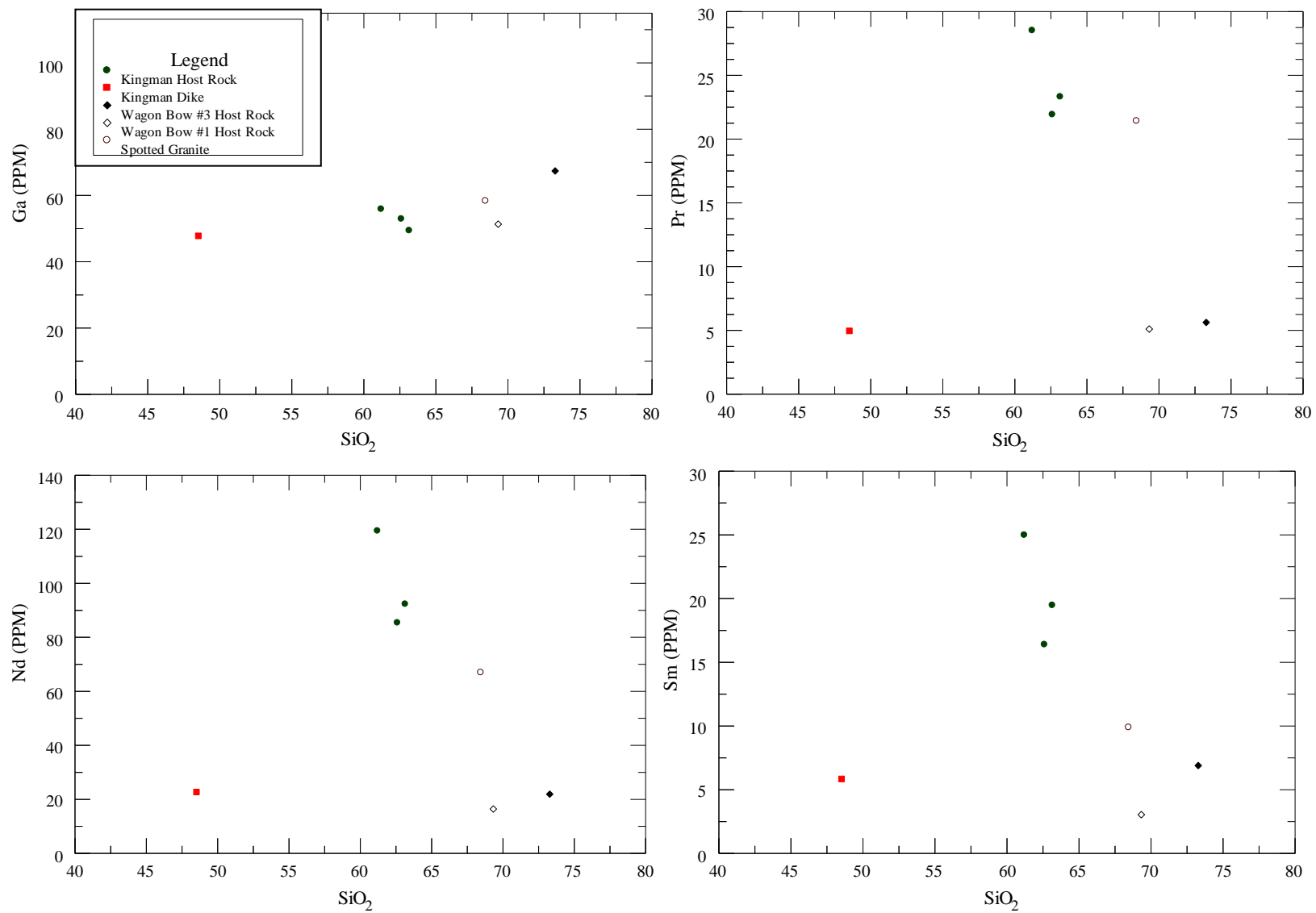


Figure 38. Continued

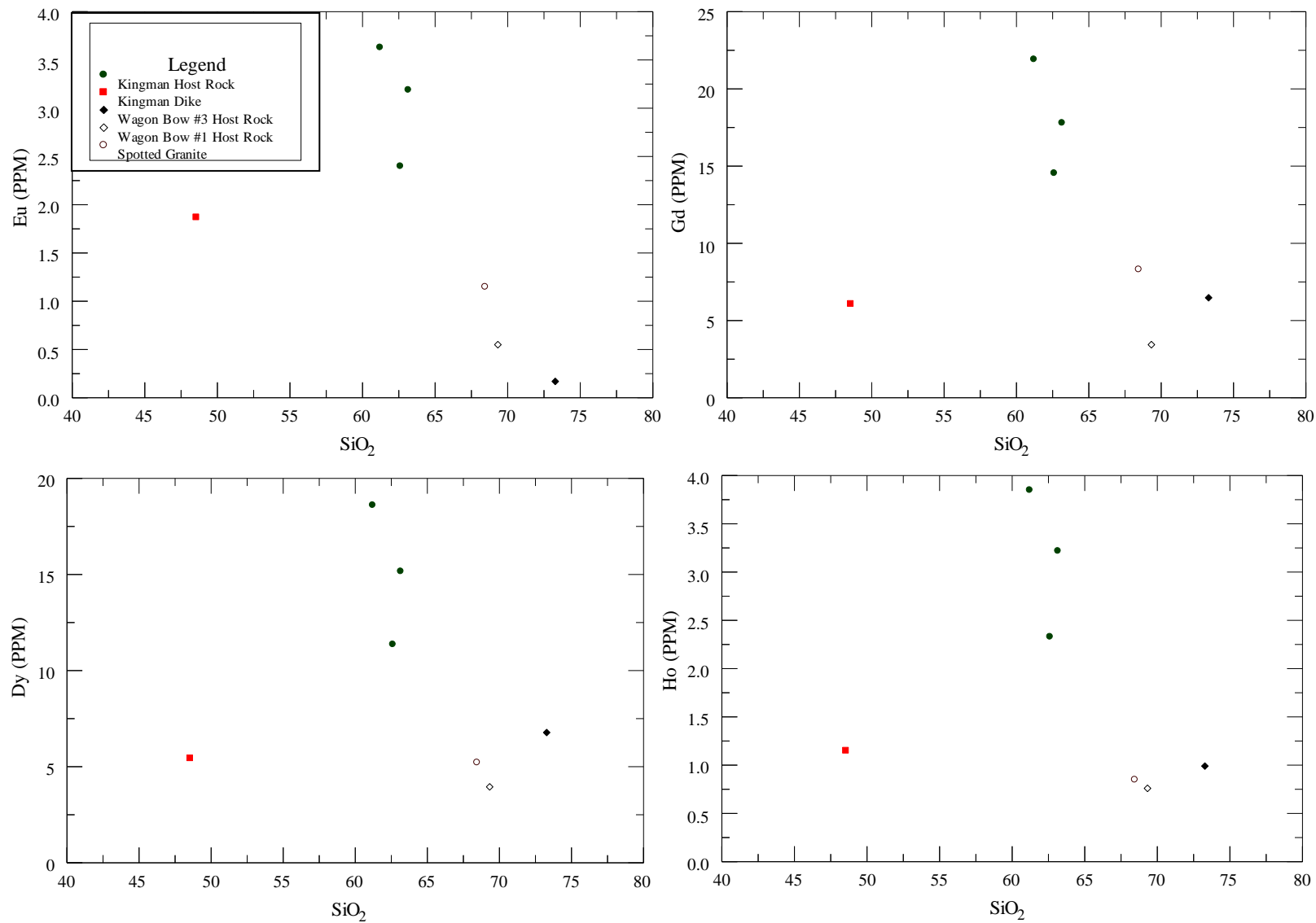


Figure 38. Continued

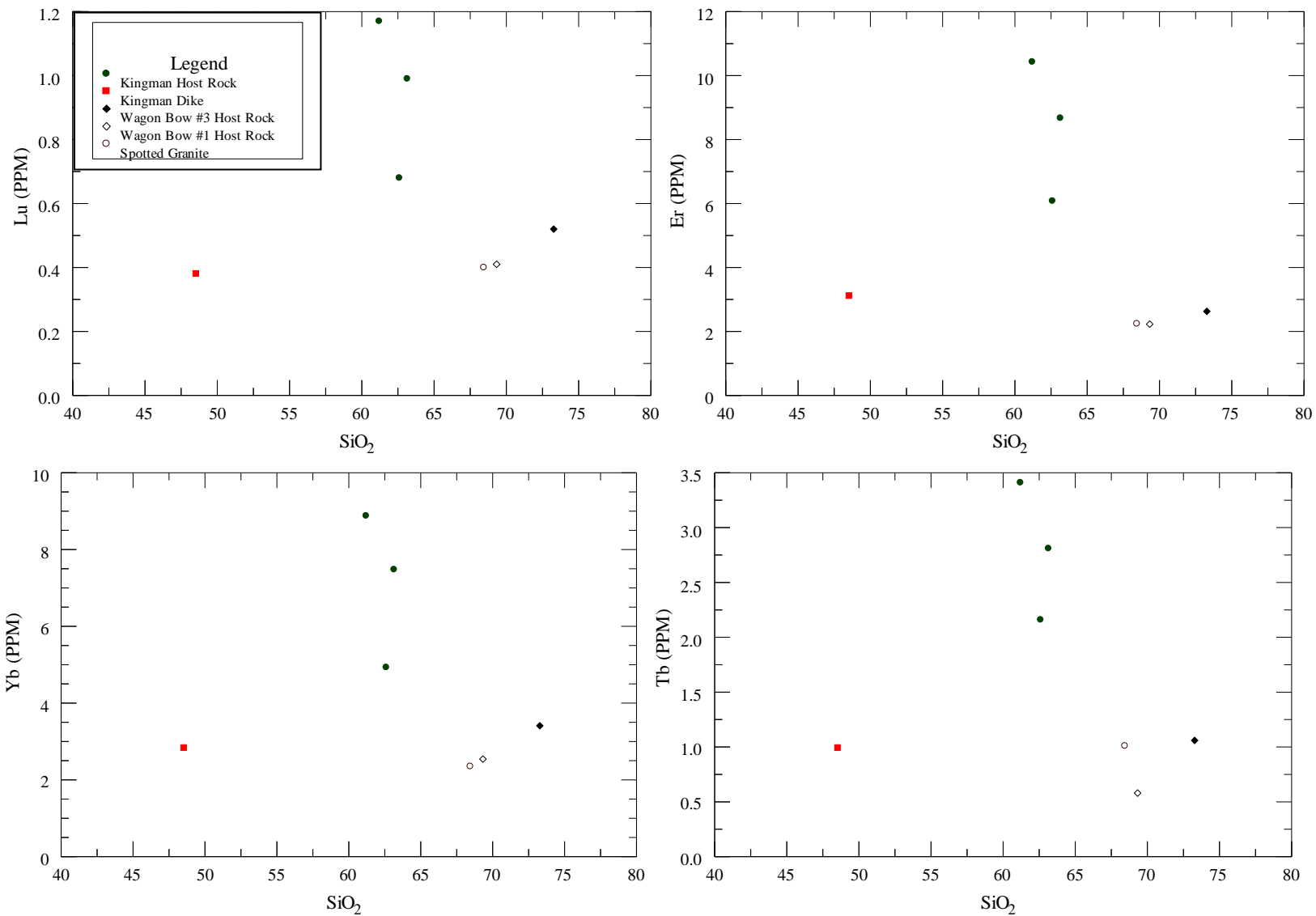


Figure 38. Continued

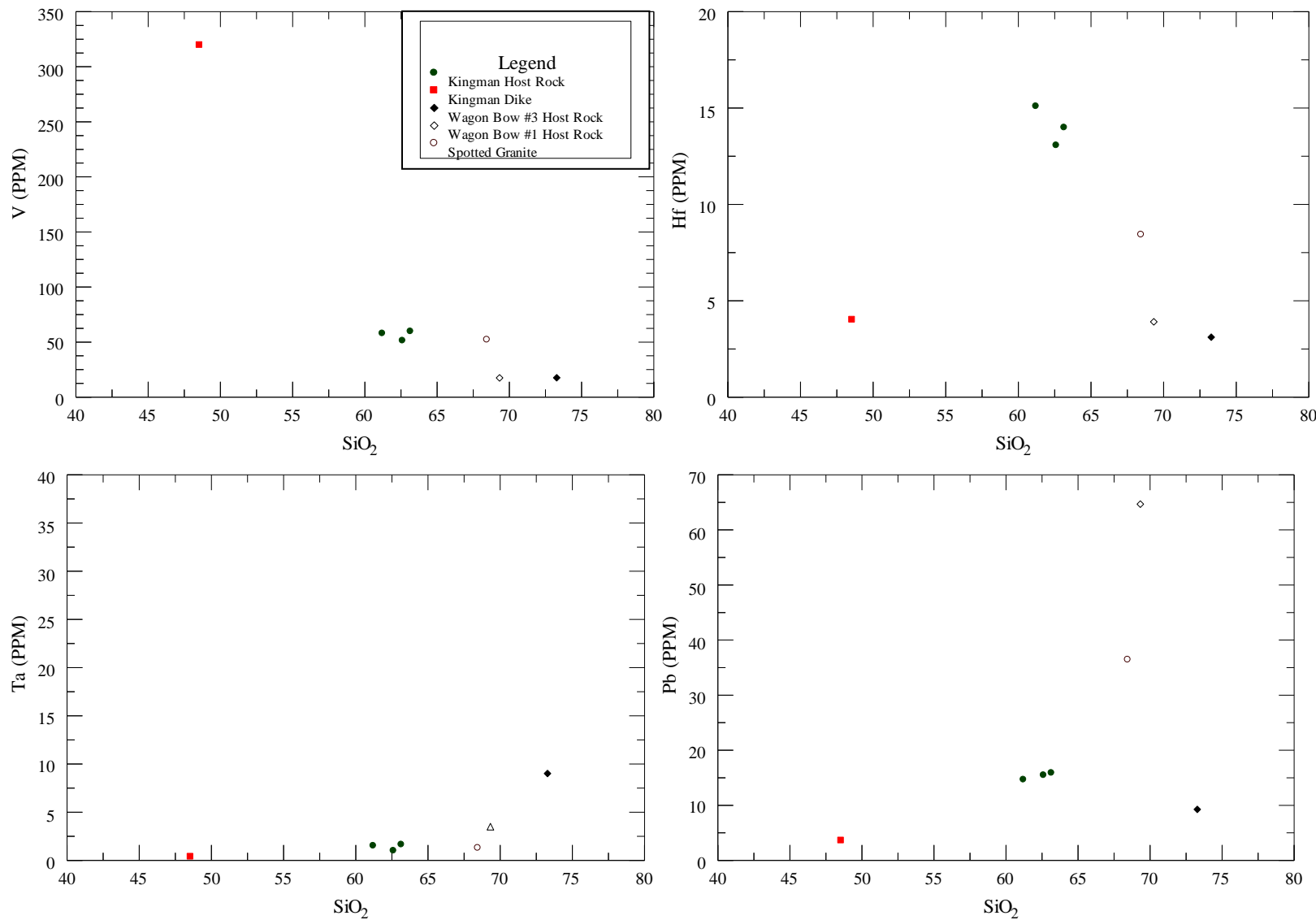


Figure 38. Continued

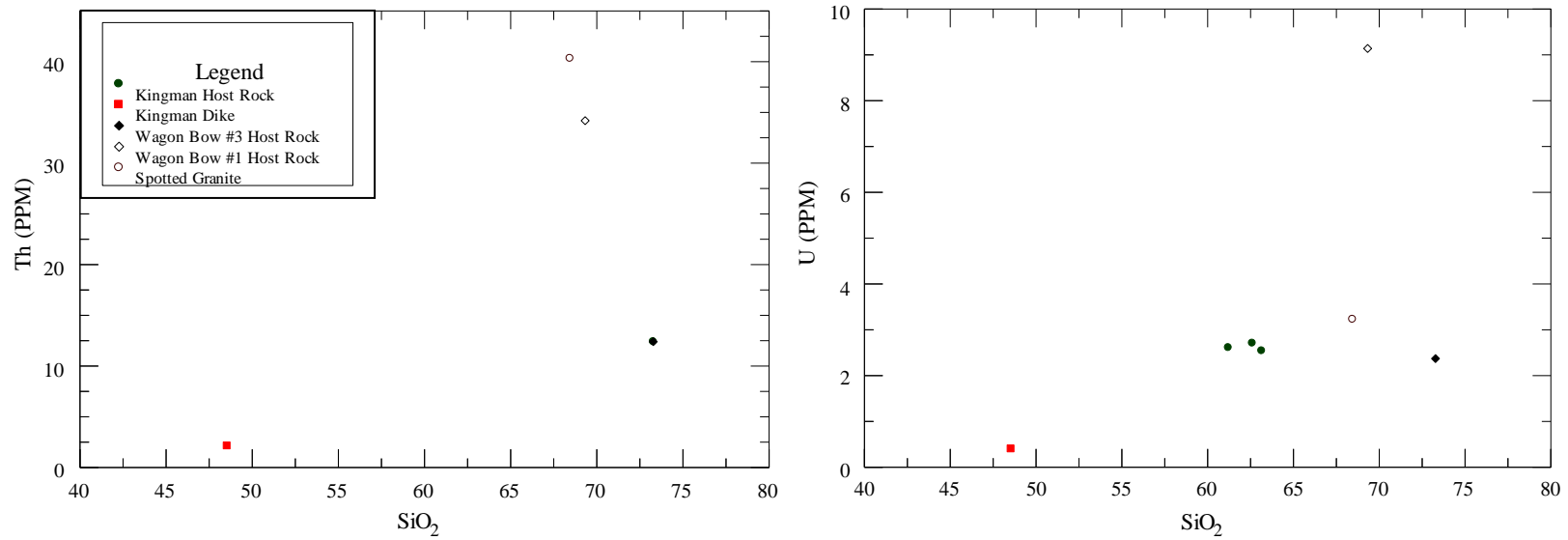


Figure 38. Continued

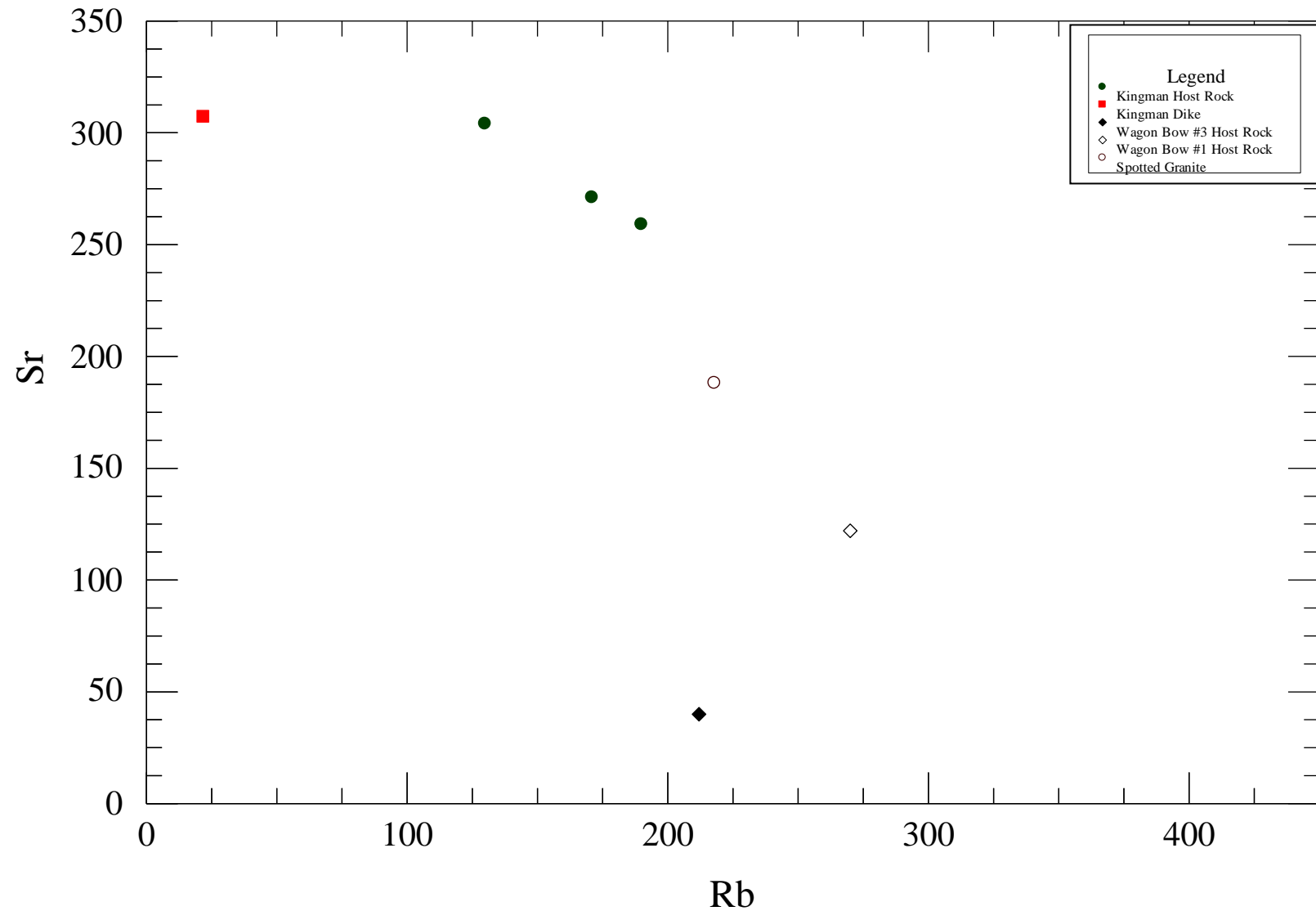


Figure 39. Rb versus Sr variation diagram for pegmatites and host rocks.

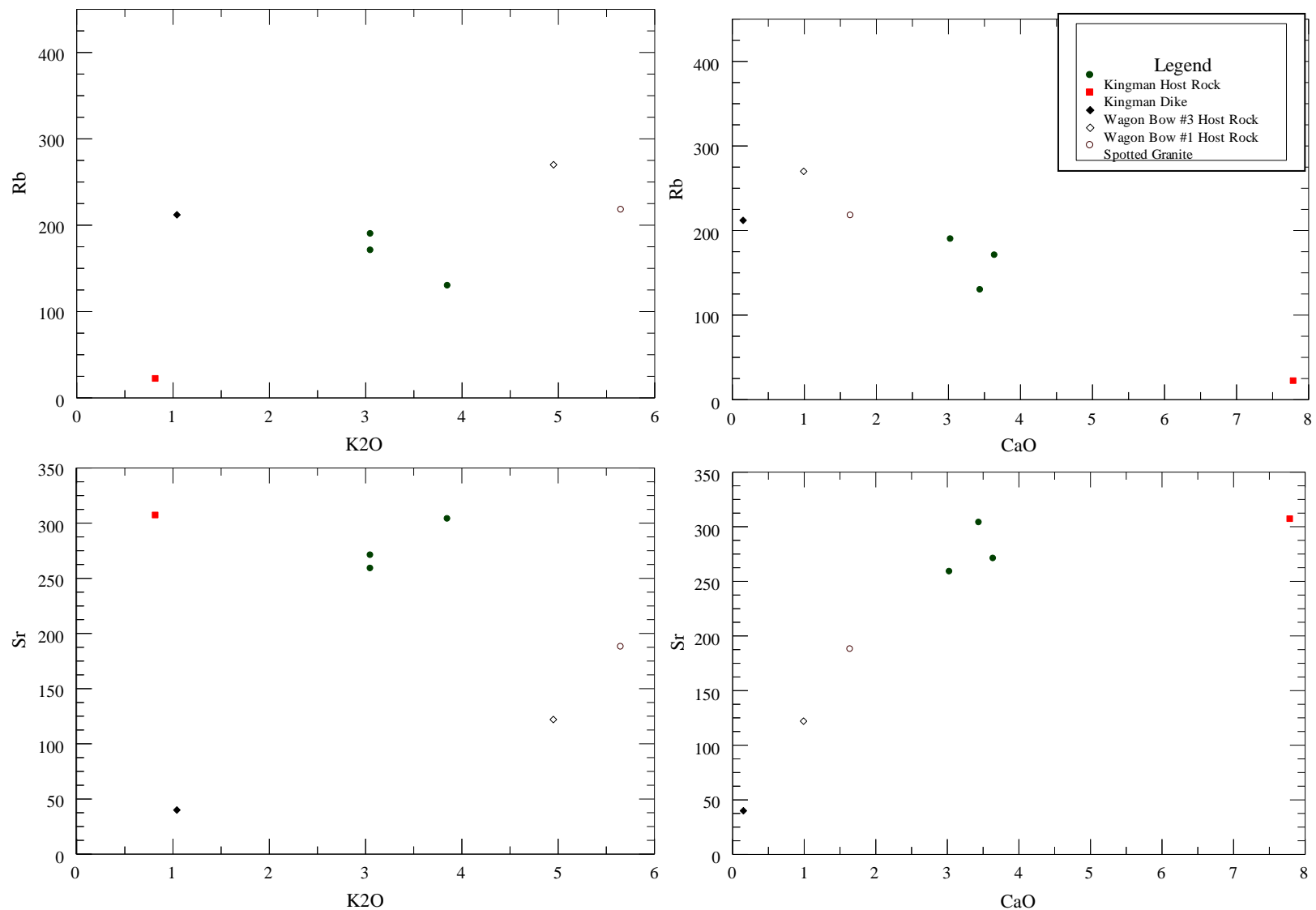


Figure 40. K<sub>2</sub>O and CaO versus Rb and Sr for pegmatitic and host rocks.

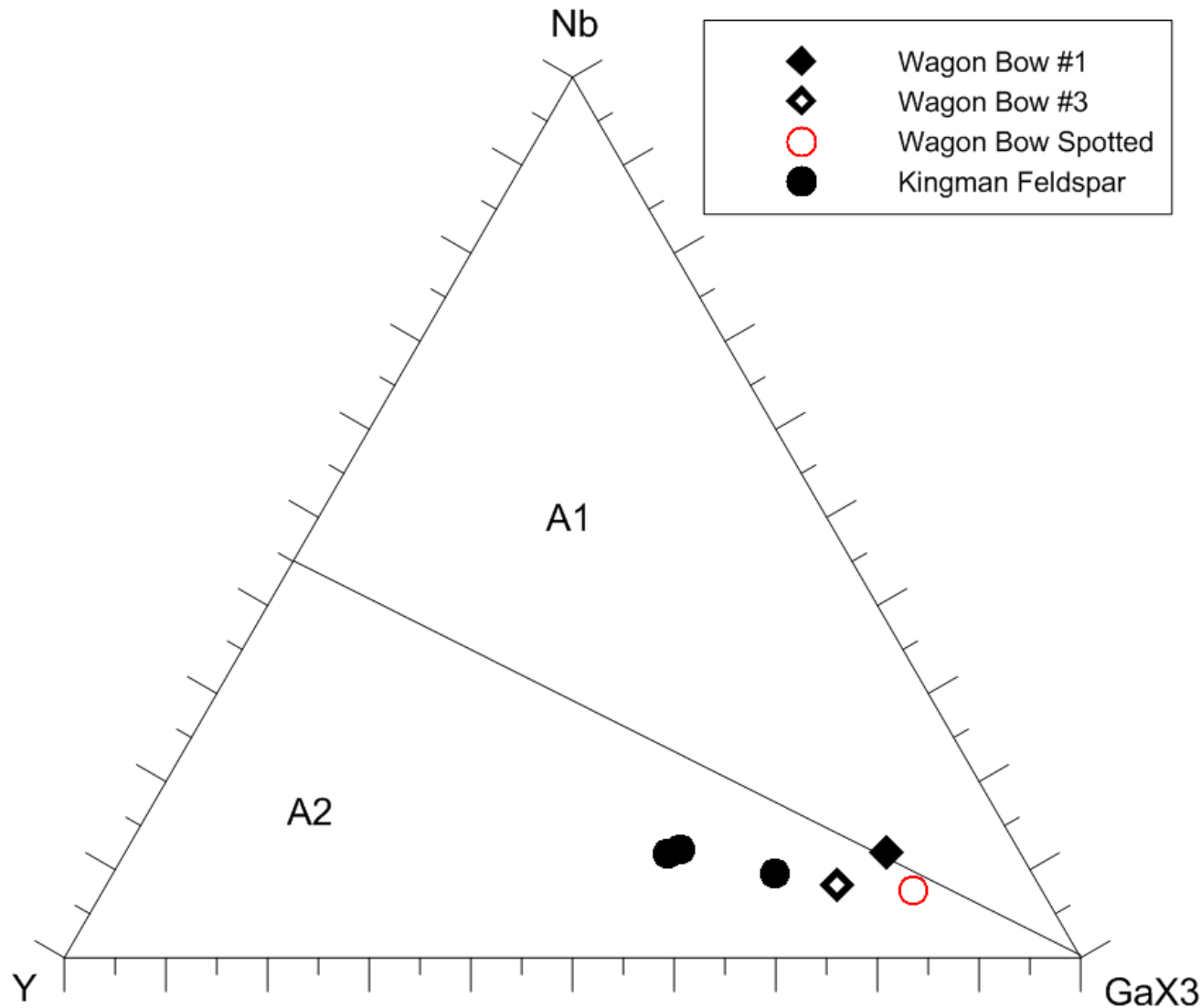


Figure 41. Ternary diagram showing that all but Wagon Bow #1 plot in the A2 section, indicating post collisional, post-orogenic and anorogenic environments. Modified from Eby (1992).

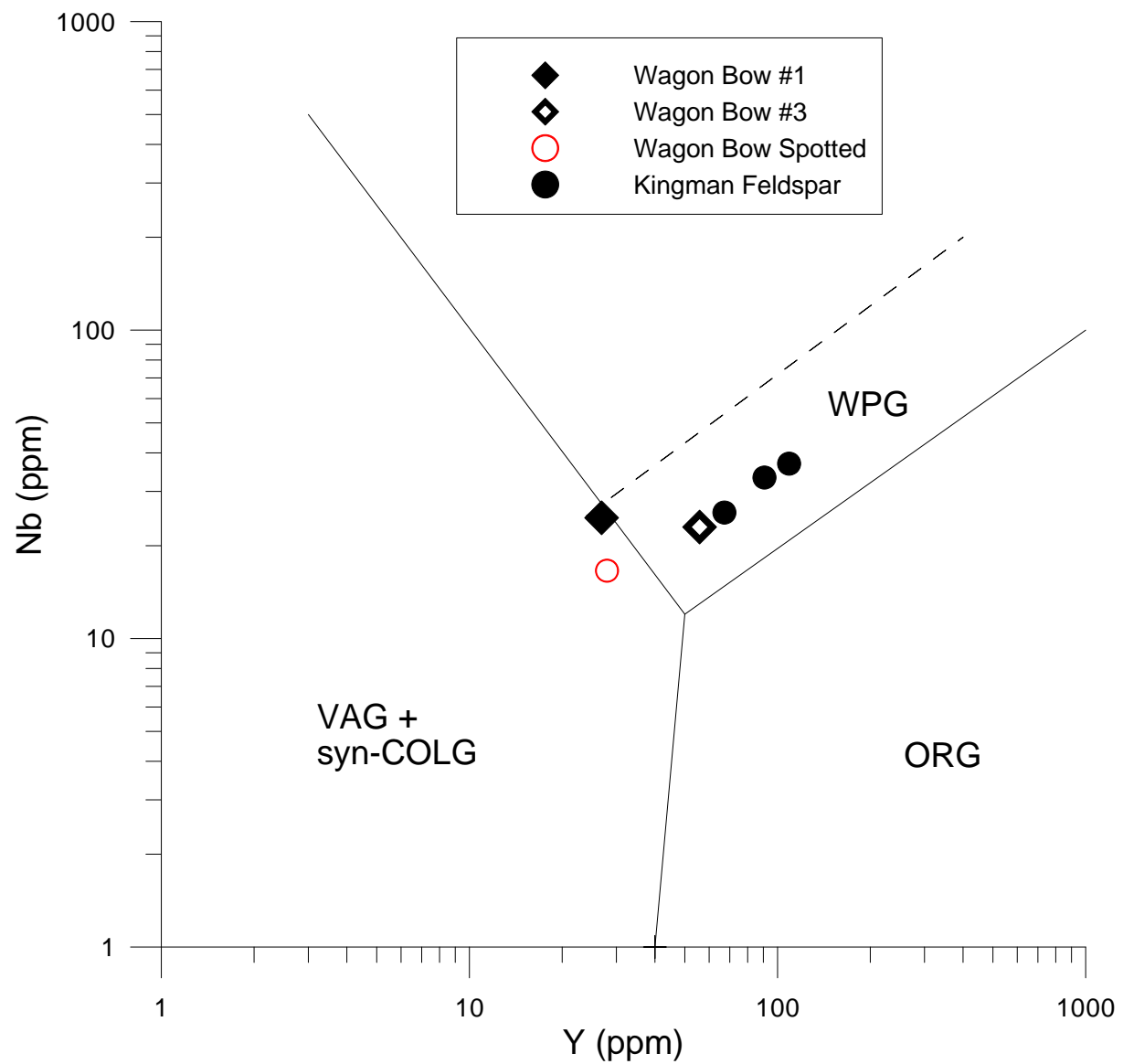


Figure 42. Pearce tectonic discrimination diagram for the Wagon Bow and Kingman host rocks. Modified from Pearce et al. (1984).

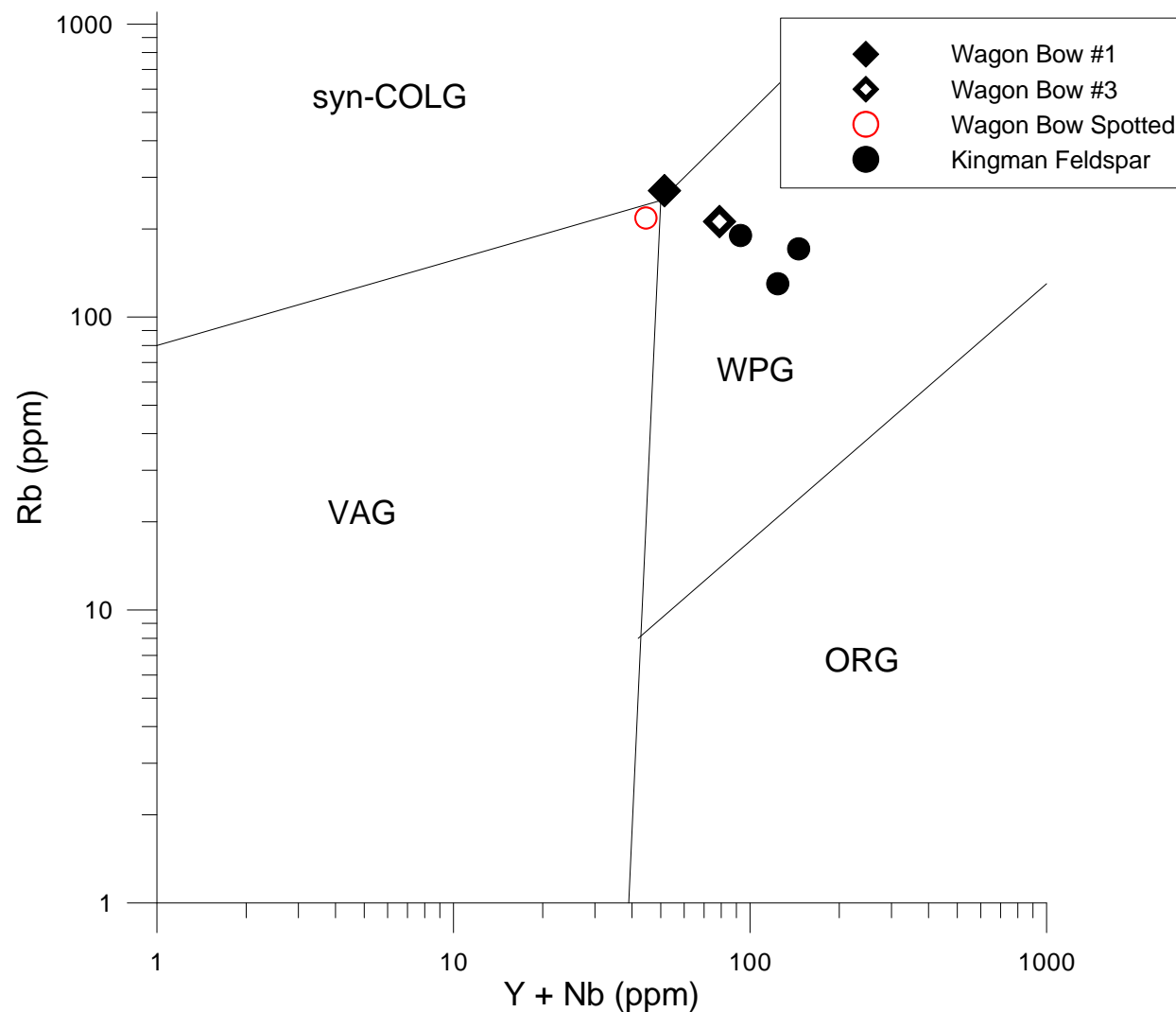


Figure 43. Pearce tectonic discrimination diagram for the Wagon Bow and Kingman host rocks. Modified from Pearce et al. (1984).

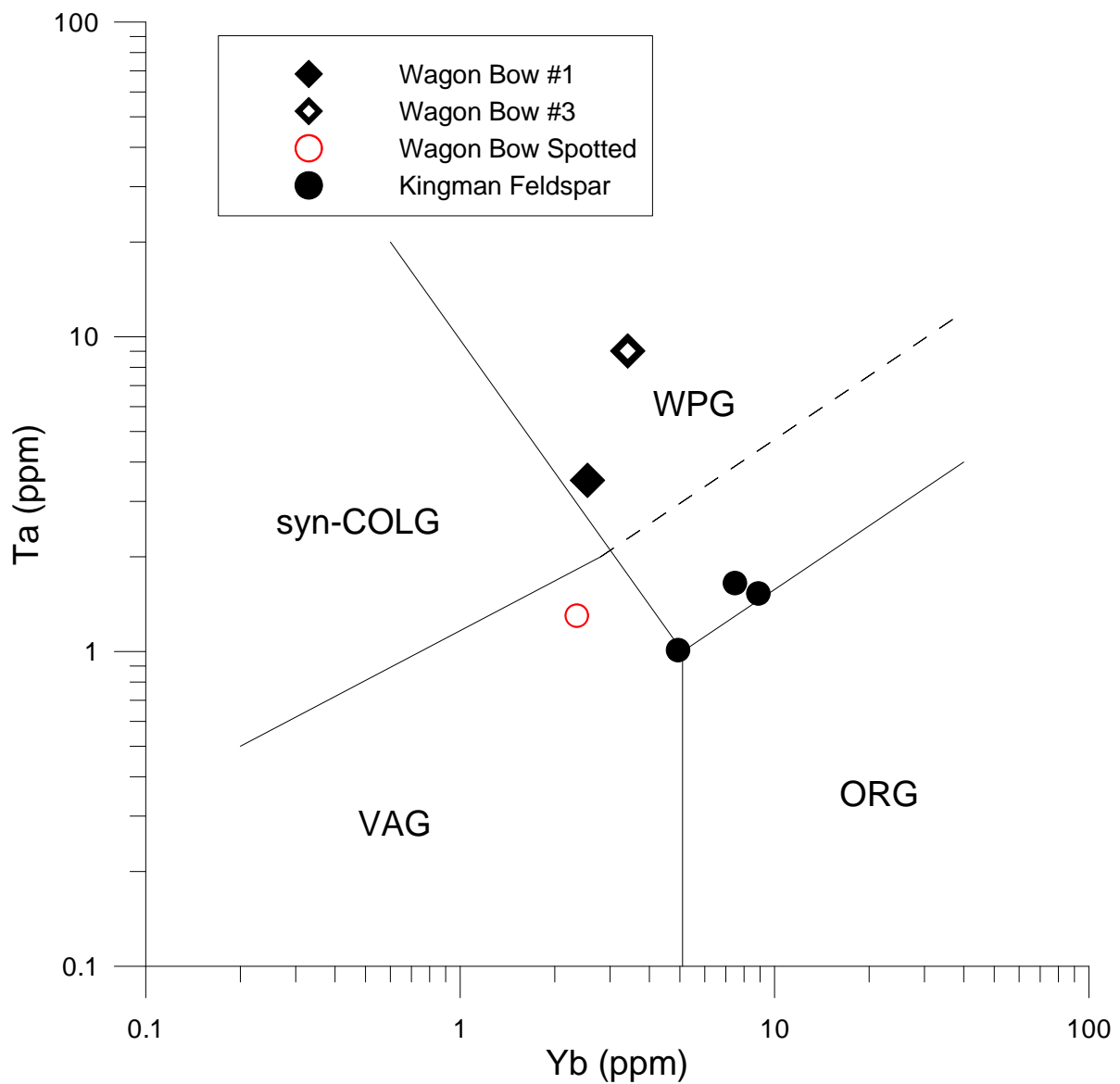


Figure 44. Pearce tectonic discrimination diagram for the Wagon Bow and Kingman host rocks. Modified from Pearce et al. (1984).

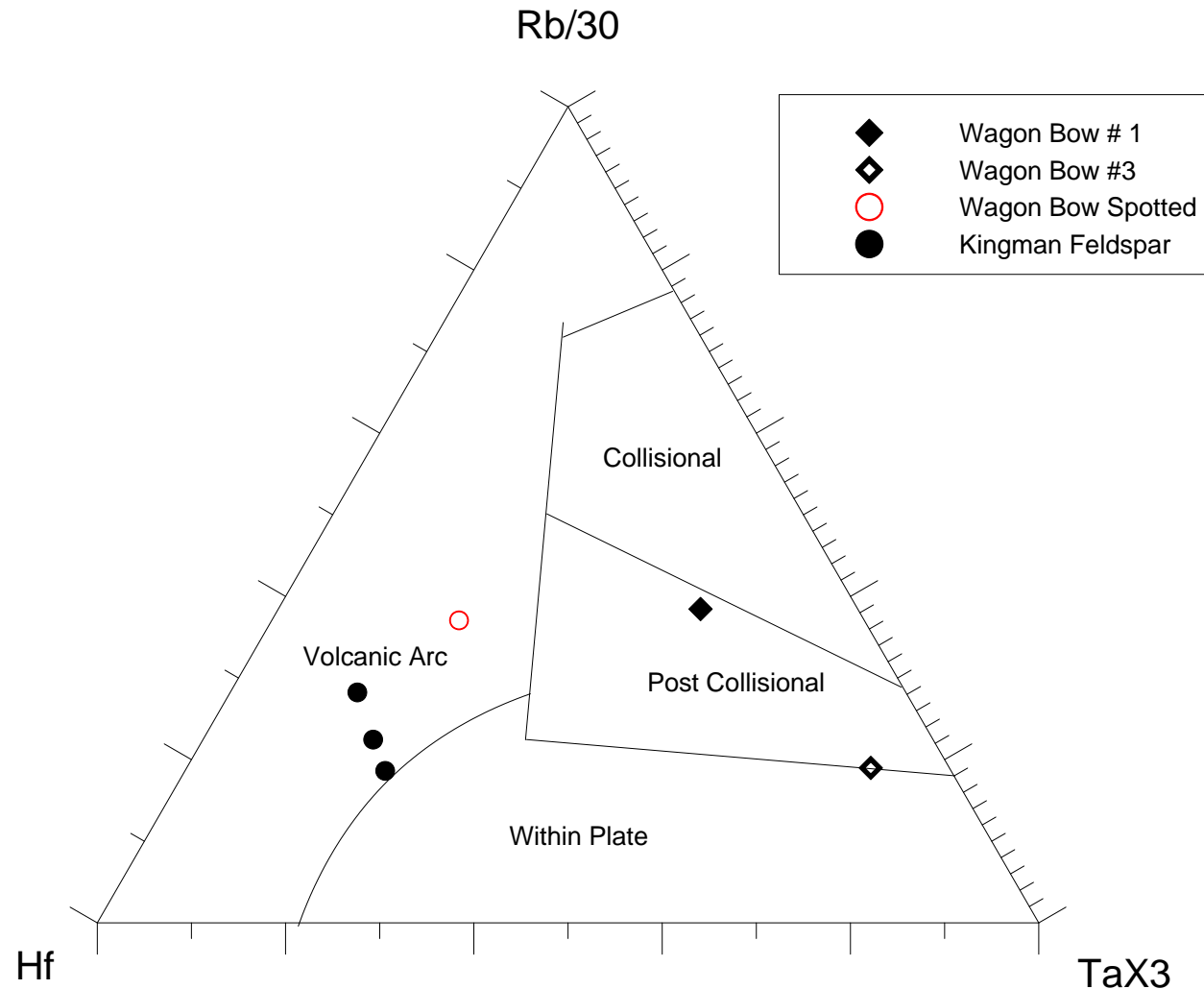


Figure 45. Ternary diagram showing tectonic discrimination for the Wagon Bow and Kingman host rocks. After Harris, Pearce, & Tindle (1986).

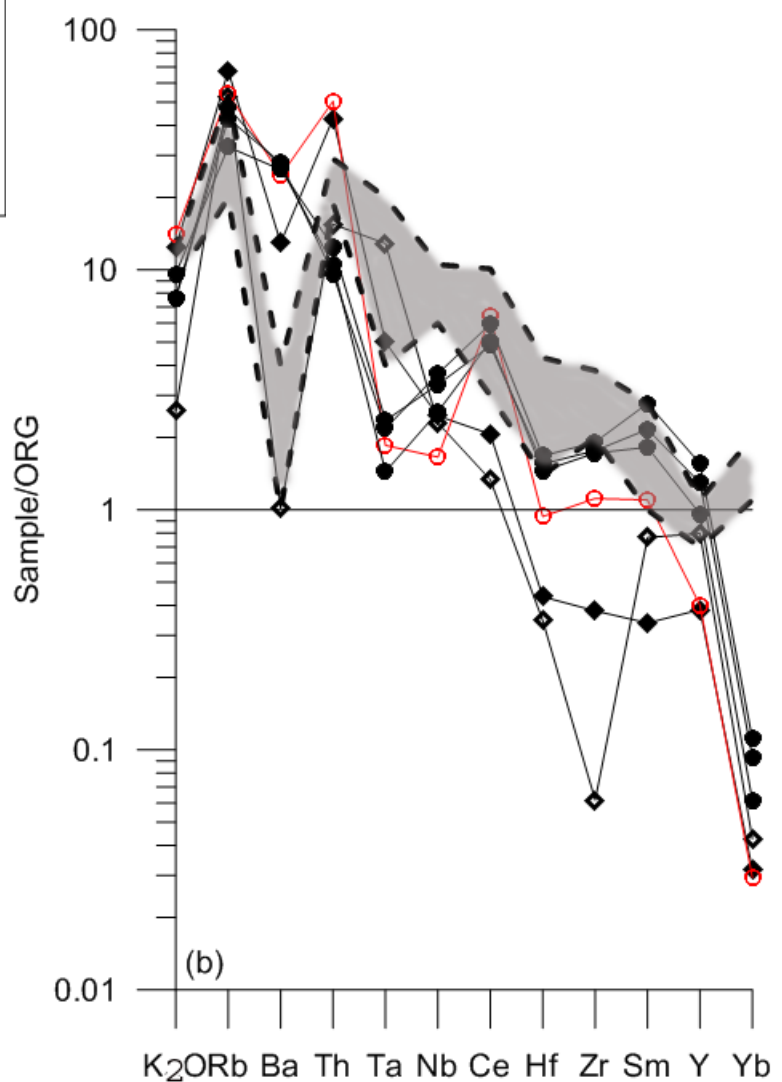
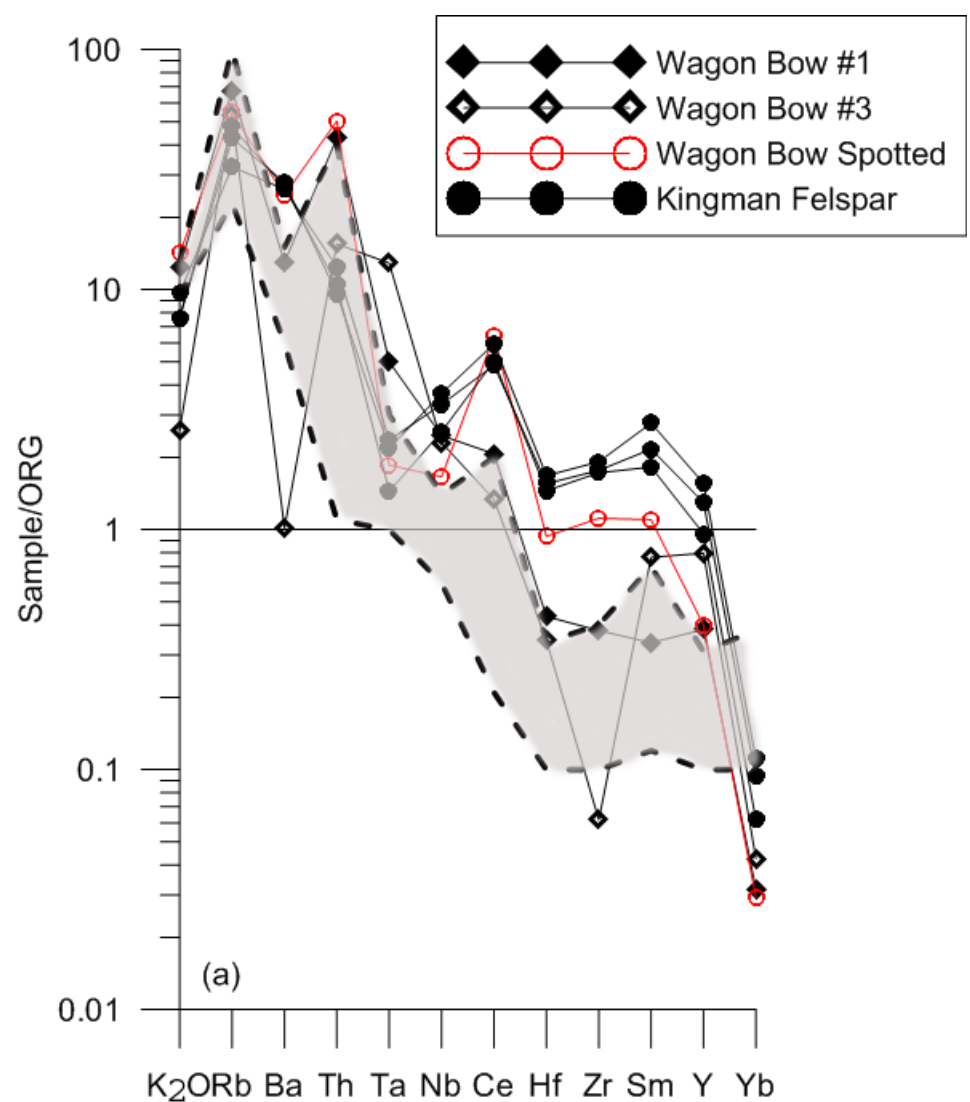


Figure 46. Spider diagrams for Wagon Bow and Kingman Feldspar host rock samples normalized to Ocean Ridge Granite. The shaded represent fields for (a) syn-collisional granite, (b) within plate granites, (c) volcanic arc, and (d) rift. After Pearce et al., (1984).

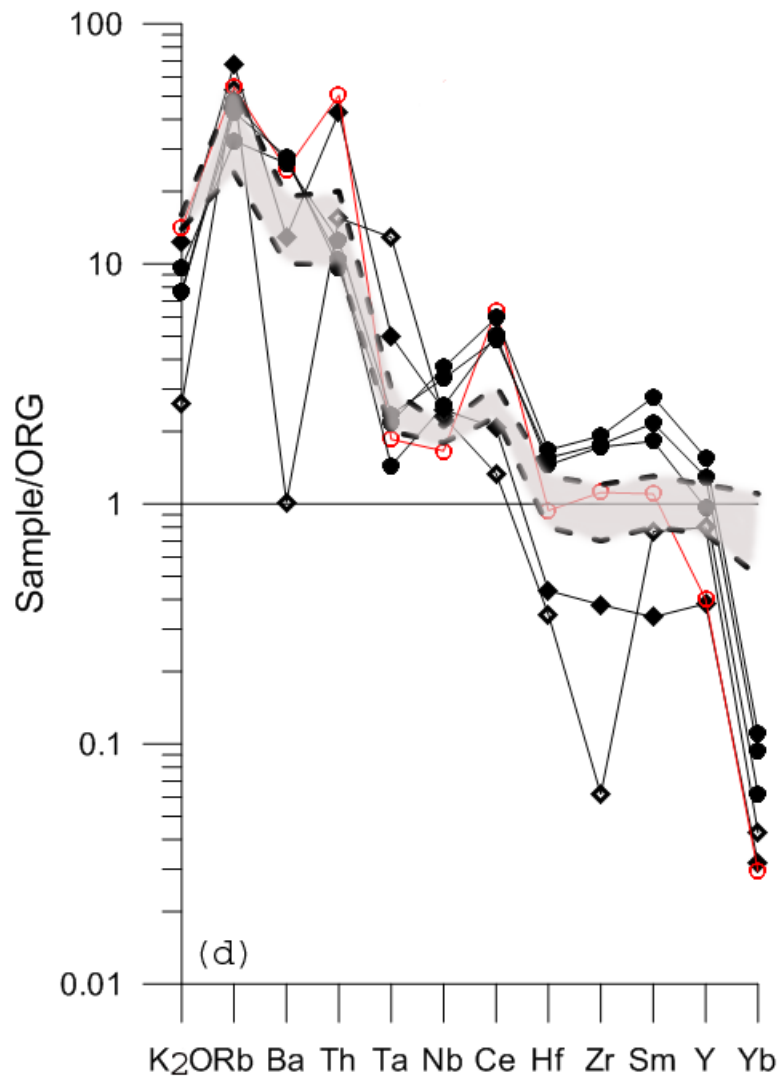
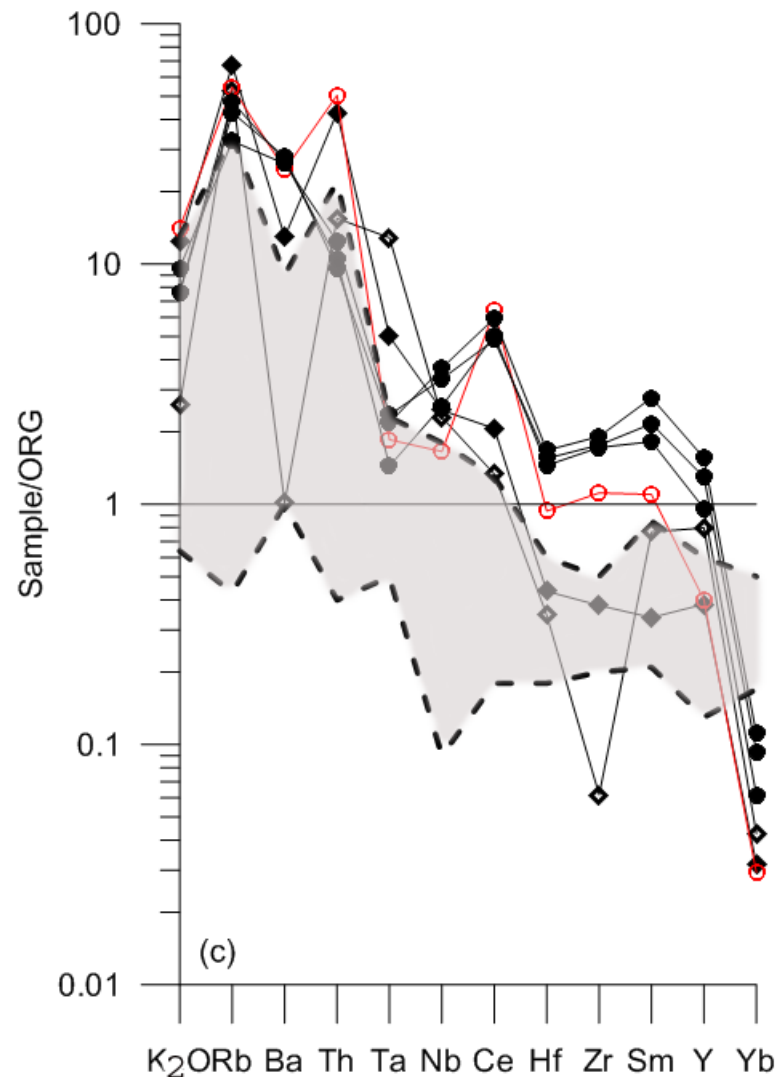


Figure 46. Continued

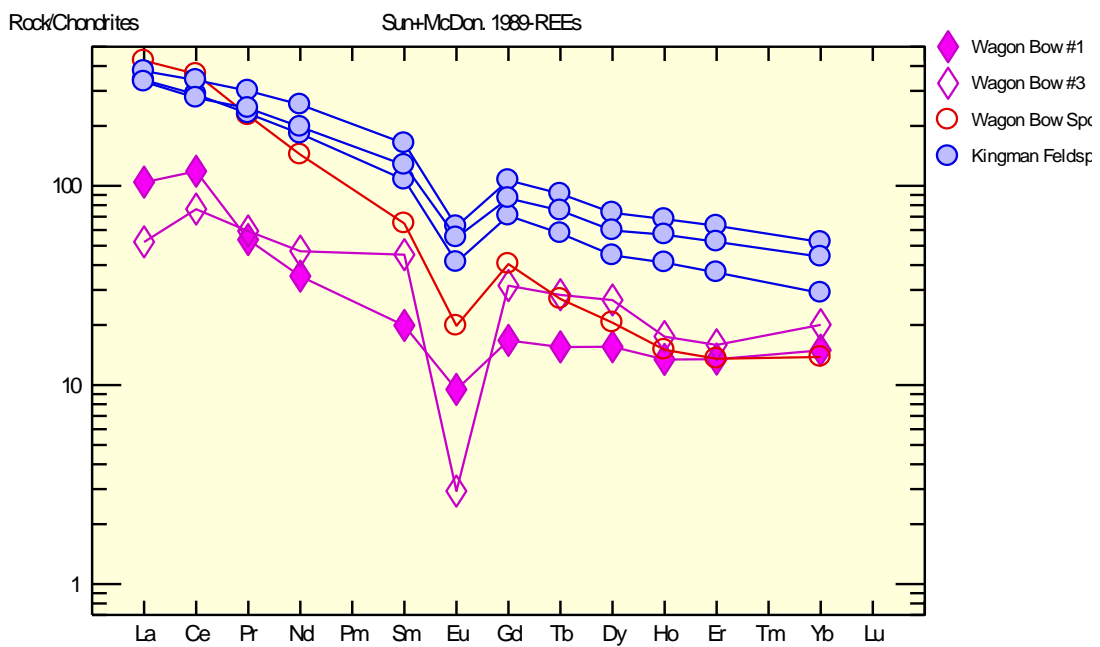


Figure 47. Chondrite diagram showing LREE enrichment trend and negative Eu anomaly, noticeably in the Wagon Bow #3 granite.

## **Discussion and Conclusions**

Five pegmatites were included in this study; the Kingman Feldspar, Rare Metals, and three Wagon Bow pegmatites. The Kingman Feldspar pegmatite is located in the Cerbat Range and the Rare Metals and Wagon Bow pegmatites crop out in the Aquarius range 65 km to the SSE.

All of the pegmatites are intruded into Paleoproterozoic granitic rocks. The Cerbat Range, which hosts the Kingman Feldspar pegmatite, lies in the Mojave terrane. Ages of these granitic plutons are generally contemporaneous with the juxtaposition of the Mojave and Yavapai terranes (1740 – 1720 Ma) (Duebendorfer et al., 2001). The Aquarius Range, which hosts the Wagon Bow and Rare Metals pegmatites, lies within the Boundary Zone between the Mojave and Yavapai terranes. The Boundary Zone is isotopically mixed and marked by both syn- and post-collisional modification (Duebendorfer et al., 2001). Although there are no age dates available for granitic plutons from the Aquarius Range, granites in the Hualapai Range, which lie in the Boundary zone just to the west, range in age from 1718 - 1675 Ga (Chamberlain et al., 1989). Thus the Aquarius Range granites may be slightly younger than those in the Cerbat Range and are likely associated with the subsequent docking of the sutured Mojave and Yavapai terranes to North America during the Yavapai Orogeny (1710 – 1680 Ma) (Duebendorfer et al., 2001).

Major and trace element chemistry is consistent with a diverse origin for the Cerbat and Aquarius range granitic host rocks. The quartz diorites exposed in the Cerbat range have significantly higher Nb and La as compared to the Wagon Bow granites, thus precluding a genetic relationship. Additionally, the higher Ba content for the quartz

diorites, likely reflecting the presence of K-feldspar megacrysts, suggests a different origin for these rocks. Within the Aquarius range, the Wagon Bow spotted granite has higher Zr as well as abundant muscovite, indicating that it is not genetically related to other Wagon Bow granites.

Geochemically, these plutons generally show mixed tectonic signatures which reflect the complex tectonic setting of the area. Rather than resulting from the melting of a single, well-defined source, these post-collisional melts reflect the complex chemistry of the protolith. The Kingman quartz diorite and the Wagon Bow #1 and #3 granites show strong attenuated within plate signatures with some within plate characteristics. The spotted granite from the Wagon Bow #1 pegmatite exhibits both of the above signatures as well as Paleoproterozoic subduction volcanic arc affinities. This variability is attributed to early Proterozoic rifting which produced crust of both attenuated within plate crust and juvenile volcanic arc composition in the Boundary Zone (Duebendorfer et al., 2001). Subsequent remelting of this crust during the Yavapai Orogeny produced granites with complex hybrid compositions that are the result of the relative contribution of the diverse rifted crustal material.

The Kingman Feldspar pegmatite in the Cerbat range was intruded into the host granite in a sill-like fashion whereas the Rare Metals and Wagon Bow pegmatites are segregations within discordant granitic dikes in the Aquarius Range granite. The pegmatites were emplaced either during or subsequent to the Yavapai orogeny (1710 – 1680 Ma) when the sutured terranes docked with North America. Thus, the field relationships suggest that the Mojave district pegmatites are not genetically related to their granitic hosts.

All the pegmatites studied are enriched in REE as indicated by the presence of monazite, allanite, bastnaesite, polycrase-(Y) and euxenite-(Y). They also lack tourmaline, spodumene, and Ta-rich columbite. Pegmatites with this characteristic mineralogy and chemistry generally fall into the NYF type classification of Černý and Ercit (2005). However, these pegmatites differ from typical NYF pegmatites in several significant ways. Perhaps the most obvious difference is the absence of F, which is abundant in classic NYF pegmatites. While this is unusual, it is not the first occurrence of F poor NYF pegmatites as those in the Trout Creek Pass pegmatite district in Colorado are F deficient as well (Hanson et al., 1992).

Second, Nb is very low in abundance or absent. The Kingman Feldspar pegmatite contains abundant LREE minerals, but, Nb- and Ta-enriched phases are notably absent. In the Rare Metals pegmatite, rare euxenite-(Y) and polycrase-(Y) in replacement units contain some Nb and Ta. The Wagon Bow pegmatites appear to be less evolved with lower concentrations of Nb, Ta, and REE, thus the necessary constituents to form columbite may simply not have been available.

Third, the white color of the K-feldspar, reflecting the lower than usual trivalent iron content, is unusual for NYF pegmatites which generally contain pink or red K-feldspar.

Finally, in the Rare Metals pegmatite, the presence of minor lithium in the rare beryl and muscovite may represent minor contamination of less depleted upper crustal material.

In summary, these pegmatites do not lie clearly within the NYF categories of Černý and Ercit (2005) and implies that perhaps a new category of pegmatite may be needed to classify these pegmatites.

The crystallization sequence observed in the pegmatites from this study is similar to other NYF pegmatites. They are all zoned with a composite quartz microcline core although the internal zonation is variable among the pegmatites. The Kingman Feldspar pegmatite is composed of a border zone, wall zone, intermediate zone and a composite quartz-microcline core. The Rare Metals pegmatite, however, has no border zone and Wagon Bow #3 lacks both border and an intermediate zones. Following emplacement of the pegmatite melt, inward crystallization formed the border zone first followed by the wall zone, intermediate zone (when present) and composite core. As crystallization progressed, the incompatible elements became progressively enriched producing accessory minerals including bastnaesite, Ca-rich bastnaesite, zircon, and monazite. Late in the crystallization history of the Rare Metals pegmatite HREE a enriched fluid evolved from the melt producing replacement pods along the core-wall zone boundary.

The Aquarius range pegmatites are the only pegmatites that contain line rock. Line rock is an oscillatory effect in which two minerals, in this case muscovite and albite, develop as the dominant crystallizing mineral switches. Whole rock analyses of Rare Metals line rock show significant differences in major and trace element compositions from the top to the bottom of the line rock series. These differences most likely represent differences in modal percentages of the minerals present in the samples analyzed. The analyzed sample with Na and Sr abundances has higher modal percentages of albite, whereas samples with higher modal percentages of muscovite exhibit elevated Rb

contents. Niobium, which does not partition into either of the above minerals, is constant in all three samples.

There are substantial mineralogical differences in the REE mineralogy in pegmatites from the Cerbat Mountains as compared to those from the Aquarius range. Generally in F-rich environments such as the South Platte pegmatite district, F complexes with the HREE's whereas LREE's form minerals such as allanite and monazite from a late stage melt. Subsequent replacement by the HREE enriched fluid phases, generally along the core-wall zone boundary, form replacement pods that contain HREE-enriched Nb- Ta- Ti-oxides (Simmons et al., 1987). Alternatively, F-poor pegmatites such as the Trout Creek Pass pegmatite district, exhibit the same REE separation (Hanson, et al. 1992). These authors attributed this separation to two phases of mineral crystallization with the LREE being preferentially incorporated into primary allanite and monazite. The HREE remained in the melt and were subsequently incorporated into a later evolving fluid phase that formed the HREE Nb-Ta- Ti-oxide minerals.

The Kingman Feldspar pegmatite, with massive allanite pods, is exceptionally enriched in LREE and depleted in HREE, as no HREE phases are present. The Rare Metals pegmatite contains both HREE enriched phases including euxenite, polycrase, and betafite as well as LREE enriched monazite. The Wagon Bow pegmatites have only very small amounts of REE minerals, but both HREE and LREE minerals are present.

The Rare Metals pegmatite exhibits a REE distribution similar to the Trout Creek pegmatites. LREE enriched primary monazite occurs in the core zone and sparse amounts of HREE enriched polycrase-(Y) and euxenite-(Y) form in replacement units. However, the Kingman Feldspar pegmatite exhibits a very unusual REE distribution.

Notably large concentrations of LREE's are present; hosted by the large allanite pods located in cuts B and C. However, to date, no HREE enriched phases have been reported from this pegmatite. This may be the result of either (a) incorporation of HREE into a late-stage fluid that was subsequently lost to the system or (b) having been formed by partial melting of within plate granites where the HREE were sequestered into residual garnet, thus were never present. Furthermore, the LREE distribution in the Kingman pegmatite is significantly Nd enriched. This is reflected in the higher Nd content in the allanite which, in some cases, is sufficiently high that  $\text{Nd} > \text{Ce}$ . Because Nd dominant allanites are currently not an accepted mineral species, they represent a new mineral species; allanite-Nd.

## References

- ANDERSON, Phillip. (1989): Proterozoic Plate Tectonic Evolution of Arizona. *Arizona Geological Society Digest.* **17**. 17-55.
- BENNETT, V.C & DEPAOLO, D.J. (1987): Proterozoic crustal history of the western United States as determined by neodymium isotopic mapping. *Geological Society of America Bulletin.* **99**. 674-685
- BOWEN, N. L. and Tuttle O.F. (1950): NaAlSi<sub>3</sub>O<sub>8</sub>-KAlSi<sub>3</sub>O<sub>8</sub>-H<sub>2</sub>O. *Journal of Geology.* **58** 489-511.
- DUEBENDORFER, E.M., CHAMBERLAIN, K.R., JONES, C.S.(2001): Paleoproterozoic Tectonic History of the Cerbat Mountains, northwestern Arizona: Implications for crustal assembly in the southwestern United States. *GSA Bulletin.* **113**. No. 5. 575-590
- ČERNÝ, P. & ERCIT, T. (2005): The Classification of Granitic Pegmatites Revisited. *The Canadian Mineralogist.* **43**. 2005-2026.
- CHAMBERLAIN, K.R. & BOWRING, S.A. (2000): Proterozoic Geochronologic and Isotope Boundary in NW Arizona. *Journal of Geology,* **98**. 399-416.
- CRISS, J.W. (1980): Fundamental parameters calculations on a laboratory microcomputer. *Advances X-Ray Analysis.* **23**. 93-97.
- EBY, G.N. (1992): Chemical subdivision of the A-type granitoids: petrogenetic and tectonic implications. *Geology.* **20**. 641-644
- ENGLAND, P. & THOMPSON, A. B. (1984): Pressure-temperature-time paths of regional metamorphism. Part 1. Heat transfer during the evolution of regions of thickened continental crust. *Journal of Petrology.* **25**. 894-928.
- ERCIT, T. S. (2002): The Mess that is “Allanite”. *The Canadian Mineralogist.* **40**. 1411-1419.
- FALSTER, A.U., SIMMONS, W.B., WEBBER, K.L. & BUCHOLTZ, T. (2000): Pegmatites and pegmatite minerals of the Wausau complex, Marathon County, Wisconsin. *Memorie Soc. It. Sci. Nat. Museo Civico Storia Nat. Milan.* **30**. 13-28.
- GOOGLE EARTH. 34° 91'4.92"N, 113° 52'3.85"W. November 26, 2007.
- GULSON, B.L. and KROGH, T.E. (1973): Old Lead Compositions in the Young Bergell Massif, South-East Swiss Alps. *Contributions to Mineralogy and Petrology.* **40**. 239-252.

- HANSON, S.L., FALSTER, A.U. & SIMMONS, W.B. (2008): Rare-Earth Element Distribution in the Mojave County Pegmatites, Northwestern Arizona. *Cordilleran Rocky Mountain Section GSA Abstracts with Programs*. **40**. No.1. 34.
- HANSON, S.L., SIMMONS, W.B., & FALSTER, A.U. (2007): A Reevaluation of Nb-Ta-Ti Oxides from the Rare Metals Mine, Mojave County Pegmatite District, Northwestern Arizona. *Rochester Mineralogical Symposium Abstracts*. No. 34. 13-14.
- HANSON, S.L., SIMMONS, W.B. & FALSTER, A.U. (2006): Quest for the Rare Metals Mine, Mojave County Pegmatite District, Northwestern Arizona. *Rochester Mineralogical Symposium Abstracts*. No. 33. 18-19.
- HANSON, S.L., FALSTER, A.U. and SIMMONS, W.B. (2005) Rare-Earth Mineralogy of the Mojave County Pegmatites, Northwestern Arizona. *Rochester Mineralogical Symposium Abstracts*. 14-15.
- HANSON, S.L., SIMMONS, W.B., WEBBER, K. L., and FALSTER, A.U. (1992) Rare-Earth-Element Mineralogy of Granitic Pegmatites in the Trout Creek Pass Pegmatite District, Chaffee County, Colorado. *Canadian Mineralogist*. **30**. 673-686.
- HARRIS, N.B.W. (1981): The role of fluorine and chlorine in the petrogenesis of a peralkaline complex from Saudi Arabia. *Chemical Geology*. **31**. 301-310.
- HARRIS, N.B.W., PEARCE, J.A. and TINDLE. (1986): Chemical Characteristics of Collision Sone magmatism. In: COWARD, M.P, and RIES, A.C. (eds) *Collision Tectonics, Geological Special Publication*. **19**. 67-81.
- HEINRICH, E. William. (1960): Some Rare-Earth Mineral Deposits in Mojave County, Arizona. The Arizona Bureau of Mines. *Bulletin* 167.
- HOFFMAN, P.E. (1988): United plates of America, the birth of a craton: Early Proterozoic assembly and growth of Laurentia. *Annual Review of Earth and Planetary Sciences*. **16**. 543-603.
- KARLSTROM, K. E & BOWING, S.A. (1993): Proterozoic orogenic history of Arizona. In Van Schmus, W.R. et al. (1993): Transcontinental Proterozoic provinces. In Reed, J.C., Jr. et al. ers. Precambrian: Conterminous U.S.: Boulder, Colorado. Geological Society of America. *Geology of North America*. **C-2**. 188-211.
- KARLSTROM, K. E & BOWING, S.A. (1988): Early Proterozoic assembly of tectonostratigraphic terranes in southwestern North America. *Journal of Geology*. **96**. 561-576
- LE MAITRE, R.W. (1989): A Classification of Igneous Rocks and Glossary of Terms: Recommendations of the International Union of Geological Sciences

- Subcommission on the Systematics of igneous rocks. Blackwell, Oxford. 193.
- LEVINSON, A.A. (1966): A system of nomenclature for rare earth minerals. *Am. Mineral.* **51**, 152-158.
- NELSON, B.K. & DEPAOLO, D.J. (1985): Rapid production of continental crust 1.7 to 1.9 b.y. ago: Nd isotopic evidence from the basement of the North American mid-continent. *Geological Society of America Bulletin*. **96**. 746-754
- NIELSON, J.E., LUX, D.R., DALRYMPLE, G.B., GLAZNER, A.F. (1990): Age of the Peace Springs Tuff, southeastern California and Western Arizona. *Journal of Geophysical Research*. **95**. No. B1. 571-580.
- PEARCE, J.R., HARRIS, N.B., & TINDLE, A.G. (1984): Trace element discrimination diagrams for the tectonic interpretation of granitic rocks. *J. Petrol.* **25**. 956-983.
- POUCHOU, J. -L., & PICHOIR, F. (1991): Quantitative analysis of homogenous or stratified microvolumes applying the model "PAP," in Heinrich, K.F.J. and Newbury, D.E. eds., *Electron Probe Quantitation*. Plenum, NY. 31-75.
- SCHALLER, W.T., STEVENS, R.E., and JAHNS, RH. (1962): An unusual beryl from Arizona. *The American Mineralogist*. **47**. May-June
- SCHRADER, F.C. (1909): Mineral deposits of the Cerbat range, Black Mountains and Grand Wash Cliffs, Mojave county, Arizona. Dept. of the Interior. *UGS. Bulletin* **397**. 1-226.
- SILVER, L.T. (1965): Mazatzal orogeny and tectonic episodicity. In Abstracts for 1964. *Geological Society of America Special Paper* 82. 185-186.
- SILVER, L.T., ANDERSON, C.A., CRITTENDEN, M., and ROBERTSON, J.M. (1977): Chronostratigraphic elements of the Precambrian rocks of the southwestern and far western United States. *Geological Society of America Abstracts with Programs*. **9**. 1176.
- SIMMONS, W.B. & HEINRICH, E.W. (1980): Rare-earth pegmatites of the South Platte district, Colorado. *Colo. Geol. Surv., Res. Ser.* 11.
- SIMMONS, W.B., Lee, M.T., and Brewster, R.H. (1987): Geochemistry and evolution of the South Platte granite-pegmatite system, Jefferson County, Colorado. *Geochemica et Cosmochimica Acta*. **51**. 455-471.

WISE, M.A. (1999): Characterization and classification of NYF-type pegmatites. *In The Eugene E. Foord Memorial Symp. on NYF-type Pegmatites* (Denver). *Can Mineral.* **37**. 802-803 (abstr.).

WOLFHARD, M.R. (1984): Structure and Mineralization. 1984 Fall Field Trip. Arizona Geological Society.

WOODEN, J.L., STACEY, J.S., DOE, B., HOWARD, K.A., and HILLER, D.M. (1988): Pb isotopic evidence for the formation of Proterozoic crust in the southwestern United States. *In* Ernst, W.G. ed. Metamorphism and crustal evolution of the western United States. **Rubey Volume VII**. 68-86.

## Analytical Methods

### Petrographic Analysis

Blocks were cut from hand samples using a water cooled saw with diamond blade. These chips were sent to National Petrographic, INC. to be made into petrographic thin sections.

### Heavy Mineral Separation

Heavy minerals were separated using lithium metatungstate adjusted to a density of 2.9 grams per cubic centimeter. Heavy minerals were frozen using liquid nitrogen separate from the light minerals, cleaned in distilled water, dried and handpicked for further investigation.

### Scanning Electron Microscopy

Analyses were completed using an AMRAY 1820 Digital SEM with an acceleration potential of 20 kV. The working distance was 18 mm and a 400 micron final aperture was used with a sample tilt between 0° and 35°. Backscattered electron images were collected using EDS 2009, an integrated software package, by IXRF systems, INC. Images were captured at a resolution of 512 by 512 pixels and 16 frame averages were employed. EDS spectra were acquired for 60 seconds. X-ray maps were collected at a resolution of 256 by 256 pixels, a dwell time of 50 milliseconds and 25 frame averages.

### Direct Coupled Plasma Spectroscopy

A Spectronics Spectraspan V was used to collect data on certain trace elements. Data were collected of Rb and Tl to compare in a ratio (Rb to K to Tl) to determine pegmatite evolution. Boron and Li data were collected to determine if they were in existence in the samples and if so how much. Collecting times were 10-20 seconds. Ytterbium was measured at 398.799 nm with a 20 second count time at 20,000 V and

varied from 1-0.001. Tantalum was measured at 296.513 nm at a 20 second count time at 20,000 V and varied from 10-0.001. Gallium was measured at 417.206 nm with a 15 second count time at 10,000 V and varied from 1-0.

### Electron Microprobe Analyses

Mineral grains were handpicked, placed on a labeled grid and encased in epoxy. After curing, the epoxy was ground down to intercept the grains and the mounts were polished with 1 micron, 0.3 micron and 0.05 micron alumina. Between each step the sample mounts were cleaned in an ultrasonic bath for 1 minute. After drying overnight in a desiccator, they were coated with 250 Å of carbon in a vacuum of  $1 \times 10^{-5}$  Torr. Mineral analyses were completed using an ARL-SEMQ electron microprobe with an acceleration potential of 15 kV and a beam current of 15-20 nA. Peak counts were collected for 45 seconds and background positions were determined by the mean atomic number method (MAN).

Standards included; REE orthophosphates (synthetic)(La for La, Ce, Eu, Gd, Tb, Ho, Tm, Yb, Lu and L $\beta$  for Pr, Nd, Sm, Dy and Er-MAN), YPO<sub>4</sub> (synthetic; Y<sub>La1</sub> W<sub>Ma1</sub>-MAN), CaWO<sub>4</sub> (synthetic; W<sub>Ma1</sub>-MAN ), PbO (synthetic; Pb<sub>Ma1</sub>-MAN), ZrO<sub>2</sub> (synthetic; Zr<sub>La1</sub> and Sn<sub>La1</sub>-MAN), V<sub>2</sub>O<sub>5</sub> (synthetic; V<sub>Ka</sub>-MAN), UO<sub>2</sub> (synthetic; U<sub>Ma1</sub>-MAN), ThO<sub>2</sub> (synthetic; Th<sub>Ma1</sub>-MAN), HfO<sub>2</sub> (synthetic; Hf<sub>La1</sub>-MAN), albite (Na<sub>Ka</sub>-MAN), adularia(K<sub>Ka1</sub>-MAN), clinopyroxene (Mg<sub>Ka</sub>, Ca<sub>Ka</sub> and Si<sub>Ka</sub>-MAN), corundum (MAN), quartz (MAN), hematite (Fe<sub>Ka</sub>-MAN), rutile (Ti<sub>Ka</sub>-MAN), periclaste (MAN), spessartine(Mn<sub>Ka</sub>-MAN), YNbO<sub>4</sub> (Nb<sub>La1</sub>-MAN), manganotantalite (Mn<sub>Ka</sub> and Ta<sub>La1</sub>-MAN), microlite(Ca<sub>Ka</sub>, Ta<sub>La1</sub> and F<sub>Ka</sub>-MAN), andalusite(MAN), labradolite(MAN),

fluortopaz ( $F_{K\alpha}$ -MAN) and fluorapatite(MAN). Data were processed and ZAF corrected by Probe for Windows by Microbeam Inc. : Matrix effects were corrected using a  $\phi(\rho Z)$  correction procedure (Pouchou and Pichoir 1991).

### X-ray diffraction

Certain minerals are metamict (Ex. euxenite and monazite), thus must be recrystallized prior to XRD analysis. This was accomplished by heating samples in a quartz tube with each separated from another by quartz wool. A gas mixture of 95 % Ar 5% H was percolated through the tube while it was heated to 1000°C for 12 hours. Minerals were analyzed using a SCINTAG XDS 2000 X-ray diffractometer at an operating voltage of 35 kV and a beam current of 15 mA. Step scans were run from 2° to 60° with a step increment of 0.05°and a dwell time of 6 seconds. The scans were measured using diffraction master system (DMS).

### Whole Rock Analyses

Whole rock samples were prepared from fragments, approximately 1 cm, generated by manually breaking rock samples. These samples were then crushed using a ceramic mill in a shatterbox. Major and trace elements were analyzed at Michigan State University. Major elements were analyzed on a Rigaku SMAX spectrometer and trace elements were analyzed using Inductively Coupled Plasma – Mass Spectrometry (ICP-MS). Glass disks were prepared using a low dilution fusion and were made by mixing 3.0 g of finely ground rock powder with 9.0 g lithium tetraborate as a flux, and 0.5 g ammonium nitrate as an oxidizer. These materials were fused at 1000°C in a platinum

crucible in an oxidizing flame for at least 30 minutes and then poured into platinum molds. Data were reduced by the fundamental parameter data reduction method (Criss, 1980) using XRFWIN software (Omni Instruments).

## Appendix

Table 26a. Chemical Composition of Biotite from the Wagon Bow #2 and Rare Metals

Sample	Wagon Bow # 2					Rare Metals Mine			
	WHM-2-4	WHM-2-5	B-1-D-1	B-1-D-2	B-1-D-3	B-1-D-4	RMM-3-1	RMM-3-2	RMM-3-3
SiO <sub>2</sub>	38.56	38.66	38.23	38.00	38.21	38.43	38.57	38.62	38.57
TiO <sub>2</sub>	2.78	2.94	3.13	3.21	3.43	3.65	3.02	2.98	3.01
Al <sub>2</sub> O <sub>3</sub>	14.34	14.53	14.25	14.32	14.54	14.11	14.32	14.29	14.41
SFeO	25.66	25.73	24.68	24.87	24.46	25.03	25.54	25.34	25.34
MnO	1.10	1.12	1.27	1.35	1.38	1.45	1.21	1.13	1.26
MgO	3.77	3.87	4.11	4.01	4.11	3.87	4.12	4.09	3.89
CaO	0.21	0.14	0.18	0.18	0.38	0.21	0.19	0.22	0.18
Na <sub>2</sub> O	0.31	0.29	0.21	0.24	0.17	0.11	0.30	0.28	0.31
K <sub>2</sub> O	7.89	7.80	6.77	7.02	6.73	7.23	7.05	7.23	7.66
F	0.98	1.02	0.63	0.71	0.57	0.57	0.89	1.09	1.01
Cl	0.02	0.03	0.01	0.01	0.02	0.02	0.01	0.03	0.02
Sub-Total	95.61	96.12	93.48	93.92	94.00	94.70	95.22	95.31	95.64

Table 26a continued. Chemical Formula of Biotite from the Wagon Bow #2 and Rare Metals

Sample	Wagon Bow # 2						Rare Metals Mine		
	WHM-2-4	WHM-2-5	B-1-D-1	B-1-D-2	B-1-D-3	B-1-D-4	RMM-3-1	RMM-3-2	RMM-3-3
Si	2.8098	2.8005	2.8178	2.7983	2.7995	2.8059	2.8058	2.8142	2.8066
Al(iv)	0.9840	1.1995	1.1822	1.2017	1.2005	1.1941	1.1942	1.1858	1.1934
Ti(iv)									
Al(vi)	0.338	0.042	0.056	0.042	0.056	0.020	0.034	0.042	0.043
Ti(vi)	0.163	0.160	0.173	0.178	0.189	0.201	0.165	0.163	0.164
Fe3	1.564	1.559	1.521	1.532	1.499	1.528	1.554	1.544	1.542
Fe2	0.000	0.000	0.000	0.000	0.000	0.000	0.000	0.000	0.000
Mn	0.068	0.069	0.079	0.084	0.085	0.090	0.075	0.070	0.077
Mg	0.409	0.418	0.451	0.440	0.449	0.421	0.447	0.444	0.422
Vacancy(vi)	0.459	0.752	0.719	0.725	0.722	0.739	0.725	0.737	0.751
Sum Oct Cat	2.541	2.248	2.281	2.275	2.278	2.261	2.275	2.263	2.249
Ca	0.016	0.011	0.014	0.014	0.030	0.017	0.015	0.017	0.014
Na	0.044	0.041	0.031	0.034	0.023	0.016	0.042	0.039	0.043
K	0.733	0.720	0.636	0.660	0.629	0.674	0.654	0.672	0.711
Sum(A site)	0.794	0.772	0.681	0.708	0.682	0.706	0.711	0.729	0.768
F	0.227	0.233	0.148	0.166	0.131	0.131	0.205	0.251	0.233
Cl	0.003	0.004	0.001	0.002	0.003	0.002	0.002	0.004	0.002
OH	1.771	1.764	1.851	1.832	1.866	1.867	1.793	1.745	1.765
F	0.98	1.02	0.63	0.71	0.57	0.57	0.89	1.09	1.01
Fe/Fe+Mg	0.7927	0.7887	0.7711	0.7768	0.7695	0.7839	0.7767	0.7766	0.7852
F	0.98	1.02	0.63	0.71	0.57	0.57	0.89	1.09	1.01

Table 26b. Chemical Composition of Biotite from the Rare Metals and Kingman Mine

Sample	Rare Metals Mine				Kingman Mine				
	RMM-3-4	RMM-3-5	RMM-4-1	RMM-4-2	D-4-D-1	D-4-D-2	D-4-D-3	D-4-D-4	D-4-D-5
SiO <sub>2</sub>	38.46	38.62	38.54	38.51	38.11	38.24	38.13	38.33	38.31
TiO <sub>2</sub>	2.95	2.92	3.12	3.10	2.92	2.79	2.92	2.77	2.82
Al <sub>2</sub> O <sub>3</sub>	14.31	14.32	14.34	14.37	13.83	13.78	13.87	13.56	13.73
SFeO	25.42	25.27	25.43	25.38	25.21	25.12	25.17	25.04	25.12
MnO	1.12	1.21	1.09	1.11	1.12	1.09	1.13	1.09	1.13
MgO	3.83	4.07	3.93	3.74	3.66	4.01	3.79	3.65	3.98
CaO	0.22	0.20	0.21	0.23	0.20	0.19	0.21	0.17	0.17
Na <sub>2</sub> O	0.29	0.32	0.29	0.26	0.18	0.18	0.19	0.21	0.20
K <sub>2</sub> O	7.32	7.00	6.99	6.78	7.00	6.34	6.22	6.73	6.57
F	0.99	0.97	0.89	0.79	0.56	0.51	0.52	0.49	0.50
Cl	0.01	0.03	0.02	0.09	0.01	0.02	0.01	0.02	0.02
Sub-Total	94.92	94.94	94.86	94.35	92.81	92.27	92.18	92.07	92.56

Table 26b continued. Chemical Formula of Biotite from the Rare Metals and Kingman Mine

Sample	Rare Metals Mine				Kingman Mine				
	RMM-3-4	RMM-3-5	RMM-4-1	RMM-4-2	D-4-D-1	D-4-D-2	D-4-D-3	D-4-D-4	D-4-D-5
Si	2.8129	2.8183	2.8115	2.8194	2.8333	2.8445	2.8389	2.8632	2.8452
Al(iv)	1.1871	1.1817	1.1885	1.1806	1.1667	1.1555	1.1611	1.1368	1.1548
Ti(iv)									
Al(vi)	0.047	0.050	0.045	0.059	0.046	0.053	0.057	0.058	0.047
Ti(vi)	0.162	0.160	0.171	0.170	0.163	0.156	0.163	0.156	0.158
Fe3	1.555	1.542	1.551	1.554	1.567	1.563	1.567	1.564	1.560
Fe2	0.000	0.000	0.000	0.000	0.000	0.000	0.000	0.000	0.000
Mn	0.069	0.075	0.067	0.069	0.071	0.069	0.071	0.069	0.071
Mg	0.418	0.443	0.427	0.408	0.405	0.444	0.420	0.406	0.441
Vacancy(vi)	0.749	0.730	0.737	0.739	0.748	0.715	0.721	0.748	0.723
Sum Oct Cat	2.251	2.270	2.263	2.261	2.252	2.285	2.279	2.252	2.277
Ca	0.017	0.015	0.018	0.018	0.016	0.015	0.017	0.014	0.015
Na	0.040	0.045	0.041	0.036	0.026	0.026	0.028	0.031	0.029
K	0.683	0.652	0.650	0.633	0.664	0.602	0.591	0.642	0.622
Sum(A site)	0.741	0.713	0.709	0.688	0.706	0.643	0.636	0.687	0.666
F	0.230	0.225	0.206	0.183	0.130	0.121	0.123	0.116	0.118
Cl	0.002	0.003	0.003	0.011	0.002	0.002	0.002	0.002	0.003
OH	1.768	1.772	1.791	1.806	1.868	1.877	1.875	1.881	1.879
F	0.99	0.97	0.89	0.79	0.56	0.51	0.52	0.49	0.50
Fe/Fe+Mg	0.7883	0.7769	0.7840	0.7920	0.7946	0.7788	0.7885	0.7940	0.7797
F	0.99	0.97	0.89	0.79	0.56	0.51	0.52	0.49	0.50

Table 27a. Chemical Composition of Microcline from the Kingman, Rare Metals and Wagon Bow Pegmatites

	Kingman Mine			Rare Metals Mine			Wagon Bow #3		
	KFM-site-X-7	KFM-site-X-8	KFM-site-X-9	KFM-site-X-10	RMM-24-2	RMM-24-3	RMM-24-4	WH-1-8	WH-1-9
<b>Oxides</b>									
SiO <sub>2</sub>	64.88	64.88	64.83	64.84	64.78	64.71	64.74	64.67	64.6
TiO <sub>2</sub>	0.01	0.01	0.01	0.01	0.01	0.01	0.01	0.01	0.01
Al <sub>2</sub> O <sub>3</sub>	18.32	18.3	18.33	18.33	18.31	18.35	18.35	18.34	18.32
MgO	0	0	0	0	0	0	0	0.01	0
CaO	0.03	0.02	0.03	0.03	0.02	0.02	0.02	0.02	0.03
MnO	0	0	0	0	0	0	0	0	0
FeO	0	0	0	0.02	0.01	0.01	0.01	0.03	0.01
Na <sub>2</sub> O	0.32	0.29	0.34	0.34	0.3	0.27	0.32	0.28	0.23
K <sub>2</sub> O	16.3	16.22	16.31	16.28	16.32	16.31	16.11	16.29	16.32
Rb <sub>2</sub> O	0.05	0.05	0.05	0.06	0.07	0.06	0.06	0.05	0.06
Total	99.92	99.76	99.9	99.9	99.81	99.74	99.63	99.69	99.57
<b>Ions</b>									
Ti	0	0	0	0	0	0	0	0	0
Mg	0	0	0	0	0	0	0	0.001	0
Ca	0.002	0.001	0.002	0.001	0.001	0.001	0.001	0.001	0.001
Mn	0	0	0	0	0	0	0	0	0
Fe 2+	0	0	0	0.001	0	0.001	0	0.001	0
Na	0.029	0.026	0.031	0.031	0.027	0.024	0.029	0.025	0.021
K	0.961	0.956	0.962	0.959	0.962	0.961	0.95	0.96	0.962
Rb	0.002	0.002	0.001	0.002	0.002	0.002	0.002	0.001	0.002
Σ X-Site	0.993	0.984	0.995	0.993	0.992	0.988	0.982	0.987	0.986
Σ Al	0.998	0.997	0.998	0.999	0.997	1	0.999	0.999	0.998
Σ Si	2.999	2.998	2.996	2.997	2.994	2.99	2.992	2.988	2.985
Anorthite	0.2	0.1	0.2	0.1	0.1	0.1	0.1	0.1	0.1
Albite	2.9	2.6	3.1	3.1	2.7	2.4	3	2.5	2.1
Orthoclase	96.9	97.3	96.8	96.8	97.2	97.5	96.9	97.4	97.7

Table 27b. Chemical Composition of Microcline from the Kingman, Rare Metals and Wagon Bow Pegmatites

	Kingman Mine			Rare Metals Mine			Wagon Bow #3			Wagon Bow #2
Oxides	KFM-entranc e area-10	KFM-site-X-6	KFM-entranc e area-6	RMMF-1	RMM-24-1	RMMF-2	WH-1-10	WH-1-6	WH-1-7	WH2RA D-2
SiO <sub>2</sub>	64.91	64.77	64.88	64.83	64.81	64.84	64.57	64.74	64.69	64.59
TiO <sub>2</sub>	0.01	0	0.01	0.01	0.01	0.01	0.01	0.01	0.02	0.01
Al <sub>2</sub> O <sub>3</sub>	18.34	18.37	18.46	18.39	18.37	18.35	18.33	18.35	18.3	18.41
MgO	0	0	0	0	0	0	0	0	0.01	0
CaO	0.04	0.02	0.04	0.02	0.01	0.02	0.02	0.02	0.03	0.02
MnO	0	0	0	0	0	0.01	0	0	0	0.01
FeO	0.01	0	0.01	0.02	0	0.01	0.02	0.01	0.02	0.03
Na <sub>2</sub> O	0.33	0.3	0.28	0.29	0.29	0.31	0.23	0.29	0.3	0.31
K <sub>2</sub> O	16.41	16.31	16.23	16.33	16.3	16.29	16.3	16.26	16.34	16.23
Rb <sub>2</sub> O	0.07	0.04	0.06	0.07	0.06	0.07	0.06	0.06	0.05	
Total	100.12	99.81	99.98	99.94	99.84	99.91	99.53	99.73	99.76	99.61
Ions										
Ti	0	0	0	0	0	0	0	0	0.001	0
Mg	0	0	0	0	0	0	0	0	0.001	0
Ca	0.002	0.001	0.002	0.001	0	0.001	0.001	0.001	0.002	0.001
Mn	0	0	0	0	0	0	0	0	0	0
Fe 2+	0	0	0	0.001	0	0	0.001	0	0.001	0.001
Na	0.03	0.027	0.025	0.026	0.026	0.028	0.021	0.026	0.027	0.028
K	0.967	0.962	0.957	0.963	0.961	0.96	0.961	0.958	0.963	0.957
Rb	0.002	0.001	0.002	0.002	0.002	0.002	0.002	0.002	0.002	0
Σ X-Site	1.001	0.991	0.986	0.991	0.989	0.991	0.984	0.987	0.994	0.986
Σ Al	0.999	1	1.005	1.001	1	1	0.999	0.999	0.997	1.003
Σ Si	3	2.993	2.999	2.996	2.995	2.997	2.984	2.992	2.99	2.985
Anorthite	0.2	0.1	0.2	0.1	0	0.1	0.1	0.1	0.2	0.1
Albite	3	2.7	2.5	2.6	2.6	2.8	2.1	2.6	2.7	2.8
Orthoclase	96.8	97.2	97.3	97.3	97.3	97.1	97.8	97.3	97.1	97.1

Table 27c. Chemical Composition of Microcline from the Kingman, Rare Metals and Wagon Bow Pegmatites

	Kingman Mine				Rare Metals Mine			Wagon Bow #3	
	KFM-site-X-7	KFM-site-X-8	KFM-site-X-9	KFM-site-X-10	RMM-24-2	RMM-24-3	RMM-24-4	WH-1-8	WH-1-9
<b>Oxides</b>									
SiO <sub>2</sub>	64.88	64.88	64.83	64.84	64.78	64.71	64.74	64.67	64.6
TiO <sub>2</sub>	0.01	0.01	0.01	0.01	0.01	0.01	0.01	0.01	0.01
Al <sub>2</sub> O <sub>3</sub>	18.32	18.3	18.33	18.33	18.31	18.35	18.35	18.34	18.32
MgO	0	0	0	0	0	0	0	0.01	0
CaO	0.03	0.02	0.03	0.03	0.02	0.02	0.02	0.02	0.03
MnO	0	0	0	0	0	0	0	0	0
FeO	0	0	0	0.02	0.01	0.01	0.01	0.03	0.01
Na <sub>2</sub> O	0.32	0.29	0.34	0.34	0.3	0.27	0.32	0.28	0.23
K <sub>2</sub> O	16.3	16.22	16.31	16.28	16.32	16.31	16.11	16.29	16.32
Rb <sub>2</sub> O	0.05	0.05	0.05	0.06	0.07	0.06	0.06	0.05	0.06
Total	99.92	99.76	99.9	99.9	99.81	99.74	99.63	99.69	99.57
<b>Ions</b>									
Ti	0	0	0	0	0	0	0	0	0
Mg	0	0	0	0	0	0	0	0.001	0
Ca	0.002	0.001	0.002	0.001	0.001	0.001	0.001	0.001	0.001
Mn	0	0	0	0	0	0	0	0	0
Fe 2+	0	0	0	0.001	0	0.001	0	0.001	0
Na	0.029	0.026	0.031	0.031	0.027	0.024	0.029	0.025	0.021
K	0.961	0.956	0.962	0.959	0.962	0.961	0.95	0.96	0.962
Rb	0.002	0.002	0.001	0.002	0.002	0.002	0.002	0.001	0.002
Σ X-Site	0.993	0.984	0.995	0.993	0.992	0.988	0.982	0.987	0.986
Σ Al	0.998	0.997	0.998	0.999	0.997	1	0.999	0.999	0.998
Σ Si	2.999	2.998	2.996	2.997	2.994	2.99	2.992	2.988	2.985
Anorthite	0.2	0.1	0.2	0.1	0.1	0.1	0.1	0.1	0.1
Albite	2.9	2.6	3.1	3.1	2.7	2.4	3	2.5	2.1
Orthoclase	96.9	97.3	96.8	96.8	97.2	97.5	96.9	97.4	97.7

Table 28a. Chemical Composition of Plagioclase from the Rare Metals and Wagon Bow Pegmatites

Oxides	Rare Metals Mine				Wagon Bow # 3			
	RMMF-10	RMM-24-8	RMM-24-9	RMM-24-10	WH-1-1	WH-1-2	WH-1-3	WH-1-4
SiO <sub>2</sub>	68.6	68.68	68.72	68.77	68.71	68.67	68.68	68.72
TiO <sub>2</sub>	0	0	0	0	0	0	0	0
Al <sub>2</sub> O <sub>3</sub>	19.55	19.4	19.34	19.4	19.38	19.31	19.33	19.37
MgO	0	0	0	0.01	0	0	0	0
CaO	0.12	0.21	0.24	0.25	0.27	0.29	0.23	0.32
MnO	0	0	0	0	0	0	0	0
FeO	0	0	0	0.01	0	0	0	0
Na <sub>2</sub> O	11.33	11.34	11.29	11.36	11.22	11.35	11.31	11.2
K <sub>2</sub> O	0.13	0.2	0.21	0.22	0.23	0.19	0.33	0.23
Total	99.73	99.82	99.81	100.01	99.81	99.8	99.89	99.84
Ions								
Ti	0	0	0	0	0	0	0	0
Mg	0	0	0	0	0	0	0	0
Ca	0.005	0.01	0.011	0.012	0.013	0.013	0.011	0.015
Mn	0	0	0	0	0	0	0	0
Fe 2+	0	0	0	0	0	0	0	0
Na	0.961	0.961	0.957	0.961	0.951	0.962	0.959	0.949
K	0.007	0.011	0.012	0.012	0.013	0.011	0.019	0.013
Σ X-Site	0.974	0.982	0.98	0.985	0.977	0.986	0.988	0.976
Σ Al	1.007	1	0.997	0.998	0.998	0.995	0.996	0.998
Σ Si	3	3.002	3.005	3.002	3.004	3.004	3.003	3.004
Anorthite	0.6	1	1.2	1.2	1.3	1.4	1.1	1.5
Albite	98.7	97.9	97.6	97.6	97.4	97.6	97	97.2
Orthoclase	0.8	1.1	1.2	1.2	1.3	1.1	1.9	1.3

Table 28b. Chemical Composition of Plagioclase Exsolution Lamellae from the Kingman, Rare Metals and Wagon Bow Pegmatites

Oxides	Wagon Bow #2						Wagon Bow			Rare Metals Mine		
	Kingman Mine			# 3								
	WH2RAD -1	WH2RAD -5	WH2REC -2	KFM- entranc e -2	KFM- site-X- 1	KFM- entranc e -1	WH-1-5	RMM -24-6	RMM- 24-7	RMMF-9		
SiO <sub>2</sub>	68.79	68.67	68.61	68.61	68.68	68.55	68.68	69	68.69	68.61		
TiO <sub>2</sub>	0	0	0	0	0	0.01	0	0	0	0		
Al <sub>2</sub> O <sub>3</sub>	19.34	19.44	19.51	19.44	19.46	19.58	19.31	19	19.44	19.38		
MgO	0	0	0	0	0	0	0	0	0	0		
CaO	0.48	0.54	0.4	0.16	0.31	0.19	0.26	0.2	0.23	0.19		
MnO	0	0	0	0	0	0	0	0	0	0		
FeO	0.01	0.02	0.01	0	0	0	0	0	0	0		
Na <sub>2</sub> O	10.87	10.56	10.89	11.61	11.34	11.56	11.22	11	11.29	11.37		
K <sub>2</sub> O	0.09	0.1	0.09	0.15	0.12	0.2	0.15	0.2	0.23	0.18		
Total	99.58	99.34	99.52	99.96	99.91	100.08	99.62	100	99.88	99.73		
Ions												
Ti	0	0	0	0	0	0	0	0	0	0		
Mg	0	0	0	0	0	0	0	0	0	0		
Ca	0.022	0.026	0.019	0.007	0.015	0.009	0.012	0	0.011	0.009		
Mn	0	0	0	0	0	0	0	0	0	0		
Fe 2+	0	0.001	0	0	0	0	0	0	0	0		
Na	0.922	0.897	0.924	0.983	0.961	0.978	0.952	1	0.956	0.965		
K	0.005	0.006	0.005	0.008	0.007	0.011	0.008	0	0.013	0.01		
Σ X-Site	0.95	0.929	0.948	0.999	0.982	0.998	0.973	1	0.98	0.984		
Σ Al	0.997	1.004	1.007	1.001	1.002	1.007	0.996	1	1.001	1		
Σ Si	3.009	3.008	3.003	2.998	3	2.993	3.007	3	3.001	3.002		
Anorthite	2.3	2.7	2	0.7	1.5	0.9	1.2	0.9	1.1	0.9		
Albite	97.1	96.6	97.5	98.5	97.8	98	97.9	98	97.6	98.1		
Orthoclase	0.6	0.6	0.5	0.8	0.7	1.1	0.9	1.2	1.3	1		

Table 29a. Chemical Composition of Ilmenite from the Kingman Pegmatite

Oxides	KMB-X-M-5	KFMAX-3	B-3-A-2	B-3-A-5	B-4-B-1	B-4-B-2	B-4-B-3
WO <sub>3</sub>	0	0.02	0	0	0	0	0
Nb <sub>2</sub> O <sub>5</sub>	0	0.08	0.09	0.09	0.02	0.02	0.03
Ta <sub>2</sub> O <sub>5</sub>	0	0.01	0.01	0	0	0.01	0.02
SiO <sub>2</sub>	0	0	0	0	0	0	0
TiO <sub>2</sub>	52.09	51.43	52.12	52.01	55.23	53.34	55.65
ZrO <sub>2</sub>	0	0.01	0	0	0	0	0
SnO <sub>2</sub>	0	0.21	0.07	0.09	0	0	0.01
ThO <sub>2</sub>	0	0.01	0	0	0	0	0
Al <sub>2</sub> O <sub>3</sub>	0.08	0.13	0.25	0.29	0.15	0.23	0.21
Sc <sub>2</sub> O <sub>3</sub>	0.09	0	0	0	0	0	0
Ce <sub>2</sub> O <sub>3</sub>	0	0	0	0	0	0	0
MgO	0.06	0.14	0.33	0.26	0.17	0.21	0.19
CaO	0.04	0	0.03	0.05	0	0.02	0.02
MnO	8.45	0.45	1.45	1.34	0.09	0.08	0.1
FeO	38.83	46.77	45.98	45.9	41.67	44.88	42.34
Na <sub>2</sub> O	0.05	0	0	0	0	0	0
Total	99.99	99.99	100.34	100.03	99.99	99.99	100
Ions							
Mg	0.002	0.005	0.012	0.01	0.006	0.008	0.007
Mn	0.18	0.01	0.031	0.029	0.002	0.002	0.002
Fe 2+	0.816	0.978	0.968	0.969	0.82	0.919	0.852
$\Sigma$ A-Site	0.997	0.993	1.011	1.007	0.828	0.928	0.861
W	0	0	0	0	0	0	0
Nb	0	0.001	0.001	0.001	0	0	0
Ta	0	0	0	0	0	0	0
Si	0	0	0	0	0	0	0
Ti	0.984	0.967	0.986	0.987	0.978	0.982	1.007
Zr	0	0	0	0	0	0	0
Sn	0	0.002	0.001	0.001	0	0	0
Th	0	0	0	0	0	0	0
Al	0.002	0.004	0.007	0.009	0.004	0.007	0.006
Sc	0.002	0	0	0	0	0	0
Ce	0	0	0	0	0	0	0
Ca	0.001	0	0.001	0.001	0	0.001	0
Na	0.003	0	0	0	0	0	0
$\Sigma$ B-Site	0.988	0.991	0.994	0.996	0.982	0.988	1.013

Table 29b. Chemical Composition of Ilmenite from the Kingman Pegmatite

Oxides	KMB-X-M-5	KFMAX-3	B-3-A-2	B-3-A-5	B-4-B-1	B-4-B-2	B-4-B-3
WO <sub>3</sub>	0	0.02	0	0	0	0	0
Nb <sub>2</sub> O <sub>5</sub>	0	0.08	0.09	0.09	0.02	0.02	0.03
Ta <sub>2</sub> O <sub>5</sub>	0	0.01	0.01	0	0	0.01	0.02
SiO <sub>2</sub>	0	0	0	0	0	0	0
TiO <sub>2</sub>	52.09	51.43	52.12	52.01	55.23	53.34	55.65
ZrO <sub>2</sub>	0	0.01	0	0	0	0	0
SnO <sub>2</sub>	0	0.21	0.07	0.09	0	0	0.01
ThO <sub>2</sub>	0	0.01	0	0	0	0	0
Al <sub>2</sub> O <sub>3</sub>	0.08	0.13	0.25	0.29	0.15	0.23	0.21
Sc <sub>2</sub> O <sub>3</sub>	0.09	0	0	0	0	0	0
Ce <sub>2</sub> O <sub>3</sub>	0	0	0	0	0	0	0
MgO	0.06	0.14	0.33	0.26	0.17	0.21	0.19
CaO	0.04	0	0.03	0.05	0	0.02	0.02
MnO	8.45	0.45	1.45	1.34	0.09	0.08	0.1
FeO	38.83	46.77	45.98	45.9	41.67	44.88	42.34
Na <sub>2</sub> O	0.05	0	0	0	0	0	0
Total	99.99	99.99	100.34	100.03	99.99	99.99	100
Ions							
Mg	0.002	0.005	0.012	0.01	0.006	0.008	0.007
Mn	0.18	0.01	0.031	0.029	0.002	0.002	0.002
Fe 2+	0.816	0.978	0.968	0.969	0.82	0.919	0.852
Σ A-Site	0.997	0.993	1.011	1.007	0.828	0.928	0.861
W	0	0	0	0	0	0	0
Nb	0	0.001	0.001	0.001	0	0	0
Ta	0	0	0	0	0	0	0
Si	0	0	0	0	0	0	0
Ti	0.984	0.967	0.986	0.987	0.978	0.982	1.007
Zr	0	0	0	0	0	0	0
Sn	0	0.002	0.001	0.001	0	0	0
Th	0	0	0	0	0	0	0
Al	0.002	0.004	0.007	0.009	0.004	0.007	0.006
Sc	0.002	0	0	0	0	0	0
Ce	0	0	0	0	0	0	0
Ca	0.001	0	0.001	0.001	0	0.001	0
Na	0.003	0	0	0	0	0	0
Σ B-Site	0.988	0.991	0.994	0.996	0.982	0.988	1.013

Table 30a. Chemical Composition of Hematite from the Kingman, Rare Metals and Wagon Bow Pegmatites

Oxides	Kingman Feldspar Mine							Wagon Bow #2				
	KFMAA-3	KFMAA-4	KFMAA-5	S-1-A-1	S-1-A-2	S-1-A-4	S-1-A-5	WHM-1-4	S-2-A-1	S-2-A-3	S-2-A-5	S-2-A-4
TiO <sub>2</sub>	0	0	0	0.12	0.09	0.01	0.01	0	0.1	0.03	0.04	0.04
Al <sub>2</sub> O <sub>3</sub>	0.98	0.97	0.96	0.2	0.18	0.19	0.18	0.12	0.17	0.15	0.16	0.17
Sc <sub>2</sub> O <sub>3</sub>	0.03	0.03	0.03	0.01	0.01	0	0	0.03	0.01	0.01	0.02	0.01
					100.0							
Fe <sub>2</sub> O <sub>3</sub>	96.58	96.73	96.45	100	2	99.41	99.41	97.43	96.76	99.03	98.86	98.85
Ce <sub>2</sub> O <sub>3</sub>	0	0	0	0	0	0	0	0	0	0	0	0
MgO	0	0.02	0.02	0.03	0.02	0.03	0.03	0.04	0.03	0.02	0.04	0.03
CaO	0.11	0.12	0.11	0.06	0.02	0.03	0.05	0.02	0.03	0.02	0.03	0.02
MnO	0.11	0.14	0.12	0.46	0.53	0.56	0.48	0.16	0.38	0.52	0.63	0.46
				100.8	100.8	100.2	100.1					
Total	97.8	98.01	97.68	8	8	7	7	97.8	97.48	99.83	99.78	99.6
Ions												
Ti	0	0	0	0.005	0.004	0	0.001	0	0.004	0.001	0.002	0.002
Al	0.031	0.031	0.031	0.006	0.005	0.006	0.005	0.004	0.005	0.005	0.005	0.005
Sc	0.001	0.001	0.001	0	0	0	0	0.001	0	0	0	0
Fe <sup>3+</sup>	1.964	1.964	1.964	1.939	1.941	1.939	1.946	1.973	1.948	1.944	1.934	1.946
Ce	0	0	0	0	0	0	0	0	0	0	0	0
Mg	0	0.001	0.001	0.003	0.002	0.003	0.002	0.003	0.002	0.002	0.003	0.003
Ca	0.003	0.004	0.003	0.003	0.001	0.002	0.003	0.001	0.002	0.001	0.002	0.001
Mn	0.003	0.003	0.003	0.02	0.023	0.025	0.021	0.007	0.017	0.023	0.028	0.02
Σ A-Site	2.002	2.002	2.002	1.976	1.976	1.976	1.978	1.989	1.979	1.978	1.974	1.979

Table 30b. Chemical Composition of Hematite from the Kingman, Rare Metals and Wagon Bow Pegmatites

Oxides	Kingman Feldspar Mine						Wagon Bow #2					
	KFMAA-3	KFMAA-4	KFMAA-5	S-1-A-1	S-1-A-2	S-1-A-4	S-1-A-5	WHM-1-4	S-2-A-1	S-2-A-3	S-2-A-5	S-2-A-4
TiO <sub>2</sub>	0	0	0	0.12	0.09	0.01	0.01	0	0.1	0.03	0.04	0.04
Al <sub>2</sub> O <sub>3</sub>	0.98	0.97	0.96	0.2	0.18	0.19	0.18	0.12	0.17	0.15	0.16	0.17
Sc <sub>2</sub> O <sub>3</sub>	0.03	0.03	0.03	0.01	0.01	0	0	0.03	0.01	0.01	0.02	0.01
Fe <sub>2</sub> O <sub>3</sub>	96.58	96.73	96.45	100	100.02	99.41	99.41	97.43	96.76	99.03	98.86	98.85
Ce <sub>2</sub> O <sub>3</sub>	0	0	0	0	0	0	0	0	0	0	0	0
MgO	0	0.02	0.02	0.03	0.02	0.03	0.03	0.04	0.03	0.02	0.04	0.03
CaO	0.11	0.12	0.11	0.06	0.02	0.03	0.05	0.02	0.03	0.02	0.03	0.02
MnO	0.11	0.14	0.12	0.46	0.53	0.56	0.48	0.16	0.38	0.52	0.63	0.46
Total	97.8	98.01	97.68	100.88	100.88	100.27	100.17	97.8	97.48	99.83	99.78	99.6
Ions												
Ti	0	0	0	0.005	0.004	0	0.001	0	0.004	0.001	0.002	0.002
Al	0.031	0.031	0.031	0.006	0.005	0.006	0.005	0.004	0.005	0.005	0.005	0.005
Sc	0.001	0.001	0.001	0	0	0	0	0.001	0	0	0	0
Fe <sup>3+</sup>	1.964	1.964	1.964	1.939	1.941	1.939	1.946	1.973	1.948	1.944	1.934	1.946
Ce	0	0	0	0	0	0	0	0	0	0	0	0
Mg	0	0.001	0.001	0.003	0.002	0.003	0.002	0.003	0.002	0.002	0.003	0.003
Ca	0.003	0.004	0.003	0.003	0.001	0.002	0.003	0.001	0.002	0.001	0.002	0.001
Mn	0.003	0.003	0.003	0.02	0.023	0.025	0.021	0.007	0.017	0.023	0.028	0.02
Σ A-Site	2.002	2.002	2.002	1.976	1.976	1.976	1.978	1.989	1.979	1.978	1.974	1.979

Table 31. Chemical Compositions of Nd-Dominant Allanite from the Kingman Pegmatite

	KFMBA-1-1	KFMBA-1-2	KFMBA-1-3	KFMBA-2-1	KFMBA-2-2	KFMBA-2-3	KFMBA-2-4	KFMBX-1-2	KFMBX-3-3	KFMCA-1-1
WO <sub>3</sub>	0.02	0.01	0.01	0.00	0.00	0.02	0.01	0.00	0.01	0.00
P <sub>2</sub> O <sub>5</sub>	0.00	0.00	0.00	0.00	0.02	0.00	0.00	0.02	0.01	0.00
Nb <sub>2</sub> O <sub>5</sub>	0.01	0.01	0.01	0.01	0.01	0.00	0.00	0.00	0.00	0.00
Ta <sub>2</sub> O <sub>5</sub>	0.00	0.00	0.00	0.00	0.00	0.00	0.00	0.00	0.00	0.00
SiO <sub>2</sub>	29.59	29.66	29.58	29.68	29.84	29.76	29.66	29.88	29.86	29.87
TiO <sub>2</sub>	0.45	0.62	0.34	0.54	0.63	0.59	0.68	0.48	0.61	0.44
ZrO <sub>2</sub>	0.02	0.01	0.01	0.01	0.02	0.03	0.03	0.00	0.00	0.00
SnO <sub>2</sub>	0.00	0.00	0.00	0.00	0.00	0.00	0.00	0.00	0.00	0.00
HfO <sub>2</sub>	0.00	0.00	0.00	0.00	0.00	0.00	0.00	0.00	0.00	0.00
ThO <sub>2</sub>	0.90	0.90	0.87	0.78	0.80	0.76	0.72	0.47	0.42	0.40
UO <sub>2</sub>	0.11	0.14	0.13	0.10	0.05	0.05	0.07	0.05	0.03	0.02
Al <sub>2</sub> O <sub>3</sub>	12.20	12.32	12.72	13.09	12.46	12.33	12.56	13.95	12.64	12.90
Sc <sub>2</sub> O <sub>3</sub>	0.06	0.05	0.06	0.06	0.07	0.07	0.06	0.06	0.06	0.07
Y <sub>2</sub> O <sub>3</sub>	0.20	0.20	0.19	0.16	0.18	0.21	0.19	0.09	0.08	0.10
La <sub>2</sub> O <sub>3</sub>	3.09	3.01	2.98	4.98	4.65	5.00	4.98	5.06	5.30	3.79
Ce <sub>2</sub> O <sub>3</sub>	7.88	8.10	7.89	5.78	5.57	5.89	5.69	6.45	6.88	6.78
Pr <sub>2</sub> O <sub>3</sub>	1.83	1.89	1.78	1.77	1.90	1.89	1.88	1.34	1.45	1.83
Nd <sub>2</sub> O <sub>3</sub>	9.03	8.78	8.60	7.97	8.66	7.89	7.78	6.77	7.09	6.99
Sm <sub>2</sub> O <sub>3</sub>	1.15	1.15	1.32	1.11	1.09	1.09	0.97	1.11	1.32	1.22
Eu <sub>2</sub> O <sub>3</sub>	0.01	0.01	0.01	0.00	0.00	0.00	0.00	0.01	0.09	0.02
Gd <sub>2</sub> O <sub>3</sub>	0.00	0.01	0.01	0.01	0.00	0.00	0.01	0.02	0.02	0.03
Tb <sub>2</sub> O <sub>3</sub>	0.00	0.01	0.00	0.00	0.00	0.00	0.00	0.00	0.05	0.02
Dy <sub>2</sub> O <sub>3</sub>	0.02	0.03	0.03	0.03	0.03	0.03	0.03	0.00	0.02	0.03
Ho <sub>2</sub> O <sub>3</sub>	0.00	0.01	0.00	0.00	0.00	0.00	0.00	0.00	0.04	0.01
Er <sub>2</sub> O <sub>3</sub>	0.01	0.00	0.00	0.00	0.00	0.01	0.00	0.00	0.00	0.00
Tm <sub>2</sub> O <sub>3</sub>	0.00	0.00	0.00	0.00	0.00	0.00	0.00	0.00	0.01	0.00
Yb <sub>2</sub> O <sub>3</sub>	0.19	0.18	0.19	0.09	0.15	0.16	0.13	0.07	0.12	0.08
Lu <sub>2</sub> O <sub>3</sub>	0.00	0.00	0.00	0.00	0.00	0.00	0.00	0.00	0.00	0.00
MgO	0.30	0.30	0.24	0.29	0.27	0.22	0.24	0.08	0.16	0.25
CaO	9.00	9.45	9.93	9.88	9.67	9.67	9.81	10.32	9.97	9.76
MnO	1.23	1.33	1.13	1.07	1.10	1.01	1.04	0.93	1.16	1.68
FeO	16.43	16.39	16.84	17.82	16.56	16.90	17.43	15.82	16.96	16.97
PbO	0.02	0.02	0.04	0.01	0.00	0.02	0.04	0.02	0.02	0.03
Na <sub>2</sub> O	0.00	0.00	0.00	0.00	0.00	0.00	0.00	0.00	0.02	0.00
K <sub>2</sub> O	0.00	0.03	0.00	0.00	0.02	0.03	0.02	0.02	0.04	0.00
H <sub>2</sub> O	6.155	5.315	4.999	4.699	6.145	6.288	5.885	6.943	5.511	6.694
F	0.021	0	0.013	0.021	0.074	0.033	0.054	0.012	0	0
Cl	0.055	0.062	0.068	0.044	0.043	0.033	0.035	0.045	0.044	0.015
Subtotal	100	100	100	100	100	100	100	100	100	100
Less O=F	0.01	0.00	0.01	0.01	0.03	0.01	0.02	0.01	0.00	0.00
Less O=Cl	0.01	0.01	0.02	0.01	0.01	0.01	0.01	0.01	0.01	0.00
Total	99.98	99.99	99.98	99.98	99.96	99.98	99.97	99.98	99.99	100.00

Table 31 cont. Chemical Formula of Nd-Dominant Allanite from the Kingman Pegmatite

Ions	KFMBA-1-1	KFMBA-1-2	KFMBA-1-3	KFMBA-2-1	KFMBA-2-2	KFMBA-2-3	KFMBA-2-4	KFMBX-1-2	KFMBX-3-3	KFMCA-1-1
W	0	0	0	0	0	0.001	0	0	0	0
P	0	0	0	0	0.002	0	0	0.002	0.001	0
Nb	0.001	0.001	0	0	0	0	0	0	0	0
Ta	0	0	0	0	0	0	0	0	0	0
Zr	0.001	0.001	0.001	0	0.001	0.002	0.001	0	0	0
Sn	0	0	0	0	0	0	0	0	0	0
Hf	0	0	0	0	0	0	0	0	0	0
Th	0.021	0.021	0.02	0.018	0.018	0.018	0.017	0.011	0.01	0.009
U	0.003	0.003	0.003	0.002	0.001	0.001	0.002	0.001	0.001	0.001
Sc	0.006	0.005	0.005	0.005	0.006	0.006	0.005	0.005	0.005	0.006
Y	0.011	0.011	0.01	0.008	0.009	0.011	0.01	0.005	0.004	0.005
La	0.116	0.112	0.112	0.186	0.172	0.186	0.186	0.187	0.196	0.14
Ce	0.292	0.3	0.293	0.214	0.205	0.217	0.211	0.237	0.253	0.249
Pr	0.068	0.07	0.066	0.065	0.07	0.069	0.069	0.049	0.053	0.067
<b>Nd</b>	<b>0.327</b>	<b>0.317</b>	<b>0.311</b>	<b>0.288</b>	<b>0.311</b>	<b>0.284</b>	<b>0.281</b>	<b>0.243</b>	<b>0.255</b>	<b>0.251</b>
Sm	0.04	0.04	0.046	0.039	0.038	0.038	0.034	0.039	0.046	0.042
Eu	0	0	0	0	0	0	0	0	0.003	0.001
Gd	0	0	0	0	0	0	0	0.001	0.001	0.001
Tb	0	0	0	0	0	0	0	0	0.001	0.001
Dy	0.001	0.001	0.001	0.001	0.001	0.001	0.001	0	0.001	0.001
Ho	0	0	0	0	0	0	0	0	0.001	0
Er	0	0	0	0	0	0	0	0	0	0
Tm	0	0	0	0	0	0	0	0	0	0
Yb	0.006	0.005	0.006	0.003	0.004	0.005	0.004	0.002	0.004	0.002
Lu	0	0	0	0	0	0	0	0	0	0
Ca	0.977	1.024	1.079	1.07	1.042	1.045	1.063	1.11	1.074	1.05
Mn	0.105	0.114	0.097	0.091	0.094	0.086	0.089	0.079	0.099	0.143
Pb	0.001	0.001	0.001	0	0	0.001	0.001	0	0.001	0.001
Na	0	0	0	0	0	0	0	0	0.004	0
K	0	0.004	0	0	0.003	0.005	0.003	0.003	0.007	0
$\Sigma$ A-Site	1.976	2.03	2.051	1.99	1.977	1.976	1.977	1.974	2.02	1.97
Al	1.458	1.469	1.521	1.56	1.476	1.465	1.498	1.65	1.497	1.527
Ti	0.035	0.047	0.026	0.041	0.048	0.045	0.052	0.036	0.046	0.034
Mg	0.046	0.045	0.037	0.043	0.041	0.034	0.036	0.012	0.023	0.038
Fe 2+	1.393	1.386	1.428	1.507	1.392	1.425	1.474	1.328	1.425	1.426
$\Sigma$ M-Site	2.932	2.947	3.012	3.151	2.957	2.969	3.06	3.026	2.991	3.025
$\Sigma$ Si	3	3	3	3	3	3	3	3	3	3
OH	4.058	3.982	3.992	3.979	3.956	3.968	3.988	3.985	3.988	3.994
F	0.007	0	0.004	0.007	0.024	0.011	0.017	0.004	0	0
Cl	0.009	0.011	0.012	0.008	0.007	0.006	0.006	0.008	0.007	0.003
$\Sigma$ Hydroxyl	4.179	3.597	3.398	3.183	4.151	4.245	3.995	4.661	3.701	4.488

Table 32a. Chemical Compositions of Allanite from the Kingman Pegmatite

	KFMBA- 1-3b	KFMBA- 3-1	KFMBA- 3-2	KFMBA- 3-3	KFMBA- 3-4	KFMBX- 1-1	KFMBX- 1-3	KFMBX- 1-4	KFMBX- 2-1	KFMBX- 2-2
WO <sub>3</sub>	0.01	0	0	0.01	0	0	0	0	0.01	0
P <sub>2</sub> O <sub>5</sub>	0	0	0	0	0	0	0	0	0	0
Nb <sub>2</sub> O <sub>5</sub>	0.01	0	0	0	0	0	0	0	0	0
Ta <sub>2</sub> O <sub>5</sub>	0	0.02	0	0	0	0	0	0	0	0.01
SiO <sub>2</sub>	29.57	30.02	29.69	29.66	29.78	29.88	29.82	29.57	29.57	29.44
TiO <sub>2</sub>	0.31	0.77	0.76	0.83	0.75	0.52	0.56	0.5	0.68	0.66
ZrO <sub>2</sub>	0.01	0.02	0	0.02	0	0	0	0	0	0
SnO <sub>2</sub>	0	0	0	0	0	0	0	0	0	0
HfO <sub>2</sub>	0	0	0	0	0	0	0	0	0	0
ThO <sub>2</sub>	0.9	0.57	0.46	0.47	0.51	0.46	0.51	0.62	0.34	0.44
UO <sub>2</sub>	0.14	0.05	0.03	0.03	0.03	0.05	0.05	0.04	0.03	0.03
Al <sub>2</sub> O <sub>3</sub>	12.45	12.68	12.76	12.57	12.38	13.54	13.64	13.33	11.88	11.79
Sc <sub>2</sub> O <sub>3</sub>	0.06	0.06	0.06	0.05	0.04	0.07	0.06	0.05	0.07	0.06
Y <sub>2</sub> O <sub>3</sub>	0.25	0.09	0.08	0.09	0.08	0.08	0.08	0.09	0.11	0.09
La <sub>2</sub> O <sub>3</sub>	3.01	4.55	3.46	3.98	3	5.57	5.23	4.88	4.66	4.56
Ce <sub>2</sub> O <sub>3</sub>	9.33	8.88	8.98	8.99	8.66	6.57	6.98	7	8.77	8.57
Pr <sub>2</sub> O <sub>3</sub>	1.81	1.46	1.65	1.57	1.43	0.98	1.51	1.11	1.43	1.68
Nd <sub>2</sub> O <sub>3</sub>	8.9	6.79	7.09	6.33	7.34	6.55	6.55	6.72	6.23	6.34
Sm <sub>2</sub> O <sub>3</sub>	1.3	0.94	1.15	1	0.88	0.89	0.93	0.93	1.11	1.09
Eu <sub>2</sub> O <sub>3</sub>	0.01	0	0	0	0.01	0	0.01	0	0	0
Gd <sub>2</sub> O <sub>3</sub>	0	0.02	0.02	0.02	0.01	0	0	0.02	0.02	0.03
Tb <sub>2</sub> O <sub>3</sub>	0	0	0	0	0	0	0	0	0	0.01
Dy <sub>2</sub> O <sub>3</sub>	0.03	0.03	0.02	0.03	0.02	0	0	0	0	0.01
Ho <sub>2</sub> O <sub>3</sub>	0	0	0	0	0	0	0	0	0	0
Er <sub>2</sub> O <sub>3</sub>	0	0	0	0	0	0	0	0	0	0.01
Tm <sub>2</sub> O <sub>3</sub>	0	0	0	0	0	0	0	0	0	0.01
Yb <sub>2</sub> O <sub>3</sub>	0.21	0.06	0.06	0.06	0.05	0.09	0.08	0.07	0.1	0.11
Lu <sub>2</sub> O <sub>3</sub>	0	0	0	0	0	0	0	0	0	0
MgO	0.27	0.16	0.16	0.15	0.17	0.09	0.08	0.07	0.33	0.31
CaO	9.43	9.65	9.66	9.83	10.09	10.33	9.77	9.84	9.89	10.12
MnO	1.2	1.23	1.27	1.32	1.22	0.92	0.89	0.91	0.93	0.93
FeO	15.46	17.79	17.22	17.09	17.43	15.55	15.87	15.77	17.66	17.56
PbO	0.04	0.03	0.02	0.03	0.02	0.02	0.01	0.02	0.02	0.02
Na <sub>2</sub> O	0	0	0	0	0	0	0	0	0	0
K <sub>2</sub> O	0.02	0.01	0.09	0.03	0.01	0.02	0.02	0.02	0	0
H <sub>2</sub> O	5.197	4.115	5.268	5.786	6.034	7.795	7.219	8.382	6.066	6.041
F	0	0.011	0.026	0.026	0.023	0	0.021	0.018	0.073	0.034
Cl	0.055	0.022	0.023	0.031	0.028	0.043	0.088	0.045	0.023	0.031
Subtotal	100	100	100	100	100	100	100	100	100	100
Less O=F	0	0	0.01	0.01	0.01	0	0.01	0.01	0.03	0.01
Less O=Cl	0.01	0	0.01	0.01	0.01	0.01	0.02	0.01	0.01	0.01
Total	99.99	99.99	99.98	99.98	99.98	99.99	99.97	99.98	99.96	99.98

Table 32a cont. Chemical Formula of Allanite from the Kingman Pegmatite

Ions	KFMBA-1-3b	KFMBA-3-1	KFMBA-3-2	KFMBA-3-3	KFMBA-3-4	KFMBX-1-1	KFMBX-1-3	KFMBX-1-4	KFMBX-2-1	KFMBX-2-2
W	0	0	0	0	0	0	0	0	0	0
P	0	0	0	0	0	0	0	0	0	0
Nb	0.001	0	0	0	0	0	0	0	0	0
Ta	0	0.001	0	0	0	0	0	0	0	0
Zr	0.001	0.001	0	0.001	0	0	0	0	0	0
Sn	0	0	0	0	0	0	0	0	0	0
Hf	0	0	0	0	0	0	0	0	0	0
Th	0.021	0.013	0.011	0.011	0.012	0.01	0.012	0.014	0.008	0.01
U	0.003	0.001	0.001	0.001	0.001	0.001	0.001	0.001	0.001	0.001
Sc	0.005	0.005	0.005	0.004	0.004	0.006	0.005	0.005	0.006	0.005
Y	0.013	0.005	0.004	0.005	0.004	0.004	0.004	0.005	0.006	0.005
La	0.113	0.167	0.129	0.149	0.111	0.206	0.194	0.183	0.174	0.171
Ce	0.347	0.325	0.332	0.333	0.319	0.241	0.257	0.26	0.326	0.319
Pr	0.067	0.053	0.061	0.058	0.053	0.036	0.055	0.041	0.053	0.062
Nd	0.323	0.242	0.256	0.229	0.264	0.235	0.235	0.244	0.226	0.231
Sm	0.045	0.032	0.04	0.035	0.031	0.031	0.032	0.033	0.039	0.038
Eu	0	0	0	0	0	0	0	0	0	0
Gd	0	0.001	0.001	0.001	0	0	0	0.001	0.001	0.001
Tb	0	0	0	0	0	0	0	0	0	0
Dy	0.001	0.001	0.001	0.001	0.001	0	0	0	0	0
Ho	0	0	0	0	0	0	0	0	0	0
Er	0	0	0	0	0	0	0	0	0	0
Tm	0	0	0	0	0	0	0	0	0	0
Yb	0.007	0.002	0.002	0.002	0.001	0.003	0.003	0.002	0.003	0.003
Lu	0	0	0	0	0	0	0	0	0	0
Ca	1.025	1.033	1.045	1.066	1.089	1.111	1.052	1.07	1.075	1.105
Mn	0.103	0.104	0.109	0.113	0.104	0.078	0.076	0.078	0.08	0.081
Pb	0.001	0.001	0.001	0.001	0.001	0.001	0	0	0.001	0.001
Na	0	0	0	0	0	0	0	0	0	0
K	0.003	0.002	0.014	0.005	0.001	0.003	0.003	0.003	0	0
$\Sigma$ A-Site	2.079	1.989	2.012	2.015	1.996	1.966	1.929	1.94	1.999	2.033
Al	1.489	1.493	1.519	1.498	1.47	1.602	1.618	1.594	1.42	1.416
Ti	0.024	0.058	0.058	0.063	0.057	0.04	0.042	0.038	0.052	0.05
Mg	0.04	0.023	0.025	0.023	0.025	0.013	0.012	0.01	0.051	0.048
Fe 2+	1.311	1.486	1.455	1.446	1.468	1.305	1.335	1.338	1.498	1.496
$\Sigma$ M-Site	2.864	3.06	3.057	3.03	3.02	2.96	3.007	2.98	3.021	3.01
$\Sigma$ Si	3	3	3	3	3	3	3	3	3	3
OH	3.994	4	3.977	3.914	4.06	3.985	4.026	3.994	4.061	3.976
F	0	0.003	0.008	0.008	0.007	0	0.007	0.006	0.023	0.011
Cl	0.009	0.004	0.004	0.005	0.005	0.007	0.015	0.008	0.004	0.005
$\Sigma$ Hydroxyl	3.527	2.75	3.563	3.918	4.068	5.228	4.866	5.687	4.133	4.122

Table 32b. Chemical Compositions of Allanite from the Kingman Pegmatite

	KFMBX-2- 3	KFMBX-2- 4	KFMBX-3- 1	KFMBX-3- 2	KFMBX-3- 4	KFMCA-1- 2	KFMCA-1- 3	KFMCA-1- 4	KFMCA-2- 1	KFMCA-2- 2
WO <sub>3</sub>	0.00	0.00	0.00	0.00	0.01	0.00	0.02	0.02	0.00	0.00
P <sub>2</sub> O <sub>5</sub>	0.00	0.00	0.03	0.01	0.01	0.00	0.00	0.00	0.00	0.00
Nb <sub>2</sub> O <sub>5</sub>	0.00	0.00	0.00	0.00	0.00	0.00	0.00	0.00	0.00	0.00
Ta <sub>2</sub> O <sub>5</sub>	0.00	0.00	0.00	0.00	0.00	0.00	0.00	0.00	0.00	0.00
SiO <sub>2</sub>	29.54	29.54	29.88	29.70	29.64	29.88	29.53	29.98	29.68	29.84
TiO <sub>2</sub>	0.70	0.57	0.57	0.52	0.59	0.43	0.46	0.42	0.57	0.64
ZrO <sub>2</sub>	0.00	0.00	0.00	0.00	0.00	0.03	0.03	0.01	0.00	0.00
SnO <sub>2</sub>	0.00	0.00	0.00	0.00	0.00	0.02	0.03	0.01	0.00	0.00
HfO <sub>2</sub>	0.00	0.00	0.00	0.00	0.00	0.00	0.00	0.00	0.00	0.00
ThO <sub>2</sub>	0.38	0.41	0.44	0.41	0.44	0.39	0.37	0.41	0.54	0.57
UO <sub>2</sub>	0.04	0.03	0.05	0.04	0.03	0.03	0.03	0.02	0.01	0.01
Al <sub>2</sub> O <sub>3</sub>	11.92	11.56	12.54	12.60	12.55	12.87	13.03	13.32	12.78	12.96
Sc <sub>2</sub> O <sub>3</sub>	0.07	0.07	0.06	0.06	0.06	0.08	0.07	0.07	0.06	0.06
Y <sub>2</sub> O <sub>3</sub>	0.08	0.10	0.08	0.08	0.08	0.09	0.06	0.09	0.09	0.09
La <sub>2</sub> O <sub>3</sub>	4.44	4.53	5.44	5.10	5.65	4.12	4.05	3.73	3.54	3.43
Ce <sub>2</sub> O <sub>3</sub>	8.73	8.94	7.57	7.00	8.43	6.95	6.79	7.33	8.96	9.06
Pr <sub>2</sub> O <sub>3</sub>	1.68	1.80	1.57	1.76	1.23	1.68	1.60	1.55	1.89	1.77
Nd <sub>2</sub> O <sub>3</sub>	6.44	6.53	6.88	7.10	7.23	6.34	6.88	6.23	6.34	5.68
Sm <sub>2</sub> O <sub>3</sub>	1.21	1.18	1.34	1.30	1.28	1.19	1.17	1.02	1.34	1.23
Eu <sub>2</sub> O <sub>3</sub>	0.00	0.00	0.00	0.00	0.02	0.02	0.03	0.02	0.06	0.03
Gd <sub>2</sub> O <sub>3</sub>	0.02	0.02	0.00	0.02	0.02	0.02	0.02	0.02	0.03	0.03
Tb <sub>2</sub> O <sub>3</sub>	0.00	0.00	0.00	0.00	0.00	0.00	0.03	0.02	0.03	0.02
Dy <sub>2</sub> O <sub>3</sub>	0.02	0.00	0.00	0.00	0.00	0.03	0.02	0.03	0.00	0.00
Ho <sub>2</sub> O <sub>3</sub>	0.00	0.00	0.03	0.02	0.03	0.02	0.02	0.01	0.02	0.01
Er <sub>2</sub> O <sub>3</sub>	0.00	0.00	0.00	0.00	0.00	0.03	0.02	0.00	0.00	0.01
Tm <sub>2</sub> O <sub>3</sub>	0.00	0.00	0.00	0.01	0.00	0.02	0.00	0.02	0.00	0.01
Yb <sub>2</sub> O <sub>3</sub>	0.10	0.10	0.11	0.09	0.14	0.08	0.09	0.08	0.03	0.05
Lu <sub>2</sub> O <sub>3</sub>	0.00	0.01	0.00	0.00	0.00	0.00	0.01	0.00	0.00	0.01
MgO	0.26	0.30	0.15	0.17	0.17	0.27	0.24	0.30	0.12	0.13
CaO	10.22	10.23	10.00	10.22	9.90	10.33	9.66	9.83	9.79	9.90
MnO	0.94	0.94	1.22	1.18	1.10	1.73	1.79	1.72	0.88	0.95
FeO	17.88	17.66	16.89	17.06	16.89	16.73	16.26	17.07	16.79	16.83
PbO	0.02	0.02	0.02	0.02	0.03	0.01	0.02	0.03	0.02	0.02
Na <sub>2</sub> O	0.00	0.00	0.00	0.00	0.00	0.00	0.00	0.02	0.00	0.00
K <sub>2</sub> O	0.01	0.01	0.00	0.02	0.00	0.00	0.00	0.02	0.00	0.00
H <sub>2</sub> O	5.90	5.87	6.00	5.91	5.95	5.95	5.90	5.98	5.90	5.95
F	0.06	0.05	0.00	0.00	0.00	0.03	0.02	0.00	0.03	0.02
Cl	0.03	0.02	0.06	0.06	0.03	0.01	0.00	0.02	0.02	0.03
Subtotal	100.68	100.50	100.93	100.45	101.52	99.39	98.24	99.43	99.54	99.34
Less O=F	0.02	0.02	0.00	0.00	0.00	0.01	0.01	0.00	0.01	0.01
Less O=Cl	0.01	0.01	0.01	0.01	0.01	0.00	0.00	0.01	0.01	0.01
Total	100.65	100.48	100.92	100.44	101.51	99.37	98.24	99.42	99.52	99.33

Table 32b cont. Chemical Formula of Allanite from the Kingman Pegmatite

Ions	KFMBX- 2-3	KFMBX- 2-4	KFMBX- 3-1	KFMBX- 3-2	KFMBX- 3-4	KFMCA- 1-2	KFMCA- 1-3	KFMCA- 1-4	KFMCA- 2-1	KFMCA- 2-2
W	0.000	0.000	0.000	0.000	0.000	0.000	0.001	0.000	0.000	0.000
P	0.000	0.000	0.003	0.001	0.001	0.000	0.000	0.000	0.000	0.000
Nb	0.000	0.000	0.000	0.000	0.000	0.000	0.000	0.000	0.000	0.000
Ta	0.000	0.000	0.000	0.000	0.000	0.000	0.000	0.000	0.000	0.000
Zr	0.000	0.000	0.000	0.000	0.000	0.002	0.002	0.001	0.000	0.000
Sn	0.000	0.000	0.000	0.000	0.000	0.001	0.001	0.000	0.000	0.000
Hf	0.000	0.000	0.000	0.000	0.000	0.000	0.000	0.000	0.000	0.000
Th	0.009	0.009	0.010	0.009	0.010	0.009	0.008	0.009	0.013	0.013
U	0.001	0.001	0.001	0.001	0.001	0.001	0.001	0.000	0.000	0.000
Sc	0.006	0.006	0.005	0.005	0.005	0.007	0.006	0.006	0.005	0.005
Y	0.004	0.005	0.004	0.004	0.004	0.005	0.003	0.005	0.005	0.005
La	0.166	0.170	0.202	0.190	0.211	0.153	0.152	0.138	0.132	0.127
Ce	0.325	0.332	0.278	0.259	0.312	0.255	0.252	0.269	0.332	0.333
Pr	0.062	0.067	0.057	0.065	0.045	0.061	0.059	0.057	0.070	0.065
Nd	0.234	0.237	0.247	0.256	0.261	0.227	0.249	0.223	0.229	0.204
Sm	0.042	0.041	0.046	0.045	0.045	0.041	0.041	0.035	0.047	0.043
Eu	0.000	0.000	0.000	0.000	0.001	0.001	0.001	0.001	0.002	0.001
Gd	0.001	0.001	0.000	0.001	0.001	0.001	0.001	0.001	0.001	0.001
Tb	0.000	0.000	0.000	0.000	0.000	0.000	0.001	0.001	0.001	0.001
Dy	0.001	0.000	0.000	0.000	0.000	0.001	0.001	0.001	0.000	0.000
Ho	0.000	0.000	0.001	0.001	0.001	0.001	0.001	0.000	0.001	0.000
Er	0.000	0.000	0.000	0.000	0.000	0.001	0.001	0.000	0.000	0.000
Tm	0.000	0.000	0.000	0.000	0.000	0.001	0.000	0.001	0.000	0.000
Yb	0.003	0.003	0.003	0.003	0.004	0.002	0.003	0.003	0.001	0.001
Lu	0.000	0.000	0.000	0.000	0.000	0.000	0.000	0.000	0.000	0.000
Ca	1.112	1.113	1.075	1.106	1.073	1.112	1.051	1.054	1.060	1.066
Mn	0.081	0.081	0.104	0.101	0.094	0.147	0.154	0.146	0.075	0.080
Pb	0.000	0.001	0.000	0.000	0.001	0.000	0.001	0.001	0.001	0.000
Na	0.000	0.000	0.000	0.000	0.000	0.000	0.000	0.003	0.000	0.000
K	0.002	0.002	0.000	0.003	0.000	0.000	0.000	0.003	0.000	0.000
$\sum$ A-Site	2.049	2.069	2.036	2.050	2.070	2.029	1.990	1.958	1.975	1.945
Al	1.427	1.384	1.484	1.500	1.496	1.524	1.560	1.572	1.522	1.535
Ti	0.053	0.043	0.043	0.040	0.045	0.033	0.035	0.032	0.043	0.049
Mg	0.039	0.045	0.023	0.025	0.026	0.040	0.037	0.045	0.018	0.020
Fe 2+	1.518	1.499	1.418	1.441	1.430	1.405	1.381	1.428	1.419	1.415
$\sum$ M-Site	3.037	2.971	2.968	3.006	2.997	3.002	3.013	3.077	3.002	3.019
$\sum$ Si	3.000	3.000	3.000	3.000	3.000	3.000	3.000	3.000	3.000	3.000
OH	3.996	3.977	4.018	3.982	4.017	3.986	3.998	3.992	3.979	3.990
F	0.018	0.014	0.000	0.000	0.000	0.010	0.006	0.000	0.010	0.007
Cl	0.004	0.004	0.009	0.011	0.006	0.002	0.000	0.004	0.004	0.005
$\sum$ Hydroxyl	4.019	3.995	4.028	3.993	4.022	3.998	4.004	3.996	3.993	4.002

Table 32c. Chemical Compositions of Allanite from the Kingman Pegmatite

	KFMCX- 2-1	KFMCX- 2-2	KFMCX- 2-3	KFMCX- 2-4	KFMCX- 3-1	KFMCX- 3-2	KFMCX- 3-3	KFMCX- 3-4	KFMCF-2- 1	KFMCF-2- 2
WO <sub>3</sub>	0.00	0.00	0.00	0.00	0.00	0.00	0.00	0.00	0.00	0.00
P <sub>2</sub> O <sub>5</sub>	0.00	0.00	0.00	0.00	0.00	0.00	0.00	0.00	0.05	0.02
Nb <sub>2</sub> O <sub>5</sub>	0.00	0.00	0.00	0.00	0.03	0.00	0.00	0.00	0.00	0.00
Ta <sub>2</sub> O <sub>5</sub>	0.00	0.00	0.00	0.00	0.00	0.00	0.00	0.00	0.00	0.00
SiO <sub>2</sub>	29.76	29.67	29.88	29.71	29.62	29.66	29.58	29.47	29.78	29.78
TiO <sub>2</sub>	0.35	0.34	0.28	0.32	0.46	0.47	0.48	0.51	0.87	0.93
ZrO <sub>2</sub>	0.00	0.00	0.00	0.00	0.02	0.02	0.01	0.00	0.00	0.01
SnO <sub>2</sub>	0.00	0.00	0.00	0.00	0.00	0.00	0.00	0.00	0.00	0.00
HfO <sub>2</sub>	0.00	0.00	0.00	0.00	0.00	0.00	0.00	0.00	0.00	0.00
ThO <sub>2</sub>	0.88	0.90	0.77	0.79	0.54	0.49	0.50	0.51	0.95	1.02
UO <sub>2</sub>	0.09	0.07	0.05	0.07	0.03	0.06	0.06	0.05	0.11	0.10
Al <sub>2</sub> O <sub>3</sub>	12.59	12.27	12.46	12.23	13.22	12.89	13.23	13.00	12.88	12.68
Sc <sub>2</sub> O <sub>3</sub>	0.08	0.08	0.09	0.09	0.08	0.08	0.07	0.08	0.08	0.06
Y <sub>2</sub> O <sub>3</sub>	0.11	0.09	0.10	0.09	0.06	0.07	0.07	0.05	0.23	0.21
La <sub>2</sub> O <sub>3</sub>	3.33	3.24	3.26	3.44	4.23	4.63	3.43	4.54	4.10	3.65
Ce <sub>2</sub> O <sub>3</sub>	9.83	9.57	9.93	10.00	9.46	9.22	9.09	9.10	9.88	10.00
Pr <sub>2</sub> O <sub>3</sub>	1.88	1.90	1.99	2.02	2.32	2.23	2.33	2.41	1.00	1.01
Nd <sub>2</sub> O <sub>3</sub>	6.44	6.79	6.23	6.00	6.20	6.23	6.44	6.22	6.12	5.99
Sm <sub>2</sub> O <sub>3</sub>	1.22	1.27	1.32	1.28	1.45	1.50	1.45	1.38	0.88	0.78
Eu <sub>2</sub> O <sub>3</sub>	0.03	0.04	0.05	0.04	0.00	0.00	0.03	0.01	0.02	0.02
Gd <sub>2</sub> O <sub>3</sub>	0.03	0.03	0.02	0.02	0.03	0.04	0.04	0.04	0.02	0.02
Tb <sub>2</sub> O <sub>3</sub>	0.01	0.02	0.01	0.01	0.00	0.01	0.00	0.00	0.00	0.01
Dy <sub>2</sub> O <sub>3</sub>	0.00	0.00	0.01	0.01	0.01	0.02	0.03	0.02	0.03	0.00
Ho <sub>2</sub> O <sub>3</sub>	0.01	0.01	0.01	0.01	0.00	0.00	0.01	0.00	0.00	0.00
Er <sub>2</sub> O <sub>3</sub>	0.00	0.02	0.02	0.00	0.01	0.00	0.00	0.00	0.00	0.00
Tm <sub>2</sub> O <sub>3</sub>	0.00	0.01	0.01	0.00	0.00	0.00	0.00	0.00	0.00	0.00
Yb <sub>2</sub> O <sub>3</sub>	0.07	0.09	0.08	0.07	0.10	0.09	0.10	0.12	0.15	0.14
Lu <sub>2</sub> O <sub>3</sub>	0.00	0.01	0.01	0.00	0.00	0.00	0.00	0.00	0.00	0.00
MgO	0.20	0.19	0.22	0.18	0.22	0.23	0.23	0.26	0.55	0.52
CaO	9.89	9.43	9.56	9.51	10.00	10.09	10.10	10.04	9.86	9.93
MnO	1.22	1.29	1.31	1.22	0.96	0.98	0.95	0.93	1.33	1.28
FeO	17.34	17.45	17.56	17.34	16.00	15.89	16.01	15.94	17.00	17.22
PbO	0.03	0.03	0.03	0.03	0.03	0.03	0.02	0.02	0.16	0.11
Na <sub>2</sub> O	0.00	0.00	0.00	0.00	0.00	0.00	0.00	0.00	0.00	0.00
K <sub>2</sub> O	0.03	0.04	0.04	0.04	0.02	0.02	0.03	0.03	0.02	0.00
H <sub>2</sub> O	5.96	5.94	5.93	5.96	5.94	5.94	5.93	5.92	5.80	5.93
F	0.04	0.03	0.04	0.04	0.05	0.05	0.04	0.05	0.03	0.03
Cl	0.04	0.04	0.05	0.05	0.07	0.07	0.08	0.07	0.07	0.04
Subtotal	101.50	100.86	101.30	100.57	101.17	101.00	100.33	100.77	101.96	101.48
Less O=F	0.02	0.01	0.02	0.02	0.02	0.02	0.02	0.02	0.01	0.01
Less O=Cl	0.01	0.01	0.01	0.01	0.02	0.02	0.02	0.02	0.02	0.01
Total	101.47	100.84	101.27	100.54	101.14	100.97	100.29	100.74	101.93	101.46

Table 32c cont. Chemical Formula of Allanite from the Kingman Pegmatite

Ions	KFMCX-2-1	KFMCX-2-2	KFMCX-2-3	KFMCX-2-4	KFMCX-3-1	KFMCX-3-2	KFMCX-3-3	KFMCX-3-4	KFMCF-2-1	KFMCF-2-2
W	0.000	0.000	0.000	0.000	0.000	0.000	0.000	0.000	0.000	0.000
P	0.000	0.000	0.000	0.000	0.000	0.000	0.000	0.000	0.004	0.002
Nb	0.000	0.000	0.000	0.000	0.001	0.000	0.000	0.000	0.000	0.000
Ta	0.000	0.000	0.000	0.000	0.000	0.000	0.000	0.000	0.000	0.000
Zr	0.000	0.000	0.000	0.000	0.001	0.001	0.000	0.000	0.000	0.000
Sn	0.000	0.000	0.000	0.000	0.000	0.000	0.000	0.000	0.000	0.000
Hf	0.000	0.000	0.000	0.000	0.000	0.000	0.000	0.000	0.000	0.000
Th	0.020	0.021	0.017	0.018	0.013	0.011	0.012	0.012	0.022	0.023
U	0.002	0.002	0.001	0.001	0.001	0.001	0.001	0.001	0.002	0.002
Sc	0.007	0.007	0.007	0.007	0.007	0.007	0.006	0.007	0.007	0.005
Y	0.006	0.005	0.005	0.005	0.003	0.003	0.004	0.002	0.012	0.011
La	0.124	0.121	0.121	0.128	0.158	0.173	0.128	0.171	0.152	0.136
Ce	0.363	0.354	0.365	0.370	0.351	0.341	0.337	0.339	0.364	0.369
Pr	0.069	0.070	0.073	0.074	0.086	0.082	0.086	0.089	0.037	0.037
Nd	0.232	0.245	0.223	0.216	0.224	0.225	0.233	0.226	0.220	0.215
Sm	0.042	0.044	0.046	0.044	0.051	0.052	0.051	0.048	0.031	0.027
Eu	0.001	0.002	0.002	0.002	0.000	0.000	0.001	0.000	0.001	0.001
Gd	0.001	0.001	0.001	0.001	0.001	0.001	0.001	0.001	0.001	0.001
Tb	0.000	0.001	0.000	0.000	0.000	0.000	0.000	0.000	0.000	0.000
Dy	0.000	0.000	0.000	0.000	0.000	0.001	0.001	0.001	0.001	0.000
Ho	0.000	0.000	0.000	0.000	0.000	0.000	0.000	0.000	0.000	0.000
Er	0.000	0.001	0.001	0.000	0.000	0.000	0.000	0.000	0.000	0.000
Tm	0.000	0.000	0.000	0.000	0.000	0.000	0.000	0.000	0.000	0.000
Yb	0.002	0.003	0.002	0.002	0.003	0.003	0.003	0.004	0.005	0.004
Lu	0.000	0.000	0.000	0.000	0.000	0.000	0.000	0.000	0.000	0.000
Ca	1.068	1.022	1.028	1.029	1.085	1.094	1.097	1.094	1.064	1.072
Mn	0.104	0.111	0.111	0.104	0.083	0.084	0.081	0.080	0.114	0.109
Pb	0.001	0.001	0.001	0.001	0.001	0.001	0.001	0.001	0.004	0.003
Na	0.000	0.000	0.000	0.000	0.000	0.000	0.000	0.000	0.000	0.000
K	0.005	0.006	0.006	0.007	0.004	0.003	0.004	0.005	0.003	0.000
$\Sigma$ A-Site	2.047	2.017	2.010	2.009	2.073	2.083	2.047	2.081	2.044	2.017
Al	1.496	1.462	1.474	1.455	1.578	1.537	1.581	1.560	1.529	1.505
Ti	0.026	0.026	0.021	0.024	0.035	0.036	0.037	0.039	0.066	0.071
Mg	0.030	0.029	0.033	0.027	0.034	0.035	0.035	0.039	0.083	0.079
Fe 2+	1.462	1.475	1.474	1.464	1.355	1.344	1.357	1.357	1.432	1.451
$\Sigma$ M-Site	3.014	2.992	3.002	2.970	3.002	2.952	3.010	2.995	3.110	3.106
$\Sigma$ Si	3.000	3.000	3.000	3.000	3.000	3.000	3.000	3.000	3.000	3.000
OH	4.008	4.006	3.971	4.014	4.013	4.009	4.012	4.020	3.972	3.985
F	0.014	0.011	0.011	0.013	0.017	0.016	0.014	0.014	0.011	0.009
Cl	0.008	0.006	0.009	0.008	0.011	0.012	0.013	0.011	0.011	0.008
$\Sigma$ Hydroxyl	4.029	4.023	3.991	4.035	4.041	4.036	4.039	4.046	3.920	4.001

Table 32d. Chemical Compositions of Allanite from the Kingman Pegmatite

	KFMCA- 2-3	KFMCA- 2-4	KFMCA- 3-1	KFMCA- 3-2	KFMCA- 3-3	KFMCA- 3-4	KFMCAX- 1-1	KFMCA- 1-2	KFMCA- 1-3	KFMCA- 1-4
WO <sub>3</sub>	0.00	0.00	0.00	0.00	0.01	0.01	0.00	0.00	0.00	0.00
P <sub>2</sub> O <sub>5</sub>	0.00	0.00	0.00	0.02	0.00	0.00	0.00	0.00	0.00	0.00
Nb <sub>2</sub> O <sub>5</sub>	0.00	0.00	0.00	0.01	0.01	0.00	0.00	0.00	0.02	0.01
Ta <sub>2</sub> O <sub>5</sub>	0.00	0.00	0.00	0.00	0.00	0.00	0.00	0.00	0.00	0.00
SiO <sub>2</sub>	29.88	29.87	29.82	29.78	29.68	29.63	29.56	29.62	29.66	29.55
TiO <sub>2</sub>	0.63	0.67	0.45	0.45	0.45	0.51	0.34	0.35	0.36	0.34
ZrO <sub>2</sub>	0.00	0.00	0.00	0.00	0.00	0.00	0.00	0.00	0.00	0.00
SnO <sub>2</sub>	0.00	0.00	0.00	0.00	0.00	0.00	0.00	0.00	0.00	0.00
HfO <sub>2</sub>	0.00	0.00	0.00	0.00	0.00	0.00	0.00	0.00	0.00	0.00
ThO <sub>2</sub>	0.59	0.54	0.68	0.78	0.75	0.69	0.78	0.84	0.80	0.79
UO <sub>2</sub>	0.02	0.02	0.12	0.11	0.09	0.09	0.02	0.03	0.02	0.02
Al <sub>2</sub> O <sub>3</sub>	12.98	12.64	13.24	12.93	13.22	13.22	13.11	12.68	13.09	12.99
Sc <sub>2</sub> O <sub>3</sub>	0.06	0.05	0.06	0.07	0.07	0.07	0.07	0.07	0.07	0.08
Y <sub>2</sub> O <sub>3</sub>	0.09	0.08	0.12	0.09	0.08	0.09	0.11	0.10	0.10	0.09
La <sub>2</sub> O <sub>3</sub>	3.84	3.22	3.23	3.26	2.99	3.45	4.32	4.33	3.94	4.00
Ce <sub>2</sub> O <sub>3</sub>	7.99	8.43	9.00	10.01	9.21	9.99	8.68	8.88	8.54	8.90
Pr <sub>2</sub> O <sub>3</sub>	1.81	1.68	1.88	2.12	2.09	2.08	1.77	1.65	1.59	1.65
Nd <sub>2</sub> O <sub>3</sub>	6.57	6.23	7.78	6.44	6.55	6.21	6.54	6.38	6.55	6.00
Sm <sub>2</sub> O <sub>3</sub>	1.09	1.10	1.44	1.42	1.40	1.44	0.95	0.99	0.93	0.83
Eu <sub>2</sub> O <sub>3</sub>	0.04	0.03	0.03	0.02	0.02	0.02	0.00	0.01	0.00	0.00
Gd <sub>2</sub> O <sub>3</sub>	0.04	0.02	0.04	0.02	0.04	0.03	0.00	0.00	0.00	0.01
Tb <sub>2</sub> O <sub>3</sub>	0.03	0.04	0.01	0.00	0.01	0.00	0.00	0.00	0.00	0.01
Dy <sub>2</sub> O <sub>3</sub>	0.00	0.00	0.00	0.01	0.01	0.00	0.01	0.02	0.02	0.02
Ho <sub>2</sub> O <sub>3</sub>	0.01	0.02	0.00	0.00	0.00	0.00	0.00	0.00	0.00	0.00
Er <sub>2</sub> O <sub>3</sub>	0.01	0.01	0.00	0.00	0.00	0.00	0.00	0.00	0.00	0.00
Tm <sub>2</sub> O <sub>3</sub>	0.00	0.01	0.01	0.00	0.01	0.00	0.00	0.01	0.00	0.00
Yb <sub>2</sub> O <sub>3</sub>	0.04	0.05	0.10	0.09	0.12	0.10	0.07	0.07	0.08	0.08
Lu <sub>2</sub> O <sub>3</sub>	0.00	0.01	0.00	0.01	0.00	0.00	0.00	0.00	0.00	0.00
MgO	0.12	0.14	0.13	0.15	0.13	0.15	0.12	0.13	0.13	0.14
CaO	9.73	9.80	10.21	9.83	9.88	9.90	10.13	10.09	10.11	10.14
MnO	0.94	0.92	0.80	0.68	0.75	0.72	1.25	1.30	1.12	1.25
FeO	16.87	16.97	16.12	15.99	16.09	16.05	16.77	16.87	16.34	16.68
PbO	0.02	0.01	0.04	0.02	0.04	0.04	0.04	0.04	0.04	0.03
Na <sub>2</sub> O	0.00	0.02	0.00	0.00	0.00	0.00	0.00	0.02	0.00	0.00
K <sub>2</sub> O	0.00	0.00	0.00	0.02	0.01	0.02	0.01	0.03	0.03	0.01
H <sub>2</sub> O	5.96	5.97	5.95	5.96	5.93	5.94	5.96	5.98	5.95	5.93
F	0.02	0.02	0.02	0.02	0.02	0.01	0.02	0.03	0.02	0.02
Cl	0.03	0.03	0.02	0.02	0.03	0.03	0.00	0.01	0.00	0.01
Subtotal	99.41	98.62	101.29	100.34	99.68	100.50	100.62	100.53	99.52	99.59
Less O=F	0.01	0.01	0.01	0.01	0.01	0.00	0.01	0.01	0.01	0.01
Less O=Cl	0.01	0.01	0.01	0.00	0.01	0.01	0.00	0.00	0.00	0.00
Total	99.39	98.61	101.28	100.33	99.66	100.49	100.61	100.52	99.51	99.58

Table 32d cont. Chemical Formula of Allanite from the Kingman Pegmatite

Ions	KFMCA- 2-3	KFMCA- 2-4	KFMCA- 3-1	KFMCA- 3-2	KFMCA- 3-3	KFMCA- 3-4	KFMCX- 1-1	KFMCX- 1-2	KFMCX- 1-3	KFMCX- 1-4
W	0.000	0.000	0.000	0.000	0.000	0.000	0.000	0.000	0.000	0.000
P	0.000	0.000	0.000	0.002	0.000	0.000	0.000	0.000	0.000	0.000
Nb	0.000	0.000	0.000	0.001	0.000	0.000	0.000	0.000	0.001	0.000
Ta	0.000	0.000	0.000	0.000	0.000	0.000	0.000	0.000	0.000	0.000
Zr	0.000	0.000	0.000	0.000	0.000	0.000	0.000	0.000	0.000	0.000
Sn	0.000	0.000	0.000	0.000	0.000	0.000	0.000	0.000	0.000	0.000
Hf	0.000	0.000	0.000	0.000	0.000	0.000	0.000	0.000	0.000	0.000
Th	0.014	0.012	0.015	0.018	0.017	0.016	0.018	0.019	0.018	0.018
U	0.000	0.001	0.003	0.002	0.002	0.002	0.001	0.001	0.000	0.000
Sc	0.005	0.004	0.005	0.006	0.006	0.006	0.006	0.007	0.007	0.007
Y	0.005	0.004	0.006	0.005	0.004	0.005	0.006	0.005	0.005	0.005
La	0.142	0.119	0.120	0.121	0.112	0.129	0.162	0.162	0.147	0.150
Ce	0.294	0.310	0.332	0.369	0.341	0.370	0.322	0.329	0.316	0.331
Pr	0.066	0.061	0.069	0.078	0.077	0.077	0.065	0.061	0.058	0.061
Nd	0.235	0.224	0.279	0.232	0.236	0.225	0.237	0.231	0.237	0.217
Sm	0.038	0.038	0.050	0.049	0.049	0.050	0.033	0.034	0.033	0.029
Eu	0.001	0.001	0.001	0.001	0.001	0.001	0.000	0.000	0.000	0.000
Gd	0.001	0.001	0.001	0.001	0.001	0.001	0.000	0.000	0.000	0.000
Tb	0.001	0.001	0.000	0.000	0.000	0.000	0.000	0.000	0.000	0.000
Dy	0.000	0.000	0.000	0.000	0.000	0.000	0.000	0.001	0.001	0.001
Ho	0.000	0.001	0.000	0.000	0.000	0.000	0.000	0.000	0.000	0.000
Er	0.000	0.000	0.000	0.000	0.000	0.000	0.000	0.000	0.000	0.000
Tm	0.000	0.000	0.000	0.000	0.000	0.000	0.000	0.000	0.000	0.000
Yb	0.001	0.002	0.003	0.003	0.004	0.003	0.002	0.002	0.002	0.003
Lu	0.000	0.000	0.000	0.000	0.000	0.000	0.000	0.000	0.000	0.000
Ca	1.047	1.054	1.101	1.061	1.069	1.074	1.102	1.095	1.095	1.103
Mn	0.080	0.079	0.068	0.058	0.064	0.062	0.108	0.112	0.096	0.108
Pb	0.000	0.000	0.001	0.001	0.001	0.001	0.001	0.001	0.001	0.001
Na	0.000	0.003	0.000	0.000	0.000	0.000	0.000	0.005	0.000	0.000
K	0.000	0.000	0.000	0.003	0.002	0.004	0.001	0.005	0.005	0.002
$\Sigma$ A-Site	1.930	1.915	2.054	2.011	1.986	2.026	2.064	2.070	2.022	2.036
Al	1.535	1.497	1.570	1.535	1.575	1.578	1.568	1.513	1.561	1.555
Ti	0.048	0.050	0.034	0.034	0.035	0.039	0.026	0.026	0.027	0.026
Mg	0.018	0.021	0.020	0.023	0.020	0.023	0.018	0.020	0.020	0.021
Fe 2+	1.416	1.425	1.356	1.346	1.360	1.358	1.423	1.429	1.383	1.415
$\Sigma$ M-Site	3.017	2.993	2.980	2.938	2.990	2.998	3.035	2.988	2.991	3.017
$\Sigma$ Si	3.000	3.000	3.000	3.000	3.000	3.000	3.000	3.000	3.000	3.000
OH	3.991	3.999	3.993	4.005	3.999	4.011	4.035	4.040	4.015	4.015
F	0.006	0.007	0.007	0.006	0.005	0.003	0.007	0.009	0.007	0.006
Cl	0.006	0.006	0.004	0.003	0.005	0.005	0.000	0.002	0.000	0.002
$\Sigma$ Hydroxyl	4.00	4.01	4.00	4.01	4.01	4.02	4.04	4.05	4.02	4.02

Table 32e. Chemical Compositions of Allanite from the Kingman Pegmatite

	KFMCM-3-1	KFMCM-3-2	KFMCM-3-3	KFMCM-3-4	KFMCM-3-5	KFMCM-4-1	KFMCM-4-2	KFMCM-4-3	KFMCM-4-4	KFMCM-4-5
WO <sub>3</sub>	0.00	0.00	0.00	0.00	0.00	0.00	0.00	0.00	0.00	0.00
P <sub>2</sub> O <sub>5</sub>	0.04	0.04	0.01	0.02	0.04	0.02	0.03	0.03	0.03	0.03
Nb <sub>2</sub> O <sub>5</sub>	0.00	0.00	0.00	0.00	0.00	0.00	0.00	0.00	0.00	0.00
Ta <sub>2</sub> O <sub>5</sub>	0.00	0.00	0.00	0.00	0.00	0.00	0.00	0.00	0.00	0.00
SiO <sub>2</sub>	30.02	30.12	29.94	29.98	30.03	29.85	29.80	29.83	29.84	29.83
TiO <sub>2</sub>	0.93	0.92	0.93	0.88	0.92	0.93	0.97	0.96	0.98	0.94
ZrO <sub>2</sub>	0.00	0.00	0.00	0.00	0.00	0.00	0.00	0.00	0.00	0.00
SnO <sub>2</sub>	0.00	0.00	0.00	0.00	0.00	0.00	0.00	0.00	0.00	0.00
HfO <sub>2</sub>	0.00	0.00	0.00	0.00	0.00	0.00	0.00	0.00	0.00	0.00
ThO <sub>2</sub>	1.22	1.14	1.23	1.32	1.28	1.31	1.34	1.29	1.37	1.30
UO <sub>2</sub>	0.10	0.10	0.10	0.09	0.11	0.13	0.14	0.14	0.14	0.14
Al <sub>2</sub> O <sub>3</sub>	14.61	14.48	14.45	14.73	14.58	14.45	14.34	14.31	14.23	14.27
Sc <sub>2</sub> O <sub>3</sub>	0.08	0.07	0.07	0.08	0.08	0.10	0.08	0.07	0.07	0.07
Y <sub>2</sub> O <sub>3</sub>	0.10	0.11	0.12	0.09	0.09	0.11	0.09	0.10	0.12	0.08
La <sub>2</sub> O <sub>3</sub>	4.79	4.68	4.70	4.68	4.55	4.12	4.32	4.23	4.09	4.27
Ce <sub>2</sub> O <sub>3</sub>	10.13	10.08	9.88	9.78	9.66	9.02	9.10	9.03	9.12	9.23
Pr <sub>2</sub> O <sub>3</sub>	1.26	1.34	1.30	1.35	1.38	1.46	1.43	1.38	1.30	1.38
Nd <sub>2</sub> O <sub>3</sub>	6.88	6.89	7.01	6.89	6.89	7.05	7.12	7.17	7.20	7.09
Sm <sub>2</sub> O <sub>3</sub>	0.59	0.61	0.56	0.58	0.57	0.51	0.49	0.51	0.52	0.52
Eu <sub>2</sub> O <sub>3</sub>	0.03	0.03	0.03	0.02	0.03	0.03	0.02	0.02	0.02	0.03
Gd <sub>2</sub> O <sub>3</sub>	0.03	0.04	0.04	0.04	0.04	0.03	0.03	0.04	0.03	0.03
Tb <sub>2</sub> O <sub>3</sub>	0.00	0.00	0.01	0.00	0.00	0.00	0.00	0.00	0.00	0.00
Dy <sub>2</sub> O <sub>3</sub>	0.03	0.04	0.05	0.03	0.04	0.03	0.03	0.04	0.03	0.03
Ho <sub>2</sub> O <sub>3</sub>	0.00	0.00	0.00	0.00	0.00	0.00	0.00	0.00	0.00	0.00
Er <sub>2</sub> O <sub>3</sub>	0.00	0.00	0.00	0.00	0.00	0.00	0.00	0.00	0.00	0.00
Tm <sub>2</sub> O <sub>3</sub>	0.00	0.00	0.00	0.00	0.00	0.00	0.00	0.00	0.00	0.00
Yb <sub>2</sub> O <sub>3</sub>	0.06	0.06	0.06	0.07	0.07	0.09	0.08	0.10	0.07	0.08
Lu <sub>2</sub> O <sub>3</sub>	0.00	0.00	0.00	0.00	0.00	0.00	0.00	0.00	0.00	0.00
MgO	0.10	0.09	0.11	0.09	0.09	0.13	0.10	0.13	0.11	0.12
CaO	10.11	10.11	10.14	10.14	10.10	9.85	9.95	9.93	10.02	9.92
MnO	1.34	1.38	1.41	1.39	1.41	0.95	1.11	1.16	1.06	1.10
FeO	14.87	15.09	15.32	15.34	15.40	16.13	16.11	16.25	16.43	16.09
PbO	0.08	0.09	0.08	0.08	0.08	0.10	0.11	0.09	0.10	0.09
Na <sub>2</sub> O	0.00	0.00	0.00	0.00	0.00	0.00	0.00	0.01	0.00	0.00
K <sub>2</sub> O	0.00	0.00	0.03	0.02	0.00	0.00	0.00	0.00	0.00	0.00
H <sub>2</sub> O	4.20	4.30	4.10	4.20	4.20	5.20	5.00	5.00	5.00	5.00
F	0.06	0.05	0.06	0.05	0.06	0.06	0.05	0.05	0.04	0.04
Cl	0.05	0.06	0.05	0.05	0.04	0.04	0.05	0.05	0.05	0.04
Subtotal	101.71	101.90	101.79	102.00	101.74	101.69	101.88	101.88	101.97	101.70
Less O=F	0.02	0.02	0.03	0.02	0.02	0.02	0.03	0.02	0.02	0.02
Less O=Cl	0.01	0.01	0.01	0.01	0.01	0.01	0.01	0.01	0.01	0.01
Total	101.68	101.87	101.75	101.96	101.70	101.66	101.85	101.85	101.94	101.67

Table 32e cont. Chemical Formula of Allanite from the Kingman Pegmatite

Ions	KFMCM-3-1	KFMCM-3-2	KFMCM-3-3	KFMCM-3-4	KFMCM-3-5	KFMCM-4-1	KFMCM-4-2	KFMCM-4-3	KFMCM-4-4	KFMCM-4-5
W	0.000	0.000	0.000	0.000	0.000	0.000	0.000	0.000	0.000	0.000
P	0.004	0.003	0.001	0.002	0.003	0.002	0.002	0.003	0.003	0.002
Nb	0.000	0.000	0.000	0.000	0.000	0.000	0.000	0.000	0.000	0.000
Ta	0.000	0.000	0.000	0.000	0.000	0.000	0.000	0.000	0.000	0.000
Zr	0.000	0.000	0.000	0.000	0.000	0.000	0.000	0.000	0.000	0.000
Sn	0.000	0.000	0.000	0.000	0.000	0.000	0.000	0.000	0.000	0.000
Hf	0.000	0.000	0.000	0.000	0.000	0.000	0.000	0.000	0.000	0.000
Th	0.028	0.026	0.028	0.030	0.029	0.030	0.031	0.029	0.031	0.030
U	0.002	0.002	0.002	0.002	0.002	0.003	0.003	0.003	0.003	0.003
Sc	0.007	0.006	0.006	0.007	0.007	0.008	0.007	0.006	0.006	0.006
Y	0.005	0.006	0.006	0.005	0.005	0.006	0.005	0.005	0.007	0.004
La	0.176	0.172	0.174	0.173	0.168	0.153	0.160	0.157	0.152	0.158
Ce	0.371	0.368	0.362	0.358	0.353	0.332	0.335	0.333	0.335	0.340
Pr	0.046	0.049	0.047	0.049	0.050	0.053	0.052	0.050	0.047	0.050
Nd	0.245	0.245	0.251	0.246	0.246	0.253	0.256	0.258	0.258	0.255
Sm	0.020	0.021	0.019	0.020	0.020	0.018	0.017	0.018	0.018	0.018
Eu	0.001	0.001	0.001	0.001	0.001	0.001	0.001	0.001	0.001	0.001
Gd	0.001	0.001	0.001	0.001	0.001	0.001	0.001	0.001	0.001	0.001
Tb	0.000	0.000	0.000	0.000	0.000	0.000	0.000	0.000	0.000	0.000
Dy	0.001	0.001	0.001	0.001	0.001	0.001	0.001	0.001	0.001	0.001
Ho	0.000	0.000	0.000	0.000	0.000	0.000	0.000	0.000	0.000	0.000
Er	0.000	0.000	0.000	0.000	0.000	0.000	0.000	0.000	0.000	0.000
Tm	0.000	0.000	0.000	0.000	0.000	0.000	0.000	0.000	0.000	0.000
Yb	0.002	0.002	0.002	0.002	0.002	0.003	0.002	0.003	0.002	0.002
Lu	0.000	0.000	0.000	0.000	0.000	0.000	0.000	0.000	0.000	0.000
Ca	1.083	1.078	1.089	1.087	1.081	1.060	1.073	1.071	1.079	1.069
Mn	0.114	0.116	0.120	0.117	0.119	0.080	0.095	0.098	0.090	0.094
Pb	0.002	0.002	0.002	0.002	0.002	0.002	0.003	0.002	0.002	0.002
Na	0.000	0.000	0.000	0.000	0.000	0.000	0.000	0.002	0.000	0.000
K	0.000	0.000	0.005	0.003	0.000	0.000	0.000	0.000	0.000	0.000
$\Sigma$ A-Site	2.108	2.099	2.117	2.106	2.090	2.006	2.044	2.041	2.036	2.036
Al	1.721	1.700	1.706	1.737	1.717	1.712	1.701	1.696	1.686	1.692
Ti	0.070	0.069	0.070	0.066	0.069	0.070	0.074	0.072	0.074	0.071
Mg	0.014	0.013	0.017	0.013	0.013	0.020	0.015	0.019	0.016	0.017
Fe 2+	1.243	1.257	1.284	1.284	1.286	1.356	1.357	1.366	1.381	1.353
$\Sigma$ M-Site	3.048	3.039	3.077	3.100	3.085	3.158	3.147	3.153	3.157	3.133
$\Sigma$ Si	3.000	3.000	3.000	3.000	3.000	3.000	3.000	3.000	3.000	3.000
OH	3.966	3.966	3.990	3.978	3.965	3.983	3.983	3.972	3.970	3.979
F	0.019	0.017	0.017	0.016	0.020	0.017	0.016	0.016	0.014	0.011
Cl	0.008	0.009	0.009	0.008	0.007	0.007	0.008	0.009	0.009	0.007
$\Sigma$ Hydroxyl	2.827	2.883	2.766	2.827	2.826	3.512	3.382	3.380	3.375	3.373

Table 32f. Chemical Compositions of Allanite from the Kingman Pegmatite

	KFMCF-2-3	KFMCSW-1	KFMCSW-2	KFMCSW-3	KFMCSW-4	KFMCSW-5	KFMCM-1-6	KFMCM-2-1	KFMCM-2-4	KFMCM-2-5
WO <sub>3</sub>	0.00	0.00	0.00	0.00	0.00	0.00	0.00	0.00	0.00	0.00
P <sub>2</sub> O <sub>5</sub>	0.03	0.04	0.05	0.04	0.05	0.02	0.04	0.03	0.02	0.02
Nb <sub>2</sub> O <sub>5</sub>	0.00	0.00	0.00	0.00	0.00	0.00	0.00	0.00	0.00	0.00
Ta <sub>2</sub> O <sub>5</sub>	0.01	0.00	0.00	0.00	0.00	0.00	0.00	0.00	0.00	0.00
SiO <sub>2</sub>	30.03	29.89	29.78	29.98	29.67	29.83	30.03	29.96	29.94	29.96
TiO <sub>2</sub>	1.00	0.88	0.97	0.93	0.90	0.87	0.90	0.87	0.93	0.85
ZrO <sub>2</sub>	0.00	0.00	0.00	0.00	0.00	0.00	0.00	0.00	0.00	0.00
SnO <sub>2</sub>	0.00	0.00	0.00	0.00	0.00	0.00	0.00	0.00	0.00	0.00
HfO <sub>2</sub>	0.00	0.00	0.00	0.00	0.00	0.00	0.00	0.00	0.00	0.00
ThO <sub>2</sub>	0.95	0.88	0.90	0.90	0.97	0.98	1.06	1.11	1.03	1.00
UO <sub>2</sub>	0.10	0.09	0.11	0.10	0.11	0.10	0.09	0.11	0.10	0.10
Al <sub>2</sub> O <sub>3</sub>	13.00	13.78	13.87	13.87	13.80	13.78	14.45	14.61	14.47	14.55
Sc <sub>2</sub> O <sub>3</sub>	0.06	0.07	0.07	0.06	0.07	0.07	0.07	0.08	0.08	0.09
Y <sub>2</sub> O <sub>3</sub>	0.23	0.20	0.17	0.12	0.13	0.14	0.09	0.14	0.12	0.12
La <sub>2</sub> O <sub>3</sub>	3.77	3.54	4.03	3.89	4.16	3.95	4.22	4.45	4.32	4.40
Ce <sub>2</sub> O <sub>3</sub>	10.04	10.57	10.33	9.90	9.76	9.70	9.00	9.66	9.93	9.68
Pr <sub>2</sub> O <sub>3</sub>	0.94	1.15	1.00	1.32	1.28	1.23	1.12	1.26	1.31	1.28
Nd <sub>2</sub> O <sub>3</sub>	6.08	6.34	6.75	7.76	6.87	7.13	7.67	7.22	7.12	7.43
Sm <sub>2</sub> O <sub>3</sub>	0.75	0.63	0.56	0.65	0.57	0.53	0.54	0.62	0.59	0.62
Eu <sub>2</sub> O <sub>3</sub>	0.02	0.02	0.02	0.03	0.02	0.02	0.02	0.03	0.04	0.03
Gd <sub>2</sub> O <sub>3</sub>	0.00	0.00	0.00	0.00	0.00	0.00	0.00	0.04	0.01	0.02
Tb <sub>2</sub> O <sub>3</sub>	0.00	0.00	0.00	0.00	0.00	0.00	0.00	0.00	0.00	0.00
Dy <sub>2</sub> O <sub>3</sub>	0.00	0.00	0.04	0.04	0.04	0.04	0.04	0.04	0.04	0.05
Ho <sub>2</sub> O <sub>3</sub>	0.00	0.00	0.00	0.00	0.00	0.00	0.00	0.00	0.00	0.00
Er <sub>2</sub> O <sub>3</sub>	0.00	0.00	0.00	0.00	0.00	0.00	0.00	0.00	0.01	0.00
Tm <sub>2</sub> O <sub>3</sub>	0.00	0.00	0.00	0.00	0.00	0.00	0.00	0.00	0.00	0.00
Yb <sub>2</sub> O <sub>3</sub>	0.16	0.15	0.11	0.10	0.09	0.08	0.09	0.06	0.06	0.05
Lu <sub>2</sub> O <sub>3</sub>	0.00	0.00	0.00	0.00	0.00	0.00	0.00	0.00	0.00	0.00
MgO	0.49	0.36	0.28	0.33	0.32	0.30	0.27	0.10	0.09	0.10
CaO	10.00	10.21	9.96	10.05	10.10	10.04	10.77	10.06	10.00	10.01
MnO	1.34	1.21	1.11	0.90	1.06	1.01	0.98	1.21	1.10	1.22
FeO	17.12	16.79	16.77	16.56	16.67	16.45	15.99	16.10	15.98	16.02
PbO	0.10	0.10	0.10	0.12	0.09	0.09	0.11	0.09	0.09	0.09
Na <sub>2</sub> O	0.00	0.00	0.00	0.00	0.00	0.00	0.00	0.00	0.00	0.00
K <sub>2</sub> O	0.02	0.00	0.03	0.00	0.02	0.00	0.00	0.00	0.00	0.00
H <sub>2</sub> O	5.00	4.50	4.60	4.00	5.10	5.50	4.20	4.00	4.50	4.00
F	0.03	0.04	0.04	0.04	0.03	0.03	0.04	0.05	0.06	0.05
Cl	0.04	0.06	0.04	0.04	0.03	0.03	0.04	0.03	0.04	0.04
Subtotal	101.33	101.49	101.69	101.72	101.90	101.95	101.82	101.94	101.97	101.80
Less O=F	0.01	0.02	0.02	0.02	0.02	0.02	0.01	0.01	0.02	0.02
Less O=Cl	0.01	0.01	0.01	0.01	0.01	0.01	0.01	0.01	0.01	0.01
Total	101.30	101.46	101.66	101.69	101.87	101.92	101.80	101.92	101.94	101.77

Table 32f cont. Chemical Formula of Allanite from the Kingman Pegmatite

Ions	KFMCF- 3	KFMCSW- 1	KFMCSW- 2	KFMCSW- 3	KFMCSW- 4	KFMCSW- 5	KFMCM- 1-6	KFMCM- 2-1	KFMCM- 2-4	KFMCM- 2-5
W	0.000	0.000	0.000	0.000	0.000	0.000	0.000	0.000	0.000	0.000
P	0.003	0.004	0.004	0.004	0.004	0.002	0.004	0.003	0.002	0.002
Nb	0.000	0.000	0.000	0.000	0.000	0.000	0.000	0.000	0.000	0.000
Ta	0.000	0.000	0.000	0.000	0.000	0.000	0.000	0.000	0.000	0.000
Zr	0.000	0.000	0.000	0.000	0.000	0.000	0.000	0.000	0.000	0.000
Sn	0.000	0.000	0.000	0.000	0.000	0.000	0.000	0.000	0.000	0.000
Hf	0.000	0.000	0.000	0.000	0.000	0.000	0.000	0.000	0.000	0.000
Th	0.022	0.020	0.021	0.020	0.022	0.023	0.024	0.025	0.024	0.023
U	0.002	0.002	0.003	0.002	0.002	0.002	0.002	0.002	0.002	0.002
Sc	0.005	0.006	0.006	0.005	0.006	0.006	0.006	0.007	0.007	0.007
Y	0.012	0.011	0.009	0.006	0.007	0.007	0.005	0.007	0.006	0.006
La	0.139	0.131	0.150	0.143	0.155	0.146	0.155	0.164	0.160	0.162
Ce	0.367	0.388	0.381	0.363	0.361	0.357	0.329	0.354	0.364	0.355
Pr	0.034	0.042	0.037	0.048	0.047	0.045	0.041	0.046	0.048	0.047
Nd	0.217	0.227	0.243	0.277	0.248	0.256	0.273	0.258	0.255	0.266
Sm	0.026	0.022	0.019	0.022	0.020	0.018	0.019	0.021	0.020	0.021
Eu	0.001	0.001	0.001	0.001	0.001	0.001	0.001	0.001	0.001	0.001
Gd	0.000	0.000	0.000	0.000	0.000	0.000	0.000	0.001	0.000	0.001
Tb	0.000	0.000	0.000	0.000	0.000	0.000	0.000	0.000	0.000	0.000
Dy	0.000	0.000	0.001	0.001	0.001	0.001	0.001	0.001	0.001	0.002
Ho	0.000	0.000	0.000	0.000	0.000	0.000	0.000	0.000	0.000	0.000
Er	0.000	0.000	0.000	0.000	0.000	0.000	0.000	0.000	0.000	0.000
Tm	0.000	0.000	0.000	0.000	0.000	0.000	0.000	0.000	0.000	0.000
Yb	0.005	0.004	0.003	0.003	0.003	0.002	0.003	0.002	0.002	0.002
Lu	0.000	0.000	0.000	0.000	0.000	0.000	0.000	0.000	0.000	0.000
Ca	1.070	1.098	1.075	1.077	1.094	1.081	1.152	1.079	1.074	1.074
Mn	0.113	0.103	0.095	0.076	0.090	0.086	0.083	0.103	0.094	0.104
Pb	0.002	0.003	0.002	0.003	0.002	0.002	0.003	0.002	0.002	0.002
Na	0.000	0.000	0.000	0.000	0.000	0.000	0.000	0.000	0.000	0.000
K	0.003	0.000	0.005	0.000	0.003	0.000	0.000	0.000	0.000	0.000
$\Sigma$ A-Site	2.021	2.062	2.055	2.051	2.066	2.035	2.101	2.076	2.062	2.077
Al	1.531	1.629	1.646	1.636	1.645	1.634	1.702	1.724	1.708	1.717
Ti	0.075	0.067	0.073	0.070	0.068	0.066	0.068	0.066	0.070	0.064
Mg	0.073	0.053	0.042	0.050	0.047	0.045	0.039	0.015	0.013	0.016
Fe 2+	1.430	1.409	1.413	1.385	1.410	1.383	1.335	1.348	1.339	1.341
$\Sigma$ M-Site	3.109	3.158	3.174	3.141	3.170	3.128	3.144	3.153	3.130	3.138
$\Sigma$ Si	3.000	3.000	3.000	3.000	3.000	3.000	3.000	3.000	3.000	3.000
OH	3.978	3.997	3.985	3.978	3.980	3.978	3.985	3.981	3.984	3.987
F	0.010	0.011	0.013	0.012	0.011	0.011	0.014	0.016	0.018	0.015
Cl	0.007	0.010	0.007	0.006	0.005	0.006	0.007	0.006	0.006	0.007

Table 33a. Chemical Composition of Monazite from the Wagon Bow and Rare Metals Pegmatites

Oxides	Wagon Bow # 3					Rare Metals Mine				
	WHRADM-1	WHRADM-2	MONWH-4	MONWH-5	RMM-1-1	RMM-1-2	RMM-2-2	RMM-2-3	RMM-2-4	RMM-2-5
P <sub>2</sub> O <sub>5</sub>	30.12	29.88	29.56	29.63	29.50	29.54	29.61	29.70	29.56	29.61
SiO <sub>2</sub>	1.43	1.57	1.27	1.22	0.88	0.92	0.65	0.50	0.35	0.34
TiO <sub>2</sub>	0.01	0.01	0.00	0.00	0.00	0.00	0.00	0.00	0.00	0.00
ThO <sub>2</sub>	2.90	3.00	2.70	2.57	3.11	2.93	2.90	3.01	2.89	2.84
ThO <sub>2</sub>	0.23	0.31	0.31	0.29	0.33	0.38	0.28	0.27	0.28	0.28
UO <sub>2</sub>	0.09	0.11	0.12	0.10	0.21	0.18	0.27	0.52	0.18	0.16
Sc <sub>2</sub> O <sub>3</sub>	0.03	0.04	0.03	0.05	0.04	0.04	0.04	0.04	0.03	0.04
Y <sub>2</sub> O <sub>3</sub>	0.27	0.31	0.14	0.13	0.12	0.15	0.09	0.09	0.12	0.12
La <sub>2</sub> O <sub>3</sub>	8.21	8.44	8.44	8.12	7.90	8.23	8.57	8.57	8.46	8.60
Ce <sub>2</sub> O <sub>3</sub>	22.12	21.57	22.92	23.01	23.55	22.13	22.51	22.33	22.13	22.40
Pr <sub>2</sub> O <sub>3</sub>	3.54	3.41	3.32	3.09	3.23	3.18	3.32	3.16	3.27	3.28
Nd <sub>2</sub> O <sub>3</sub>	20.99	19.91	20.04	20.11	18.77	19.34	21.01	21.34	21.65	21.00
Sm <sub>2</sub> O <sub>3</sub>	4.54	4.32	2.78	2.92	3.11	3.21	3.13	3.19	3.43	3.62
Eu <sub>2</sub> O <sub>3</sub>	0.26	0.22	0.16	0.17	0.15	0.13	0.17	0.18	0.15	0.17
Gd <sub>2</sub> O <sub>3</sub>	2.57	2.22	1.77	1.82	1.54	1.57	2.09	1.91	1.88	1.92
Tb <sub>2</sub> O <sub>3</sub>	0.55	0.46	0.06	0.06	0.05	0.05	0.08	0.05	0.05	0.07
Dy <sub>2</sub> O <sub>3</sub>	0.25	0.21	0.10	0.09	0.07	0.09	0.04	0.04	0.03	0.04
Ho <sub>2</sub> O <sub>3</sub>	0.01	0.01	0.00	0.00	0.00	0.00	0.00	0.00	0.00	0.00
Er <sub>2</sub> O <sub>3</sub>	0.01	0.02	0.02	0.01	0.00	0.00	0.00	0.01	0.00	0.01
Tm <sub>2</sub> O <sub>3</sub>	0.01	0.01	0.01	0.00	0.00	0.00	0.00	0.00	0.00	0.00
Yb <sub>2</sub> O <sub>3</sub>	0.13	0.12	0.10	0.08	0.06	0.05	0.08	0.08	0.06	0.07
Lu <sub>2</sub> O <sub>3</sub>	0.00	0.00	0.00	0.00	0.00	0.00	0.00	0.00	0.00	0.00
MgO	0.21	0.16	0.09	0.09	0.10	0.11	0.05	0.04	0.04	0.06
CaO	0.79	0.94	0.54	0.50	0.43	0.42	0.46	0.42	0.39	0.40
MnO	0.06	0.06	0.03	0.04	0.08	0.21	0.03	0.02	0.03	0.02
FeO	0.57	0.91	0.78	0.93	1.21	1.00	0.70	0.56	0.55	0.56
PbO	0.21	0.20	0.16	0.15	0.18	0.17	0.16	0.19	0.17	0.20
Total	100.11	98.42	95.46	95.18	94.62	94.04	96.23	96.23	95.69	95.81

Table 33a. Chemical Composition of Monazite from then Wagon Bow and Rare Metals Pegmatites

Oxides	Wagon Bow # 3					Rare Metals Mine				
	WHRADM-1	WHRADM-2	MONWH-4	MONWH-5	RMM-1-1	RMM-1-2	RMM-2-2	RMM-2-3	RMM-2-4	RMM-2-5
P <sub>2</sub> O <sub>5</sub>	30.12	29.88	29.56	29.63	29.5	29.54	29.61	29.7	29.56	29.61
SiO <sub>2</sub>	1.43	1.57	1.27	1.22	0.88	0.92	0.65	0.5	0.35	0.34
TiO <sub>2</sub>	0.01	0.01	0	0	0	0	0	0	0	0
ThO <sub>2</sub>	2.9	3	2.7	2.57	3.11	2.93	2.9	3.01	2.89	2.84
ThO <sub>2</sub>	0.23	0.31	0.31	0.29	0.33	0.38	0.28	0.27	0.28	0.28
UO <sub>2</sub>	0.09	0.11	0.12	0.1	0.21	0.18	0.27	0.52	0.18	0.16
Sc <sub>2</sub> O <sub>3</sub>	0.03	0.04	0.03	0.05	0.04	0.04	0.04	0.04	0.03	0.04
Y <sub>2</sub> O <sub>3</sub>	0.27	0.31	0.14	0.13	0.12	0.15	0.09	0.09	0.12	0.12
La <sub>2</sub> O <sub>3</sub>	8.21	8.44	8.44	8.12	7.9	8.23	8.57	8.57	8.46	8.6
Ce <sub>2</sub> O <sub>3</sub>	22.12	21.57	22.92	23.01	23.55	22.13	22.51	22.33	22.13	22.4
Pr <sub>2</sub> O <sub>3</sub>	3.54	3.41	3.32	3.09	3.23	3.18	3.32	3.16	3.27	3.28
Nd <sub>2</sub> O <sub>3</sub>	20.99	19.91	20.04	20.11	18.77	19.34	21.01	21.34	21.65	21
Sm <sub>2</sub> O <sub>3</sub>	4.54	4.32	2.78	2.92	3.11	3.21	3.13	3.19	3.43	3.62
Eu <sub>2</sub> O <sub>3</sub>	0.26	0.22	0.16	0.17	0.15	0.13	0.17	0.18	0.15	0.17
Gd <sub>2</sub> O <sub>3</sub>	2.57	2.22	1.77	1.82	1.54	1.57	2.09	1.91	1.88	1.92
Tb <sub>2</sub> O <sub>3</sub>	0.55	0.46	0.06	0.06	0.05	0.05	0.08	0.05	0.05	0.07
Dy <sub>2</sub> O <sub>3</sub>	0.25	0.21	0.1	0.09	0.07	0.09	0.04	0.04	0.03	0.04
Ho <sub>2</sub> O <sub>3</sub>	0.01	0.01	0	0	0	0	0	0	0	0
Er <sub>2</sub> O <sub>3</sub>	0.01	0.02	0.02	0.01	0	0	0	0.01	0	0.01
Tm <sub>2</sub> O <sub>3</sub>	0.01	0.01	0.01	0	0	0	0	0	0	0
Yb <sub>2</sub> O <sub>3</sub>	0.13	0.12	0.1	0.08	0.06	0.05	0.08	0.08	0.06	0.07
Lu <sub>2</sub> O <sub>3</sub>	0	0	0	0	0	0	0	0	0	0
MgO	0.21	0.16	0.09	0.09	0.1	0.11	0.05	0.04	0.04	0.06
CaO	0.79	0.94	0.54	0.5	0.43	0.42	0.46	0.42	0.39	0.4
MnO	0.06	0.06	0.03	0.04	0.08	0.21	0.03	0.02	0.03	0.02
FeO	0.57	0.91	0.78	0.93	1.21	1	0.7	0.56	0.55	0.56
PbO	0.21	0.2	0.16	0.15	0.18	0.17	0.16	0.19	0.17	0.2
Total	100.11	98.42	95.46	95.18	94.62	94.04	96.23	96.23	95.69	95.81

Table 33a cont. Chemical Formula of Monazite from then Wagon Bow and Rare Metals Pegmatites

Ions	Wagon Bow # 3					Rare Metals Mine																			
	Ti	Th	U	Al	Sc	Y	La	Ce	Pr	Nd	Sm	Eu	Gd	Tb	Dy	Ho	Er	Tm	Yb	Lu	Mg	Ca	Mn	Fe 2+	Pb
Ti	0.000	0.000	0.000	0.000	0.000	0.000	0.000	0.027	0.026	0.027	0.027	0.026	0.027	0.027	0.027	0.027	0.002	0.002	0.003	0.003	0.003	0.003	0.003	0.003	
Th	0.025	0.026	0.024	0.023	0.028	0.027	0.026	0.027	0.026	0.027	0.027	0.026	0.027	0.027	0.027	0.027	0.002	0.002	0.002	0.002	0.003	0.003	0.003	0.003	
U	0.004	0.005	0.003	0.003	0.003	0.003	0.003	0.003	0.002	0.003	0.003	0.002	0.002	0.003	0.002	0.002	0.002	0.002	0.002	0.002	0.002	0.002	0.002	0.002	
Al	0.004	0.005	0.006	0.005	0.010	0.008	0.012	0.012	0.012	0.025	0.025	0.025	0.025	0.025	0.025	0.025	0.025	0.009	0.009	0.007	0.009	0.007	0.009	0.007	0.009
Sc	0.001	0.001	0.001	0.002	0.001	0.001	0.001	0.001	0.001	0.001	0.001	0.001	0.001	0.001	0.001	0.001	0.001	0.001	0.001	0.001	0.001	0.001	0.001	0.001	
Y	0.005	0.006	0.003	0.003	0.003	0.003	0.002	0.002	0.002	0.002	0.002	0.002	0.002	0.002	0.002	0.002	0.002	0.003	0.003	0.003	0.003	0.003	0.003	0.003	0.003
La	0.116	0.120	0.124	0.119	0.117	0.122	0.126	0.126	0.126	0.126	0.126	0.126	0.126	0.126	0.126	0.126	0.126	0.126	0.126	0.126	0.126	0.126	0.126	0.126	0.126
Ce	0.311	0.305	0.334	0.335	0.346	0.326	0.329	0.329	0.329	0.326	0.326	0.326	0.326	0.326	0.326	0.326	0.326	0.327	0.327	0.330	0.327	0.330	0.327	0.330	0.327
Pr	0.050	0.048	0.048	0.045	0.047	0.047	0.048	0.048	0.048	0.046	0.046	0.046	0.046	0.046	0.046	0.046	0.048	0.048	0.048	0.048	0.048	0.048	0.048	0.048	
Nd	0.287	0.275	0.285	0.286	0.269	0.278	0.299	0.299	0.299	0.304	0.304	0.304	0.304	0.304	0.304	0.304	0.302	0.312	0.312	0.302	0.312	0.302	0.312	0.302	0.312
Sm	0.060	0.058	0.038	0.040	0.043	0.045	0.043	0.043	0.043	0.044	0.044	0.044	0.044	0.044	0.044	0.044	0.048	0.048	0.050	0.048	0.050	0.048	0.050	0.048	
Eu	0.003	0.003	0.002	0.002	0.002	0.002	0.002	0.002	0.002	0.002	0.002	0.002	0.002	0.002	0.002	0.002	0.002	0.002	0.002	0.002	0.002	0.002	0.002	0.002	
Gd	0.033	0.029	0.023	0.024	0.021	0.021	0.028	0.028	0.028	0.025	0.025	0.025	0.025	0.025	0.025	0.025	0.025	0.025	0.025	0.026	0.025	0.025	0.025	0.026	
Tb	0.007	0.006	0.001	0.001	0.001	0.001	0.001	0.001	0.001	0.001	0.001	0.001	0.001	0.001	0.001	0.001	0.001	0.001	0.001	0.001	0.001	0.001	0.001	0.001	
Dy	0.003	0.003	0.001	0.001	0.001	0.001	0.000	0.000	0.000	0.000	0.000	0.000	0.000	0.000	0.000	0.000	0.000	0.000	0.000	0.000	0.000	0.000	0.000	0.000	
Ho	0.000	0.000	0.000	0.000	0.000	0.000	0.000	0.000	0.000	0.000	0.000	0.000	0.000	0.000	0.000	0.000	0.000	0.000	0.000	0.000	0.000	0.000	0.000	0.000	
Er	0.000	0.000	0.000	0.000	0.000	0.000	0.000	0.000	0.000	0.000	0.000	0.000	0.000	0.000	0.000	0.000	0.000	0.000	0.000	0.000	0.000	0.000	0.000	0.000	
Tm	0.000	0.000	0.000	0.000	0.000	0.000	0.000	0.000	0.000	0.000	0.000	0.000	0.000	0.000	0.000	0.000	0.000	0.000	0.000	0.000	0.000	0.000	0.000	0.000	
Yb	0.002	0.001	0.001	0.001	0.001	0.001	0.001	0.001	0.001	0.001	0.001	0.001	0.001	0.001	0.001	0.001	0.001	0.001	0.001	0.001	0.001	0.001	0.001	0.001	
Lu	0.000	0.000	0.000	0.000	0.000	0.000	0.000	0.000	0.000	0.000	0.000	0.000	0.000	0.000	0.000	0.000	0.000	0.000	0.000	0.000	0.000	0.000	0.000	0.000	
Mg	0.012	0.018	0.005	0.006	0.006	0.007	0.003	0.003	0.002	0.002	0.003	0.002	0.003	0.002	0.003	0.002	0.003	0.003	0.004	0.003	0.004	0.003	0.004	0.003	
Ca	0.032	0.078	0.023	0.021	0.019	0.018	0.019	0.019	0.018	0.019	0.018	0.018	0.018	0.018	0.018	0.018	0.017	0.017	0.017	0.017	0.017	0.017	0.017	0.017	
Mn	0.002	0.004	0.001	0.001	0.003	0.007	0.001	0.001	0.001	0.001	0.001	0.001	0.001	0.001	0.001	0.001	0.001	0.001	0.001	0.001	0.001	0.001	0.001	0.001	
Fe 2+	0.018	0.059	0.026	0.031	0.041	0.034	0.023	0.023	0.019	0.019	0.019	0.019	0.019	0.019	0.019	0.019	0.019	0.019	0.019	0.019	0.019	0.019	0.019	0.019	
Pb	0.002	0.004	0.002	0.002	0.002	0.002	0.002	0.002	0.002	0.002	0.002	0.002	0.002	0.002	0.002	0.002	0.002	0.002	0.002	0.002	0.002	0.002	0.002	0.002	
$\Sigma$ A-Site	0.978	1.056	0.951	0.950	0.962	0.953	0.971	0.974	0.974	0.970	0.971	0.971	0.971	0.971	0.971	0.971	0.971	0.971	0.971	0.971	0.971	0.971	0.971	0.971	
P	0.978	0.979	0.995	0.998	1.002	1.006	1.001	1.002	1.002	1.009	1.009	1.009	1.009	1.009	1.009	1.009	1.009	1.009	1.009	1.009	1.009	1.009	1.009	1.009	
Si	0.055	0.061	0.051	0.049	0.035	0.037	0.026	0.026	0.020	0.020	0.014	0.014	0.014	0.014	0.014	0.014	0.014	0.014	0.014	0.014	0.014	0.014	0.014	0.014	
$\Sigma$ B-Site	1.033	1.039	1.045	1.047	1.038	1.043	1.027	1.022	1.022	1.023	1.023	1.023	1.023	1.023	1.023	1.023	1.023	1.023	1.023	1.023	1.023	1.023	1.023	1.023	

Table 33b. Chemical Composition of Monazite from then Wagon Bow and Rare Metals Pegmatites

Oxides	Wagon Bow # 3						Rare Metals Mine			
	WHRADM-3	WHRADM-4	WHRADM-5	MONWH-1	MONWH-2	MONWH-3	RMM-1-3	RMM-1-4	RMM-1-5	RMM-2-1
P <sub>2</sub> O <sub>5</sub>	29.92	30.01	29.82	29.82	29.92	29.32	29.41	29.23	29.57	29.63
SiO <sub>2</sub>	1.43	1.33	1.56	1.23	1.09	1.33	0.63	1.75	0.83	0.55
TiO <sub>2</sub>	0.01	0.01	0.01	0.01	0.01	0.01	0.01	0	0	0
ThO <sub>2</sub>	3.23	2.88	3.03	2.89	2.78	2.82	2.89	2.78	2.81	2.79
ThO <sub>2</sub>	0.22	0.28	0.26	0.3	0.31	0.28	0.28	0.22	0.31	0.23
UO <sub>2</sub>	0.08	0.23	0.19	0.11	0.09	0.06	0.21	0.19	0.18	0.2
Sc <sub>2</sub> O <sub>3</sub>	0.04	0.04	0.03	0.02	0.04	0.04	0.03	0.03	0.03	0.04
Y <sub>2</sub> O <sub>3</sub>	0.28	0.23	0.25	0.18	0.13	0.14	0.12	0.16	0.13	0.11
La <sub>2</sub> O <sub>3</sub>	7.99	8.22	8.3	7.98	8.21	8.05	8.63	8.88	8.73	8.89
Ce <sub>2</sub> O <sub>3</sub>	22.01	20.94	22.33	23.12	23.03	22.83	22.54	22.19	21.23	22.43
Pr <sub>2</sub> O <sub>3</sub>	3.63	3.3	3.42	3.22	3.14	3.09	3.34	3.21	3.12	2.99
Nd <sub>2</sub> O <sub>3</sub>	19.22	21.43	19.83	19.57	19.43	19.99	19.77	19.93	21.34	21.21
Sm <sub>2</sub> O <sub>3</sub>	4.77	4.3	4.23	3.21	2.98	2.93	3.19	3.23	3	3.02
Eu <sub>2</sub> O <sub>3</sub>	0.2	0.21	0.21	0.13	0.14	0.11	0.16	0.17	0.18	0.12
Gd <sub>2</sub> O <sub>3</sub>	2.09	2.33	2.3	1.68	1.89	1.78	1.82	1.92	1.88	1.99
Tb <sub>2</sub> O <sub>3</sub>	0.51	0.5	0.52	0.08	0.09	0.07	0.04	0.05	0.07	0.07
Dy <sub>2</sub> O <sub>3</sub>	0.23	0.23	0.24	0.11	0.09	0.08	0.09	0.06	0.03	0.04
Ho <sub>2</sub> O <sub>3</sub>	0	0	0.01	0	0	0	0	0	0	0
Er <sub>2</sub> O <sub>3</sub>	0.01	0.01	0.01	0.01	0.02	0.01	0.01	0	0.01	0
Tm <sub>2</sub> O <sub>3</sub>	0	0.01	0.02	0	0	0	0	0	0	0
Yb <sub>2</sub> O <sub>3</sub>	0.14	0.12	0.12	0.08	0.09	0.08	0.06	0.08	0.08	0.06
Lu <sub>2</sub> O <sub>3</sub>	0	0	0.01	0	0	0	0	0	0	0
MgO	0.24	0.21	0.18	0.09	0.07	0.08	0.14	0.09	0.09	0.03
CaO	0.89	0.83	0.73	0.56	0.59	0.56	0.38	0.38	0.54	0.77
MnO	0.08	0.05	0.05	0.03	0.05	0.04	0.19	0.08	0.03	0.02
FeO	0.78	0.78	0.46	1.12	1	0.93	1.12	0.99	0.78	0.66
PbO	0.23	0.2	0.22	0.16	0.16	0.13	0.19	0.16	0.17	0.2
Total	98.23	98.69	98.37	95.73	95.37	94.76	95.26	95.76	95.18	96.05

Table 33b cont. Chemical Formula of Monazite from then Wagon Bow and Rare Metals Pegmatites

Ions	Wagon Bow # 3						Rare Metals Mine			
	WHRADM-3	WHRADM-4	WHRADM-5	MONWH-1	MONWH-2	MONWH-3	RMM-1-3	RMM-1-4	RMM-1-5	RMM-2-1
Ti	0	0	0	0	0	0	0	0	0	0
Th	0.029	0.025	0.027	0.026	0.025	0.026	0.026	0.025	0.026	0.025
U	0.004	0.005	0.005	0.003	0.003	0.003	0.002	0.002	0.003	0.002
Al	0.003	0.011	0.009	0.005	0.004	0.003	0.01	0.009	0.009	0.009
Sc	0.001	0.001	0.001	0.001	0.001	0.001	0.001	0.001	0.001	0.001
Y	0.006	0.005	0.005	0.004	0.003	0.003	0.003	0.003	0.003	0.002
La	0.114	0.117	0.119	0.116	0.12	0.119	0.128	0.13	0.129	0.131
Ce	0.313	0.296	0.317	0.334	0.334	0.335	0.332	0.322	0.311	0.328
Pr	0.051	0.046	0.048	0.046	0.045	0.045	0.049	0.046	0.046	0.044
Nd	0.266	0.296	0.275	0.276	0.275	0.286	0.284	0.282	0.305	0.303
Sm	0.064	0.057	0.057	0.044	0.041	0.04	0.044	0.044	0.041	0.042
Eu	0.003	0.003	0.003	0.002	0.002	0.002	0.002	0.002	0.002	0.002
Gd	0.027	0.03	0.03	0.022	0.025	0.024	0.024	0.025	0.025	0.026
Tb	0.007	0.006	0.007	0.001	0.001	0.001	0.001	0.001	0.001	0.001
Dy	0.003	0.003	0.003	0.001	0.001	0.001	0.001	0.001	0	0.001
Ho	0	0	0	0	0	0	0	0	0	0
Er	0	0	0	0	0	0	0	0	0	0
Tm	0	0	0	0	0	0	0	0	0	0
Yb	0.002	0.001	0.001	0.001	0.001	0.001	0.001	0.001	0.001	0.001
Lu	0	0	0	0	0	0	0	0	0	0
Mg	0.028	0.024	0.021	0.006	0.004	0.005	0.009	0.005	0.005	0.002
Ca	0.074	0.069	0.061	0.023	0.025	0.024	0.016	0.016	0.023	0.033
Mn	0.005	0.003	0.003	0.001	0.002	0.001	0.007	0.003	0.001	0.001
Fe 2+	0.05	0.051	0.03	0.037	0.033	0.031	0.038	0.033	0.026	0.022
Pb	0.005	0.004	0.004	0.002	0.002	0.001	0.002	0.002	0.002	0.002
Σ A-Site	1.053	1.054	1.025	0.952	0.948	0.951	0.979	0.952	0.961	0.977
P	0.983	0.982	0.98	0.998	1.004	0.994	1.001	0.98	1.003	1.003
Si	0.056	0.052	0.061	0.049	0.043	0.053	0.025	0.069	0.033	0.022
Σ B-Site	1.039	1.034	1.04	1.047	1.047	1.047	1.026	1.049	1.036	1.025

Rb, 10-0.01 780.206 nm 15 sec	mass	volume	ppm detected in solution	ppm per L	wt percent element	ppm of element in sample	wt %
K-spar downslope from Z	199.0	0.035	1.410	5685.714	0.024798995	247.9899497	0.024798995
slab site F K spar	193.0	0.035	1.850	5514.286	0.033549223	335.492228	0.033549223
host granite KFM b-1 mica	42.8	0.035	0.210	1222.857	0.017172897	171.728972	0.017172897
mica pieces WH2	193.6	0.035	2.560	5531.429	0.046280992	462.8099174	0.046280992
biotite KFM b	201.9	0.035	2.420	5768.571	0.041951461	419.5146112	0.041951461
granite piece WH-2 K-spar	195.7	0.035	0.876	5591.429	0.015666837	156.66837	0.015666837
host rock WH1 mica	10.0	0.035	0.040	285.714	0.014	140	0.014
RMM Mi 21 muscovite	200.9	0.035	3.000	5740.000	0.052264808	522.6480836	0.052264808
WB1M muscovite	193.9	0.035	2.670	5540.000	0.048194946	481.9494585	0.048194946
host rock WH2 K-spar	192.2	0.035	0.900	5491.429	0.016389178	163.8917794	0.016389178
mica pieces WH2 K-spar	202.7	0.035	2.550	5791.429	0.044030587	440.3058707	0.044030587
K-spar + quartz WH2	198.3	0.035	1.450	5665.714	0.025592537	255.9253656	0.025592537
granite piece WH2 mica	47.2	0.035	0.233	1348.571	0.017277542	172.7754237	0.017277542
perthite per5 RMM	199.0	0.035	3.340	5685.714	0.058743719	587.4371859	0.058743719
beryl RNN RMM-5	208.2	0.035	0.060	5948.571	0.001008646	10.08645533	0.001008646

Table 34. DCP analysis of Rb from multiple pegmatites.

Li, 10-01 15 sec	mass	volume	ppm detected in solution	ppm per L	wt percent element	ppm of element in sample	wt %
K-spar downslope from Z	199.0	0.035	0.000	5685.714	0	0	0
slab site F K spar	193.0	0.035	0.000	5514.286	0	0	0
host granite KFM b-1 mica	42.8	0.035	0.000	1222.857	0	0	0
mica pieces WH2	193.6	0.035	0.934	5531.429	0.016885331	168.8533058	0.016885331
biotite KFM b	201.9	0.035	1.360	5768.571	0.023576028	235.7602774	0.023576028
granite piece WH-2 K-spar	195.7	0.035	0.000	5591.429	0	0	0
host rock WH1 mica	10.0	0.035	0.000	285.714	0	0	0
RMM Mi 21 muscovite	200.9	0.035	1.430	5740.000	0.024912892	249.1289199	0.024912892
WB1M muscovite	193.9	0.035	1.120	5540.000	0.020216606	202.166065	0.020216606
host rock WH2 K-spar	192.2	0.035	0.033	5491.429	0.000600937	6.009365245	0.000600937
mica pieces WH2 K-spar	202.7	0.035	1.880	5791.429	0.032461766	324.6176616	0.032461766
K-spar + quartz WH2	198.3	0.035	0.000	5665.714	0	0	0
granite piece WH2 mica	47.2	0.035	0.043	1348.571	0.003188559	31.88559322	0.003188559
perthite per5 RMM	199.0	0.035	0.000	5685.714	0	0	0
beryl RNN RMM-5	208.2	0.035	2.100	5948.571	0.035302594	353.0259366	0.035302594

Table 35. DCP analysis of Li from multiple pegmatites.

Tl, 10-01 15 sec	mass	volume	ppm detected in solution	ppm per L	wt percent element	ppm of element in sample	wt %
K-spar downslope from Z	199.0	0.035	0.070	5685.714	0.001231156	12.31155779	0.001231156
slab site F K spar	193.0	0.035	0.037	5514.286	0.000670984	6.70984456	0.000670984
host granite KFM b-1 mica	42.8	0.035	0.026	1222.857	0.002126168	21.26168224	0.002126168
mica pieces WH2	193.6	0.035	0.087	5531.429	0.001572831	15.72830579	0.001572831
biotite KFM b	201.9	0.035	0.078	5768.571	0.001352155	13.52154532	0.001352155
granite piece WH-2 K-spar	195.7	0.035	0.042	5591.429	0.00075115	7.51149719	0.00075115
host rock WH1 mica	10.0	0.035	0.044	285.714	0.0154	154	0.0154
RMM Mi 21 muscovite	200.9	0.035	0.090	5740.000	0.001567944	15.67944251	0.001567944
WB1M muscovite	193.9	0.035	0.101	5540.000	0.001823105	18.23104693	0.001823105
host rock WH2 K-spar	192.2	0.035	0.067	5491.429	0.001220083	12.20083247	0.001220083
mica pieces WH2 K-spar	202.7	0.035	0.052	5791.429	0.000897879	8.978786384	0.000897879
K-spar + quartz WH2	198.3	0.035	0.022	5665.714	0.000388301	3.883005547	0.000388301
granite piece WH2 mica	47.2	0.035	0.006	1348.571	0.000444915	4.449152542	0.000444915
perthite per5 RMM	199.0	0.035	0.121	5685.714	0.002128141	21.28140704	0.002128141
beryl RNN RMM-5	208.2	0.035	0.052	5948.571	0.000874159	8.741594621	0.000874159

Table 36. DCP analysis of Tl from multiple pegmatites.

B, 10-0.01 15 sec	mass	volume	ppm detected in solution	ppm per L	wt percent element	ppm of element in sample	wt %
K-spar downslope from Z	199.0	0.035	0.000	5685.714	0	0	0
slab site F K spar	193.0	0.035	0.000	5514.286	0	0	0
host granite KFM b-1 mica	42.8	0.035	0.000	1222.857	0	0	0
mica pieces WH2	193.6	0.035	0.000	5531.429	0	0	0
biotite KFM b	201.9	0.035	0.011	5768.571	0.000190688	1.906884596	0.000190688
granite piece WH-2 K-spar	195.7	0.035	0.013	5591.429	0.000232499	2.324987225	0.000232499
host rock WH1 mica	10.0	0.035	0.000	285.714	0	0	0
RMM Mi 21 muscovite	200.9	0.035	0.000	5740.000	0	0	0
WB1M muscovite	193.9	0.035	0.000	5540.000	0	0	0
host rock WH2 K-spar	192.2	0.035	0.007	5491.429	0.000127471	1.27471384	0.000127471
mica pieces WH2 K-spar	202.7	0.035	0.000	5791.429	0	0	0
K-spar + quartz WH2	198.3	0.035	0.000	5665.714	0	0	0
granite piece WH2 mica	47.2	0.035	0.008	1348.571	0.00059322	5.93220339	0.00059322
perthite per5 RMM	199.0	0.035	0.000	5685.714	0	0	0
beryl RNN RMM-5	208.2	0.035	0.000	5948.571	0	0	0

Table 37. DCP analysis of B from multiple pegmatites.

## **Vita**

TJ A. Brown was born on January 23, 1986 in Bryan, Ohio. Thirteen years later he moved to Cambria, Michigan where he graduated from Camden-Frontier High School in 2004. In fall of that year he began attending Adrian College full time where he spent two years as an undeclared undergraduate. In his junior year he finally declared a double major in Earth Science and Environmental Science with a minor in Biology. He graduated from Adrian College in the spring of 2008 with a B.A. In the fall of 2008 he moved to New Orleans and attended the University of New Orleans as a graduate student. He will receive an M.S. degree in December of 2010.